

UNIVERSITY COLLEGE LONDON

CIVIL & ENVIRONMENTAL ENGINEERING

TANYA KENT

**The Effect of Media Size on Biological Aerated Filter (BAF)
Performance**

**Thesis submitted for the degree of Doctor of Philosophy
March 1998**

ProQuest Number: 10010655

All rights reserved

INFORMATION TO ALL USERS

The quality of this reproduction is dependent upon the quality of the copy submitted.

In the unlikely event that the author did not send a complete manuscript and there are missing pages, these will be noted. Also, if material had to be removed, a note will indicate the deletion.



ProQuest 10010655

Published by ProQuest LLC(2016). Copyright of the Dissertation is held by the Author.

All rights reserved.

This work is protected against unauthorized copying under Title 17, United States Code.
Microform Edition © ProQuest LLC.

ProQuest LLC
789 East Eisenhower Parkway
P.O. Box 1346
Ann Arbor, MI 48106-1346

ABSTRACT

BAFs are used for the secondary treatment of wastewater and combine biological treatment with suspended solids capture, negating the need for a separate solids removal stage. The costs associated with BAFs (apart from construction costs) are mainly due to aeration and backwashing. Further research is needed to optimise the process and decrease energy requirements and associated costs. One area which may be important in this respect is the size of media employed.

Research was carried out to compare the performance of four different sizes of the same media type at different hydraulic/organic loading rates. A number of process variables (including effluent quality, headloss, oxygen transfer) were monitored to gain an understanding of how the process as a whole was affected by changing the size of media employed.

Results showed that effluent quality in terms of BOD, SS and $\text{NH}_4\text{-N}$ generally improved with decreasing media size. The smallest media size (2-4mm) had a decrease in nitrification above loads of $0.6\text{kg NH}_4\text{-N/m}^3\text{/d}$ whilst 2.8-5.6mm media nitrified up to $1\text{kg NH}_4\text{-N/m}^3\text{/d}$, this suggests that there may be an optimum size for combined carbonaceous treatment and nitrification.

Oxygen transfer rates were similar for three of the media sizes with the small media having high transfer rates, this was reflected in the low denitrification rates seen in small media.

The small media sizes accumulate more solids than large media, this leads to shorter run times and more frequent backwashing than in large media. Large media sizes are therefore useful for decreasing high BOD/SS loads (roughing filtration), whilst small media can be used for tertiary nitrification processes where there are strict $\text{NH}_4\text{-N}$ consents.

ACKNOWLEDGEMENTS

I would like to thank a number of people from Cranfield University, UCL and Thames Water R&D for their help in completing my research.

Thanks to Rukhsana Ormesher, Dave Hemmings and Allan Mann for helping me with my early attempts at producing a pilot rig at Cranfield University. Thanks to Ian at UCL for help with the video of my pilot plant. From Thames Water, Wayne Edwards, Richard Harris and Adrian Mercer proved invaluable in helping me maintain my pilot rig in working order.

Special thanks go to Pete Pearce who has been a font of knowledge throughout my time at Thames and provided badly needed support to a very nervous speaker at her first international conference.

In the last three years the support of my family and friends has been as important as the help I have received from colleagues at work. Special mentions must go to Jason for encouraging me not to give up when my enthusiasm waned and to Bev and family for taking me in when I needed a home.

Finally I would like to thank Thames Water for funding this project and providing the pilot rig and laboratory budget! Also Steve Williams from Thames Water R&D (who only laughed at me occasionally for my 'blonde' moments) and Dr Caroline Fitzpatrick from UCL for all their supervision.

CONTENTS

ABSTRACT	i
ACKNOWLEDGEMENTS	ii
CONTENTS	iii
LIST OF FIGURES	xi
LIST OF TABLES	xix
LIST OF EQUATIONS	xxiii
NOMENCLATURE	xxiv
1.0 INTRODUCTION	1
2.0 LITERATURE REVIEW	3
2.1 Introduction	3
2.2 Wastewater Treatment Processes	3
2.3 Biological Treatment of Wastewater	3
2.4 Filtration Theory	5
2.4.1 Microscopic Theory	6
2.4.2 Macroscopic Theory	6
2.4.3 The Effect of Media, Bed Depth and Velocity on Filtration	8
2.4.4 Wastewater Filtration	8
2.4.5 Biological Filtration	9
2.5 Development of Biological Aerated Filters	10
2.6 Operation and Use of Biological Aerated Filters	11
2.7 Aeration	12
2.8 Oxygen Transfer	12
2.8.1 Two Film Theory	13
2.8.2 Effect of Physical Properties on Oxygen Transfer	13
2.8.3 Effect of Biological Constituents on Oxygen Transfer	14
2.9 Off-Gas Analysis	15
2.10 Headloss Development	15
2.11 Backwashing of Filter Media	17
2.11.1 Minimum Fluidisation Velocities (V_{mf})	18

2.11.2 Backwashing Techniques	21
2.11.3 Collapse-Pulsing Mechanism	23
2.12 Biological Aerated Filter Media	26
2.12.1 Alternative Media	26
2.12.2 Characterisation of Filter Media	28
2.13 Important Filter Media Characteristics	29
2.13.1 Voidage and Porosity	29
2.13.2 Specific Surface Area and Surface Characteristics	30
2.13.3 Shape	30
2.13.4 Bulk Density	31
2.13.5 Grain Specific Gravity	31
2.13.6 Grain Settling Velocity	31
2.13.7 Minimum Fluidisation Velocity (V_{mf})	32
2.13.8 Attrition Resistance	32
2.13.9 Friability	32
2.13.10 Size	32
3.0 AIMS	34
4.0 MEDIA CHARACTERISATION	35
4.1 Introduction	35
4.2 Media Tested	35
4.3 Media Characterisation Tests	35
4.3.1 Sieve Size Analysis	35
4.3.2 Shape and Appearance	36
4.3.3 Specific Surface Area (SSA) and Internal Porosity	36
4.3.4 Acid Solubility	36
4.3.5 Grain Specific Gravity	36
4.3.6 Bulk Density	37
4.3.7 Voidage	37
4.3.8 Minimum Fluidisation Velocity	37
4.3.9 Attrition	38
4.3.10 Friability	38

4.4 Results	40
4.4.1 Sieve Size Analysis	40
4.4.2 Shape and Appearance	40
4.4.3 Specific Surface Area and Porosity	48
4.4.4 Acid Solubility	49
4.4.5 Grain Specific Gravity and Bulk Density	49
4.4.6 Voidage	50
4.4.7 Minimum Fluidisation Velocity	50
4.4.8 Attrition and Friability	54
4.5 Discussion	59
4.5.1 Media Size	59
4.5.2 Chemical Inertness	60
4.5.3 Biofilm Attachment	61
4.5.4 Fluidisation Behaviour	62
4.5.5 Attrition	66
4.5.6 Friability	67
4.6 Conclusions	68
5.0 PILOT SCALE PERFORMANCE OF ARLITA MEDIA	69
5.1 Introduction	69
5.2 Methodology	69
5.2.1 Description of the Pilot Plant	69
5.2.2 Column Configuration	70
5.2.3 Media Utilised	70
5.2.3.1 Sieve Size Analysis	71
5.2.3.2 Fluidisation Velocities	71
5.2.3.3 Friability and Attrition	71
5.2.4 Air Supply	73
5.3 Plant Operation	73
5.3.1 Commissioning	73
5.3.2 Backwashing	74
5.3.3 Operating Conditions	74
5.4 Data	75

5.4.1 Effluent Quality	75
5.4.2 Biomass Samples	75
5.4.3 Headloss	75
5.4.4 Backwash Sludge Samples	76
5.4.5 Off-Gas Analysis	76
5.5 Data analysis	77
5.5.1 Effluent Quality	77
5.5.2 Biomass Samples	77
5.5.2.1 Mass/Concentration of Biomass	77
5.5.2.2 Scanning Electron Micrographs	78
5.5.3 Headloss	78
5.5.4 Backwash Samples	78
5.5.4.1 Pressure Filtration Time (PFT)	78
5.5.4.2 Capillary Suction Time (CST)	79
5.6 Results	80
5.6.1 Steady State Results	80
5.6.2 Diurnal Variations	83
5.6.3 Bed Profiles	85
5.6.4 Biomass Profiles	86
5.6.5 Headloss	87
5.6.6 Backwash Samples	87
5.6.7 Sludge Samples	88
5.6.8 Off-Gas Analysis	88
5.7 Discussion	90
5.7.1 Steady State Operation	90
5.7.2 Carbonaceous Removal	91
5.7.3 Suspended Solids Removal	92
5.7.4 Nitrification	93
5.7.5 Overall Effluent Quality	95
5.7.6 Biofilm Growth	96
5.7.7 Headloss Development	97
5.7.8 Backwashing and Sludges	98
5.7.9 Oxygen Transfer	99

5.8 Conclusion - Overall Comparison of Arlita Media	101
6.0 PILOT SCALE PERFORMANCE OF LYTAG MEDIA	
<i>- Methodology</i>	103
6.1 Introduction	103
6.2 Methodology	103
6.2.1 Media Utilised	103
6.2.2 Sieve Size Analysis	103
6.2.3 Specific Surface Area and Porosity Data	104
6.2.4 Minimum Fluidisation Velocities	105
6.2.5 Friability	105
6.2.6 Attrition	105
6.3 Plant Operation	106
6.3.1 Commissioning	106
6.3.2 Operating Conditions	106
6.3.3 Backwashing	107
6.4 Data	109
6.4.1 Effluent Quality	109
6.4.2 Biomass Samples	109
6.4.3 Headloss	110
6.4.4 Backwash Sludge Samples	110
6.4.5 Off-Gas Analysis	110
6.4.6 Hydraulic Regime	110
6.5 Data analysis	111
7.0 PILOT SCALE PERFORMANCE OF LYTAG MEDIA	
<i>- Results: 2-4mm Lytag</i>	112
7.1 Introduction	112
7.2 Steady State Results	112
7.2.1 Settled Sewage	112
7.2.2 Effluent Quality	113
7.2.3 Diurnal Variation	116
7.2.4 Bed Profiles	118

7.3 Biofilm Growth	121
7.3.1 Biomass Samples	121
7.3.2 Microbiological Analyses	122
7.3.3 'Slime' Growth on Media Particles	123
7.3.4 Scanning Electron Micrographs	124
7.4 Headloss	125
7.5 Backwash Samples	126
7.6 Sludge Samples	128
7.7 Off-Gas Analysis	128
7.8 Hydraulic Regime	131
7.9 Decommissioning	131
8.0 PILOT SCALE PERFORMANCE OF LYTAG MEDIA	
<i>- Results: 2.8-5.6mm Lytag</i>	133
8.1 Introduction	133
8.2 Steady State Results	133
8.2.1 Settled Sewage	133
8.2.2 Effluent Quality	133
8.2.3 Diurnal Variation	137
8.2.4 Bed Profiles	138
8.3 Biofilm Growth	141
8.3.1 Biomass Samples	141
8.3.2 Microbiological Analyses and SEMs	142
8.3.3 'Slime' Growth on Media Particles	142
8.4 Headloss	143
8.5 Backwash Samples	144
8.6 Sludge Samples	146
8.7 Off-Gas Analysis	146
8.8 Hydraulic Regime	148
8.9 Decommissioning	149
9.0 PILOT SCALE PERFORMANCE OF LYTAG MEDIA	
<i>- Results: 4-8mm Lytag</i>	151

9.1 Introduction	151
9.2 Steady State Results	151
9.2.1 Settled Sewage	151
9.2.2 Effluent Quality	151
9.2.3 Diurnal Variation	154
9.2.4 Bed Profiles	156
9.3 Biofilm Growth	158
9.3.1 Biomass Samples	158
9.3.2 Microbiological Analyses and SEMs	159
9.3.3 'Slime' Growth on Media Particles	159
9.4 Headloss	160
9.5 Backwash Samples	161
9.6 Sludge Samples	162
9.7 Off-Gas Analysis	162
9.8 Hydraulic Regime	165
9.9 Decommissioning	166
10.0 PILOT SCALE PERFORMANCE OF LYTAG MEDIA	
<i>- Results: 5.6-11.2mm Lytag</i>	167
10.1 Introduction	167
10.2 Steady State Results	167
10.2.1 Settled Sewage	167
10.2.2 Effluent Quality	167
10.2.3 Diurnal Variation	170
10.2.4 Bed Profiles	172
10.3 Biofilm Growth	174
10.3.1 Biomass Samples	174
10.3.2 Microbiological Analyses and SEMs	175
10.3.3 'Slime' Growth on Media Particles	175
10.4 Headloss	176
10.5 Backwash Samples	177
10.6 Sludge Samples	179
10.7 Off-Gas Analysis	179

10.8 Hydraulic Regime	181
10.9 Decommissioning	182
11.0 PILOT SCALE RESULTS OF LYTAG MEDIA	
- <i>Discussion: The Effect of Media Size on BAF Performance</i>	184
11.1 Introduction	184
11.2 Carbonaceous Removal	184
11.3 Suspended Solids Removal	187
11.4 Nitrification	189
11.5 Denitrification	201
11.6 Overall Effluent Quality	202
11.7 Biofilm Growth	203
11.8 Headloss Development	203
11.9 Backwashing and Sludge Production	206
11.10 Oxygen Transfer	208
11.11 Hydraulic Regime	212
11.12 Decommissioning	214
12.0 PILOT SCALE PERFORMANCE OF LYTAG MEDIA	
- <i>Conclusions</i>	216
12.1 Conclusions	216
12.2 Future Work	219

APPENDIX I - Testing of Biological Aerated Filter (BAF) Media

Kent, T. D., Fitzpatrick, C. S. B & Williams, S. C.

Wat. Sci. Tech. **34** (3/4) pp363 - 370. 1996.

REFERENCES

FIGURES

2.0 LITERATURE REVIEW

2.1 Simplified Schematic of Downflow BAF	12
2.2 Optimised Filter Conditions	16
2.3 Headloss Curves	17
2.4 Minimum Fluidisation Velocity	19
2.5 Headloss Characteristics	19
2.6 Microscopic View of Air Cavities and Sand Grains During Air Scour	24
2.7 Schematic of Air Motion Corresponding to Conditions Below, At and Above Collapse-Pulsing	25

4.0 MEDIA CHARACTERISATION

4.1 Laboratory Column	39
4.2 EFG	41
4.3 'Starlight'	41
4.4 Molochite	42
4.5 Old Expanded Shale	42
4.6 New Expanded Shale	43
4.7 Lytag	43
4.8 Arlita	44
4.9 EFG	44
4.10 'Starlight'	45
4.11 Molochite	45
4.12 Old Expanded Shale	46
4.13 New Expanded Shale	46
4.14 Lytag	47
4.15 Arlita	47
4.16 Fluidisation of 2-6mm EFG at 8°C	50
4.17 Fluidisation of + 2.8mm 'Starlight'	51
4.18 Fluidisation of 2-6mm Molochite at 8°C	51
4.19 Fluidisation of 2.5-4mm Old Expanded Shale at 8°C	51
4.20 Fluidisation of 3-6mm New Expanded Shale at 8°C	52

4.21 Fluidisation of 2.36 - 4.75mm Lytag 8°C	52
4.22 Fluidisation of 3-6mm Arlita at 8°C	52
4.23 Sieve Analysis of EFG (including after attrition and friability tests)	56
4.24 Sieve Analysis of 'Starlight' (including after attrition and friability tests)	56
4.25 Sieve Analysis of Molochite (including after attrition and friability tests)	57
4.26 Sieve Analysis of Old Expanded Shale (including after attrition and friability tests)	57
4.27 Sieve Analysis of New Expanded Shale (including after attrition and friability tests)	58
4.28 Sieve Analysis of Lytag (including after attrition and friability tests)	58
4.29 Sieve Analysis of Arlita (including after attrition and friability tests)	59
5.0 PILOT SCALE PERFORMANCE OF ARLITA MEDIA	
5.1 Schematic of Single Pilot Column	69
5.2 Sieve Analysis of Arlita Media	70
5.3 Fluidisation of Arlita Media	71
5.4 Sieve Analysis of 3-6mm Arlita After Attrition and Friability Tests	72
5.5 Sieve Analysis of 4-8mm Arlita	72
5.6 'Sewage Fungus'	73
5.7 Pilot Columns at Manor Farm STW	79
5.8 Composite BOD Removal	81
5.9 Composite COD Removal	81
5.10 Composite SS Removal	82
5.11 Composite NH ₄ -N Removal	82
5.12 Composite TKN Removal	82
5.13 Diurnal BOD Removal	83
5.14 Diurnal COD Removal	83
5.15 Diurnal SS Removal	84
5.16 Diurnal NH ₄ -N Removal	84
5.17 Diurnal TKN Removal	84
5.18 NH ₄ -N Profiles	85

5.19 NO ₂ -N Profiles	85
5.20 SS Profiles	86
5.21 Biomass Profiles Before Backwashing	86
5.22 Biomass Profiles After Backwashing	87
5.23 Backwash Profiles for Arlita Media	87
5.24 Cumulative Removal of Solids During Backwash	88
5.25 Operational Oxygen Transfer Efficiency (OTE) (HLR 2)	89
5.26 Corrected OTE (HLR 2)	89
5.27 Oxygenation Capacity (OC) (HLR 2)	89
5.28 DO Profiles for 3-6mm Arlita (HLR 2)	90
5.29 DO Profiles for 4-8mm Arlita (HLR 2)	90
5.30 Effect of Backwash on NH ₄ -N Removal in 3-6mm Arlita (HLR 1)	94
5.31 Effect of Backwash on NH ₄ -N Removal in 3-6mm Arlita (HLR 2)	94
5.32 Biofilm Coverage on Arlita Media	96
5.33 Species of Ciliated Protozoa on Arlita Media	97

6.0 PILOT SCALE PERFORMANCE OF LYTAG MEDIA

- Methodology

6.1 Sieve Analysis of Lytag Media	104
-----------------------------------	-----

7.0 PILOT SCALE PERFORMANCE OF LYTAG MEDIA

- Results: 2-4mm Lytag

7.1 Composite BOD Removal	113
7.2 Composite COD Removal	114
7.3 Composite SS Removal	114
7.4 Composite NH ₄ -N Removal	114
7.5 Composite TKN Removal	115
7.6 Comparison of BOD Removal at 1.35m and 1.6m (Spot Samples)	116
7.7 Comparison of NH ₄ -N Removal at 1.35m and 1.6m (Spot Samples)	116
7.8 Diurnal BOD Removal	117
7.9 Diurnal SS Removal	117
7.10 Diurnal NH ₄ -N Removal	117
7.11 Diurnal SS Removal (HLR 1)	118

7.12 Diurnal NH ₄ -N Removal (HLR 1)	118
7.13 BOD Profiles	119
7.14 COD Profiles	119
7.15 SS Profiles	119
7.16 NH ₄ -N Profiles	120
7.17 TON Profiles	120
7.18 NO ₂ -N Profiles	120
7.19 Biomass Profiles (Before Backwashing)	122
7.20 Zoogloea	122
7.21 Media Particles From Middle of Filter Bed (HLR 1)	123
7.22 Media Particles From Middle of Filter Bed (HLR 4)	123
7.23 Biofilm Coverage on Media Particle	124
7.24 Ciliated Protozoan Species on Media Particle	124
7.25 Head Profile (HLR 1)	125
7.26 Head Profile (HLR 4)	125
7.27 Backwash Profiles	126
7.28 Suspended Solids Removed During Backwash	127
7.29 Operational Oxygen Transfer Efficiency (OTE)	129
7.30 Corrected OTE	129
7.31 Oxygenation Capacity	129
7.32 Dissolved Oxygen Profiles (Air Flow 13m/h)	130
7.33 Tracer Tests (HLR = 1m/h)	131
7.34 Sieve Analysis of 2-4mm Lytag After Decommissioning	132

8.0 PILOT SCALE PERFORMANCE OF LYTAG MEDIA

- Results: 2.8-5.6mm Lytag

8.1 Composite BOD Removal	134
8.2 Composite COD Removal	134
8.3 Composite SS Removal	134
8.4 Composite NH ₄ -N Removal	135
8.5 Composite TKN Removal	135
8.6 Comparison of BOD Removal at 1.35m and 1.6m (Spot Samples)	136
8.7 Comparison of NH ₄ -N Removal at 1.35m and 1.6m (Spot Samples)	137

8.8 Diurnal BOD Removal	137
8.9 Diurnal SS Removal	138
8.10 Diurnal NH ₄ -N Removal	138
8.11 BOD Profiles	139
8.12 COD Profiles	139
8.13 SS Profiles	139
8.14 NH ₄ -N Profiles	140
8.15 TON Profiles	140
8.16 NO ₂ -N Profiles	140
8.17 Biomass Profiles (Before Backwashing)	142
8.18 Media Particles From Middle of Filter Bed (HLR 1)	142
8.19 Media Particles From Middle of Filter Bed (HLR 4)	143
8.20 Head Profile (HLR 1)	143
8.21 Head Profile (HLR 4)	144
8.22 Backwash Profiles	145
8.23 Suspended Solids Removed During Backwash	145
8.24 Operational Oxygen Transfer Efficiency (OTE)	147
8.25 Corrected OTE	147
8.26 Oxygenation Capacity	147
8.27 Dissolved Oxygen Profiles (Air Flow 13m/h)	148
8.28 Tracer Tests (HLR = 1m/h)	149
8.29 Sieve Analysis of 2-4mm Lytag After Decommissioning	150
9.0 PILOT SCALE PERFORMANCE OF LYTAG MEDIA	
<i>- Results: 4-8mm Lytag</i>	
9.1 Composite BOD Removal	152
9.2 Composite COD Removal	152
9.3 Composite SS Removal	152
9.4 Composite NH ₄ -N Removal	153
9.5 Composite TKN Removal	153
9.6 Comparison of BOD Removal at 1.35m and 1.6m (Spot Samples)	154
9.7 Comparison of NH ₄ -N Removal at 1.35m and 1.6m (Spot Samples)	154
9.8 Diurnal BOD Removal	155

9.9 Diurnal SS Removal	155
9.10 Diurnal NH ₄ -N Removal	155
9.11 BOD Profiles	156
9.12 COD Profiles	156
9.13 SS Profiles	157
9.14 NH ₄ -N Profiles	157
9.15 TON Profiles	157
9.16 NO ₂ -N Profiles	158
9.17 Biomass Profiles (Before Backwashing)	159
9.18 Media Particles From Middle of Filter Bed (HLR 1)	159
9.19 Media Particles From Middle of Filter Bed (HLR 4)	160
9.20 Head Profile (HLR 1)	160
9.21 Backwash Profiles	161
9.22 Suspended Solids Removed During Backwash	161
9.23 Operational Oxygen Transfer Efficiency (OTE)	163
9.24 Corrected OTE	163
9.25 Oxygenation Capacity	164
9.26 Dissolved Oxygen Profiles (Air Flow 13m/h)	164
9.27 Tracer Tests (HLR = 1m/h)	165
9.28 Sieve Analysis of 2-4mm Lytag After Decommissioning	166

10.0 PILOT SCALE PERFORMANCE OF LYTAG MEDIA

- Results: 5.6-11.2mm Lytag

10.1 Composite BOD Removal	168
10.2 Composite COD Removal	168
10.3 Composite SS Removal	168
10.4 Composite NH ₄ -N Removal	169
10.5 Composite TKN Removal	169
10.6 Comparison of BOD Removal at 1.35m and 1.6m (Spot Samples)	170
10.7 Comparison of NH ₄ -N Removal at 1.35m and 1.6m (Spot Samples)	170
10.8 Diurnal BOD Removal	171
10.9 Diurnal SS Removal	171
10.10 Diurnal NH ₄ -N Removal	171

10.11 BOD Profiles	172
10.12 COD Profiles	172
10.13 SS Profiles	173
10.14 NH ₄ -N Profiles	173
10.15 TON Profiles	173
10.16 NO ₂ -N Profiles	174
10.17 Biomass Profiles (Before Backwashing)	175
10.18 Media Particles From Middle of Filter Bed (HLR 1)	176
10.19 Media Particles From Middle of Filter Bed (HLR 4)	176
10.20 Head Profile (HLR 1)	177
10.21 Head Profile (HLR 4)	177
10.22 Backwash Profiles	178
10.23 Suspended Solids Removed During Backwash	178
10.24 Operational Oxygen Transfer Efficiency (OTE)	180
10.25 Corrected OTE	180
10.26 Oxygenation Capacity	180
10.27 Dissolved Oxygen Profiles (Air Flow 13m/h)	181
10.28 Tracer Tests (HLR = 1m/h)	182
10.29 Sieve Analysis of 2-4mm Lytag After Decommissioning	183

11.0 PILOT SCALE PERFORMANCE OF LYTAG MEDIA

- Discussion

11.1 BOD Removals for Different Media Sizes	184
11.2 BOD Profiles for Different Media Sizes (HLR 2)	186
11.3 The Effect of SSA on BOD Removals	187
11.4 SS Removals for Different Media Sizes	188
11.5 SS Profiles for Different Media Sizes (HLR 3)	189
11.6 NH ₄ -N Removals for Different Media Sizes	190
11.7 NH ₄ -N Profiles for Different Media Sizes (HLR 2)	193
11.8 NH ₄ -N Profiles for Different Media Sizes (HLR 4)	193
11.9 TON Profiles for Different Media Sizes (HLR 2)	194
11.10 TON Profiles for Different Media Sizes (HLR 4)	194
11.11 TKN Removals for Different Media Sizes	195

11.12 Effect of BOD Loading Rate on Nitrification	196
11.13 Wastewater Treatment According to Filter Depth	197
11.14 Effect of Surface Area on Nitrification	200
11.15 Filter Run Times	204
11.16 Operational OTE for Different Media Sizes (HLR 3)	209
11.17 Corrected OTE for Different Media Sizes (HLR 3)	210
11.18 Oxygen Capacity for Different Media Sizes (HLR 3)	211

TABLES

2.0 LITERATURE REVIEW

2.1 Biological Processes	5
2.2 Media Use by Different Companies	26

4.0 MEDIA CHARACTERISATION

4.1 Details and Suppliers of Media	35
4.2 Sieve Analysis of all Media Types	40
4.3 Surface Area and Porosity	48
4.4 Dirt Content and Acid Solubility of all Media	49
4.5 Grain Specific Gravity and Bulk Density	49
4.6 Voidage (External Porosity)	50
4.7 Experimental and Theoretical Fluidisation Velocities	53
4.8 Attrition and Friability Tests	54
4.9 Sieve Analysis of all Media Types after Friability Test	55
4.10 Sieve Analysis of all Media Types after Attrition Test	55

5.0 PILOT SCALE PERFORMANCE OF ARLITA MEDIA

5.1 Sieve Analysis of Arlita Media	71
5.2 Sieve Analysis of Arlita Media after Attrition Test	71
5.3 Backwashing Procedure for Arlita Media	74
5.4 Backwash Regimes for Arlita Media	74
5.5 Loading Rates	80
5.6 Effluent Quality	80
5.7 Percentage Removals	80
5.8 Sludge Data	88
5.9 Oxygen Demand	101

6.0 PILOT SCALE PERFORMANCE OF LYTAG MEDIA

- Methodology

6.1 Sieve Size Analysis of Lytag	103
6.2 Surface Area and Porosity Data	104

6.3 Theoretical Minimum Fluidisation Velocities	105
6.4 Sieve Size Analysis of Lytag after Friability Tests	105
6.5 Operational Loading Rates	106
6.6 Theoretical Collapse-Pulsing Rates for Lytag Media	107
6.7 Backwash Rates Investigated	108

7.0 PILOT SCALE PERFORMANCE OF LYTAG MEDIA

- Results: 2-4mm Lytag

7.1 Composite Settled Sewage Concentrations	112
7.2 Loading Rates for Composite Samples	112
7.3 Percentage Removals by 2-4mm Lytag	113
7.4 Effluent Concentrations for 2-4mm Lytag (Port 5 Composites)	115
7.5 Denitrification	121
7.6 Flood Times from Ranger Data	126
7.7 Total Suspended Solids Removed During Backwash	127
7.8 Percentage of Treated Effluent Used for Backwash	127
7.9 Sludge Data	128
7.10 Oxygen Demand for 2-4mm Lytag	130
7.11 Clean Bed Retention Times for 2-4mm Lytag (After Backwash)	131
7.12 Sieve Analysis of 2-4mm Lytag After Filter Operation	132

8.0 PILOT SCALE PERFORMANCE OF LYTAG MEDIA

- Results: 2.8-5.6mm Lytag

8.1 Loading Rates for Composite Samples	133
8.2 Percentage Removals by 2.8-5.6mm Lytag	133
8.3 Effluent Concentrations for 2.8-5.6mm Lytag	136
8.4 Denitrification	141
8.5 Flood Times from Ranger Data	144
8.6 Total Suspended Solids Removed During Backwash	145
8.7 Percentage of Treated Effluent Used for Backwash	146
8.8 Sludge Data	146
8.9 Oxygen Demand for 2-4mm Lytag	148
8.10 Retention Times After Backwash	149

8.11 Sieve Analysis of 2.8-5.6mm Lytag After Filter Operation	149
---	-----

9.0 PILOT SCALE PERFORMANCE OF LYTAG MEDIA

- Results: 4-8mm Lytag

9.1 Loading Rates for Composite Samples	151
9.2 Percentage Removals by 4-8mm Lytag	151
9.3 Effluent Concentrations for 4-8mm Lytag	153
9.4 Denitrification	158
9.5 Flood Times from Ranger Data	161
9.6 Total Suspended Solids Removed During Backwash	162
9.7 Percentage of Treated Effluent Used for Backwash	162
9.8 Sludge Data	162
9.9 Oxygen Demand for 4-8mm Lytag	164
9.10 Retention Times After Backwash	165
9.11 Sieve Analysis of 4-8mm Lytag After Filter Operation	165

10.0 PILOT SCALE PERFORMANCE OF LYTAG MEDIA

- Results: 5.6-11.2mm Lytag

10.1 Loading Rates for Composite Samples	167
10.2 Percentage Removals by 5.6-11.2mm Lytag	167
10.3 Effluent Concentrations for 5.6-11.2mm Lytag	169
10.4 Denitrification	174
10.5 Flood Times from Ranger Data	177
10.6 Total Suspended Solids Removed During Backwash	178
10.7 Percentage of Treated Effluent Used for Backwash	179
10.8 Sludge Data	179
10.9 Oxygen Demand for 5.6-11.2mm Lytag	181
10.10 Retention Times After Backwash	182
10.11 Sieve Analysis of 5.6-11.2mm Lytag After Filter Operation	182

11.0 PILOT SCALE PERFORMANCE OF LYTAG MEDIA

- Discussion

11.1 Theoretical SSA	199
11.2 Predicted Headloss	204
11.3 Removal of Suspended Solids	206
11.4 Total Solids Yield	207
11.5 Actual Effluent Reuse for Backwashing	207
11.6 Sludge Volatile Solids	208
11.7 Operational OTE	210
11.8 Oxygen Demand	211
11.9 Retention Times	213

12.0 PILOT SCALE PERFORMANCE OF LYTAG MEDIA

- Conclusions

12.1 Advantages and Disadvantages of Different Media Sizes	216
--	-----

EQUATIONS

2.0 LITERATURE REVIEW

2.1 Kinetic Equation	7
2.2 Continuity Equation	7
2.3 Continuity Equation (2)	7
2.4 Nitrogen Metabolism (<i>Nitrosomonas</i>)	9
2.5 Nitrogen Metabolism (<i>Nitrobacter</i>)	9
2.6 Denitrification	9
2.7 OTR	13
2.8 α Factor	14
2.9 β Factor	14
2.10 Effect of Microorganism on OTR	14
2.11 Hydraulic Gradient	16
2.12 Total Headloss	16
2.13 Minimum Fluidisation Velocity	20
2.14 Reynold's Number	20
2.15 Galileo's Number	20
2.16 Carman-Kozeny Equation	20
2.17 Collapse-Pulsing Rates	23

4.0 MEDIA CHARACTERISATION

4.1 Acid Solubility	36
4.2 Poured Voidage	37
4.3 Packed Voidage	37

NOMENCLATURE

ANOVA	Analysis of Variance
AS	Activated Sludge
BAF	Biological Aerated Filter
BOD	Biochemical Oxygen Demand (mg/l)
BW	Backwash
C^*	Saturation concentration of oxygen (mg/l)
C_1	Bulk liquid oxygen concentration (mg/l)
C_0	Initial solids concentration
COD	Chemical Oxygen Demand (mg/l)
CO_2	Carbon Dioxide
CP	Collapse-Pulsing
CST	Capillary Suction Time (seconds)
d	Diameter of media particles (mm)
DO	Dissolved Oxygen (mg/l)
e^-	Electrons
g	Gravity (m/s^2)
Ga	Galileo's number
GAC	Granular Activated Carbon
GSG	Grain Specific Gravity
H	Total headloss (m)
H_0	Initial headloss (m)
H^+	Hydrogen ions
H_2O	Water
HLR	Hydraulic Loading Rate ($kg/m^3/d$)
K_a	Overall oxygen mass transfer coefficient (h^{-1})
NH_4-N	Ammoniacal Nitrogen (mg/l)
NO_2-N	Nitrite Nitrogen (mg/l)
NO_3-N	Nitrate Nitrogen (mg/l)
O_2	Oxygen
OC	Oxygenation Capacity (kg/h)
OH^-	Hydroxide ions

OLR	Organic Loading Rate (kg/m ³ /d)
OTE	Oxygen Transfer Efficiency (%)
OTR	Oxygen Transfer Rate (kg O ₂ /m ³ /h)
pe	Population equivalent
P	Pressure (mmHg)
PFT	Pressure Filtration Time (seconds)
Q _a	Air flow rate (m ³ /h)
r _m	Removal of oxygen by microorganisms (kg/h)
Re	Reynolds number
RBC	Rotating Biological Contactor
RT	Retention Time
RTD	Residence Time Distribution
SAFe	Submerged Aerated Filter
SEM	Scanning Electron Microscope
SS	Suspended Solids (mg/l)
SSA	Specific Surface Area (m ² /m ³)
STW	Sewage Treatment Works
SVI	Sludge Volume Index
sBOD/sCOD	Soluble BOD/COD (mg/l)
tBOD	Total BOD (mg/l)
TKN	Total Kjeldhal Nitrogen (mg/l)
TON	Total Organic Nitrogen (mg/l)
UC	Uniformity coefficient of media
UWWTD	Urban Waste Water Treatment Directive
VLR	Volumetric Loading Rate (kg/m ³ /d)
V	Subfluidisation water velocity (m/h)
V _{mf}	Minimum Fluidisation Velocity (m/h)
α	α factor
β	β factor
λ	Filter coefficient
σ	Specific deposit
ν	Superficial velocity of fluid (m/h)

ε_d	Porosity of deposit
ε	Voidage
μ	Dynamic viscosity (Ns/m ²)
ρ	Density of water (kg/m ³)
ρ_s	Density of media (kg/m ³)

1.0 INTRODUCTION

The biological aerated filter (BAF) has been in use for 50-60 years for the secondary treatment of wastewater but is not widespread in the UK. BAFs combine biological treatment with suspended solids capture, negating the need for a separate solids removal stage. They are an aerobic fixed film process employing media to provide a large surface area for biofilm attachment - this allows them to be used in areas where available land is limited i.e. they have a 'small footprint'.

It has been shown that BAFs are also adequate for treatment of industrial wastes (Adachi & Fuchi, 1991) and on-site treatment of leachate polluted groundwaters (Mose Pedersen & la Coeur Jansen, 1992). BAFs may also be chemically dosed and used in combination with anoxic filters for phosphorus removal (Clarke, 1995). Their compact nature also makes BAFs ideal for coastal sewage treatment (Upton & Churchley, 1996).

BAFs can treat high organic loads and there have been claims of final effluent qualities of 30mg/l BOD at loading rates of up to 5kg BOD/m³/d and 90% NH₄ removal at 0.6 - 1 kg NH₄/m³/d (Stensel *et al*, 1988). These rates are higher than alternative processes such as trickling filters and activated sludge. Following the introduction of the European Urban Waste Water Treatment Directive (UWWTD) and the Bathing Waters Directive stricter consent limits have come into force and there is a need to upgrade existing treatment works. It is therefore important to improve 'small footprint' processes such as BAFs which can be used for carbonaceous treatment, nitrification or both where there is limited land availability (such as coastal areas).

Dillon & Thomas (1990), produced an economic evaluation of one BAF process (Biocarbone) and compared it to trickling filters and the activated sludge process. It was found that for complete treatment of settled sewage the Biocarbone process was comparable to activated sludge for plants greater than 50,000 pe, (population equivalent), but for plants less than 10,000 pe the Biocarbone process was most expensive. The costs associated with BAFs (apart from construction costs) are mainly due to aeration and backwashing. Further research is needed to optimise the process and decrease energy requirements and associated costs. One area which may be

important in this respect is the size of media employed, for instance small media will provide a high surface area for biomass growth whereas large media may need less frequent backwashing due to low solids accumulation, and could be used in certain situations rather than smaller media. A detailed study of the use of different media sizes in BAFs is necessary to determine how a change in media size can effect the overall BAF performance.

2.0 LITERATURE REVIEW

2.1: Introduction

Early wastewater or sewage treatment in the UK consisted of collecting sewage draining down to the River Thames in interceptor sewers - this was then discharged to the estuary on the ebb tide and diluted in the sea. The Royal Commission on Sewage Disposal (1898-1915) later outlined requirements for sewage treatment to produce effluents with 30mg/l suspended solids (SS) and 20mg/l biochemical oxygen demand (BOD). Currently due to the high population and high water demand, treatment consents for wastewater treatment are becoming more strict especially with the introduction of the Urban Wastewater Treatment Directive and the Bathing Water Directive. Wastewater treatment processes must therefore be optimised in order to meet these consents, one available treatment option is the biological aerated filter (BAF).

2.2: Wastewater Treatment Processes

Conventional sewage treatment unit processes are split into different stages:

- 1) Preliminary and Primary (1°) - Screening and sedimentation to remove floating and settleable solids. This makes sewage more amenable to treatment and prevents blockage of pumps and pipework in later processes.
- 2) Secondary (2°) - Biological and chemical processes which remove most of the organic matter. They are the main treatment processes and usually consist of activated sludge (AS) or trickling filters.
- 3) Tertiary (3°) or Advanced - This is used to further decrease nitrogen and phosphorus levels in areas where consent levels are imposed.

2.3: Biological Treatment of Wastewater

Biological processes used to treat wastewater are classified in a number of ways:

- 1) Suspended growth (e.g. activated sludge) or attached growth (e.g. trickling filters, rotating biological contactors (RBCs), BAFs)
 - 2) Aerobic (presence of air), anaerobic (absence of air) or a combination of both.
- There may also be anoxic systems which are similar to anaerobic processes in that they

do not utilise dissolved oxygen but their biochemical pathways are modified forms of the aerobic pathways.

Aerobic biological treatment processes are often used for treatment of organics in wastewaters as well as ammoniacal nitrogen oxidation (nitrification). One of the earliest biological processes for treating wastewater, the activated sludge process, was devised in Manchester towards the beginning of this century (Arden & Lockett, 1914). This is the most common aerobic suspended-growth treatment process, and was named activated sludge because it employs a mass of flocculent micro-organisms which are capable of aerobically denaturing pollutants found in domestic sewage and industrial effluent.

Fixed-film or attached growth biological processes employ micro-organisms attached to an inert medium to convert organic matter to gases and cell constituents (Hamoda & Abd-El-Bary, 1986). One of the most commonly used processes for wastewater treatment is the trickling filter (otherwise known as a percolating filter), which is also an aerobic treatment process. The first operation of a trickling filter in England was in 1893, and the first municipal example of this in the US was installed in 1908, (Metcalf & Eddy, 1991).

Anaerobic suspended-growth systems include anaerobic digestion which is used to stabilise concentrated sludges from wastewater treatment and the anaerobic contact process which treats untreated wastes mixed with recycled sludge solids. Again an example of anaerobic attached-growth systems is the anaerobic filter which is run in the same manner as an upflow aerobic fixed-film filter except that no process oxygen is introduced.

Denitrification or conversion of nitrate to nitrogen gas is often carried out using anoxic suspended-growth or attached-growth processes.

A comparison of biological processes is given in Table 2.1.

Table 2.1: Biological Processes

Process	Aerobic/anaerobic?	Fixed/suspended growth	Treatment stage
Activated Sludge	Aerobic/Anoxic	Suspended	Secondary
Airlift Reactor	Aerobic	Suspended	Secondary
Anaerobic ponds	Anaerobic	Suspended	Secondary
Biological aerated filters	Aerobic	Attached	Secondary
Fluidised Beds	Aerobic	Attached	Secondary
Maturation ponds	Aerobic/anoxic	Suspended	Tertiary
Oxidation ponds	Aerobic	Suspended	Secondary
Rotating biological contactors	Aerobic	Attached	Secondary
Roughing filters	Aerobic	Attached	Secondary
Trickling Filters	Aerobic	Attached	Secondary

From Table 2.1 it can be seen that BAFs are aerobic attached film processes that are generally used for secondary treatment of wastewater once a high proportion of suspended and colloidal matter has been removed by settlement. They use a combination of biological treatment and filtration to remove BOD, SS and NH_4 .

2.4: Filtration Theory

The objective of filtration in both water and wastewater treatment is to produce a good effluent or filtrate by removing solids from the influent suspension. Particles in suspension are removed by different mechanisms which are influenced by a number of factors including the physical and chemical characteristics of the suspension and filter media, rate of filtration and filter operation.

Much of the theoretical work on understanding mechanisms of filtration has been based on idealised conditions with spherical media, spherical particles in suspension, monodisperse suspensions, clean bed situations and especially with reference to potable water treatment. There has more recently been development towards looking at heterodisperse suspensions and filter ripening plus breakthrough as well as extending the theory to wastewater situations.

The common mechanisms of suspended solids removal are described by two different theoretical approaches:

- 1) Microscopic or trajectory theory which looks at particles being transported towards a single collector
- 2) Macroscopic or phenomenological theory which looks at the filter bed as a whole.

2.4.1: Microscopic Theory

Trajectory modelling was first proposed in 1931 for air filtration where it is now common (Langmuir, 1942). O'Melia and Stumm (1967) adapted the theory for water filtration, the theory was more fully developed by Tien and coworkers and details of their work can be found in a number of papers (Payatakes *et al*, 1974; Rajagopalan & Tien, 1976; 1977; Tien & Payatakes, 1979).

Trajectory analysis involves the modelling of particle movement from a clear space or streamline to resting on a grain of media. Particle collection is based on the limiting trajectory of the suspended particle, particles approaching on one side of the trajectory are captured whilst those on the other side are not captured.

A variety of combinations and conditions can be used for the calculation of collection efficiency based on the collector geometry, size and size distribution, the flow field around/within the specified collector and forces acting on the suspension particles.

2.4.2: Macroscopic Theory

Trajectory analysis cannot be used for design and operation of filters as real suspensions and media are unlike the idealised versions used for modelling. A number of semiempirical models have therefore been developed which utilise the concepts of the filter coefficient (λ) and the specific deposit (σ). The filter coefficient is the proportion of particles removed per unit layer of filter and must be determined by model-scale tests for different suspensions and media types. The specific deposit is the accumulation of particles removed from suspension upon the grain surfaces and is calculated from changes in concentration with depth.

The two main equations used in macroscopic theory are the kinetic equation and the continuity equation. The kinetic equation was first put forward by Iwasaki in 1937 and describes the change in concentration throughout the depth of a filter bed:

Equation 2.1: $\frac{\partial C}{\partial L} = -\lambda C$

Where C = concentration at depth L

λ = filter coefficient

The continuity equation describes a mass balance of the solids removed from suspension and solids deposited in pores across the whole bed:

Equation 2.2: $\frac{\partial \sigma}{\partial t} + v \frac{\partial C}{\partial L} = 0$

Where C = concentration at depth L and time t

v = superficial velocity of fluid

σ = specific deposit

If the bulk specific deposit (σ') is used the continuity equation becomes:

Equation 2.3: $(1 - \varepsilon_d - C) \frac{\partial \sigma'}{\partial t} + v \frac{\partial C}{\partial l} = 0$

Where: ε_d = porosity of deposit

The simple forms of the kinetic and continuity equations are only approximations to the exact equations but it has been argued that the additional terms in the exact equations are negligible and can therefore be neglected (Ives, 1970). The work of Dabrowski (1988) using experimental data from Ives (1960) found that using the simplified versions of the equations do not significantly affect the calculations of headloss and solids concentration.

Macroscopic theory allows the entire filter cycle to be modeled but requires pilot scale experiments in order to determine different parameters. These parameters are very site specific and cannot be used to predict values for other applications.

Overall macroscopic theory shows that at a given filter depth the concentration of solids initially decreases with time (ripening), remains at a good quality and then increases (breakthrough).

2.4.3: The effect of media, bed depth and velocity on filtration

Filters may have a number of different configurations dependent on situation and process consents. Using plastic microsphere suspensions it has been found that filtration efficiency varies inversely with media grain size (Ives, 1965). Experimental work also showed that filtrate quality improves with filter depth but headloss increases. Kau & Lawler (1995) specifically looked at the effect of media type, depth and size on particle removal during filtration. They found that at the same depth removal increased with decreasing media size but particle removal was more evenly distributed throughout the bed with larger media. Moran *et al* (1993) found that an increase in filter bed depth may prevent complete breakthrough from occurring in the filter.

The work of Kau & Lawler (1995) showed that lower filtration velocity experiments removed particles better than high velocity experiments but penetration into the bed was greater at high velocities.

2.4.4: Wastewater Filtration

Filtration in a wastewater filter rather than a potable water filter is affected by the higher solids loading and difference in particle size distribution. The process of filtration in the two cases can be thought to be similar immediately after backwashing but wastewater filters may never gain a truly clean bed.

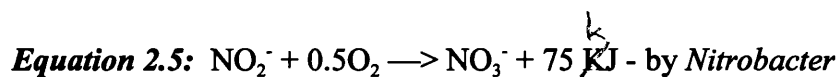
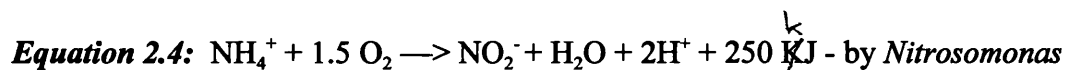
A number of studies have been carried out on wastewater filtration (Tchobanoglous & Eliassen, 1970; Tebbutt, 1971; O'Melia, 1974; Dahab & Young, 1977). These mainly concentrated on the effects of media size and filtration rate in single-sized media filters on suspended solids removal. Conflicting evidence was produced as to whether changing media size greatly affects suspended solids removal but it would appear that changing media size is more important than changing filtration rate.

Darby *et al* (1991) looked at particle size in wastewater filtration at laboratory scale using spherical glass media and found that ripening was a function of particle size, with large particle sizes being effectively captured throughout the experiment and small particles experiencing low removal for a few hours followed by a dramatic increase in removal efficiency. The highest flow rate investigated (0.37cm/s) resulted in more uniform capture of particles throughout the bed whilst decreasing overall particle removal efficiency. It was found that filters with a high filtration rate, large media and deep beds will have satisfactory removal of solids, lower headloss and longer filter runs.

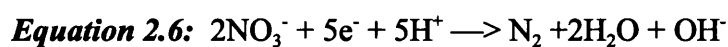
2.4.5: Biological Filtration

In BAFs bacterial activity is again responsible for breakdown of organic materials alongside filtration of particulates. Microorganisms present require a carbon source for synthesis of new biomass. Different bacteria may use organic (heterotrophs) or inorganic (autotrophs) carbon sources. Heterotrophic organisms are energetically more advantaged and in a complex wastewater environment will generally grow faster and outcompete the autotrophs.

Nitrogen metabolism is carried out by autotrophic bacteria which utilise energy generated from the oxidation of inorganic compounds according to the following equations.



In denitrification the nitrate nitrogen is reduced to elementary nitrogen by heterotrophic bacteria according to the following equation.



The kinetics of biological attachment of bacteria on the solid support is related to their growth rate with growth being proportional to the uptake of directly useable substrates.

The rate of increase depends on the growth rate of adsorbed and already attached bacteria in relation to the room available on 'protected sites' on media particles (i.e. surface roughness of media may be important for biofilm attachment and growth).

Detachment from biofilms or the loss of cells and other particles also occurs within the filter. In BAFs erosion of small particles from the outer surface is caused by shear stress created by water flowing past the biofilm, abrasion is caused by collision/rubbing together of particles and sloughing of patches of biofilm may also occur periodically. Detachment may affect the solids concentration in the bulk liquid, the substrate concentration, biofilm activity, biofilm speciation and the characteristics of biomass support particles (media).

Under dynamic conditions growth and loss of the biofilm occur simultaneously during film development (Rao Bhamidimarri & See, 1992).

2.5: Development of Biological Aerated Filters

One of the first examples of a BAF could have been tanks containing slate layers in Lawrence, US - these were termed submerged contact aerators (Clark, 1930). This was followed by the Emscher or Tank filter after the First World War. This utilised coarse slag instead of slate (Bach, 1937) and was described as exhibiting the advantages of the contact bed and trickling filter whilst eliminating the disadvantages of both. It was also compared with activated sludge and came off favourably due to producing sludge in the form of 'humus' and not activated flocs. Submerged contact aerators are constructed as compartments into which media is packed, inside larger tanks. A continuous circulation of waste and air is maintained through the contact units with waste passing again and again over the bed. In the 1940's it was reported that some contact aeration plants were difficult to operate (Fair *et al*, 1948), but there is now renewed interest in the process.

A large amount of the developmental work on aerated biofilters was carried out by French companies in the 1970s (Upton & Churchley, 1996). The Biological Aerated Filter has also been known as a submerged filter and a flooded filter, with the term BAF only becoming common since the 1980's. They have been used for treating

domestic and commercial wastewaters for a number of years in Canada, Europe, North-America and Japan (Smith & Hardy, 1992), with BAF technology being relatively new to the UK.

2.6: Operation and Use of Biological Aerated Filters

There are a number of configurations of BAF available i.e.: upflow or downflow (Figure 2.7), counter-current or co-current and utilising either sunken, structured or floating media . Each design has a number of advantages and disadvantages which have been discussed by Stephenson *et al* (1993). The common factors in BAF technology are that process air passes upward through the reactor and media is selected to provide sites for the growth and capture of biomass (Upton & Stephenson, 1993).

Advantage claims for the process as a whole include:

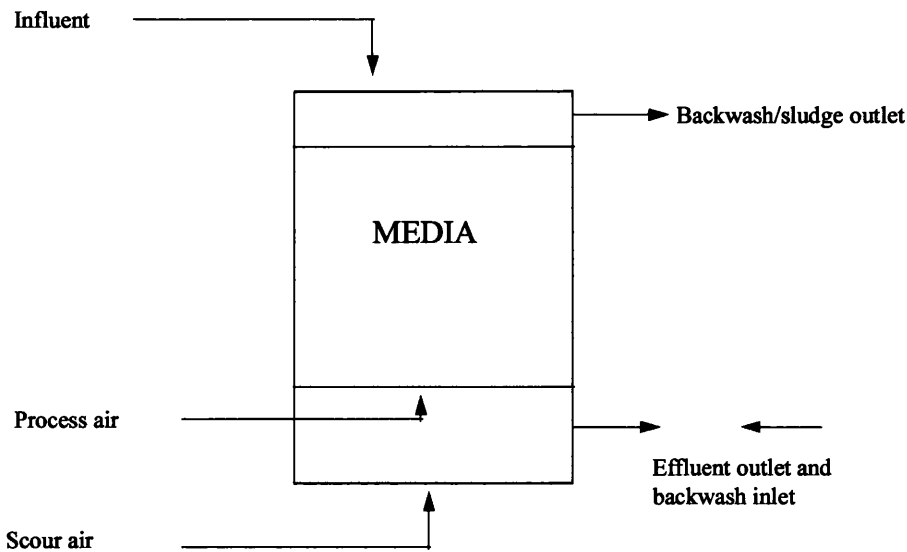
1. Limited land requirement ('small footprint plant')
2. Simple automated operation
3. Reliable effluent quality (Leglise *et al*, 1980)

Disadvantages include:

1. Complex pipework and control systems for backwash
2. Reservoirs of cleaned effluent for backwash
3. Balancing tanks for dirty backwash water

Problems with the volume of washwater used may be combated with continuous filtration systems such as REBAF which incorporates media recycle and wash systems allowing uninterrupted treatment to occur (Stevenson, 1995). More work is needed to optimise these systems before they can be relied upon for use in wastewater treatment.

Figure 2.1: Simplified Schematic of Downflow BAF



2.7: Aeration

Wastewater treatment is dependent on microorganisms receiving enough oxygen for metabolism. Process air is usually supplied in excess of process requirements, this has led to high costs as blower systems are high energy users. Despite being used at separate times, process air and backwash air are generally supplied using separate blower systems and pipework, meaning that there are high capital costs involved in the overall supply of air.

The optimisation of oxygen transfer to microorganisms may allow a reduction in costs involved in the BAF process, studies have been carried out into measuring oxygen transfer by off-gas analysis and applying this to aeration in full-scale plants.

2.8: Oxygen Transfer

The transfer of oxygen from the gaseous to the liquid phase is thought to occur in two stages with oxygen first dissolving in the liquid so there is a high concentration from which oxygen can then be transferred into the bulk liquid. A number of theories exist as to how the oxygen is then transferred to the biofilm.

The general equation given for the oxygen transfer rate is:

Equation 2.7: $OTR = dC/dt = K_1a (C^* - C_1)$

Where: dC/dt = rate of change of oxygen concentration /unit time/ unit volume

K_1a = mass transfer coefficient (a = interfacial area/ unit volume, K_1 = liquid phase mass transfer coefficient for oxygen)

C^* = saturation concentration of oxygen

C_1 = bulk liquid concentration

2.8.1: Two Film Theory

This theory proposed in 1924 by Lewis & Whitman assumes that oxygen diffuses through both a gas and a liquid film layer at the interface with the biofilm. The transfer rate of oxygen is affected by the thickness of the gas and liquid films. This may be reduced by turbulence which will affect the oxygen concentration gradient and increase oxygen transfer. More recent models have been proposed which develop the two-film theory such as the Surface Renewal Model (Winkler, 1981) and the Mass Transfer Model (Hoyland, 1979).

2.8.2: Effect of Physical Properties On Oxygen Transfer

A number of different properties can alter oxygen transfer such as temperature, air flow, bubble size, presence of media and wastewater characteristics.

The addition of media to a reactor has been seen to increase the efficiency of oxygen transfer over a clear water system with the degree of enhancement being dependent on the media used. In packed beds the void size (which in turn is dependent on media size) affects bubble size and shape. There may be undesirable effects if the media promotes bubble coalescence but generally the media should produce higher gas hold-up by producing a more tortuous path and increased residence time. This allows more time for oxygen transfer to occur. Small bubble size will generally be found in media where there are small voids and are beneficial in that they have a high surface area available for oxygen transfer.

The rate of air flow can affect oxygen transfer with high air flows generally leading to high bubble concentrations and bubble coalescence. This leads to decreased oxygen

transfer efficiencies although the reactor as a whole has an increased oxygenation capacity due to the increased mass of available oxygen.

The presence of different constituents in wastewater may also affect the transfer of oxygen. These effects are generally accounted for by α and β factors which compare wastewater with clean water. The α factor is dependent on presence of surfactants, turbulence and the aeration method whilst β factor is dependent on the dissolved solids present.

$$\text{Equation 2.8: } \alpha = \frac{\text{process water } K_1 a}{\text{clean water } K_1 a}$$

$$\text{Equation 2.9: } \beta = \frac{\text{process water } C^*}{\text{clean water } C^*}$$

In live systems the continuous removal of dissolved oxygen by microorganisms is accounted for by another factor - r_m . The equation for oxygen transfer rate becomes:

$$\text{Equation 2.10: } dC/dt = \alpha K_1 a (\beta C^* - C_1) - r_m$$

2.8.3: Effect of Biological Constituents on Oxygen Transfer

There have been a number of reports on the biological enhancement of oxygen transfer including by Reiber & Stensel (1985) and Sundararajan & Ju (1995). It is thought that the presence of biofilm affects transfer both by its physical presence, which changes the hydrodynamics around the gas-liquid interface, and due to respiration. Wise *et al* (1969, reported in Sundararajan & Ju, 1995) found that the presence of particulates alone led to a higher mass transfer rate. The opposite of this was found by Sundararajan & Ju (1995). The presence of respiring cells leads to an increase in transfer with oxygen transferring directly from the gas bubble to microorganisms accumulated at the gas-liquid interface - this is termed interfacial oxygen transfer and has also been found in RBCs (Paolini, 1986). Interfacial transfer can only occur where there is oxygen limitation at the biofilm surface, it increases with increasing bubble-biofilm contact, biomass concentration and substrate utilisation rates. It appears to

have a large role in BAFs and may account for two thirds of the total oxygen transferred (Reiber & Stensel, 1985).

Interfacial transfer of oxygen cannot be measured separately from bulk liquid transfer and the overall transfer rates are generally measured by off-gas analysis.

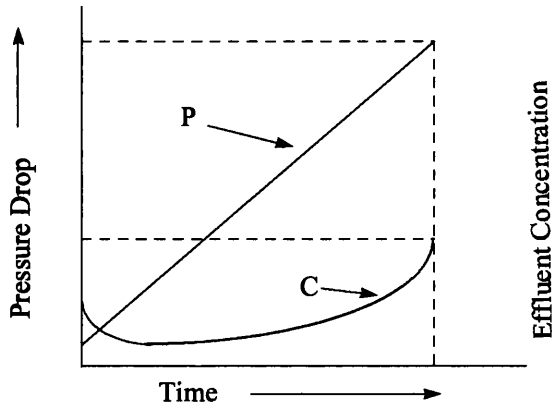
2.9: Off-Gas Analysis

Off-gas analysis is a mass-balance technique which measures the oxygen transfer efficiency (OTE) and the mass transfer coefficient in live systems at steady-state. It assumes that oxygen transferred from process air is the same as the oxygen uptake rate of the biofilm, i.e there is no change in the oxygen concentration in the liquid. When off-gas analysis is carried out further assumptions are that inerts such as nitrogen gas are not absorbed or desorbed and that process conditions do not change rapidly (Boyle *et al*, 1988).

2.10: Headloss Development

The headloss in filters is the pressure drop caused by the liquid flow passing through the filter bed. The clean filter headloss is proportional to the flow rate following Darcy's Law and dependent on grain size and porosity according to the Carmen-Kozeny equation. Goldgrabe *et al* (1993) found a correlation between effective media size and filter run times, therefore a compromise has to be reached between run time and particle removal. Optimum conditions of filter operation are thought to occur if both the filtrate quality and headloss reach their allowable upper limit at the same time.

Figure 2.2: Optimised Filter Conditions (Mintz, 1967)



In a working filter there will be an accumulation of deposits leading to a consequent increase in the hydraulic gradient which is proportional to the quantity of deposit present:

Equation 2.11:
$$\frac{\partial H}{\partial L} = \left(\frac{d H}{d L} \right)_0 + K\sigma$$

Where: $(dH/dL)_0$ = initial hydraulic gradient across clean filter material

σ = quantity of deposit per unit filter volume (specific deposit)

K = constant

The total headloss can be given by:

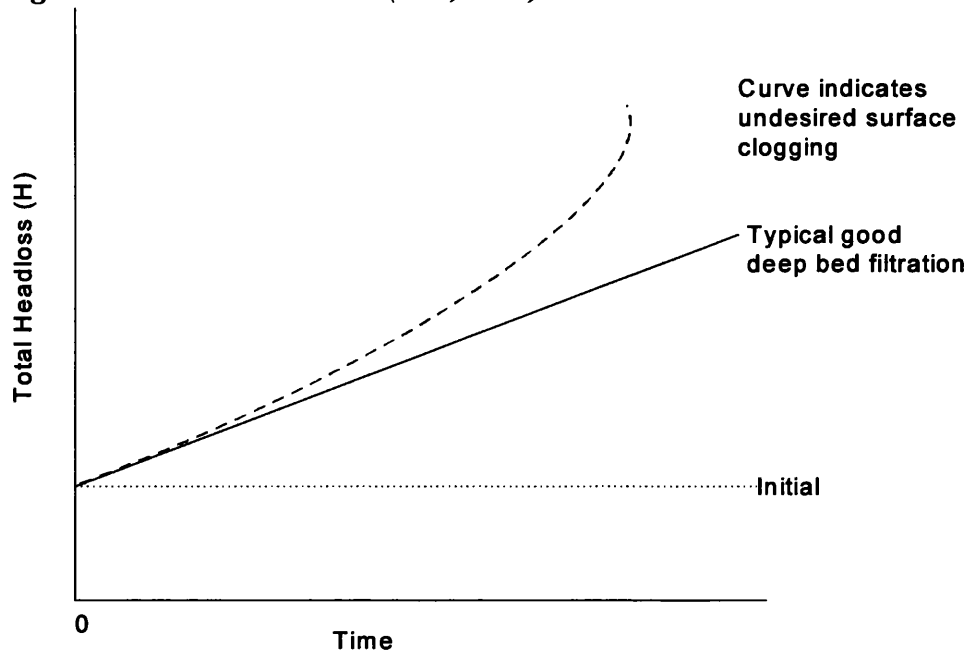
Equation 2.12:
$$H = H_0 + K\upsilon C_0 t$$

Where: H_0 = initial clean bed headloss across all layers

υ = approach velocity

C_0 = Initial concentration

Figure 2.3: Headloss Curves (Ives, 1980)



Wastewater solids removed by granular-media filters tend to accumulate at the filter surface or within the pore spaces in the top few inches of the bed. This surface straining usually causes a rapid build-up of headloss rather than the gradual increase associated with depth filtration (Figure 2.3). To combat the problems of high headloss build-up and short filter run times larger media grain sizes can be used, allowing better penetration of suspended solids and less surface straining.

2.11: Backwashing of Filter Media

When headloss reaches a maximum BAFs must be backwashed to remove excess biofilm growth. Problems occurring in filtration facilities of water treatment plants, such as mudballs and poor initial filtrate quality are associated with the effectiveness of backwashing (Amirtharajah, 1993). The rate of formation of mudballs and their effect on filter performance are more pronounced in wastewater treatment because the solids are more cohesive and influent concentrations are higher than for potable water filters (Young, 1985). Once formed, mudballs tend to grow larger and more compact by incorporating grains of media and filamentous materials carried by the wastewater.

In BAFs backwashing is designed to remove excess biomass, allowing treatment to be resumed directly after washing (Smith & Hardy, 1992), and is carried out by reversing the flow of water causing deposits to dislodge from the filter media surfaces.

Dislodgement of deposits is affected by the rate of upflow, creating shear forces on deposits and grain surfaces and leading to fluidisation and bed expansion (Fitzpatrick, 1993). Only when the upflow water is at a rate greater than the minimum fluidisation velocity, does bed expansion occur. A number of different parameters can affect the efficiency of backwashing such as the size, shape and type of media, the type of deposits that need to be removed and the detachment forces involved in cleaning the deposits from grain surfaces. Fluid shear forces cause most of the particle detachment (as shown by Fitzpatrick, 1993) but grain collisions and abrasion between grains also contribute to the removal of deposits.

The timing of backwash is usually determined by a limiting condition such as headloss or quality of effluent. The length of a filter run before backwashing is necessary can vary from a few hours to 2-3 days (Baylis, 1959) and is affected by a number of parameters such as the loading rate of the filter and the capacity of the filter as well as the efficiency of backwash.. If the run time of a filter is only a few hours it becomes very uneconomical to run the filter as backwashing expends a high amount of energy to run backwash pumps and increases the hydraulic load to upstream treatment processes as the backwash liquors must be treated. The volume and proportions of backwash are important in determining further treatment costs. Upton and Churchley (1996) reported that BAF sludges produced by backwashing are typical of high rate sludges with a volatile proportion in the order of 80% and don't provide particular operational problems.

2.11.1: Minimum Fluidisation Velocities (V_{mf})

The V_{mf} is important for determining the water rates necessary for use in backwashing of granular filters. Fluidisation is the upward flow of a fluid (gas or liquid) through a granular bed at sufficient velocity to suspend the grains in the fluid (Cleasby & Fan, 1981). As the upward flow of liquid through the filter bed increases a resistance of flow is exerted by the granular particles until eventually the resistance equals the gravitational force acting on the granular particles. This causes them to become suspended, any further increase of the flow leads to bed expansion. At the same time the pressure drop (headloss) increases linearly as the water flow increases at low rates

and levels off to a constant value as the resistance force becomes equal to the gravitational force. This process can be seen in Figure 2.4.

Figure 2.4: Minimum Fluidisation Velocity

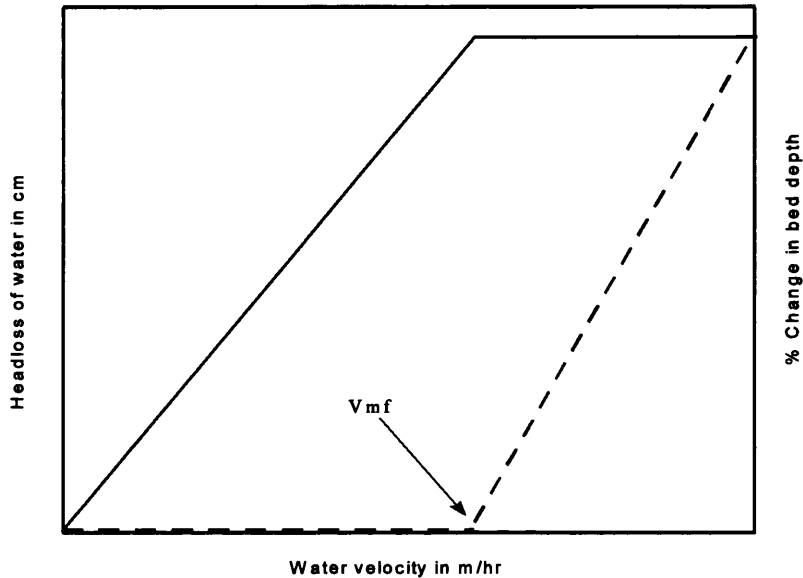
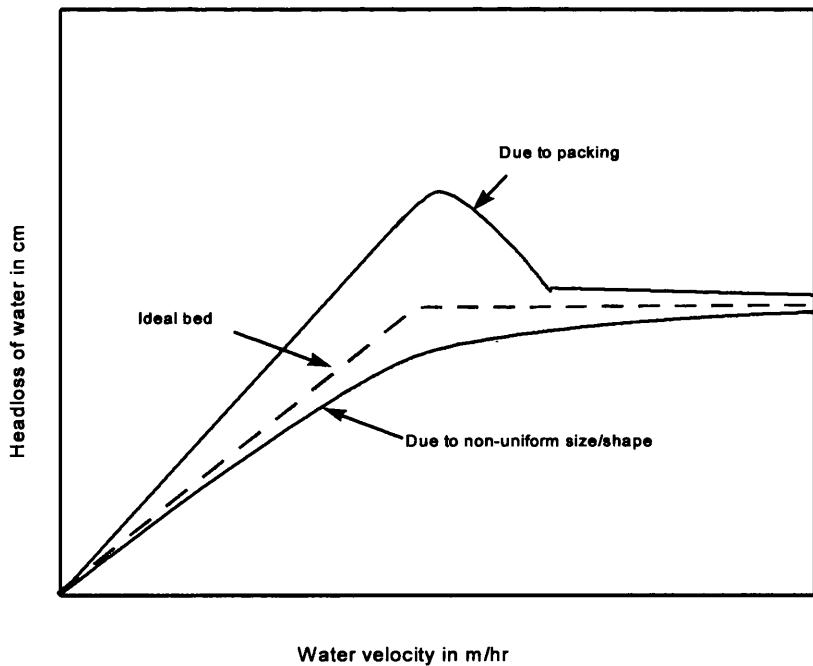


Figure 2.5: Headloss Characteristics



In a filter bed that contains a gradation in particle sizes, the V_{mf} will not be the same for all particles, with smaller grains being fluidised at a lower superficial velocity than large grains. This leads to a gradual change from a fixed bed to a totally fluidised bed making it more difficult to interpret experimental data. In some cases pressure drop or headloss may rise slightly above the constant headloss level observed after fluidisation

before dropping back down (Cleasby & Fan, 1981). This is due to packing of angular grains which prevents them going into a fluidised state and again it can affect interpretation of results (Figure 2.5).

There are a number of different equations available for predicting the V_{mf} of filter media. One of the most widely used equations is that developed by Wen & Yu (1966). Experimental work by Amirtharajah & Cleasby (1972) showed that this model gave excellent predicted values for expansion of graded sands. The equation as it stands states that:

$$\text{Equation 2.13: } V_{mf} = \frac{(Re \mu)}{d_{eq} \rho}$$

$$\text{Equation 2.14: } Re = [33.7^2 + 0.0408 Ga]^{\frac{1}{2}} - 33.7$$

$$\text{Equation 2.15: } Ga = \frac{[d_{eq}^3 \rho (\rho_s - \rho) g]}{\mu^2}$$

Where: μ = dynamic viscosity (Ns/m²)

ρ = density of water (kg/m³)

ρ_s = density of media (kg/m³)

g = acceleration due to gravity (= 9.81 m/s²)

$d_{eq} = d_{90}$ = size of media for which 90 % is smaller by weight (m)

Ga = Galileo's number

Re = Reynolds number at minimum fluidisation

The use of d_{90} should allow the minimum velocity necessary for fluidising the whole bed to be predicted. Most of the particles should be expanded and mobile at this point.

Another method is using the Carman-Kozeny equation which takes into account the bed voidage (Stevenson, 1995):

$$\text{Equation 2.16: } V_{mf} = 0.0055 \left(\frac{\epsilon^3}{1-\epsilon} \right) \frac{d_p^2 (\rho_s - \rho)}{\mu}$$

Where: ϵ = voidage (bed porosity)

d_h = hydraulic media size (mm)

These equations can predict the minimum fluidisation velocities fairly accurately but even though the Carman-Kozeny equation takes into account the voidage of each material, neither of them considers porosity or sphericity of media, both of which could greatly affect fluidisation behaviour. It must also be remembered that in practise media will be coated by a biofilm which reduces the overall particle density and may decrease necessary fluidisation velocities up to 10 - 15% (Addicks, 1990).

2.11.2: Backwashing Techniques

A large proportion of the literature and experimental work on filter backwashing has been aimed at potable water treatment but can be related to wastewater treatment. A number of different techniques for washing filters have been used in the past, these include:

- 1) Water only backwash
- 2) Water backwash with surface water auxiliary
- 3) Water backwash with air auxiliary -
 - a) Air scour followed by water backwash
 - b) Simultaneous air scour and water backwash.

The use of water alone for backwashing is a simple process and has been used for potable water treatment but generally uses high water rates which increase costs and can lead to a high degree of disturbance to the bottom gravel layers of the filter.

Backwashing of wastewater filters with water alone would require even higher water rates and has been shown to be ineffective in adequately cleaning filter media with problems such as mudballs and filter cracks remaining apparent (Young, 1985). The use of water alone is ineffective because there are limited abrasions and collisions between fluidised particles as nearly all the energy is required to suspend the grains (Camp *et al*, 1971).

Due to the ineffectiveness of water-fluidisation alone in backwashing, the use of air scour has become more common. In the early 1900's in the US air scour was

abandoned due to problems of mud balls, strainer clogging and gravel displacement but received renewed attention in the 1960's (Cleasby *et al*, 1977). The use of air scour was originally developed to break up mudballs which could then be removed during backwash, with the air being specifically directed at the surface of the filter. This use of high air flows has been extended to penetrate the whole filter as mudball formation in potable water filters can occur throughout the filter depth if coarse grained media is used. Air scour alone does not allow fluid shear forces to act on the filter media leading to a low cleaning efficiency, therefore combined air and water systems are commonly used. This appears to be the most effective backwashing method and generally the combined phase lasts for all but the last one or two minutes of the backwash procedure, at this point water is washed through on its own in order to rinse away detached solids. The use of air scour combined with water means there is less water consumption, more effective bed cleaning and lower operating costs than for water wash alone.

There are still problems with the use of air scour as it can lead to high media loss over backwash weirs, therefore the design of combined air-water cleaning systems must take into account the control of media loss (Amirtharajah & Trusler, 1982). Similar to high-rate water washes, the use of air scour can lead to disturbance of the supporting layers and consequently may lead to sand leakage into the underdrain system, clogged filter nozzles, uneven distribution of water and air and further related problems as described by Haarhoff & Malan (1983). A number of different design and operating systems, taking into account the problems associated with the use of air scour in wastewater filters, have been described by Cleasby *et al* (1975) and it has been suggested that simultaneous air and water scour should not be used for finer/lighter filter materials such as coal and sands of the typical sizes used in dual/triple media filters (Cleasby *et al*, 1977).

Overall many variables such as media size, shape and density, as well as water quality and (more commonly in potable water treatment) coagulant use, must be taken into account when trying to determine which backwash method to use. There are even more practicalities to be considered when looking at the backwashing of dual or triple media filters such as mixing of the different layers. These factors may explain why the

same backwashing procedure may be a success in one treatment plant and a failure in another (Cleasby *et al*, 1977).

It must also be remembered that bed expansion during backwash may be affected by temperature which alters the liquid viscosity (Tebbutt & Shackleton, 1984). At low temperatures there is a higher bed expansion for a particular water flow than at a higher temperature. If the same water flow is maintained throughout the year there may be high media loss in winter months, backwash flow rates could conceivably be decreased at these times in order to decrease operating costs.

2.11.3: Collapse - Pulsing Mechanism

The most effective method of cleaning filter media is thought to be using combined air and water wash to produce a condition known as collapse-pulsing as observed by Hewitt & Amirtharajah (1984). A theory for the collapse-pulsing condition has been developed (Amirtharajah, 1984), combining concepts from soil mechanics and porous media hydraulics. An empirical equation was produced (Hewitt & Amirtharajah, 1984) to describe the onset of collapse-pulsing and the theory was tested with experimental data collected for three different sizes of sand media (0.62mm, 0.86mm and 1.54mm), and two different sand depths. The detailed development of the equation is beyond the scope of this review but can be found in a number of papers (Amirtharajah, 1984; Amirtharajah *et al*, 1991) and in its simplest form is quoted as:

$$\text{Equation 2.17: } aQ_a^2 + \left(\% \frac{V}{V_{mf}} \right) = b$$

Where: Q_a = air flow rate in m/h

V = subfluidisation water velocity in m/h

a, b = constants

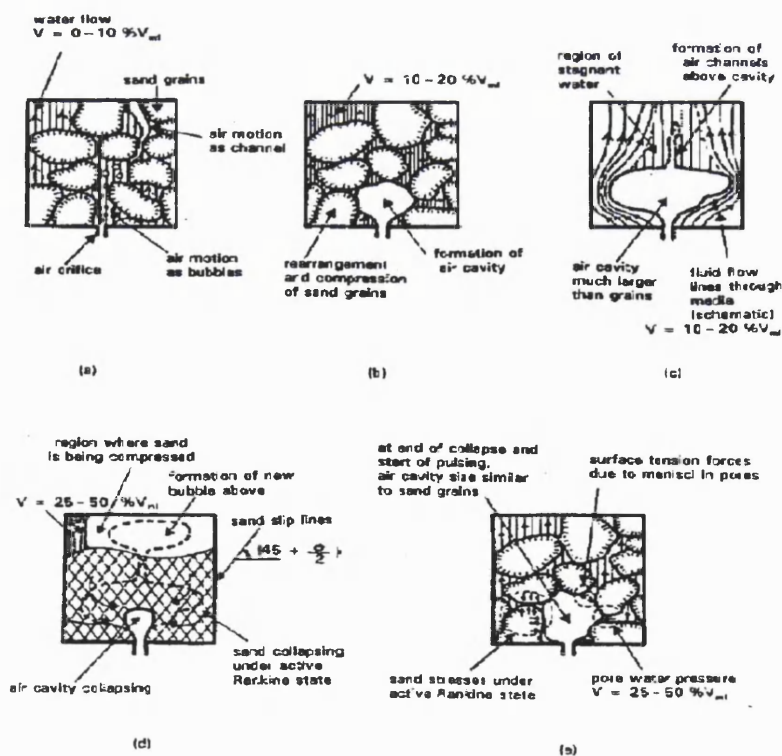
And where limits of observation were in the water flow range of 23.5 - 43.5% V_{mf} and air flow was in the range of 25 - 125m/h.

The theoretical aspects of backwashing, specifically with respect to collapse-pulsing, have been further confirmed at a pilot scale by detailed studies using endoscopes to

provide direct visual evidence of the characteristics of deposits on filter media surfaces (Ives, 1989; Fitzpatrick, 1990; 1993). The theory has also been confirmed at plant scale at the Quarles water treatment plant (Amirtharajah *et al*, 1991) and an engineering chart for operation of air scour backwash systems has been developed.

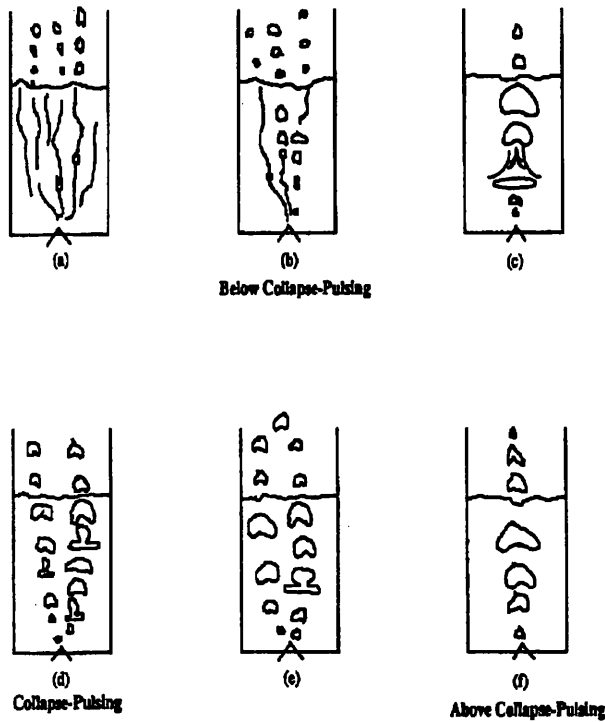
Studies have shown that air can move through filter media in different ways depending on the rate of water flow. More specifically, at a water flow rate of approximately 40 - 60% of the minimum fluidisation velocity the condition known as collapse-pulsing is observed. At this point the air flow moves through a vein or channel and forms an air pocket. Air continues to flow up into this pocket and then a channel can form above the original pocket. Following this a further pocket is able to form above the first one which then collapses. The whole process moves up the filter bed and can be easily seen as a series of pulses as media flows back into the collapsed pockets. It is the abrasion between sand grains caused by the process of collapse-pulsing that leads to thorough cleaning of the filter bed. Also large flocs are broken down within the bed allowing them to be flushed out easily and discouraging mudball formation.

Figure 2.6: Microscopic View During Air Scour (Amirtharajah, 1984)



Low water flow rates in conjunction with air flow produce streaming of air throughout the bed but this does not agitate the bed sufficiently for effective cleaning. At the other extreme, with high water flow rates between 75 and 100% of V_{mf} , the air movement follows that of water and takes the form of bubbles, this leads to fluidisation of the bed but again without the violent agitation necessary for cleaning. The pattern of air motion at different water flow rates has been described in more detail by Hewitt & Amirtharajah (1984) and Amirtharajah (1984).

Figure 2.7: Schematic of Air Motion Corresponding to Conditions Below, At and Above Collapse-Pulsing (From Amirtharajah, 1984)



Within the condition of collapse-pulsing the most effective cleaning of particles occurs at higher air flows which increase stress between media grains. It is still necessary though to follow collapse-pulsing with a water alone wash in order to flush away any detached solids.

Filter sands are the most commonly observed media so a large amount of the above theory and experimental work has been produced specifically in connection with sands. As has already been mentioned a large number of different natural materials as well as

newer synthetic materials are used as granular media in wastewater filters. It has not yet been seen whether this theory will therefore apply to all new types of media.

2.12: Biological Aerated Filter Media

BAFs employ different types of filter media for immobilisation of biomass - these are usually granular media such as sand, expanded clay, expanded slate and polystyrene beads. The selection of media and correct maintenance of media are essential for effective filter performance.

The media used in BAFs is often dependent on the company involved. In many cases companies have sole-use agreements for the use of a certain type of media, examples of this include Biolite and Biobead as seen in Table 2.2.

Table 2.2: Media Use by Different Companies

Process	Company	Media Name	Media Description	Size in mm	Specific Surface Area	Upflow or downflow
Biocarbone	Biwater - OTV	Biodagene	Expanded shist	3 - 6 (BOD) 2 - 5 (NH ₄)	800m ² /m ³	
Biobead	Brightwater	Biobead	Buoyant polypropylene rod			
SAFe	PWT	Expanded Shale	Expanded shale	2 - 6	100m ² /m ³	Downflow
Stereau BAF	Stereau / Purac	Volcanic Pozzolana	Volcanic pozzolana			Downflow
Biofor	Degremont	Biolite	Expanded clay			Upflow
Colox	Tetra	Silica	Silica	2 - 3		
Biopur	Sulzer/John Brown		Structured plastic	N/A	125 - 500 m ² /m ³	Downflow
Copa BAF	Copa	Biodek	Plastic			
FAST	Promech		Modular plastic			

As well as immobilising biomass, filter media must remove /separate suspended solids and store the separated solids until backwashing is required (Fulton, 1988).

2.12.1: Alternative Media

In the earlier period of development most granular filters were filled with sand media. Later crushed anthracite was used instead of sand (Fulton, 1988). The anthracite had a

much lower density and therefore could be expanded sufficiently during backwash by means of a much lower upflow rate than the one required to clean sand.

Other natural materials have been looked at such as pumice (Morgeli & Ives, 1979). The use of pumice was found to be questionable for effluents which imposed filter loads requiring frequent backwashing as it abraded relatively severely during a 50 hour backwash trial with an air rate of 100 m/h and water rate of 75m/h. In the same study expanded slate showed much less attrition.

Alternative media may also consist of locally available materials, for example Ogedengbe (1982), looked at locally available sands in Nigeria for use in rapid gravity filtration of potable water in response to the expense of importing sand and gravel. Again local sands were looked at by Odumosu & Muyibi (1983), but this time in respect to slow sand filters. In both cases fairly good filtration results were reported. Palm kernel shells have also been investigated by Ogedengbe & Olawale (1983), due to their abundance and wastage in rain forest regions of Nigeria, and were found to have good potential in water filtration and tertiary treatment of wastewaters.

Plastic media was developed for use in trickling filters from as early as 1954 by the Dow Chemical Company (Bryan, 1982), and was in the form of a 'honeycomb' structure. The use of plastics has become more common mainly due to it being lighter than conventional media therefore allowing taller, more compact plants to be built. Additionally the characteristics of the media are more controllable ensuring that spontaneous attachment of micro-organisms can occur. The potential of using plastic media for biomass support media in submerged aerated filters was realised fairly recently. Structured packings have also been developed for biological filters by Sulzer in the form of the Biopur system, (Ryhiner *et al*, 1992). The claimed advantages of using these types of media are that there is no attrition or loss of media during backwashing which only need occur after several days of normal operation. There is a disadvantage in that there may be less filtration than in granular media systems.

It was thought that a number of problems associated with the use of BAFs could be overcome by using a buoyant, granular plastic media instead of sunken media,

(Cantwell & Whitaker, 1989). The Biobead system was therefore developed by Brightwater Engineering and consists of a media with a furrowed structure on the surface to improve biomass attachment during backwashing. Another similar novel carrier system is in the form of Immobasil which consists of silicone rubber formed into a sponge-like structure with randomly connecting pores. The work of Mann *et al* (1995) predicts that during start-up, in upflow filters, floating media is more efficient at treating high suspended solids wastewater than sunken media, this work though does not cover steady-state reactor performance. Synthetic media can be fabricated for any process requirements allowing a high degree of control over important media characteristics. It must be remembered though that synthetic materials are costly to produce so their benefits must outweigh these costs.

2.12.2: Characterisation of Filter Media

The variation in filter mechanisms has led to the need to be able to characterise media in order to determine its suitability for use in different filters and to help in the choice of alternative materials. Every new granular material must first satisfy various requirements before it can be considered for use (Morgeli & Ives, 1979). These concern its form, grain size, grain surface, density, pore volume, solubility, durability and settling rate.

A number of filtration media standards have been developed including BS1438: 1971 which is a specification for Media for Biological Percolating Filters, the Indian Standard (Anon, 1977) which specifies in particular the characteristics of filter sand and gravel, the American Waterworks Association (AWWA) standard (Anon, 1989) which concentrates on anthracite and silica sand, and the recent British Effluent and Water Association Granular Filtering Materials Standard (BEWA, 1993). The BEWA Standard and its background has been reviewed by Stevenson (1994) and was intended for use by UK utilities, consultants, contractors, suppliers and manufacturers to define the terminology, requirements, inspection and approval procedures for all types of granular filtration material intended for water and wastewater filtration. It can also be used in connection with materials for biological filters which undergo backwashing.

2.13 Important Filter Media Characteristics

The choice of media can greatly affect wastewater treatment in economic terms. Although the filter material only represents a small proportion of the initial capital outlay, it does affect day to day running costs such as energy costs necessary for backwashing (Letterman, 1980). It is therefore important to choose media with appropriate characteristics e.g. low density and fluidisation rates, as these factors influence the amount of air and water necessary to carry out effective backwashing.

In 1984, Shah *et al* considered a number of general criteria to be important when choosing an ideal filter media. These were:

- i) it should be inert, hard and durable
- ii) it should store a large quantity of particulate matter with low headloss
- iii) it should be easily cleaned by backwashing
- iv) it should give an effluent of an acceptable quality
- v) it should not leach any undesirable substance
- vi) it should be readily available.

These points are valid but do not consider specific characteristics of media such as density, size and porosity. From the following sub-sections it can be seen that there are a number of characteristics that must be considered before using new media for filtration of wastewater.

2.13.1: Voidage and Porosity

In this study the term voidage is used to describe external or bed porosity and porosity is used to describe internal or grain porosity.

Voidage is defined as the pore volume per unit filter volume and is dependent on the shape of the grains. Orr (1966), stated that in general, the greater the deviation of a smooth-surfaced particle's shape from spherical, the closer will be the packing (and correspondingly lower voidage) that can be achieved from it by vibration or moderate pressure compaction. This is due to the particles orientating themselves so that projections on some fit into indentations on others. Rounded grains tend to produce a voidage of 40% allowing them to be cleaned at low backwash rates (Stevenson, 1994), as a filtering material though this means there is less space to hold suspended solids

and higher headloss is produced. A high voidage minimises filter clogging and short-circuiting (Anderson *et al*, 1994) and results in a decrease in the overall reactor volume but with each percentage change in voidage there may be a 9.5% change in the required backwash water rates (less for combined air and water).

Anderson *et al* (1994) looked at filter media used in anaerobic treatment of wastewater. They showed that porous media had a much better performance than non-porous media at high organic loading rates (more than 4kg COD/m³/day) due to high biomass attachment to the porous media. These results can be related to media used for aerobic filtration as well as anaerobic filtration.

2.13.2: Specific Surface Area and Surface Characteristics

Where there are high concentrations of biomass there will be a high degree of wastewater treatment and a good quality of effluent. A large surface area enhances biomass attachment to filter media, with high surface roughness also increasing the rate of attachment and accumulation of biomass on packing media (Anderson *et al*, 1994).

A small media size will have a high surface area to volume ratio and therefore comparatively high biomass concentrations. A number of papers have discussed the use of open-pore sintered glass as support media in anaerobic treatment of wastewater (e.g. Breitenbacher *et al*, 1989; Keim *et al*, 1988). These modified carriers showed that a very high specific surface area was available for colonisation by biomass and again characteristics such as pore size and volume could be easily controlled in manufacture. These properties led to a rapid start-up and high process stability during steady-state performance.

2.13.3: Shape

It is not certain how important the shape of media is for the process of filtration itself. Ives & Coad (1987), argued that there is evidence to show that more angular grains perform better as filter media and there is agreement that flaky shapes are not beneficial but most argument centres around whether grains should be spherical and if this is beneficial to filtration.

The shape of grains can be specified by their sphericity, which is the diameter of a sphere that is made of the same material as the grains and that falls through water at the same velocity, divided by the mean sieve size of the grains. Ives & Coad (1987), stated that sphericities of less than 0.6 should be avoided because of the problems associated with plate-like grains.

The sphericity of media influences the fluidisation behaviour of the media along with the fixed bed headloss, the minimum fluidisation velocity and the bed expansion as a function of upflow rate (Cleasby & Fan, 1981). Spherical particles need higher fluidisation velocities as they have lower drag forces acting on them than irregular shaped particles and therefore tend to settle out quicker.

2.13.4: Bulk Density

The bulk density is the dry weight of the material divided by the volume that it occupies and is used to quantify the amount of media necessary for filter operation. It is affected by conditions employed such as air/water backwash rates, work by Bayfield (1993) showed that even specific parameters such as the rate that backwashing is switched off will affect the result for bulk density measures. The relevant conditions should therefore be specified when quoting a bulk density value.

2.13.5: Grain Specific Gravity

Density after allowing for buoyancy (i.e.: the density of the solid grain material divided by the density of water - usually at 25°C), is important as, together with the size, it determines the degree of separation of the media layers (Morgeli & Ives, 1979). The grain specific gravity data is used to calculate fluidisation thresholds which are important in determining backwash rates (Stevenson, 1994). Generally the density of media needs to be higher than that of water if it is to be submerged and to prevent high media loss during backwashing, but not so dense that it increases backwash rates.

2.13.6: Grain Settling Velocity

The grain settling velocity is measured in water of known temperature and is useful in determining the stratification behaviour of the media if water alone is used for the final

stage of backwashing (Ives, 1990). It is also related to the minimum fluidisation velocity.

2.13.7: Minimum Fluidisation Velocity (V_{mf})

The minimum fluidisation velocity of different media is an important consideration for the process of backwashing filters - this has been discussed in depth in section 2.11.

2.13.8: Attrition Resistance

If materials are readily broken down during filter use and especially during backwashing they will produce a high volume of fines which could block filter nozzles and affect subsequent processes, for example it may lead to early breakthrough or reduced filtrate quality. It is generally expected that angular brittle grains may have prominent parts of their surfaces removed during the first few backwashes but this shouldn't persist in media that is going to be used in BAFs. Synthetic media is generally less prone to attrition than natural materials.

2.13.9: Friability

According to Fulton (1988), the friability of media is the measure of the relative 'crushability' of a particular granular material, it was noted that wear of media may not only round off the shape of the grains, but may also break down the grains into smaller-sized particles. The fines produced from a friable material could lead to blockage of nozzles and filters in BAFs and a subsequent deterioration in performance.

2.13.10: Size

According to Ives (1990), the grain size specification must be appropriate to the water to be filtered: its pre-treatment, flow rate, desired filtrate quality, length of filter run and backwash conditions.

The grain size is determined by screening and is indicated by the grain size distribution curve, which shows the percentage of the different sizes (Morgeli & Ives, 1979). Conventionally, filter sand is specified on the basis of 'effective size' and 'uniformity coefficient' (UC) (Ogedengbe, 1982). The ideal UC purely in terms of size would

have a value of 1.0 indicating that all media grains are of identical size, this is feasible with synthetic material but would be costly to achieve.

The 'effective size' has no relevance to backwashing (Stevenson, 1994) therefore it is recommended that the 'hydraulic size' (d_h), or the grain size that would produce the same resistance to flow as the material under consideration, be used to describe media size. It is also an easy parameter to calculate. Media is often described by the actual size range, with stated sizes understood to be between d_5 and d_{95} .

The size of media grains often varies depending on the company involved and the use of the BAF. Biocarbone's expanded clay has a diameter of 3 - 6mm in cases where it is used for carbonaceous (Biochemical Oxygen Demand - BOD) removal and a diameter of 2 - 5mm where it is used for nitrification (Dillon & Thomas, 1990). The Biofor process also reserves the finest sizes of media for nitrification and phosphate removal (Sagberg *et al.* 1992).

It is known that media size can affect a number of different process variables in BAFs, for example it has been noted that the smaller the media the higher the percentage particulate removal but this is outweighed by high headloss development and therefore shorter run times before backwashing must be carried out. Stensel *et al* (1988) found that backwash requirements were significantly reduced by a change to a larger media size but lower average hydraulic application rates and loadings had to be used to achieve similar effluent quality to that gained with smaller media. Detailed studies have not been carried out to investigate the effect of different media size on the BAF process as a whole in terms of effluent quality, headloss development and oxygen transfer. This study aims to measure the effect of media size on all important variables incorporated into the treatment of wastewater by BAFs.

3.0 AIMS

The overall aim of this study was to produce an understanding of the BAF process as a whole and how individual components of the process are affected by the size of media used. The different components investigated were:

1. Media characterisation - to choose the best available media type for use in BAF pilot columns
2. Effluent quality - to monitor BAF performance at different hydraulic and organic loading rates
3. Diurnal variation - to determine whether variations in settled sewage strength affect performance
4. Filter bed profiles - to monitor how removals of BOD, SS and $\text{NH}_4\text{-N}$ change with bed depth
5. Biofilm growth - to determine how this is affected by changes in hydraulic/organic loading rate and to see if the backwashing regimes employed were efficient at removing excess biofilm
6. Headloss - to determine run times and how different sections of the filter bed contribute to pressure loss build-up
7. Backwashing - to monitor solids removed at each backwash, volumes of effluent reuse and characteristics of the resulting sludges
8. Oxygen transfer rates - to determine how oxygen transfer is affected by changes in organic and hydraulic loading as well as differing air flows
9. Hydraulic regimes - to see if plug flow conditions prevail even when there is high headloss before backwashing

4.0 MEDIA CHARACTERISATION

4.1: Introduction

A number of media types are available for use in BAFs and are chosen according to the BAF configuration and treatment needed. In this project different sizes of the same media were tested at pilot scale. The physical characteristics were determined for a number of different granular media in order to determine which would be most suitable for use in a downflow sunken media biological aerated filter.

4.2: Media Tested

The details of the media tested are given in Table 4.1.

Table 4.1: Details and Suppliers of Media

Media Name	Stated Size Range	Suppliers	Description
EFG	2 - 5mm	Alpha Aggregates	Expanded fireclay grog
'Starlight'	+ 2.8mm	ECC	Foamed cylindrical clay
Molochite	2 - 6mm	ECC	Angular calcine clay
Old Expanded Shale	2.5 - 4mm	Akdolit-Werk, GMBH	Angular shale
New Expanded Shale	3 - 6mm	Akdolit-Werk, GMBH	Angular shale
Lyttag	2.36 - 4.75mm	Lyttag Ltd	Pulverised fuel ash
Arlita	3 - 6mm	Aridos Ligeros, Spain	Expanded spherical clay

The Lytag, Arlita and expanded shales have all been used at full-scale, EFG has been used in fish farm filters and both Molochite and 'Starlight' are experimental media.

4.3: Media Characterisation Tests

The tests for media characterisation were mostly taken from the British Effluent and Water Association (BEWA) [now British Water] standard for granular filtering material, (1993). Some adaptations were necessary as the standard was originally produced with reference to potable water treatment.

4.3.1: Sieve Size Analysis

Samples of approximately 200g in weight were sieved using BS 410: 1986 standardised sieves. The procedure followed was mechanical sieving for two periods of 5 minutes. The time for sieving was calculated by first sieving one sample for different intervals of time until a further minute of sieving led to less than a 1% change

in any sieve fraction . Between each sieving the sieves were tapped to prevent blinding of the openings.

The results were plotted as a log probability graph and the hydraulic size and uniformity coefficient (UC) of each sample were calculated as described by the BEWA standard.

4.3.2: Shape and Appearance

Scanning electron micrographs were taken of unused samples of each media type at a number of different magnifications to show their surface characteristics and porosity. Samples were sputter-coated with gold (Emtech model K550) to increase the contrast of the media samples and looked at using a scanning electron microscope (SEM)[ISI model ABT-55].

4.3.3: Specific Surface Area (SSA) and Internal Porosity

The powder testing and characterisation service provided by the School of Powder Technology, University of Bradford was used to obtain measurements of surface area and porosity of each of the media samples. The particle porosity was determined using a Micromeritics ASAP Adsorption Apparatus (Allen, 1981).

4.3.4: Acid Solubility

All media samples were first washed and dried (at 105°C) and 100g of media were added to 320ml of HCL solution (ratio of 1 water: 1 HCl [32%]). The samples were allowed to stand for 30 minutes after effervescence had ceased. The samples were then washed thoroughly in distilled water and dried to a constant weight. The sample was then allowed to cool and reweighed.

$$\text{Equation 4.1: Acid solubility (\%)} = \frac{\text{loss of weight}}{\text{original weight}} \times 100$$

4.3.5: Grain Specific Gravity (GSG)

The media were all porous in nature therefore it was necessary to soak them overnight in order to eliminate air from the pores, the media was then blotted to remove excess water. The specific gravity bottle technique was used to determine GSG but a 250 ml

volumetric flask was used instead of a density bottle as this has been found to give accurate results (Humby, 1994).

4.3.6: Bulk Density

A quantity of media was dried and weighed before being placed in a column of 15 cm diameter and 2 m height (Figure 4.1). The media bed was then fluidised and the bed volume was recorded. The wash conditions are specified in the results table because the bulk density of a material after fluidisation with water will be slightly lower than that following a combination of air and water washing. The dry weight of material divided by the volume occupied was calculated as the bulk density.

4.3.7: Voidage

A sample of media was soaked overnight and then drained through a sieve in order to expel air from the pores but remove excess water. The media was then poured in the 15 cm diameter column and the volume recorded (V1). The column was then tapped in order to compact the media and the compacted volume recorded (V2). A measured volume of water (V3) was then added to the column and the new volume recorded (V4).

$$\text{Equation 4.2: Poured voidage} = \frac{V1 - (V4 - V3)}{V1}$$

$$\text{Equation 4.3: Packed voidage} = \frac{V2 - (V4 - V3)}{V2}$$

4.3.8: Minimum Fluidisation Velocity (V_{mf})

Approximately 500 - 600 mm of media was placed in the same test column. The BEWA standard stated that the diameter of the testing column should be at least 50 times the hydraulic size of the material being evaluated but a number of media had hydraulic sizes of more than 3 mm. The V_{mf} was calculated from the backwash head gradient and the bed expansion. The upflow water rate was increased in stages and the water level in the manometers and the bed depth were recorded at each step, the water flow was then turned off and the new bed depth recorded before the next step. The bed

expansion was recorded as the percentage increase in depth over the residual depth after flow had ceased.

4.3.9: Attrition

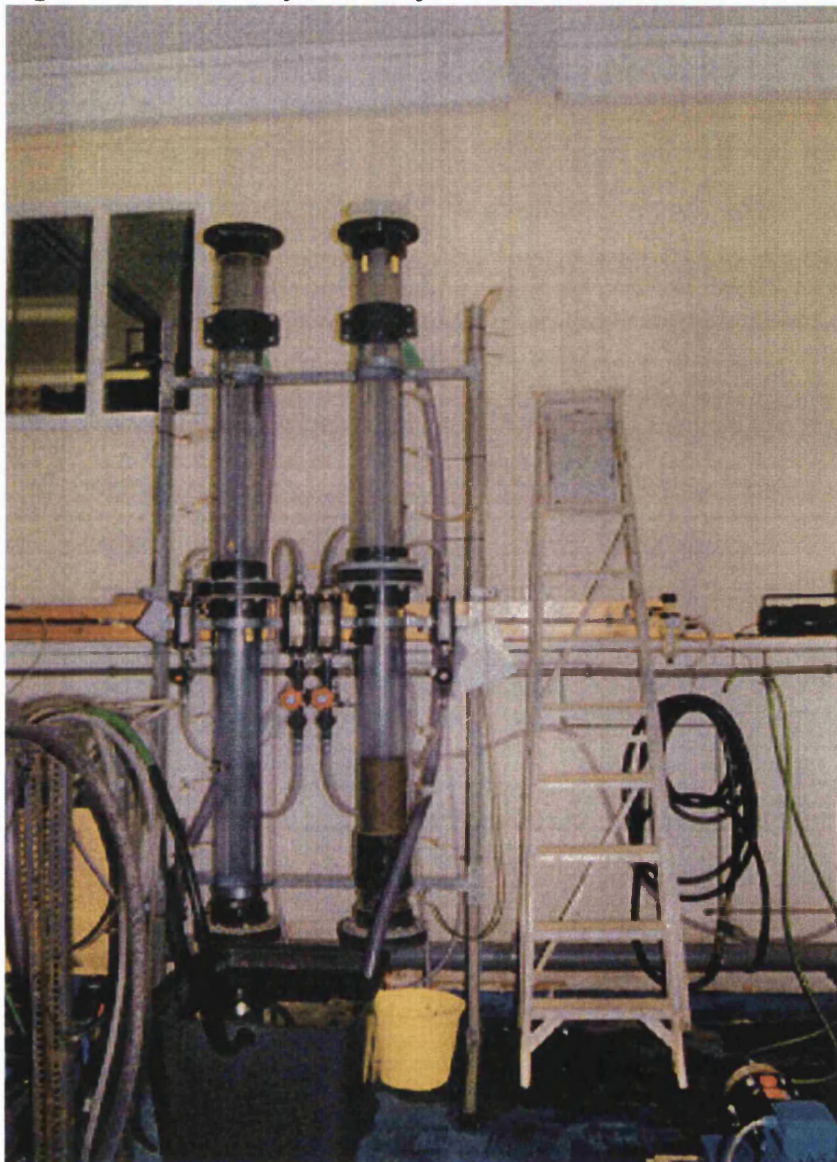
An attrition test was carried out to simulate the wearing away of media during backwashing. An accelerated backwash procedure (Ives, 1990), was carried out involving 100 hours of continuous washing to represent 3 years backwashing at 6 minutes per wash. A combined air and water wash was used as this is the normal backwashing condition employed in BAFs. Water flows of approximately 40 - 60 % V_{mf} were used and collapse-pulsing conditions (Amirtharajah, 1984) were visually determined. The backwash water was passed through a trap before flowing to drain and at the end of the test all media was dried and the percentage loss of weight of the column material was calculated.

4.3.10: Friability

The aim of the friability test is to reproduce the effect of transport and crushing during handling of filter media. The apparatus used was a simple ring shear tester as described by Humby *et al* (1995). An annular sample was subjected to a normal stress load via a shoe which was manually rotated 360° to apply a shear force. The normal load applied was equivalent to the pressure underfoot of an average person, which works out to be a loading on the sample in the ring shear tester of 300kg.

Once the samples had been subjected to the friability and attrition tests they were resieved to determine the percentage of the sample that was now undersize and the new grain size distribution.

Figure 4.1: Laboratory Column for Media Characterisation (15cm diameter)



4.4: Results

4.4.1: Sieve Size Analysis

Sieve analysis data was plotted (Figures 4.23- 4.29) and size ranges calculated as given in Table 4.2.

Table 4.2: Sieve Analysis of all Media Types

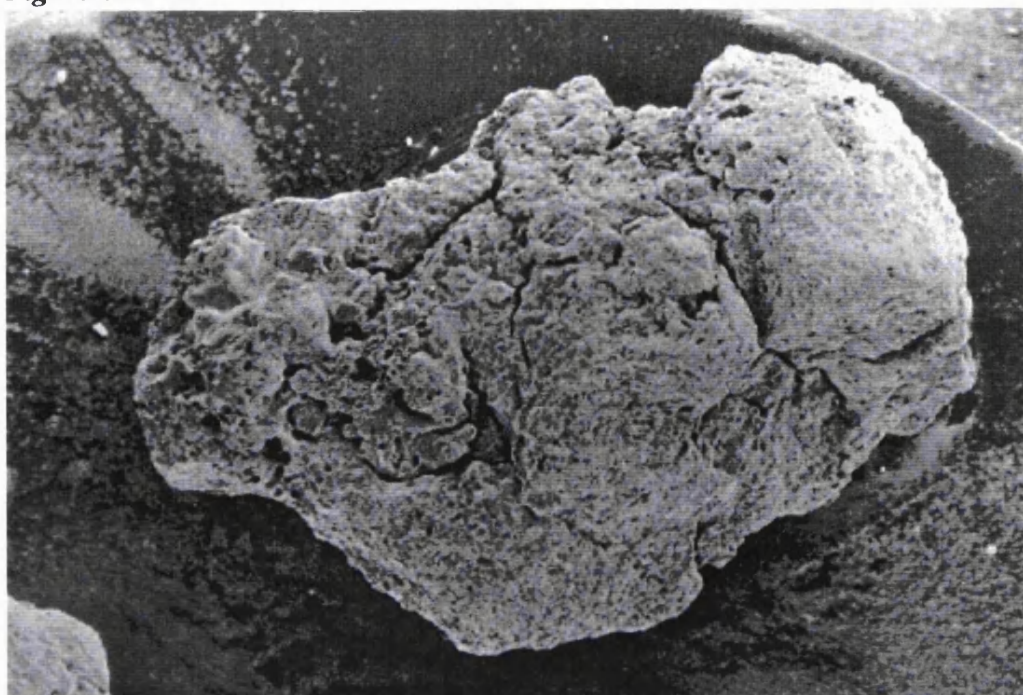
Media Type	Hydraulic Size (mm)	d₅ (mm)	Effective Size d₁₀ (mm)	d₆₀ (mm)	Uniformity Coefficient	d₉₀ (mm)	d₉₅ (mm)
'Starlight'	2.9	2.6	2.8	3.0	1.07	3.3	3.4
Molochite	3.0	1.9	2.1	3.35	1.6	4.2	4.3
EFG	3.4	2.5	2.6	3.8	1.46	4.4	4.7
Lyttag	3.5	2.6	2.9	3.8	1.31	4.2	4.3
Old Expanded Shale	2.9	2.1	2.3	3.0	1.3	3.6	3.9
New Expanded Shale	3.3	2.65	2.85	3.4	1.19	3.9	4.1
Arlita	4.7	3.5	3.7	5.0	1.35	5.8	6.2

The d₅ and d₉₅ show that Molochite and New Expanded Shale are smaller than the suppliers stated size range while the other five media are close to their stated sizes. The graphs of media size distributions also show particle size range after the attrition and friability tests.

4.4.2: Shape and Appearance

Scanning electron micrographs were taken of each of the media types at different magnifications (Figures 4.2 - 4.15). At the lowest magnification the pictures show the size and shape of single particles of the media samples. The Arlita shows the most sphericity followed by Lyttag, 'Starlight' is cylindrical and the other media have irregular shapes. At the higher magnifications we can see the surface characteristics of typical surfaces of each media type as well as the size of pores in the media. All media can be seen to have a rough surface and pores of different sizes so would be expected to be suitable for biomass attachment.

Figure 4.2: EFG



— 0.4 mm

Figure 4.3: 'Starlight'



— 1 mm

Figure 4.4: Molochite

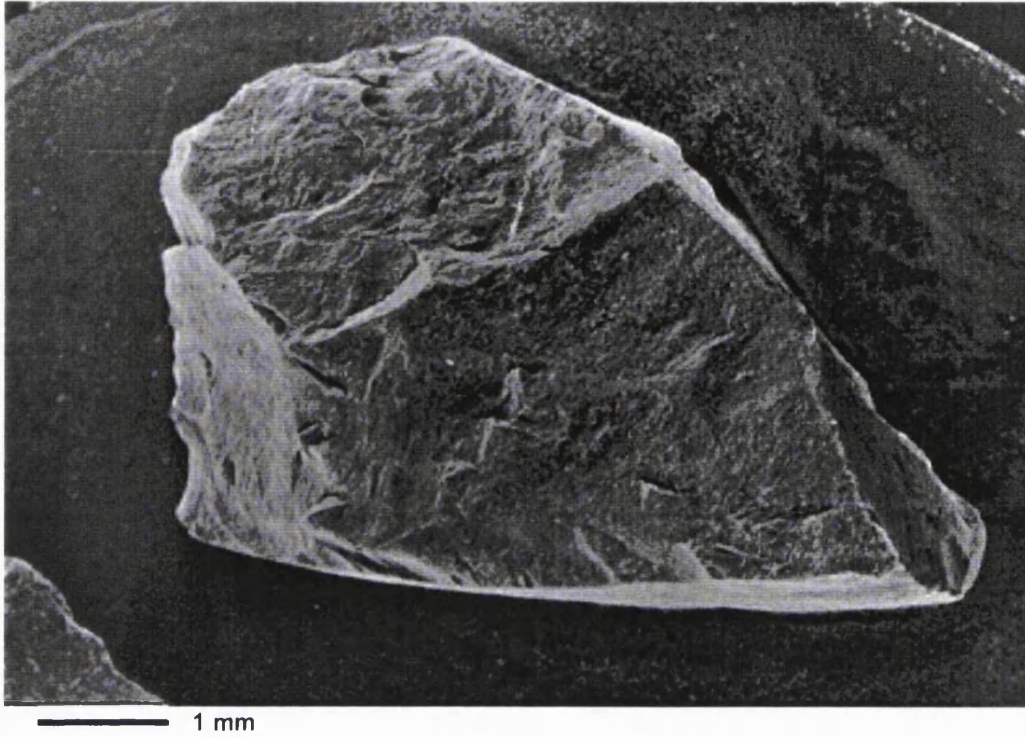


Figure 4.5: Old Expanded Shale

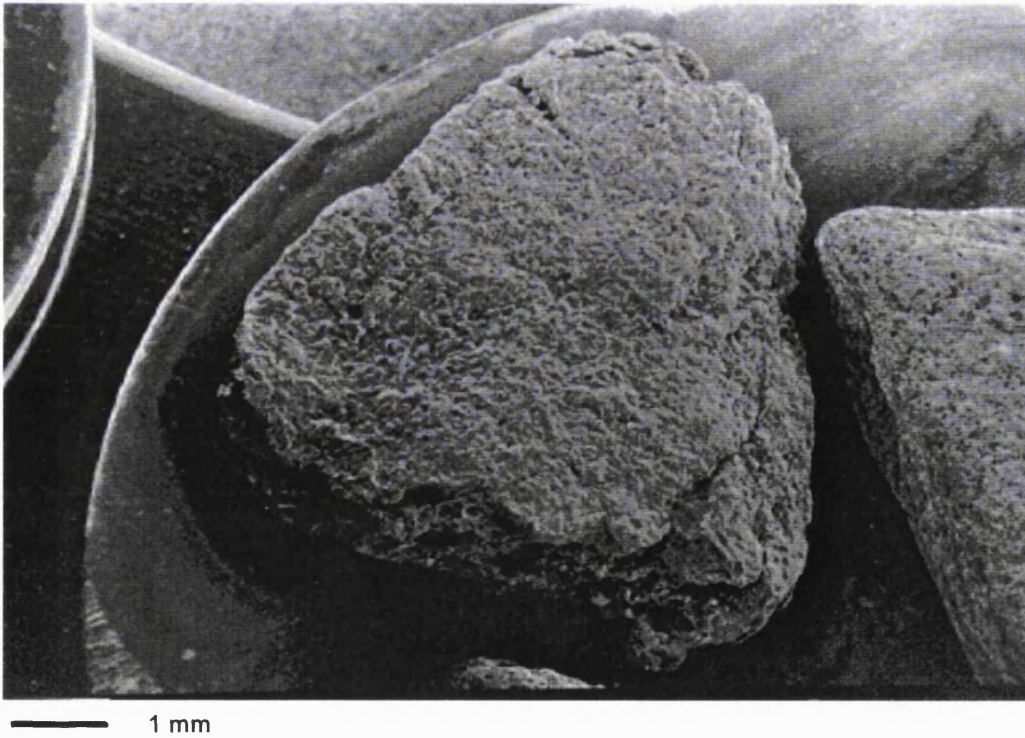


Figure 4.6: New Expanded Shale

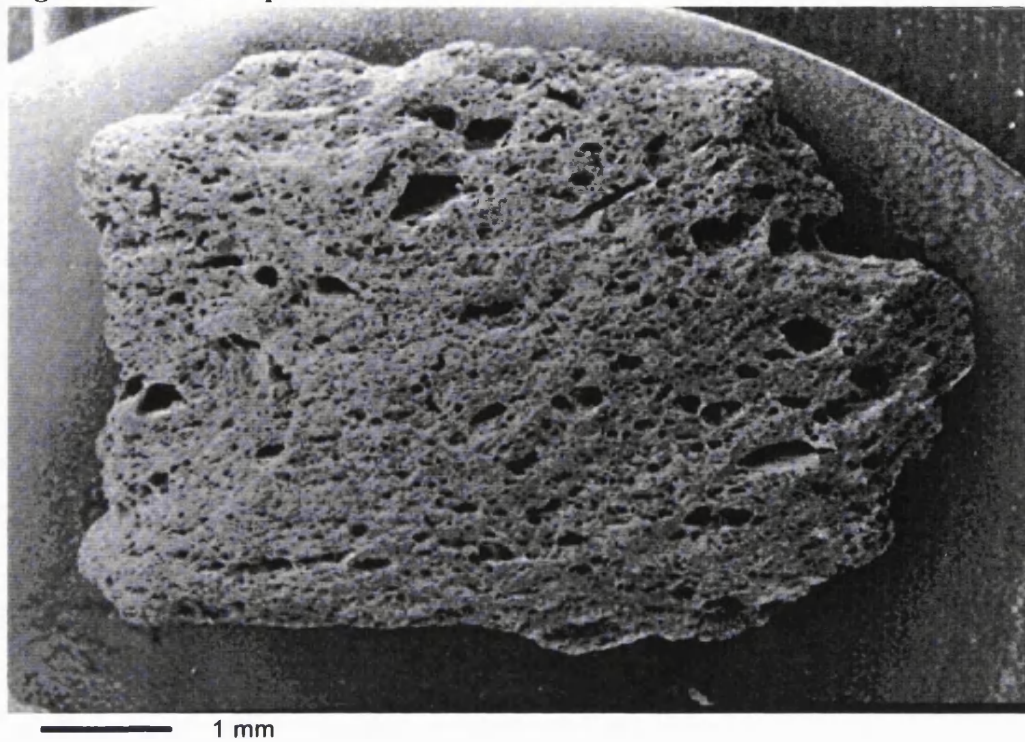


Figure 4.7: Lytag

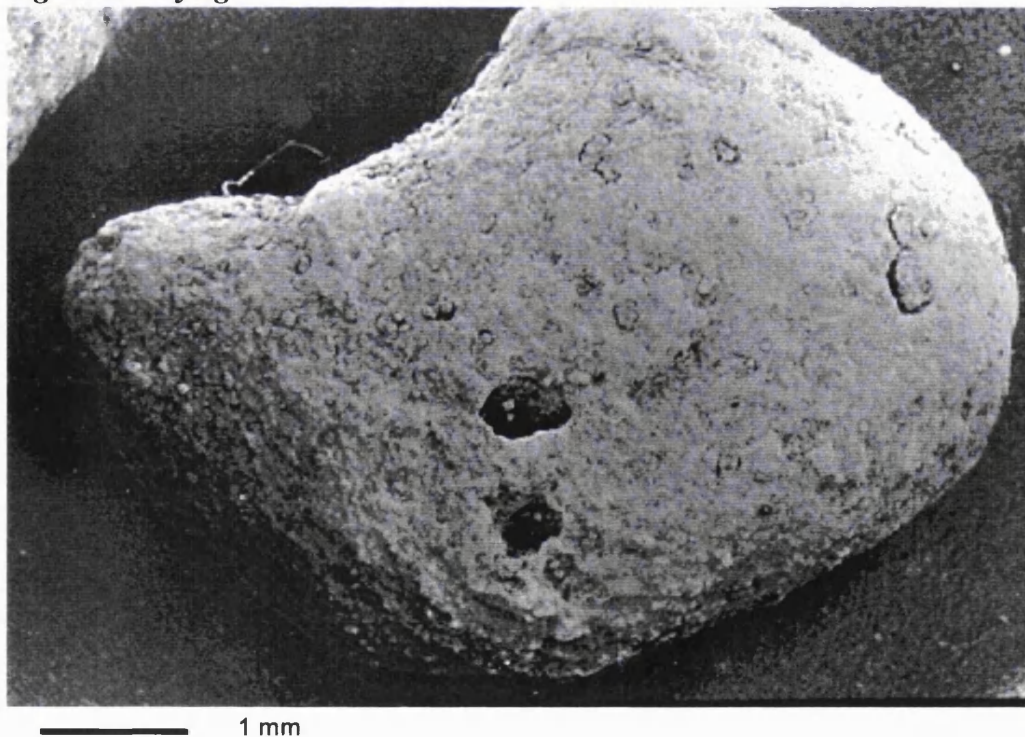


Figure 4.8: Arlita

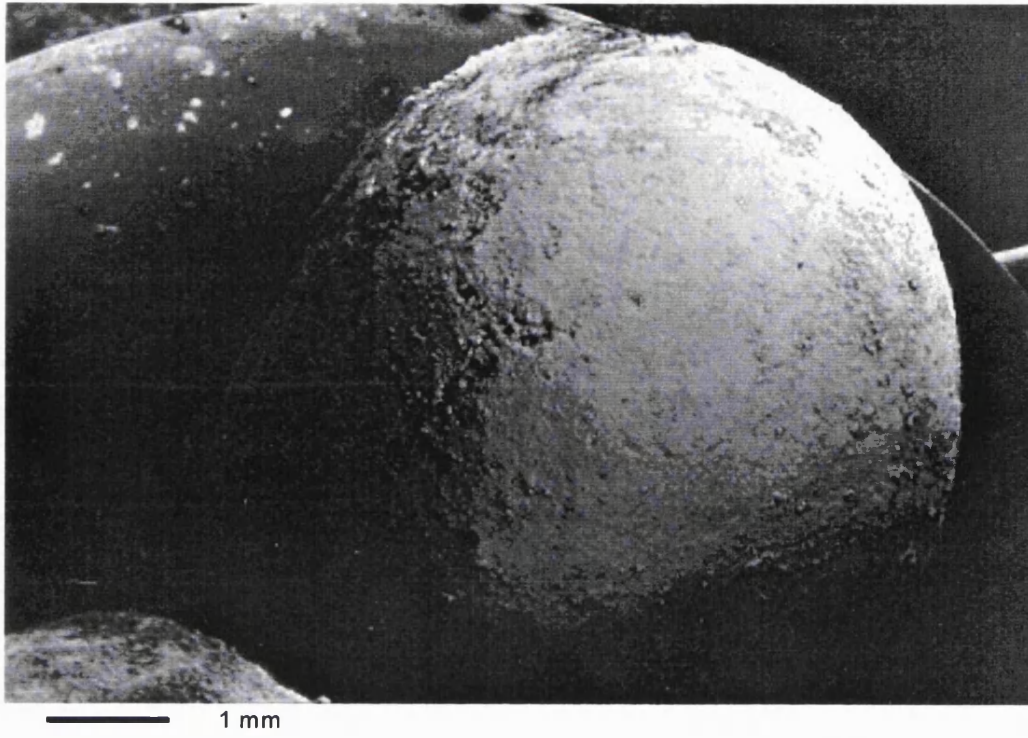


Figure 4.9: EFG

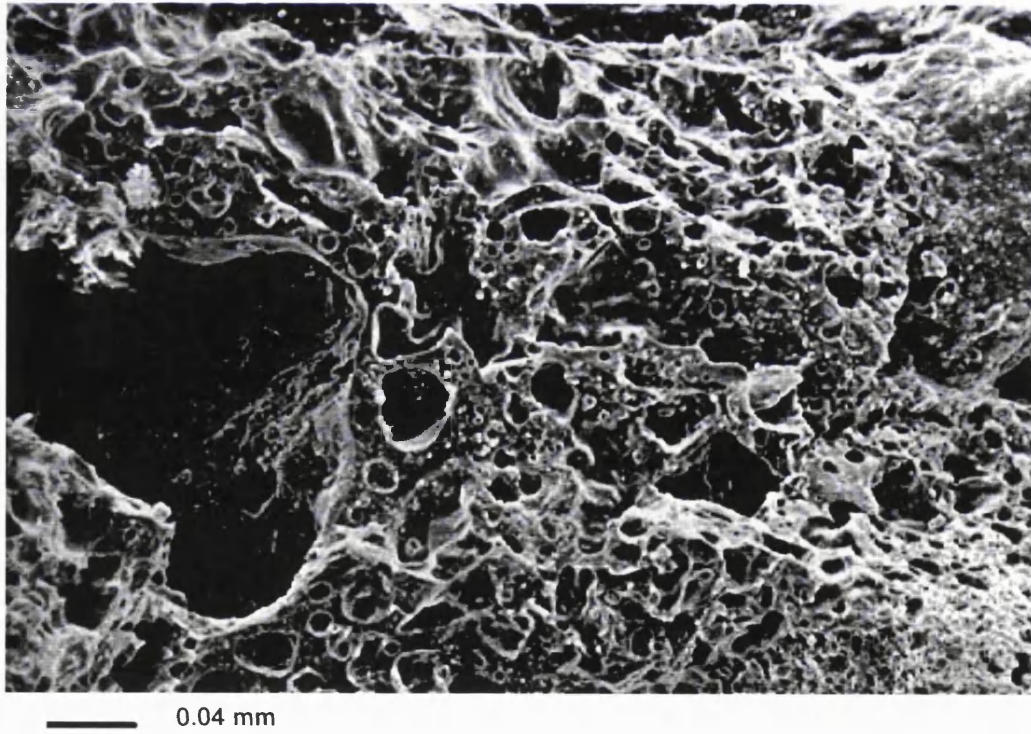
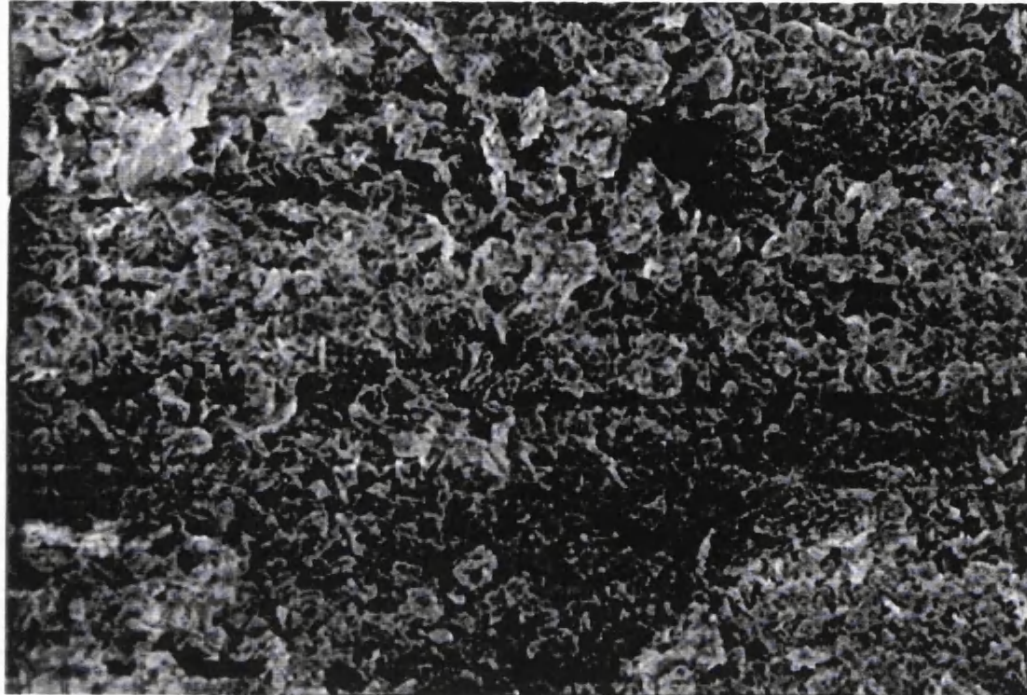
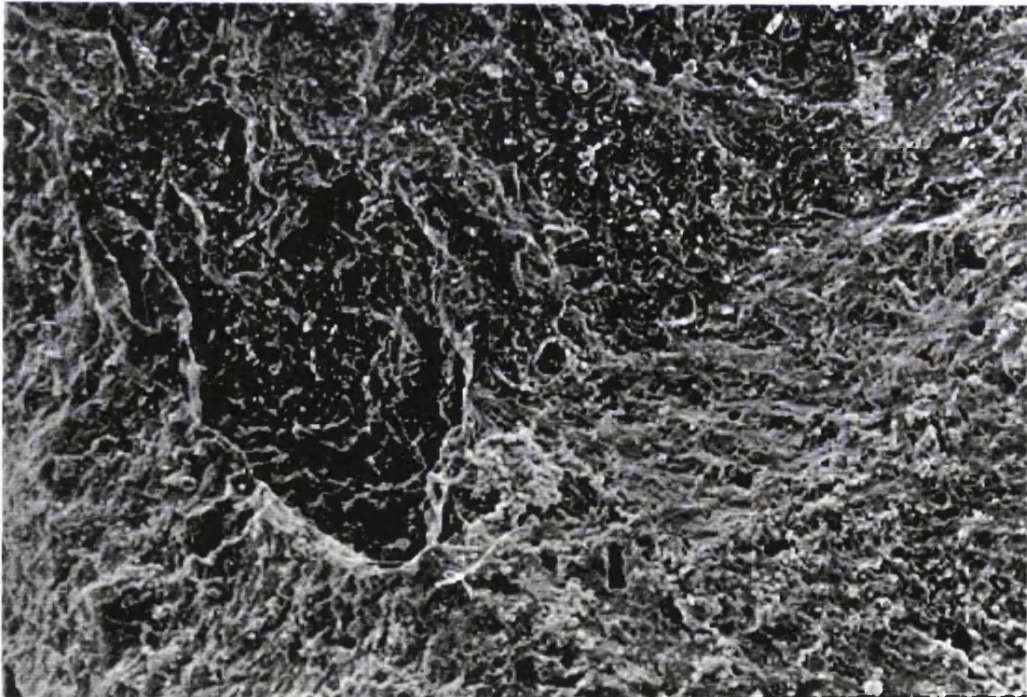


Figure 4.10: 'Starlight'



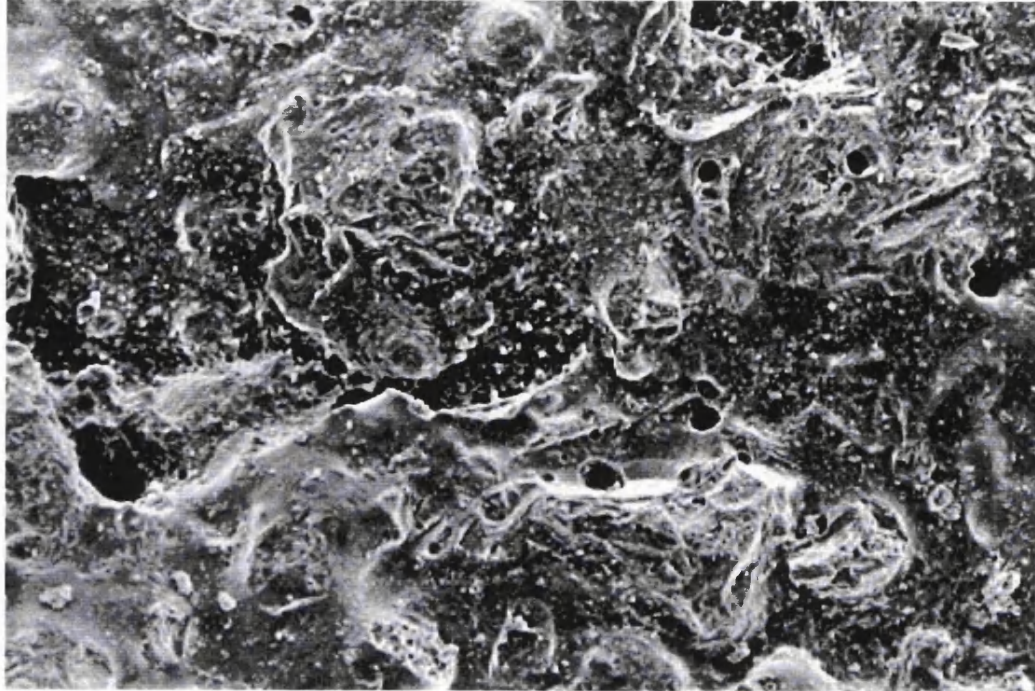
— 0.01 mm

Figure 4.11: Molochite



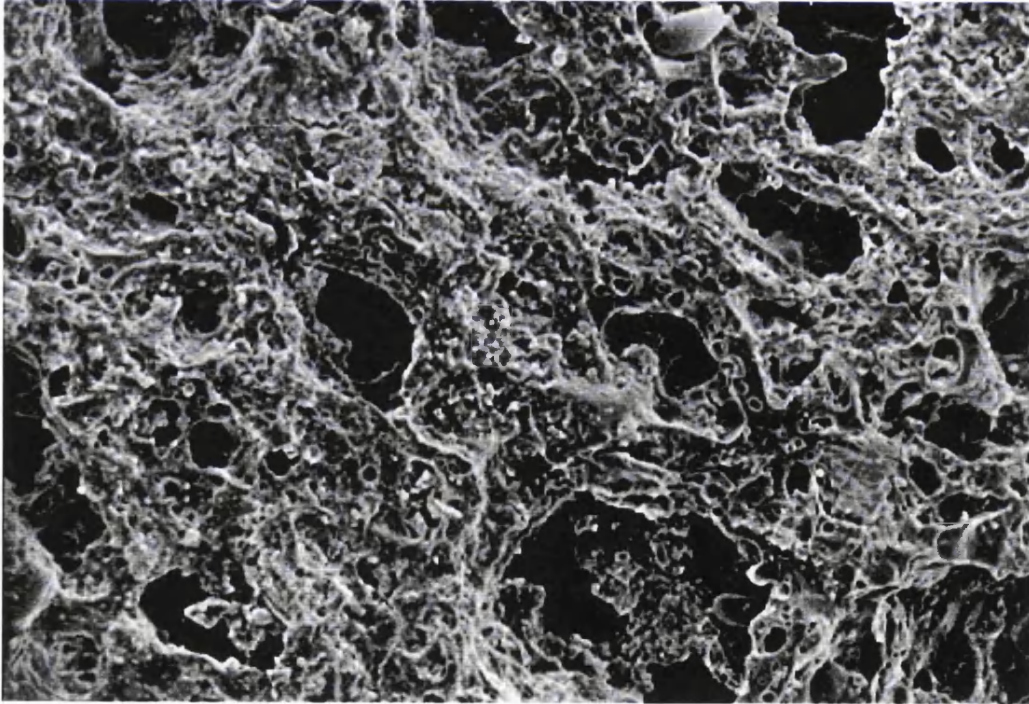
— 0.04 mm

Figure 4.12: Old Expanded Shale



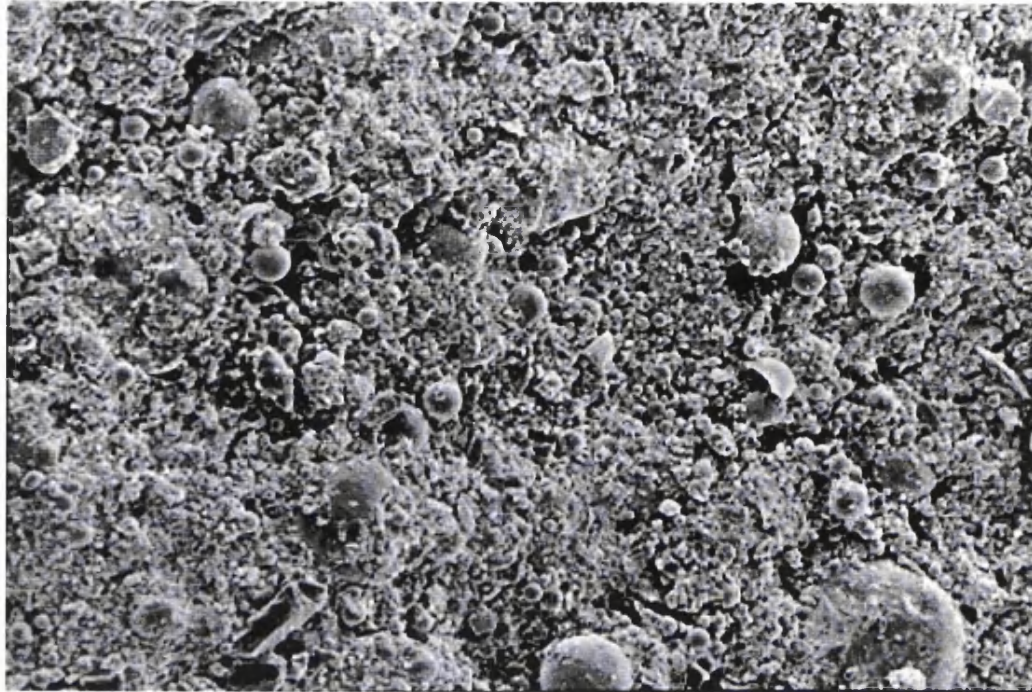
— 0.04 mm

Figure 4.13: New Expanded Shale



— 0.04 mm

Figure 4.14: Lytag



— 0.04 mm

Figure 4.15: Arlita



— 0.04 mm

4.4.3: Specific Surface Area and Porosity

The results from Bradford University for surface area and pore size are given in Table 4.3 along with calculated grain porosity and SSA. The BET surface area is the total surface area including pores and envelope density is the media density using media volume and including pores of $< 9 \mu\text{m}$. The grain SSA is a measure of the surface area of a single grain of media scaled up to allow comparison between different media types.

Table 4.3: Surface Area and Porosity Data

Media	Pore diameter (μm)	BET SA (m^2/g)	Envelope density (g/cm^3)	Grain Porosity (m^3/m^3)	Grain SSA (m^2/m^3)
EFG	44.36	0.81	1.46	0.06	1.18
	2.36			0.15	
	0.01			0.31	
'Starlight'	52.75	4.01	0.54	0.02	2.16
	2.31			0.07	
	0.01			0.81	
Molochite	52.2	0.37	2.43	0.01	0.90
	2.34			0.01	
	0.01			0.06	
Old ES	52.2	0.52	1.59	0.02	0.83
	2.35			0.08	
	0.01			0.33	
New ES	63	0.33	1.42	0.05	0.47
	2.4			0.19	
	0.01			0.42	
Lyttag	54.31	2.47	1.58	0.02	3.89
	2.35			0.07	
	0.01			0.36	
Arlita	54.31	3.11	1.28	0.01	3.98
	2.32			0.05	
	0.01			0.45	

The SSA has been calculated to include all pores down to a size of approximately $0.006\mu\text{m}$. The porosities are given to include the largest pore sizes, pores down to approximately $2.5\mu\text{m}$ and pores down to $0.006\mu\text{m}$. It can be seen that the total porosities increase significantly when the smaller pores sizes are included in the calculation, for example the 'Starlight' has a porosity of $0.02\text{m}^3/\text{m}^3$ for pores of $44.36\mu\text{m}$ and above and this increases to $0.81\text{m}^3/\text{m}^3$ for pores of $0.01\mu\text{m}$ and above.

The Arlita and Lytag have the highest total grain SSA at about $3.9 - 4 \text{ m}^2/\text{m}^3$ and the expanded shales have the lowest values of 0.5 and $0.8 \text{ m}^2/\text{m}^3$. All the media samples

have a high total SSA and some degree of porosity, again suggesting that they are all suitable for biomass attachment.

4.4.4: Acid Solubility

Table 4.4: Dirt Content and Acid Solubility of all Media.

Media	Dirt Content - %	Acid Solubility - %
'Starlight'	3.2	0.15
Molochite	0.4	0
EFG	0.6	0.1
Lyttag	1.2	0.75
Old Expanded Shale	1.0	0.35
New Expanded Shale	1.6	0.8
Arlita	1.8	1.4

The acid solubility is shown along with dirt content in Table 4.4. It can be seen that 'Starlight' has a comparatively high 'dirt' content due to a large proportion of fines but all the other samples have a fairly low dirt content. The BEWA standard stated that fine particulate material should not constitute > 1% of the material by weight. All media samples show a low acid solubility of between 0 and 1.4% (the standard quotes < 5% loss of weight).

4.4.5: Grain Specific Gravity and Bulk Density

Table 4.5: Grain Specific Gravity (GSG) and Bulk Density

Media	GSG (kg/m ³)	Bulk density (kg/m ³)	Fluidisation conditions Water flow rate (m/h) ¹
EFG	1720	661	90
'Starlight'	1340	299	45
'Starlight'	1340	291	100
Molochite	2600	1253	110
Old ES	1900	743	110
New ES	1680	572	100
Lyttag	1940	841	100
Arlita	1550	740	110

1 - From visual observation

From Table 4.5 it can be seen that 'Starlight' has a low bulk density of 291 kg/m³ when fluidised at 100m/h or 299 kg/m³ when fluidised at 45m/h. The highest bulk density is that of Molochite at 1253 kg/m³ when fluidised at 110m/h. The other samples have bulk densities of between 572 and 841 kg/m³.

The grain specific gravity follows the same pattern as bulk density with ‘Starlight’ having the lowest GSG (1.34) and Molochite having the largest (2.6). These results show that the Molochite is very dense and would require high water velocities for fluidisation making it unsuitable as a BAF media. The ‘Starlight’ is very light which would allow the use of low water velocities during backwashing.

4.4.6: Voidage (External Porosity)

Table 4.6: Voidage

Media	Poured Voidage	Packed Voidage
EFG	0.4	0.4
‘Starlight’	0.39	0.38
Molochite	0.4	0.39
Old ES	0.34	0.34
New ES	0.36	0.36
New ES	0.44	0.43
Lyttag	0.31	0.31
Arlita	0.29	0.29

Table 4.6 shows that the voidage values are all between 0.29 and 0.44 with packed voidage being slightly lower than poured voidage. The shales and Molochite appear to have the highest values of voidage with the spherical Arlita and Lytag only having values of 0.29 and 0.31 respectively.

4.4.8: Minimum Fluidisation Velocity (V_{mf})

Figures 4.16 - 4.22 show the average fluidisation of each media sample.

Figure 4.16: Fluidisation of 2-6mm EFG at 8 °C

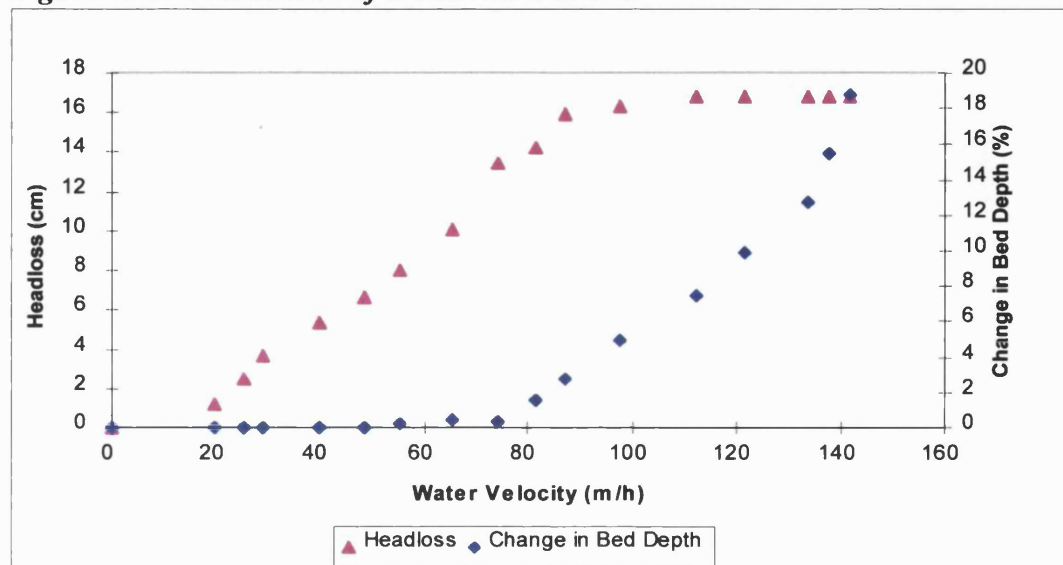


Figure 4.17: Fluidisation of + 2.8mm 'Starlight' at 8 °C

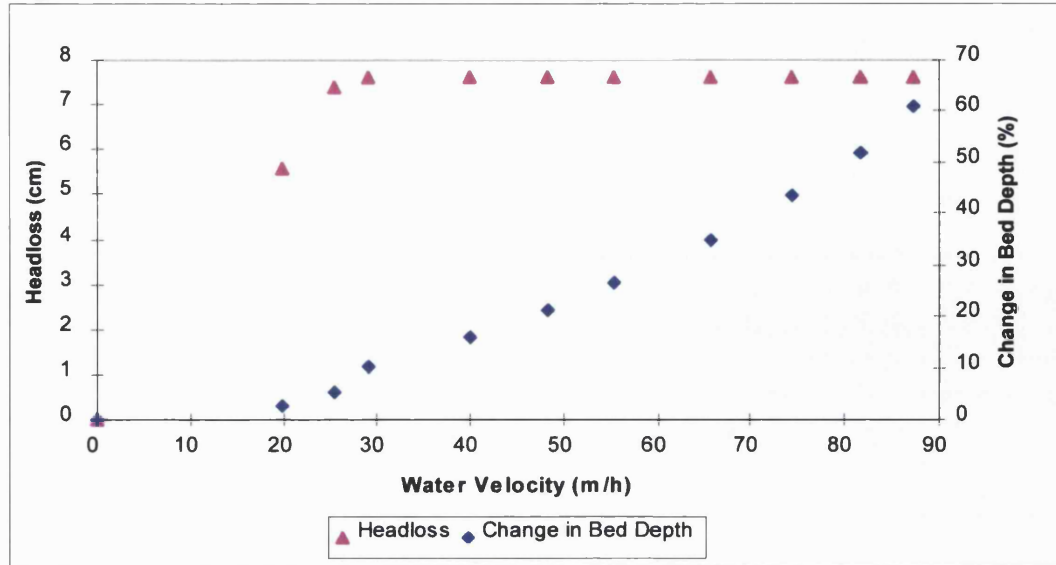


Figure 4.18: Fluidisation of 2-6mm Molochite at 8 °C

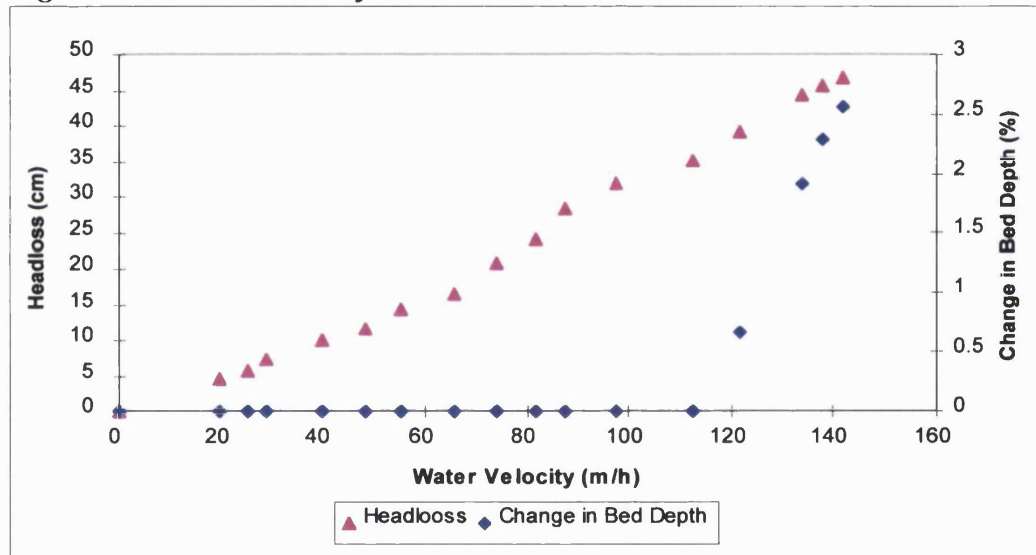


Figure 4.19: Fluidisation of 2.5-4mm Old Expanded Shale at 8 °C

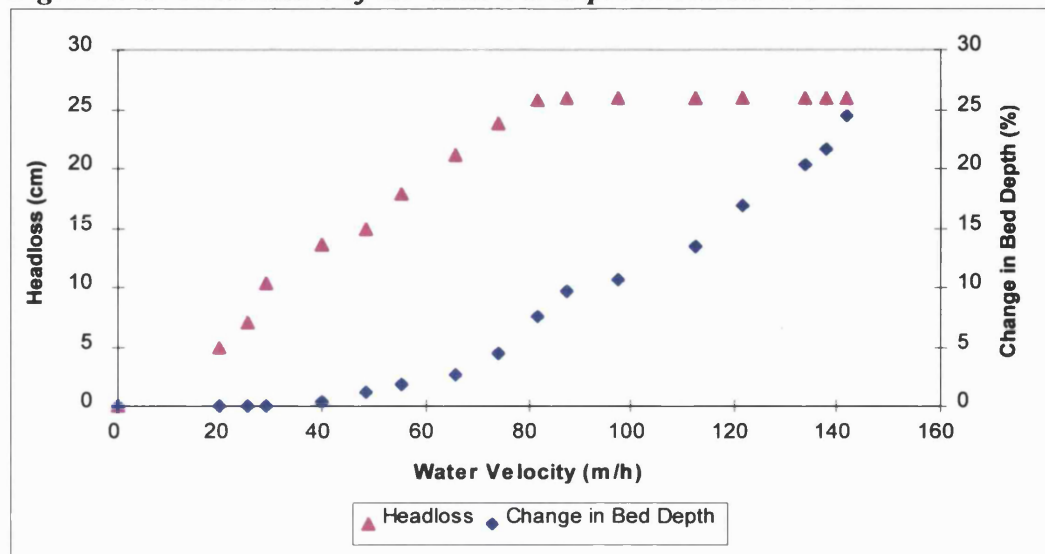


Figure 4.20: Fluidisation of 3-6mm New Expanded Shale at 8 °C

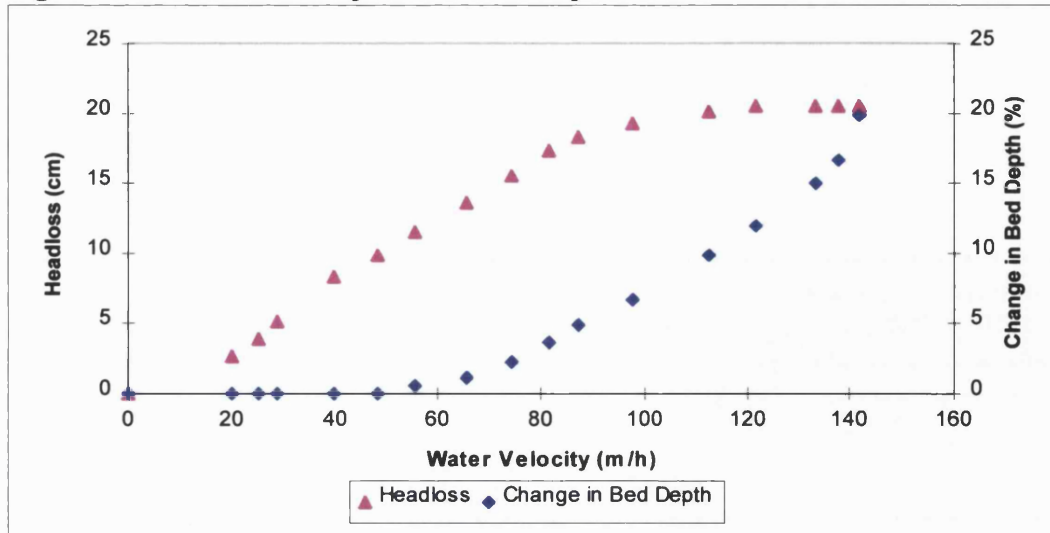


Figure 4.21: Fluidisation of 2.36-4.75mm Lytag at 8 °C

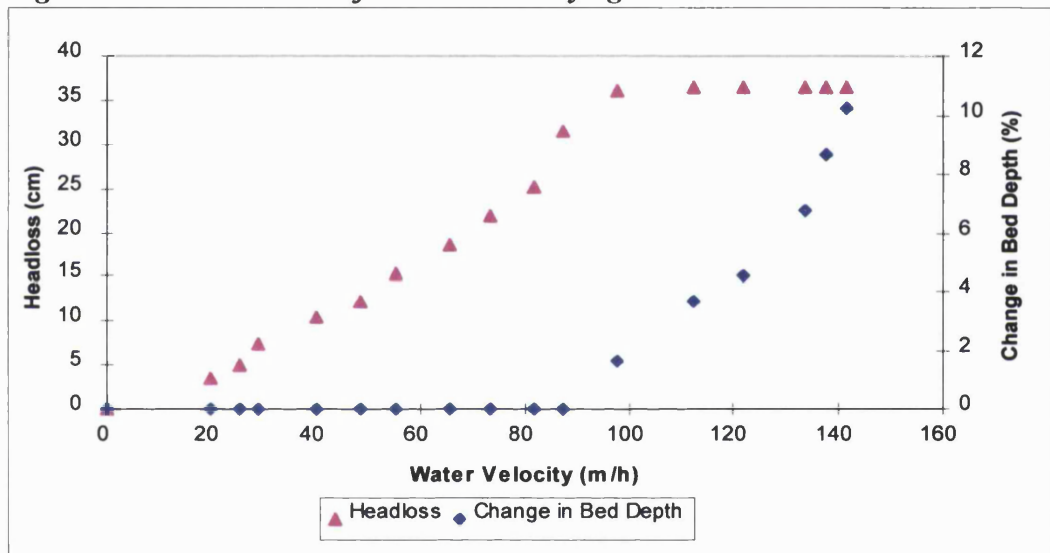


Figure 4.22: Fluidisation of 3-6mm Arlita at 8 °C

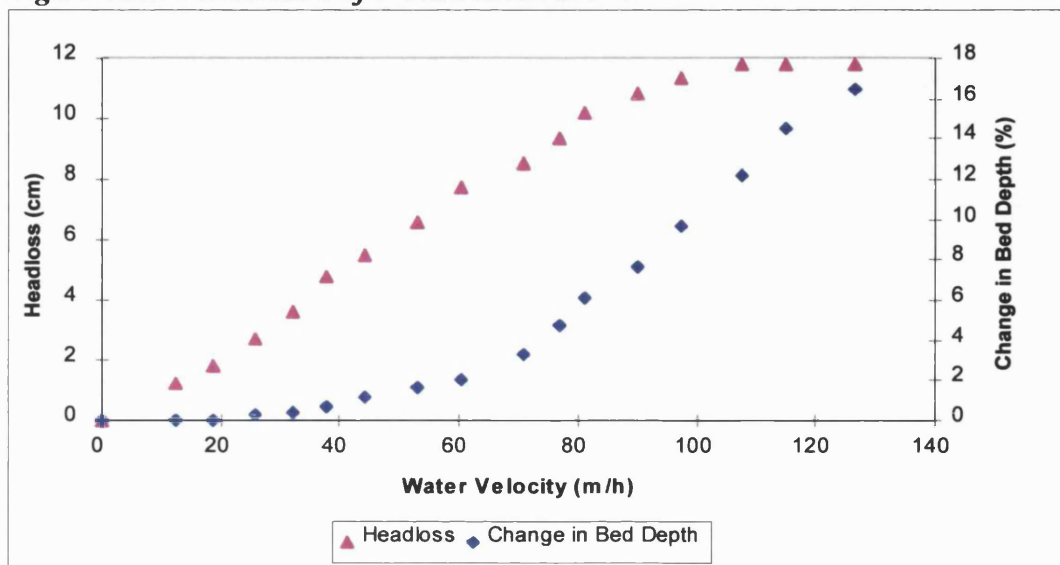


Table 4.7: Experimental and Theoretical Fluidisation Velocities

Media	Temp °C	Experimental V_{mf} at 8°C (m/h)	V_{mf} (Wen & Yu, 1966) (m/h) ¹	V_{mf} (Coulson & Richardson (1991) (m/h) ¹
EFG	8	88	97	131
	15		101	150
	25		106	192
'Starlight'	8	28	42	41
	15		45	47
	25		50	61
Molochite	8	>140	152	225
	15		157	260
	25		163	332
Old ES	8	60-80	93	66
	15		97	76
	25		103	98
New ES	8	64-96	83	79
	15		87	91
	25		93	117
Lyttag	8	92	103	73
	15		107	84
	25		113	108
Arlita	8	70-100	104	61
	15		107	71
	25		112	91

1 - Using experimental voidage

The graphs of V_{mf} show that 'Starlight' has the lowest fluidisation velocity at 28 m/h and Molochite has the highest at > 140 m/h, as predicted by their densities. The other five media types have fluidisation points between 60 and 96 m/h. Both of the shales appear to have no clear fluidisation point with the data for change in bed depth indicating a much lower V_{mf} than the headloss data. This suggests that they are not ideal as BAF media due to problems calculating backwashing rates.

The experimental V_{mf} s are generally lower than the theoretical ones at 8 °C and the effect of temperature on fluidisation can be seen in Table 4.7 for the Wen & Yu equation and Coulson & Richardson's simplification of the Carmen-Kozeny equation (as given in Chapter 2). The experimental voidage has been used in calculating Coulson & Richardson's V_{mf} , if a voidage of 0.4 for the spherical Arlita and Lyttag (i.e. assumed voidage for spherical media) is used the fluidisation velocities are calculated to be very high (208m/h for Lyttag at 15°C, 219m/h for Arlita). This suggests that the assumed voidage of 0.4 is not correct for these two media types.

4.4.9: Attrition and Friability

The water rates used for the attrition test were determined visually by determining the point of collapse-pulsing. Water flow was combined with air flow of 75m/h, the rates used are given in Table 4.8 along with percentage attrition and friability.

Table 4.8: Attrition and Friability Tests

Media	Experimental V_{mf} (m/h)	CP Water Rates (m/h) ¹	Attrition (%)	Friability (% Undersize)
EFG	88	45	6	14
'Starlight'	28	12	45.2	45
Molochite	> 140	80	1.1	3.5
Old ES	60-80	40	2.3	6.5
New ES	64-96	50	2.8	22
Lytag	92	50	5.5	6.5
Arlita	72-80	40	1.4	1.5

1 - Determined visually

From Table 4.8 it is obvious that 'Starlight' is the most friable material in the study and prone to attrition (with 45 % fines production) whilst Arlita is the least prone to attrition and friability (1.4 and 1.5%). Molochite is actually slightly less prone to attrition than Arlita but has a higher percentage friability (3.5%).

Tables 4.9 and 4.10 show the change in size range for each media type after the friability test. Where a high volume of fines have been produced due to friability the d_5 and d_{10} have not been determined, where d_{10} is missing it has also been impossible to calculate the uniformity coefficient. It can be seen that the d_5 , d_{95} and hydraulic size have decreased for all media types while the uniformity coefficient has increased. Again after the attrition test the d_5 and d_{95} have decreased for all media as has the hydraulic size. The uniformity coefficient has increased for 'Starlight' and slightly for New Expanded Shale indicating that the samples have become less uniform and have a greater range of sizes than before attrition/friability, the uniformity coefficient has decreased for all other media.

Table 4.9: Sieve Analysis of all Media Types After Friability Test

Media Type	Hydraulic Size (mm)	d₅ (mm)	Effective Size d₁₀ (mm)	d₆₀ (mm)	Uniformity Coefficient	d₉₀ (mm)	d₉₅ (mm)
'Starlight'	1.0			2.45		2.9	3.1
Molochite	2.4	1.55	1.85	3.1	1.7	4.1	4.2
EFG	2.1		0.7	3.3	4.7	4.1	4.3
Lytag	2.6		1.85	3.5	1.9	4.0	4.2
Old Expanded Shale	2.3	0.7	1.7	3.0	1.8	3.4	3.7
New Expanded Shale	1.7			2.95		3.4	3.6
Arlita	3.6	1.4	3.1	4.7	1.5	5.6	5.8

Table 4.10 : Sieve Analysis of all Media Types After Attrition Test

Media Type	Hydraulic Size (mm)	d₅ (mm)	Effective Size d₁₀ (mm)	d₆₀ (mm)	Uniformity Coefficient	d₉₀ (mm)	d₉₅ (mm)
'Starlight'	2.2	1.5	2.1	2.45	1.17	2.65	2.75
Molochite	3.2	1.7	1.95	3.1	1.59	3.6	3.7
EFG	3.2	2.3	2.5	3.5	1.4	4.1	4.2
Lytag	3.2	2.45	2.65	3.4	1.28	4	4.2
Old Expanded Shale	2.7	2.0	2.25	2.9	1.29	3.4	3.6
New Expanded Shale	3.0	2.45	2.55	3.1	1.22	3.6	3.8
Arlita	4.36	3.3	3.6	4.8	1.33	5.8	6.6

Figure 4.23: Sieve Analysis of EFG (including after attrition and friability tests)

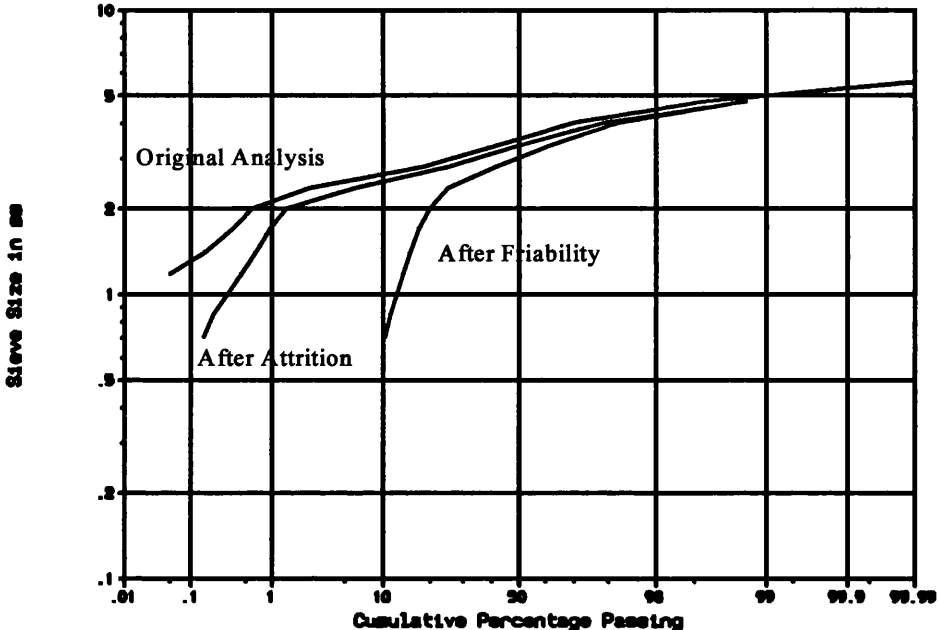


Figure 4.24: Sieve Analysis of 'Starlight' (including after attrition and friability tests)

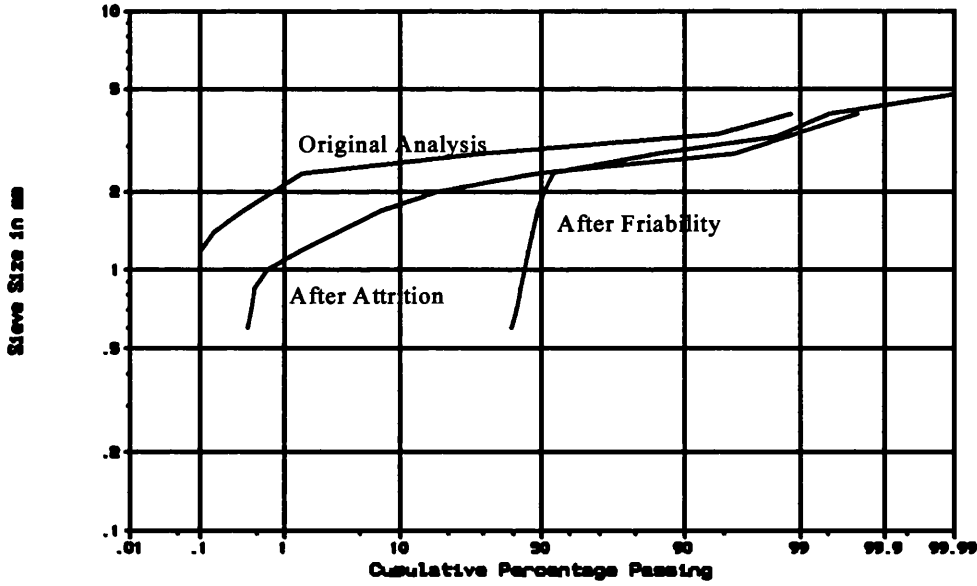


Figure 4.25: Sieve Analysis of Molochite (including after attrition and friability tests)

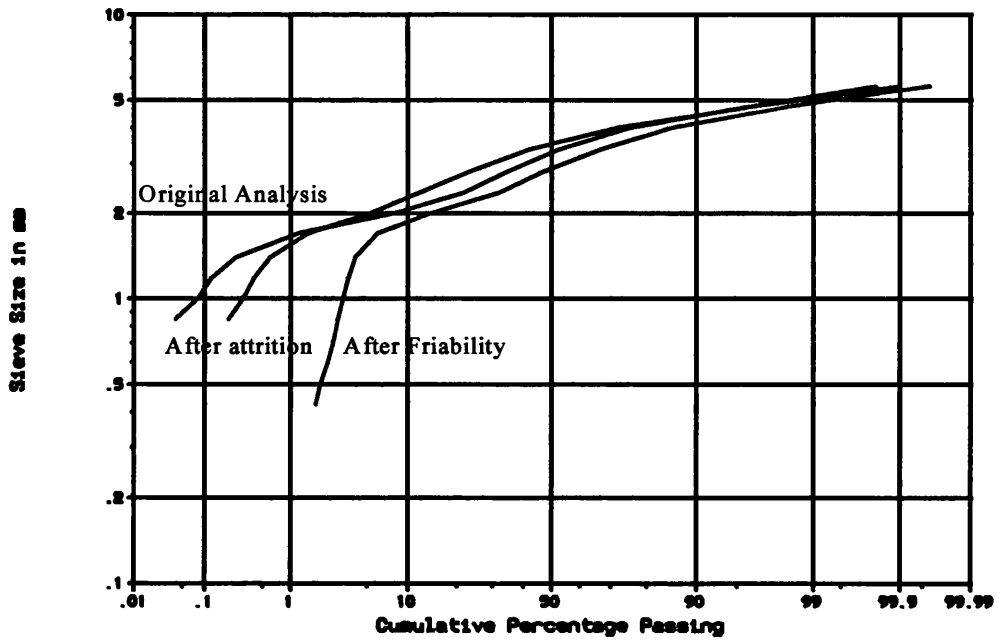


Figure 4.26: Sieve Analysis of Old Expanded Shale (including after attrition and friability tests)

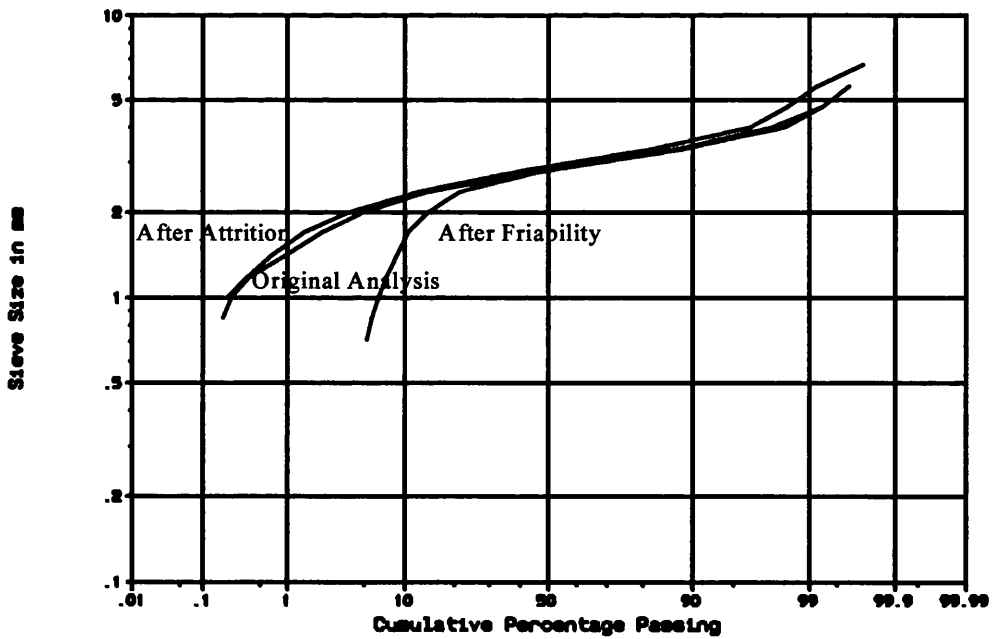


Figure 4.27: Sieve Analysis of New Expanded Shale (including after attrition and friability tests)

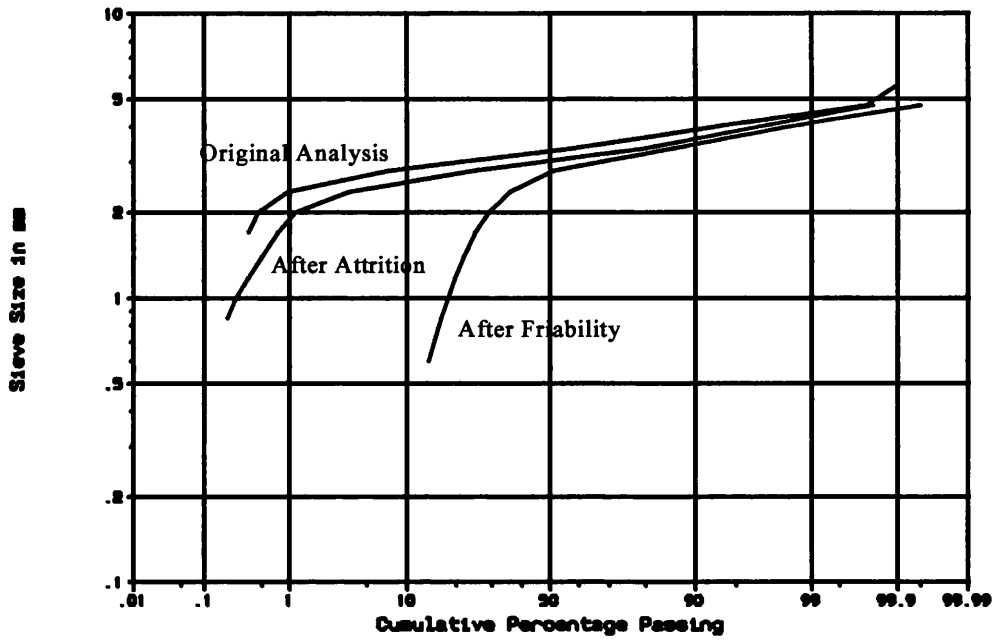


Figure 4.28: Sieve Analysis of Lytag (including after attrition and friability tests)

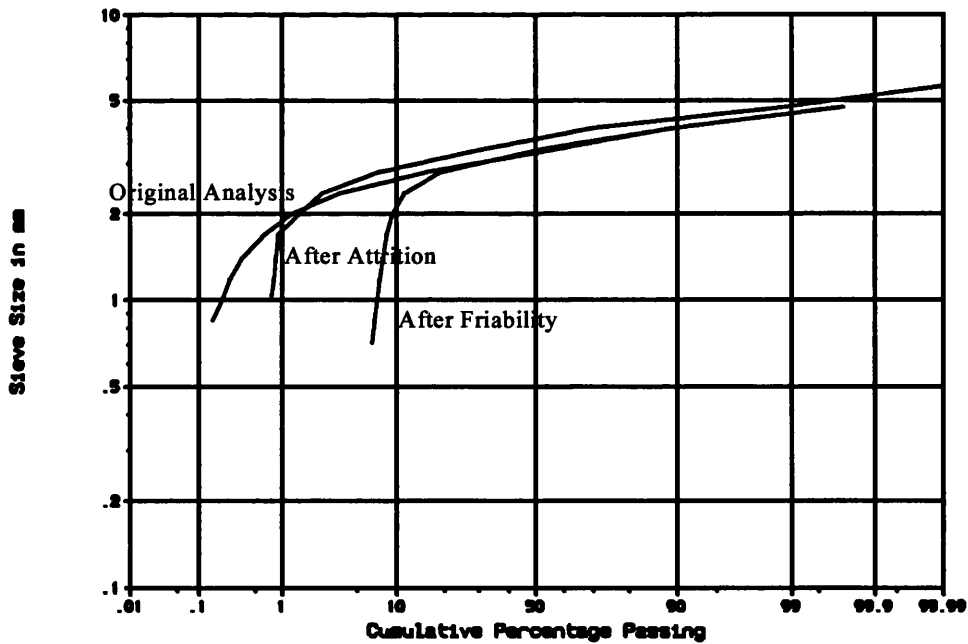
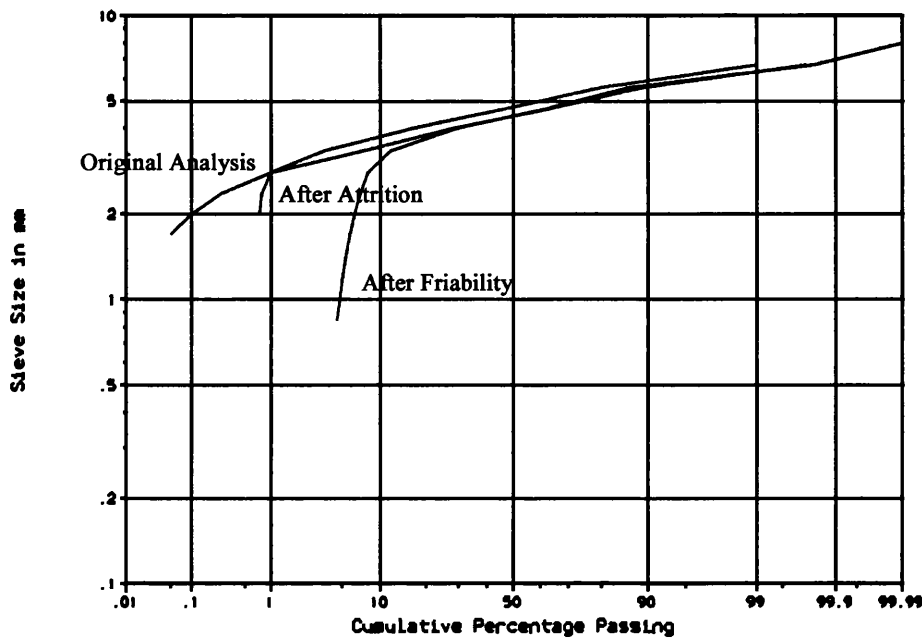


Figure 4.29: Sieve Analysis of Arlita (including after attrition and friability tests)



From the graphs it can be seen that the grain size distribution after the attrition test for Arlita, Lytag, Expanded Shale and Molochite remain close to the original. The ‘Starlight’ has a large degree of fines production (45%) making it unsuitable for use in BAFs. All the samples show high fines production after the friability test.

4.5: Discussion

4.5.1: Media Size

It is important that filter materials are supplied to the correct size range as this information will be used in calculating the backwash rates to be used in the full-scale filters. An increase in grain size of just 10% can lead to a 21% change in backwash rates (Stevenson, 1994). If we look at the original sieve size analyses of all media types in the study we can see that the samples have comparable size ranges. The range of media particle size is given by the d_5 and d_{95} and this should correspond to the suppliers stated range. From Table 4.2 it can be seen that each media sample does correspond fairly accurately with the suppliers stated size range, except for the New Expanded Shale which has a d_{95} (i.e. upper size of range) of 4.1mm but is described as being 3-6mm in diameter and the Molochite which has $d_{95} = 4.3$ compared to a stated size range of 2-6mm. This could be due to the particle shape of these two media types,

both are plate-like with different length and width sizes therefore when orientated lengthways they can pass through smaller sieve aperture sizes.

The uniformity coefficient (UC) shows the measure of spread of particle sizes and accounts for a range of 50% by weight. Media samples with all the same particle sizes would have a UC of 1.0. These ideal media samples would theoretically have identical particles which all fluidise at the same water wash rate during backwashing (if weight/density were the same for all particles). In practise even particles of the same size are likely to differ slightly in density. The data shows that the experimental 'Starlight' has the least spread of particle sizes (1.07). This is due to the manufacturing process which can control parameters such as size. The sample with the highest UC is Molochite which is also specifically manufactured so this value could possibly be improved upon during production. Lytag, Old Expanded Shale and Arlita all have UCs of approximately 1.3, this means that they have a fairly low spread of particle sizes and therefore fluidisation of all particles should occur at a reasonably well defined point, allowing backwash rates to be calculated accurately.

Another method of determining the media sample size is the hydraulic size, this is the grain size that would produce the same resistance to flow as the sample material under consideration (BEWA) or the size that gives the same surface area as this material and therefore the same hydraulic behaviour (Stevenson, 1994). The hydraulic size of the seven media types range from 2.9-4.7mm - from this value alone the backwash behaviour of the media cannot be determined.

4.5.2: Chemical Inertness

The acid solubility test has been carried out to determine whether all the media are chemically inert with reference to water. Before the acid solubility test was carried out a test for dirt content was performed. This showed a low dirt content for all of the media except 'Starlight' which had a high proportion of fines present. This could lead to problems with clogging of filter nozzles but should be acceptable if all fines are removed during the initial filter backwash. From the table it can be seen that all the media have a weight loss of less than 5% after being placed in the acid. This is the

acceptable level given by the BEWA standard. Therefore we can assume that all the media studied are chemically inert.

4.5.3: Biofilm Attachment

Biomass attachment is a very important consideration in terms of choosing BAF media. It is mainly affected by specific surface area and surface characteristics of the media. A number of scanning electron micrographs have been included in the study to show the shape and surface structure of the samples.

At a higher magnification we can see the surface characteristics of typical surface areas of each media type, this is important for biomass attachment. The molochite appears to be smooth at a low magnification but at higher magnifications it can be seen that the surface is actually rough with small pores. The EFG appears to be very porous at all the magnifications shown indicating the presence of large pores (4 - 36 μm from Figures 4.2 and 4.9). At a high magnification we can also see that the media surface is very rough. The Old Expanded Shale and Arlita show similar patterns with pores of 4 - 21 μm and 20 - 37 μm respectively. The New Expanded Shale has larger pores than the other shale sample (5 to 60 μm , Figures 4.6 and 4.13). Lytag does not appear to be porous but consists of a large proportion of spherical protrusions of 1.5 - 20 μm in diameter. These six media samples should be suitable for biofilm attachment, maybe less suitable is the 'Starlight' which looks very smooth at all magnifications and has no large pores visible. Unfortunately there were problems with charging of the 'Starlight' media during SEM analysis which is shown by bright areas within the image, this occurs due to the non-conductive nature of the specimen causing high voltage concentrations at specific points.

The specific surface area and porosity is given in Table 4.3. It can be seen that the total grain SSAs are very high (4.7 m^2/m^3 for New Expanded Shale - 3.98 m^2/m^3 for Arlita). The reason for these high values is that the method used to work out surface areas (mercury porosimetry) has accounted for all the possible pore sizes i.e.: down to 0.006 μm . In reality a high proportion of these pore sizes will not be utilised by bacteria due to problems with oxygen transfer and therefore are not important in this

instance. This means the 'useful' or 'available' specific surface area will be a lot smaller than that shown in the table.

The values for grain porosity have taken into account the pore size distribution and therefore porosity data differs according to the scale being looked at. The smallest 'useful' pore size used in the calculations is approximately 2.5 μm as at pore sizes below this point there is not enough space for bacterial reproduction or division by fission (Messing, 1988). When smaller sizes than this are included in the calculations, the grain porosity can be seen to be higher. If for instance we look at Lytag, taking the smallest pore size to be 54 μm we would have a porosity of 0.02 m^3/m^3 of media, at 2.5 μm we would have a porosity of 0.07 m^3/m^3 and at 0.01 μm we would have a porosity of 0.36 m^3/m^3 . Looking at Table 4.3 we can see that Molochite has the lowest overall porosity considering pores of 2.5 μm and above and has a relatively low SSA, the 'Starlight' has the highest overall porosity if we include all pore sizes (i.e. pores of 0.0061 μm and above), but it has the third lowest porosity if we only include pores of 2.5 μm and above. Therefore it must be remembered that the porosity and SSA data need to be interpreted carefully in relation to the pore sizes found.

There is some argument as to the importance of porosity in terms of oxygen transfer as beyond a certain pore size there will be no extra oxygen transfer to the biofilm. It could be that a rough surface is sufficient for encouraging biomass attachment and growth, therefore all samples in this study are probably suitable for biomass growth. The presence of pores is important in that the bacteria which initially colonise the media will be protected within any pores from shear stresses and environmental changes, decreasing biomass losses due to shear as found by Anderson *et al* (1994) in upflow anaerobic filters.

4.5.4: Fluidisation Behaviour

A number of physical characteristics of filter media can affect their fluidisation behaviour, these include size range (Section 4.5.1), shape, density and voidage. Looking back at the scanning electron micrographs (Figures 4.2 - 4.8) it can be seen that both Lytag and Arlita are fairly spherical, 'Starlight' is cylindrical and the other samples are irregularly shaped. There is some debate as to whether media grains

should be spherical and if this is beneficial to filtration (Ives, 1990). It is known that sphericity will affect the fluidisation behaviour of media, with spherical particles having less drag forces acting upon them than irregular shaped particles. This allows spherical particles to settle quicker therefore higher water rates are needed to combat this and allow particles to fluidise. The surface roughness of a particle may also affect fluidisation behaviour with a rough surface producing more drag than a smooth surface.

Density of granular material does not directly affect its performance as filter media (Ives, 1990), but is vital information relative to backwashing and fluidisation behaviour. There may be errors in the determination of bulk density and grain specific gravity in this study due to the porous nature of the media leading to air retention within the pores during characterisation.

Table 4.5 shows density values of all the media samples, these values correspond fairly accurately with available suppliers data (Molochite supplied as 2700 kg/m³ compared to 2600, Lytag 1950 compared to 1940 and Arlita 1350 compared to 1550). The high density of Molochite indicates that it would require high water rates for effective backwashing to prevent filter clogging and therefore would be expensive to maintain in a suitable condition. Although it might seem appropriate to choose 'Starlight' for use because of its low density and related low backwash rates there could be different problems due to loss of media across the overflow weir. This would again increase costs due to continuous topping up of the media although a shorter period of simultaneous air and water applied while the water level rises within the filter chamber can be used to combat this problem (Stevenson, 1994). Another alternative would be to use a launder system to catch the media before it flows out of the overflow pipe. All the other media types would be expected to have V_{mf} s in between those of Molochite and 'Starlight' corresponding to their densities.

The voidage is a ratio of the volume of space between grains to the overall volume of granular material and is dependent on the shape of media grains. It is again important in fluidisation as a 1% change in voidage may lead to a 9.5% change in the backwash threshold (Stevenson, 1994). A low voidage should therefore indicate a low

fluidisation value. The voidage differs with circumstances, for instance the poured voidage is different from the packed voidage. From Table 4.6 we can see the voidage values are all between 0.29 and 0.43 (the typical value for spherical media is given as 0.4). Again the porous nature of the material may have led to errors in determining voidage - the material was soaked overnight to fill the pores with water but due to the large samples used it was difficult to remove all the excess water from between media grains.

The experimental V_{mf} of each sample was recorded for a stated temperature as given in Table 4.7. All measurements were repeated a number of times with each repeat producing the same pattern of headloss and bed depth change. The actual measurement altered due to the difference caused by previous wash conditions as discussed in relation to media density.

Molochite can be seen to have a very high V_{mf} as expected from its density. Considering the change in bed depth there should be a V_{mf} of 116 m/h but at this point the headloss has not levelled off to a constant value, therefore the V_{mf} is estimated to be more than 140 m/h (the limits of the apparatus used). Molochite does have a large value of UC at 1.6 indicating a large range of particle sizes and an associated weight difference between the smallest and largest sized particles. Molochite would be expected to be a poor BAF media due to both the high backwash rates needed and the lack of a specific fluidisation point. 'Starlight' on the other hand can be seen to change with respect to both headloss and bed depth at 24 - 28 m/h, this is low as expected from the density. The fluidisation points of EFG and Lytag are easy to pinpoint at approximately 88 and 92 m/h respectively. These values are fairly similar despite the difference in density, indicating that some other parameter (such as voidage, surface roughness or shape) must have an important contribution to the V_{mf} of these samples.

The Old ES has a similar density (GSG) to Lytag and a similar voidage but appears to have a much lower V_{mf} (60-80 m/h). This is probably due to it being slightly smaller with a particle range of 2.1-3.9mm compared to 2.6-4.3mm. There are problems in interpretation for both shale samples as the change in bed depth shows a low V_{mf} but headloss data shows a high V_{mf} . This could be due to low density particles fluidising

first leading to stratification of the sample. Both the shales have a reasonably low UC therefore we can assume that the problem is caused by a difference in particle densities rather than large differences in particle size. In practise if high flows were applied there could be considerable media loss but low flows would not clean the media sufficiently. Again the New ES has a lower density than Old ES but shows similar or even higher V_{mf} , corresponding to its larger media size range of 2.65-4.1mm. Finally the Arlita has a low density and voidage which is reflected in its V_{mf} of 72-80 m/h, despite being the largest media with a size range of 3.5-6.2mm.

There may be errors in the experimental values of V_{mf} due to the diameter of the column used (150mm). Theory predicts (BEWA) that wall effects are minimised if the column diameter is at least fifty times the hydraulic size of the media being tested. In this study three of the media have hydraulic sizes less than 3mm but the other four are larger than this with Arlita being the largest at 4.7mm (ie: the column diameter is only 30 times the hydraulic size). The work of Lang *et al* (1993) suggests that column diameter should be 50 times the effective size of the media which indicates only the Arlita sample would be affected by wall effects.

The experimental values of V_{mf} are compared to theoretical values in Table 4.7. The experimental values for a temperature of 8°C are significantly lower than the theoretical values given by Wen & Yu (1966), except for the New Expanded Shale sample, this could be due to the lack of sphericity or voidage terms (Stevenson, 1994).

The Carman-Kozeny equation does incorporate voidage and corresponds more closely to the experimental data for Old ES and Arlita (at 8°C) but is still inaccurate for the other media. It uses the hydraulic size of media instead of d_{90} which is used in the Wen & Yu equation. We can see that the voidage term is important by looking at a voidage of 0.4 for Arlita (i.e. voidage expected for spherical media), this gives us a V_{mf} of 190 m/h at 8°C which is nearly 3 x that with a voidage of 0.29 and 2 x that of the experimental V_{mf} . It should be remembered that there are possibly errors in the experimental voidage value which may affect the results from the Carman-Kozeny equation but the value of V_{mf} from Coulson & Richardson may indicate that 0.29 is the

correct voidage for Arlita rather than the assumed voidage of 0.4 for spherical materials.

The theoretical values from both equations show us how V_{mf} can change with temperature. It can be seen that an increase in temperature leads to an increase in fluidisation velocity in all cases. This is due to a decrease in the viscosity and density of the water leading to increased Galileo's number and Reynolds' number and a subsequent high V_{mf} . 'Starlight' has a theoretical value of 42 m/h using Wen & Yu and 41 m/h using Coulson & Richardson (at 8°C). If we look at 15°C this increases to 45 m/h and 47 m/h respectively and at 25°C the difference between temperatures and equations has increased significantly to 50 and 60 m/h. This indicates that we could use lower backwash rates in colder weather leading to savings in backwashing costs.

As discussed in Chapter 2, collapse pulsing is thought to be the most effective method of filter backwashing (Amirtharajah, 1984). The experimental minimum fluidisation velocities were used to calculate the range of water velocity levels that could be used in combination with air for backwashing (Table 4.8). It should be remembered though that media coated with biofilm may have fluidisation levels that are 10-15% lower than clean media, (Addicks, 1990) due to a decrease in the net density of particles. The V_{mf} for different sizes of the same media will also be different due to larger particles being denser overall than small particles.

4.5.5: Attrition

As stated the backwash air and water flows were calculated and used in an extended attrition test to determine the durability of media during normal use and backwashing. From Table 4.10 it is obvious that 'Starlight' is prone to being broken down by attrition once in place in the filter. The Molochite and Arlita proved to be most resistant to attrition with 1.1% and 1.5% loss of media respectively. These values and those of the shales are within the doubtful category of 1-3% recommended for an extended attrition test (Ives, 1990) and all other media had weight losses of more than 5% which is termed unsatisfactory. The BEWA standard actually considers weight loss of more than 3% and a change in hydraulic size to be unsatisfactory. This implies that either the standard cannot be applied to BAF media in regard to attrition or the high flow rates necessary to produce collapse-pulsing in these media are too extreme,

therefore collapse-pulsing may not be appropriate for use in backwashing of BAFs. During actual filter use the period of collapse-pulsing could only last for 2-3 minutes therefore there may be less attrition over three years than suggested by the test which simulates 6 minutes collapse-pulsing.

After the attrition test the hydraulic size of all samples decreased and in most cases the UC has decreased slightly due to loss of smaller particles over the weir and a decrease in size of the larger particles (as seen in a change in d_{95}). The New Expanded Shale and 'Starlight' UC increased slightly due to fine production and an associated decrease in the uniformity of media particle sizes. Humby & Fitzpatrick (1996) found that the highest attrition occurs in the period following placement of new media in the filter therefore any further filter use should not lead to a large increase in attrition and fines production.

4.5.6: Friability

A friability test was also carried out to determine media wear during normal handling and placement. The media most resistant to wear were Molochite, Arlita, Lytag and Old Expanded Shale but they still had a small percentage of fine production. Looking at sieve data the hydraulic size has decreased and uniformity coefficient for all media types increased as a result of the friability test. The UCs of Molochite and Arlita only changed slightly corresponding to their low friability. It is possible to attribute friability to rounding of the grains (abrasion) or grain breakage (Humby, 1994). The low friability of the spherical Arlita is probably due to a lack of angular corners and large cracks on its surface. This means that any attrition is due to abrasion and this is also the case for Lytag. The Molochite is not spherical and has no large cracks but it is very angular so friability is again probably caused by abrasion. Both the EFG and 'Starlight' have large cracks present leading to grain breakage.

The BEWA standard states that for friable materials such as anthracite, GAC, pumice and other expanded inorganic materials, a special dispensation is permitted to the extent that < 10% by weight of material sampled after delivery/placing may be allowed to pass lower size limit and 5% through the next lower standard sieve size. It may therefore be necessary to include BAF materials in this section.

4.6: Conclusions

From the above discussion we can determine which of the media types in this study would be most suitable for use in biological aerated filters in terms of physical parameters. All of the media types investigated are inert and appear to be suitable for biomass attachment in terms of surface roughness, porosity and SSA.

The 'Starlight' is very light so would need very low water velocities for backwashing and therefore low energy costs but this is outweighed by the fact that it is friable and prone to attrition which would lead to problems with fines and blocking of the filters. The EFG is also friable and prone to attrition. Molochite is opposite to this, being very hard and having a low percentage attrition and friability. It is very dense though needing high backwash water velocities and energy costs. Both of the shales are problematic in that they have no clear point of fluidisation so the chosen backwash rate would either lead to underwashing of the coarser media or loss of media over the overflow weir - this could be avoided if a launder system were used. Lytag has a fairly high V_{mf} with average attrition and friabilities. The Arlita though has low attrition and friability as well as a low V_{mf} . For these reasons I chose it as being the most suitable BAF media type from those considered in this study and therefore practical for use in pilot scale trials.

The physical characteristics are not the only aspects that have to be considered in the suitability of media for use in biological filters. Other factors that must be considered are the cost and ease of supply of materials. Future work on BAF media should also take into account the establishment and growth of biomass and laboratory/pilot scale trials should be carried out to determine the importance of porosity. Pilot scale trials of wastewater treatment are ultimately important before the full-scale use of media to determine how the combination of physical characteristics and biomass establishment affect BAF performance.

5.0 PILOT SCALE PERFORMANCE OF ARLITA MEDIA

5.1: Introduction

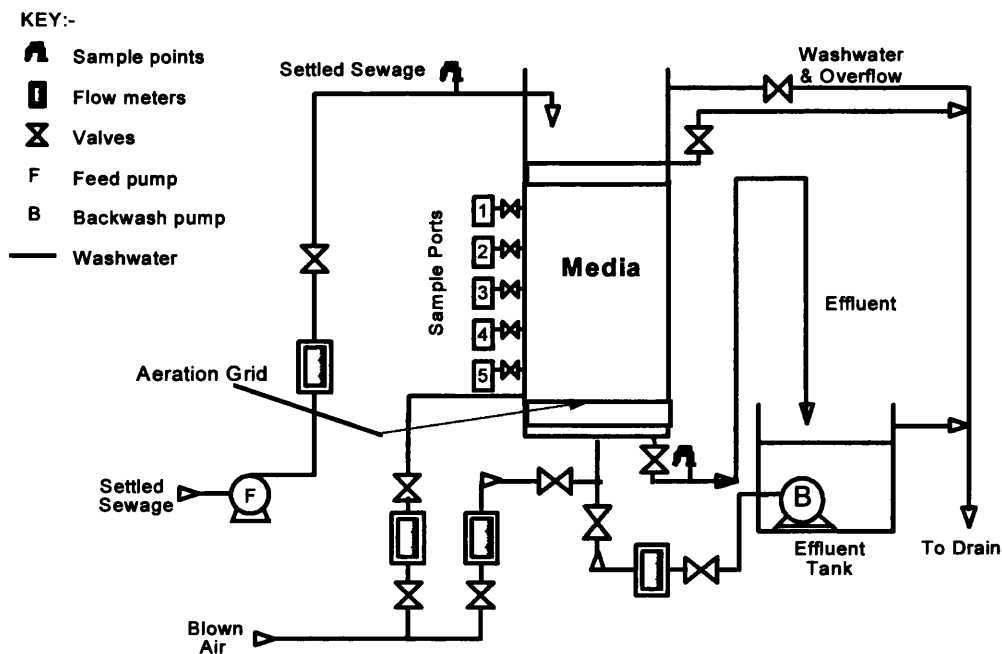
The original characterisation of media as described in Chapter 4 was used to determine which type of media was most suitable for use at pilot scale in terms of physical characters. It was shown that Lytag and Arlita media had the most appropriate characteristics. The Arlita was chosen for use at pilot scale due to its low minimum fluidisation velocity, percentage attrition and friability.

5.2: Methodology

5.2.1: Description of the Pilot Plant

The pilot plant for the original work on Arlita consisted of two downflow BAF columns, operated independently (Figures 5.1 and 5.7). The primary settled sewage from which the columns were fed was pumped from Manor Farm sewage treatment works (STW) to a holding tank. Treated effluent from the columns was collected so that some could be used for backwashing of the columns while the rest went to drain. Process air was introduced through a sparge grid at the bottom of each column.

Figure 5.1 : Schematic of Single Pilot Column



5.2.2: Column Configuration

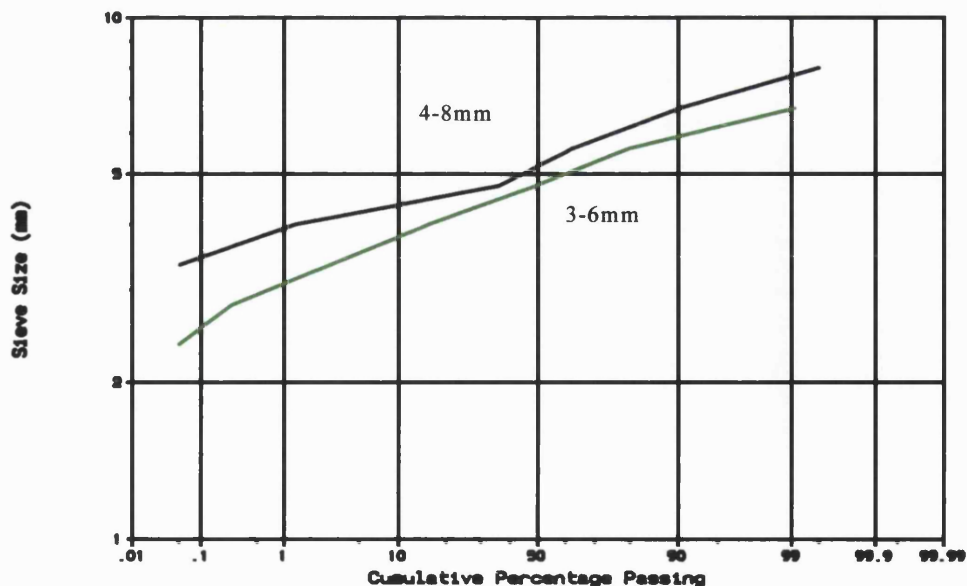
All columns were constructed from tubular stainless steel sections of 0.49m diameter. The bottom support section was 0.3m deep with a flange in the base to which an under-drain system was connected. The treated effluent was collected in this drain system and backwash air and water was supplied through it. The other three sections were 1.0m deep and sample ports were situated at filter bed depths of 0.1m, 0.35m, 0.85m, 1.1m and 1.35m from the floor of the column.

5.2.3: Media Utilised

Each column had a layer of gravel filling the support section of the column. The media utilised in this preliminary work was a pelletised expanded clay - Arlita, supplied by Aridos Ligeros, Spain. Each column had media of a different size range (3-6mm and 4-8mm) filled to approximately 1.6m from the top of the gravel layer.

Some media characterisation tests were carried out on the 4-8mm Arlita so that it could be compared to the 3-6mm Arlita. See Chapter 4 for experimental procedures for media characterisation.

Figure 5.2: Sieve Analysis of Arlita Media



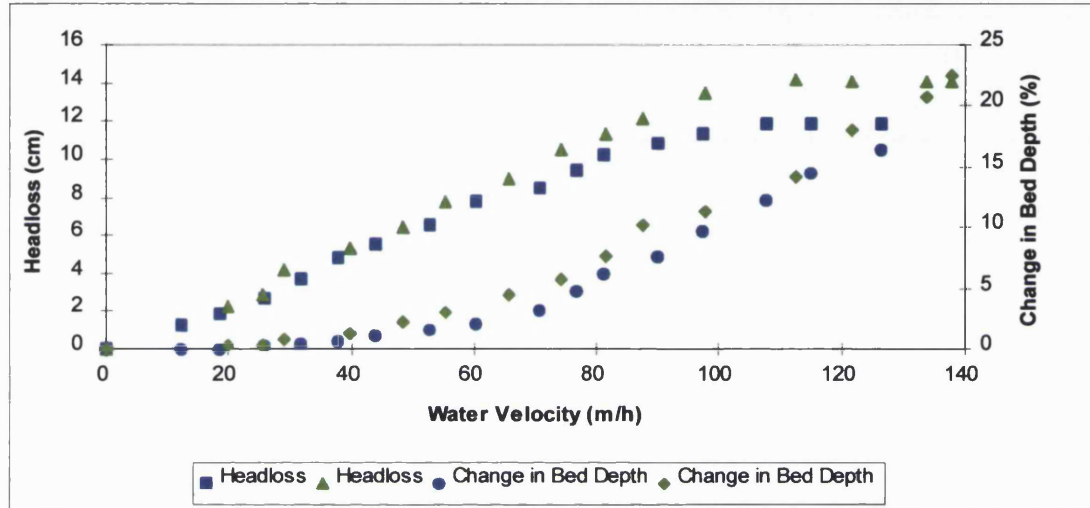
5.2.3.1: Sieve Size Analysis

Table 5.1: Sieve Analysis of Arlita Media

Media Size (mm)	Hydraulic Size (mm)	d_5 (mm)	Effective Size d_{10} (mm)	d_{60} (mm)	Uniformity Coefficient	d_{90} (mm)	d_{95} (mm)
3-6	4.7	3.5	3.7	5.0	1.35	5.8	6.2
4-8	5.23	4.2	4.3	5.5	1.28	6.5	6.8

5.2.3.2: Fluidisation Velocities

Figure 5.3: Fluidisation of Arlita Media (Green - 4-8mm, Blue - 3-6mm)



The fluidisation velocities of both sizes of Arlita were recorded from laboratory experiments at 8°C. It can be seen that there was no specific point of fluidisation in either size. The 3-6mm Arlita had a V_{mf} of 72-80m/h and the 4-8mm Arlita had a V_{mf} of 75-95m/h.

5.2.3.3: Friability and Attrition

The friability test was only carried out on the 3-6mm Arlita and details can be found in Chapter 4.

Table 5.2: Sieve Analysis of Arlita Media After Attrition Test

Media Size (mm)	Hydraulic Size (mm)	d_5 (mm)	Effective Size d_{10} (mm)	d_{60} (mm)	Uniformity Coefficient	d_{90} (mm)	d_{95} (mm)
3-6	4.4	3.2	3.5	4.7	1.34	5.7	5.8
4-8	5.0	3.95	4.2	5.2	1.24	6.2	6.8

There is some attrition of both the 3-6mm and 4-8mm Arlita, shown by a change in d_5 , d_{95} and d_h .

Figure 5.4: Sieve Analysis of 3-6mm Arlita After Attrition and Friability Tests

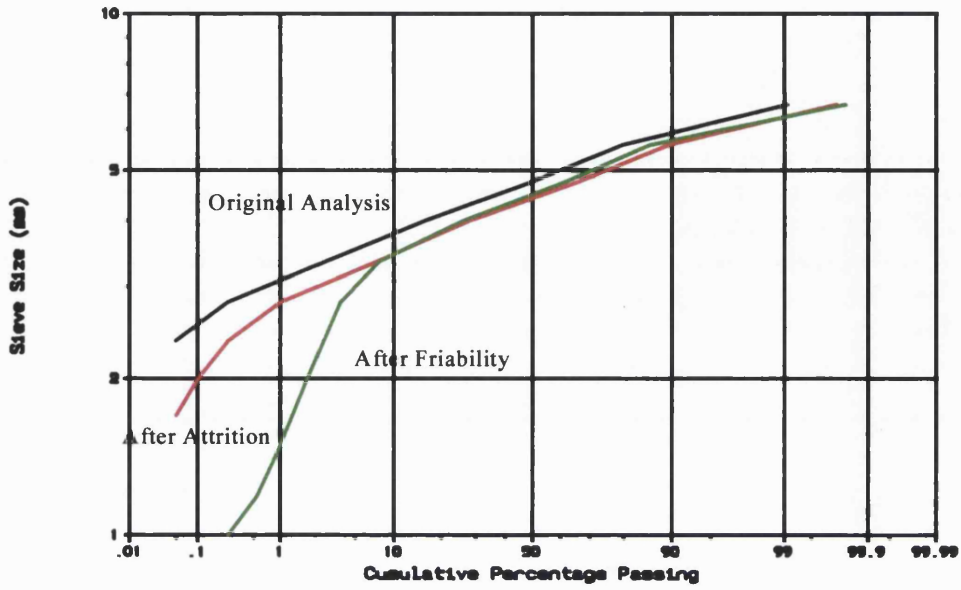
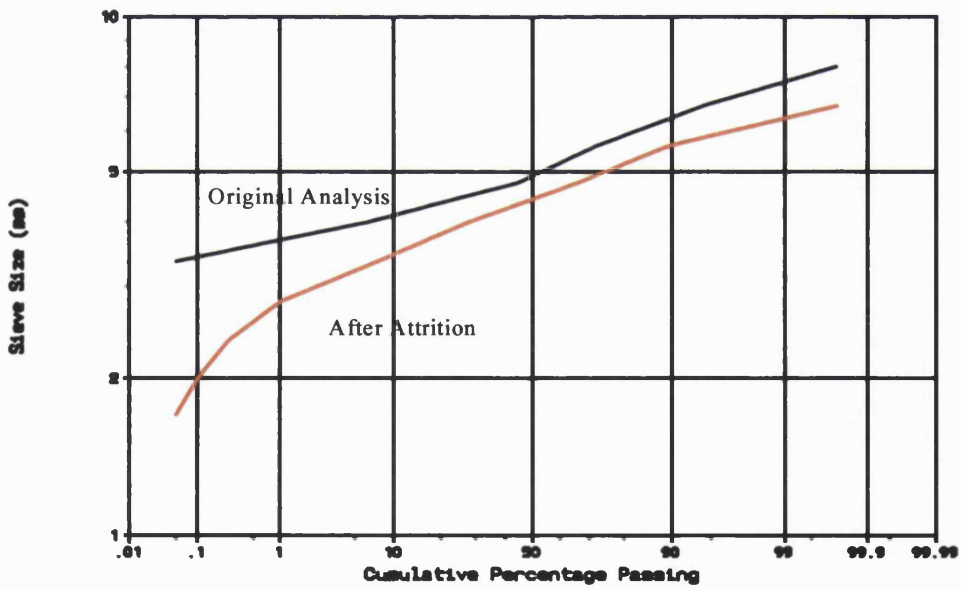


Figure 5.5: Sieve Analysis of 4-8mm Arlita



5.2.4: Air Supply

Each column had a sparge grid located in the supporting gravel layer which contain the same distribution of sparge holes, all 1.5mm in diameter.

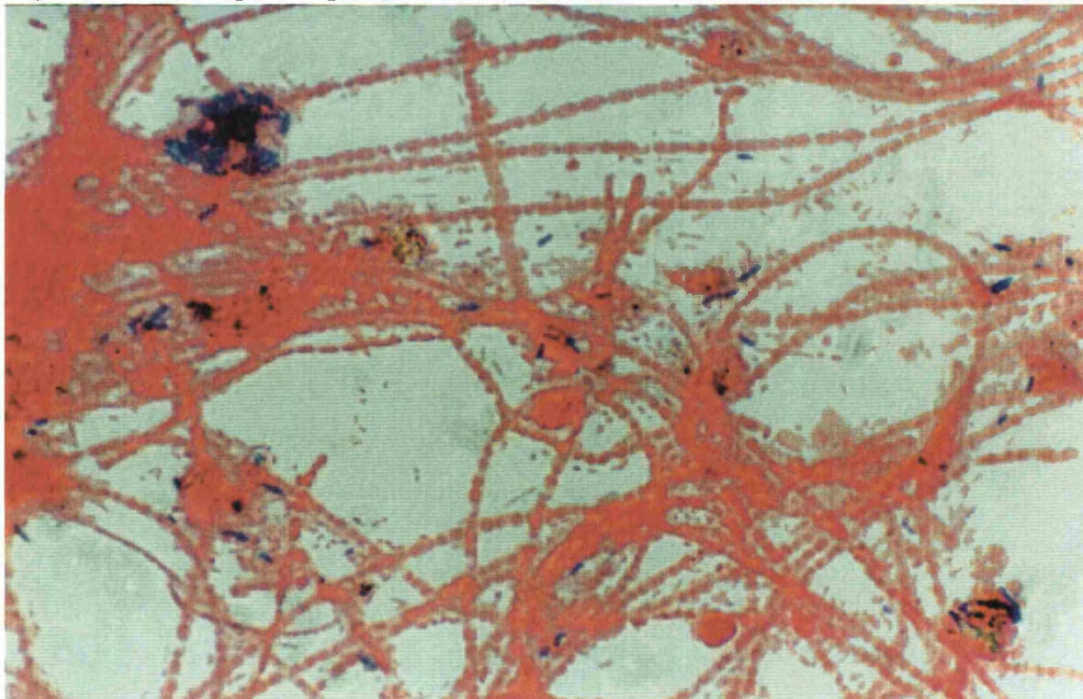
5.3: Plant Operation

5.3.1: Commissioning

In order to produce biological filters which were capable of nitrification as well as carbonaceous treatment during commissioning (17/7/95 - 14/8/95) the hydraulic loading rate (HLR) was incrementally increased when grab samples showed effluent ammonia and nitrite levels to be below 1mg/l. If the filters had been commissioned to immediately treat a high BOD/COD loading rate there would have been no opportunity for establishment of nitrifiers, as shown by the work of Ohashi *et al* (1995).

During commissioning there was little presence of 'foaming', as reported by Upton & Churchley (1996), but in both filters the presence of 'sewage fungus' was noted. This consists of masses of filaments in which the dominant bacterial type is 021N, bound into very large flocs (> 1000µm).

Figure 5.6: 'Sewage Fungus'[1cm = 0.007mm]



5.3.2: Backwashing

During commissioning with Arlita media backwash was originally only carried out when the filters flooded due to headloss build-up.

The initial procedure for backwashing is given in Table 5.3

Table 5.3: Backwashing Procedure for Arlita Media

	Rate (m/h)	Duration (mins)
Air Scour	50	1
Combined	Air - 50 Water - 40	2
Water Rinse	40	1

The top water was drained down after media had been allowed to settle and normal operation was resumed.

Once the filters were running at steady-state the backwash regime was adjusted to take into account the organic loading rate (OLR) and therefore run times, and to generate collapse-pulsing. The 3-6mm Arlita had an experimental fluidisation velocity of 72-80 m/h at 8 °C and 4-8mm Arlita had a V_{mf} of 75-95m/h. Theoretical work (Amirtharajah, 1984) shows that 40-60% of the fluidisation velocity combined with air is the optimum condition for filter backwashing and this was used to calculate the backwash rates at steady-state (Table 5.4).

Table 5.4: Backwash Regimes for Arlita Media

	3-6mm Arlita	4-8mm Arlita
Air Rate (m/h)	50	50
Air Duration (mins)	1	1
Combined Rates (m/h)	50 air + 40 water	50 air + 50 water
Combined Duration (mins)	3	3
Rinse Rate (m/h)	40	50
Rinse Duration (mins)	1	1

The columns were backwashed every 24 hours to prevent solids build-up and subsequent breakthrough in the effluent.

5.3.3: Operating Conditions

Arlita performance was investigated at two HLRs. Only one OLR was investigated as a period of rain led to a dilution in strength of the sewage for the second HLR making the strength approximately 1.0 kg BOD/m³/d in both instances.

At normal operation the air flow rate was set at 30 l/min to ensure that oxygen was not limiting for biofilm growth. This corresponds to an air flow of 9.5m/h which is well above the 2:1 air:water ratio suggested as sufficient to satisfy the oxygen demand of biomass in an upflow fixed bed reactor (Amar *et al*, 1986).

5.4: Data

5.4.1: Effluent Quality

During start-up treated effluent was sampled every 24 hours for ammoniacal nitrogen ($\text{NH}_4\text{-N}$), nitrite nitrogen ($\text{NO}_2\text{-N}$) and suspended solids (SS), in order to determine when the loading rate could be increased. The loading rate was determined by analysing a sample from a branch in the feed system for biochemical oxygen demand (BOD), chemical oxygen demand (COD), SS, total Kjeldhal nitrogen (TKN) and $\text{NH}_4\text{-N}$.

Once the filters were running at steady-state, sampling was again carried out every 24 hours, with 24 hour profile samples being analysed at each loading rate.

At each loading rate, ammoniacal nitrogen profiles were also taken to represent biomass activity, samples for this being taken from each sample port.

5.4.2: Biomass Samples

At steady-state conditions, biomass profiles were taken every week using an auger to sample at the same depths as the liquid sample ports. The mass/concentration of biomass was determined and scanning electron micrographs taken of media and biomass samples from each depth so that biomass build-up could be compared. Microbiological identifications were made using Eikelboom & van Buijgen (1981).

5.4.3: Headloss

Data from manometers set at the same depths as the sample ports were recorded in order to determine headloss throughout the filter bed.

5.4.4: Backwash Sludge Samples

It is important to know the characteristics and quantities of solids and sludge from the BAFs which need processing, treatment and disposal. Once steady-state performance had been reached by the pilot columns the backwash liquors were tested for suspended solids, settleability, pressure filtration time (PFT) and capillary suction time (CST) to see if they are affected by media size.

5.4.5: Off-Gas Analysis

One important factor in wastewater treatment by biological aerated filters is the transfer of oxygen to the microorganisms involved in the process. Off-gas analyses were therefore carried out at one loading rate over a range of air flows, covering 1 - 15m/h to see how oxygen transfer is affected by air flow rate and media size.

To measure the volume of oxygen released by the filters the pilot columns were capped and backwash pipes blocked off so that air could only escape through flexible hose attached to the oxygen measuring equipment. The oxygen concentration in the off-gas from the columns was detected using a Model 6509 gas monitor from Kent Industrial Measurements Ltd. The mA signal generated was measured with a multimeter (Fluke 79/29 series ii) and converted to a true oxygen concentration. The readings were calibrated from readings for dry air (20.95% oxygen) and readings from a special gas mixture (18.92% oxygen).

The CO₂ concentrations were measured using an infra-red gas analyser produced by Geotechnical Instruments (UK) Ltd. This device was calibrated for low CO₂ levels (0 - 5%). The ambient temperature and relative humidity of ambient air and off-gas samples were measured using a Vaisali portable HMI 31 meter and the pressure of the air flow into the filters was measured using a Digitron hand held manometer. Dissolved oxygen (DO) concentrations and effluent temperatures were measured with a WTW Oxi 323 B oxygen probe. Samples were taken from each port and of the effluent. All data was taken once steady-state conditions had been reached.

5.5: Data Analysis

5.5.1: Effluent Quality

Suspended solids: Method in Part SMP1 of "Suspended, settleable and total dissolved solids in waters and effluents, 1980" - Methods for the examination of waters and associated materials (ISBN 011 751957-X).

BOD: Method outlined in "5 day biochemical oxygen demand (BOD₅)", printed by HMSO (ISBN 011 752212-0).

COD: Method outlined in "Chemical oxygen demand (dichromate value) of polluted wastewaters", printed by HMSO (ISBN 011 751957-X).

Ammoniacal nitrogen: An 'Aqua 800 Analyser' was used to determine ammonia levels.

TKN: Method outlined in "Kjeldhal nitrogen in waters (1987)" Part D, (ISBN 011 752129-9).

Nitrite- N: An 'Aqua 800 Analyser' is used to determine nitrite levels.

TON: An 'Aqua 800 Analyser' was used to determine total oxidisable nitrogen.

Nitrate-N: Nitrate levels were calculated from TON and NO₂-N results.

All above analyses were performed by Thames Water laboratory services.

5.5.2: Biomass Samples

5.5.2.1: Mass/Concentration of biomass:

The mass and concentration of biomass is determined by adding a sample of media to a weighed crucible (A) and dried in an oven for 24 hours (at 105°C). The crucible and dry media are then reweighed (B) before being put in a furnace at 550 °C for 2 hours (with lid). Finally the crucible and media are cooled and weighed (C) (without lid).

Calculations: 1) Mass biomass = B – C (g) (D)

$$2) \% \text{ biomass} = \frac{D}{(B - A)} \times 100$$

3) Concentration of biomass = % biomass x 10,000 (mg/kg dry media)

5.5.2.2: Scanning electron micrographs:

A method of fixing and dehydrating samples was adapted from Ellis & Aydin (1995). Samples of media were fixed in a 5% solution of glutaraldehyde in phosphate buffer solution (pH 7.0) overnight. The samples were then washed with the buffer solution before being dehydrated by rinsing with consecutively stronger solutions of ethanol in distilled water (30%, 50%, 70%, 80% and 100%). Each rinsing lasted for 10 minutes. Once samples were rinsed in 100% ethanol they could be stored until it was possible to coat them. Samples were sputter coated in gold and investigated using a scanning electron microscope (SEM).

5.5.3: Headloss

Manometer readings were used to determine headloss build-up in metres of water for each filter after backwashing.

5.5.4: Backwash Samples

Samples of backwash liquors were collected from each filter every 30 seconds during the combined and rinse phases of backwash and then analysed for suspended solids (by T.Kent) before being settled out for sludge analysis.

Suspended solids, settleability and sludge volume index (SVI) were determined from standard methods (WPCF, 1985a and b).

5.5.4.1: Pressure filtration time (PFT):

A PFT meter developed by WRc measures the time taken for a fixed volume of filtrate to pass through the filter medium under a certain pressure, which is defined as the PFT. The meter is operated by first loading a sample of 50ml of unconditioned sludge into the filter assembly which consists of a brass cylinder which fits into a brass end cap that contains a porous filter paper support and a standard Whatman grade 17 filter paper. This is then loaded into the front of the meter and perspex safety guard slid into place. Filtrate is forced through the filter paper in the base of the cylinder and the time recorded for it to reach the stop electrode - the PFT for a fixed volume of liquid to be filtered.

5.5.4.2: Capillary suction time (CST):

The CST apparatus is a simple automatic measuring device which gives a reasonable approximation of the specific resistance to filtration (Baskervill & Gale, 1968). It consists of a pair of concentric circular electrodes separated by 1 cm, which are mounted in a perspex plate. The perspex plate is placed on a rectangular filter paper (Whatman No.17 grade), and the sludge sample is loaded into the central cylindrical reservoir. The time taken for the filtrate to be drawn from the sample of sludge under capillary suction pressure is measured.

Figure 5.7: Pilot Columns at Manor Farm STW



5.6 Results

5.6.1 Steady State Results

The performance of Arlita media was determined from spot samples of settled sewage and effluent taken twice a day at approximately the same time. The average settled sewage concentrations were 197.6mg/l BOD (HLR 1), 125.1mg/l BOD (HLR 2), 441.8mg/l COD, 317.8mg/l COD, 121.8mg/l SS, 118.7mg/l SS, 31mg/l NH₄-N, 29.6mg/l NH₄-N, 40.9mg/l TKN and 36.9mg/l TKN. These correspond to the average VLRs shown in Table 5.5. The average effluent qualities and removal rates are shown in Tables 5.6 and 5.7.

Table 5.5: Loading Rates

Media Size (mm)	Load	Hydraulic Load m/h	BOD Load kg/m ³ /d	SS Load kg/m ³ /d	NH ₄ -N Load kg/m ³ /d	COD Load kg/m ³ /d
4-8	1	0.4	1.09	0.77	0.2	2.78
3-6	1	0.4	1.08	0.77	0.17	2.76
4-8	2	0.57	1	1.08	0.27	2.83
3-6	2	0.57	1	1.08	0.27	2.83

Table 5.6: Effluent Quality

Media Size (mm)	Load	Effluent BOD mg/l	Effluent SS mg/l	Effluent NH ₄ -N mg/l	Effluent COD mg/l
4-8	1	6.9	10.1	1.6	69.8
3-6	1	5.2	8.0	0.7	63.1
4-8	2	9.1	9.2	4.6	72.7
3-6	2	5.4	6.8	2.2	76.6

Table 5.7: Percentage Removals

Media Size (mm)	Load	BOD Removal (%)	COD Removal (%)	SS Removal (%)	NH ₄ -N Removal (%)
4-8	1	96.4	84.3	91.6	94.9
3-6	1	97.4	84.9	94	97.9
4-8	2	93.2	74	92.3	85.8
3-6	2	95.6	78.5	94.2	93.5

At an HLR of 0.4m/h there was an OLR of approximately 1kg BOD/m³/d. At HLR 2 (0.6m/h) an OLR of 1.5kg BOD/m³/d was expected but high rainfall led to a decrease in sewage strength so again the OLR was approximately 1kg BOD/m³/d. The COD load also remained similar for both phases but SS and NH₄-N increased at the slightly higher HLR. Figures 5.8 - 5.12 show graphs of removal rate against loading rate for

the different effluent parameters, HLRs 1 and 2 have been combined as there appears to be no hydraulic effect on the effluent quality.

Figure 5.8: Composite BOD Removals

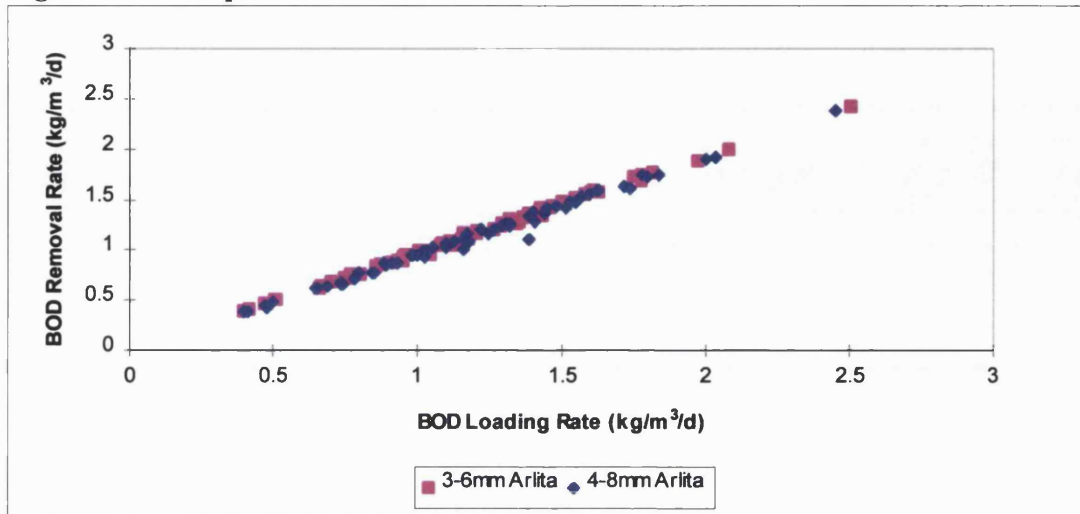


Figure 5.9: Composite COD Removals

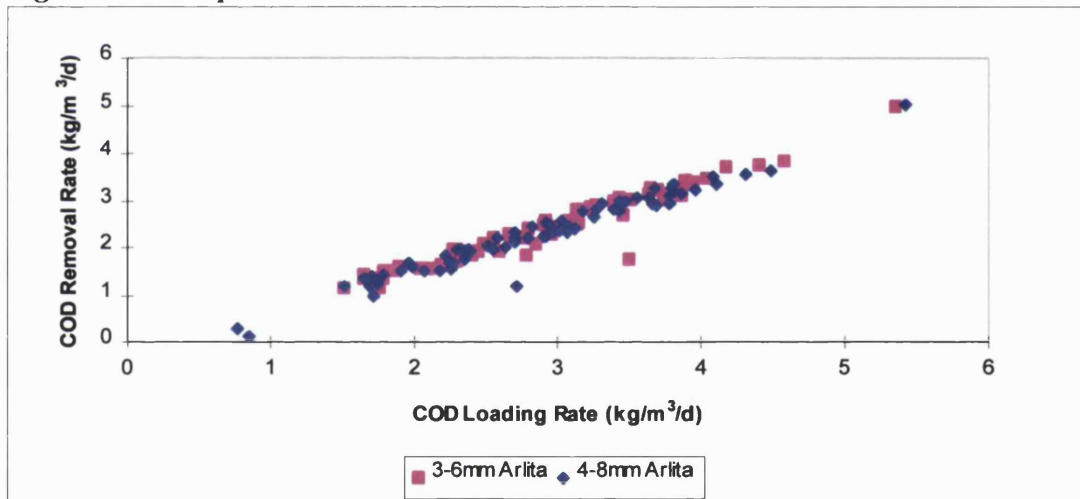


Figure 5.10: Composite SS Removals

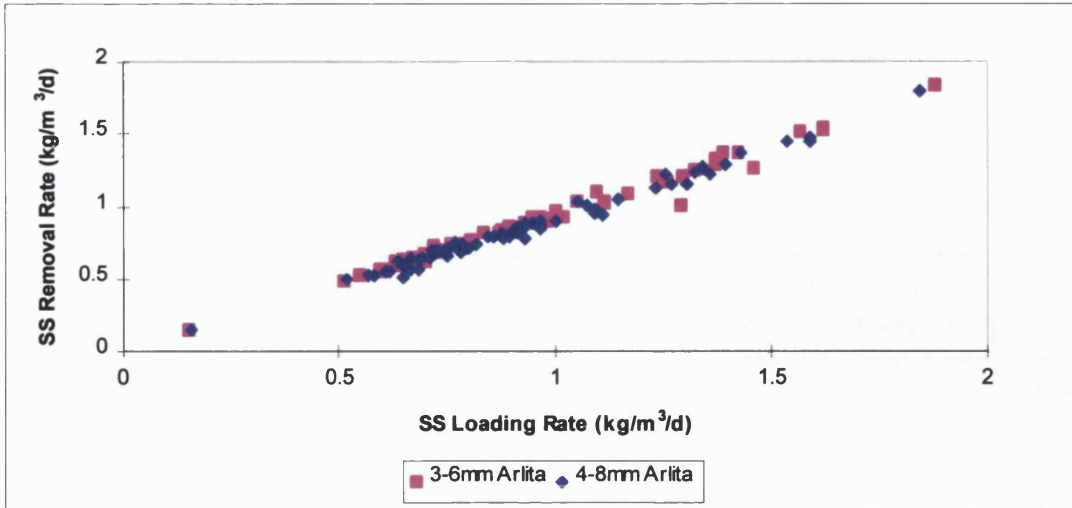


Figure 5.11: Composite NH₄-N Removals

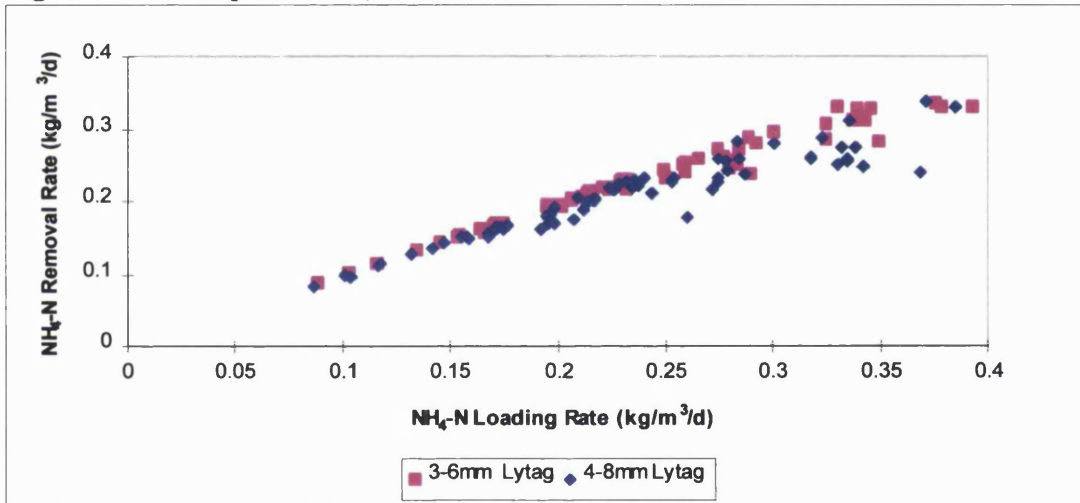
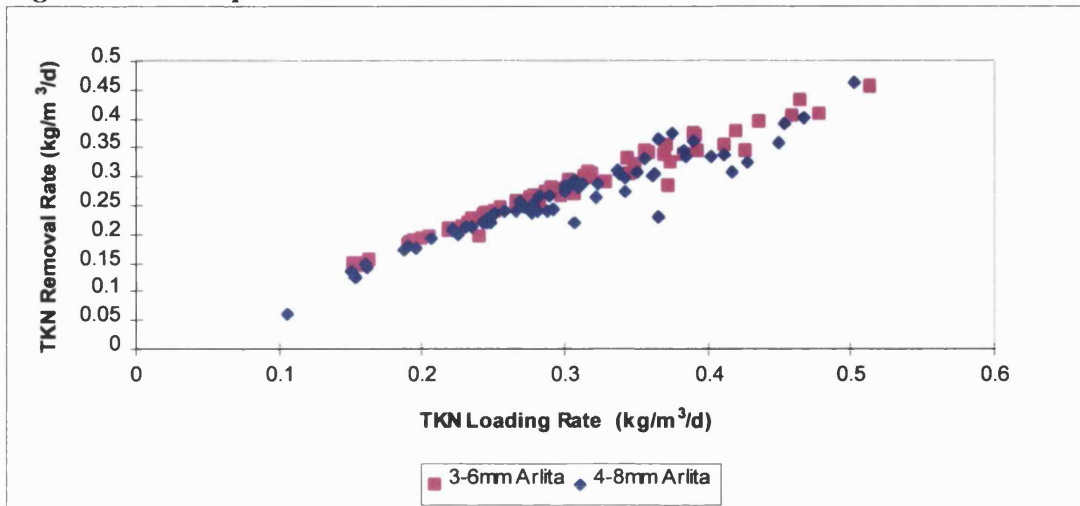


Figure 5.12: Composite TKN Removals



5.6.2: Diurnal Variations

At each loading rate 24 hour profiles were taken for each media sample as shown by Figures 5.13 - 5.17 for BOD, COD, SS, NH₄-N and TKN removal rates. Samples were taken every two hours.

Figure 5.13: Diurnal BOD Removals

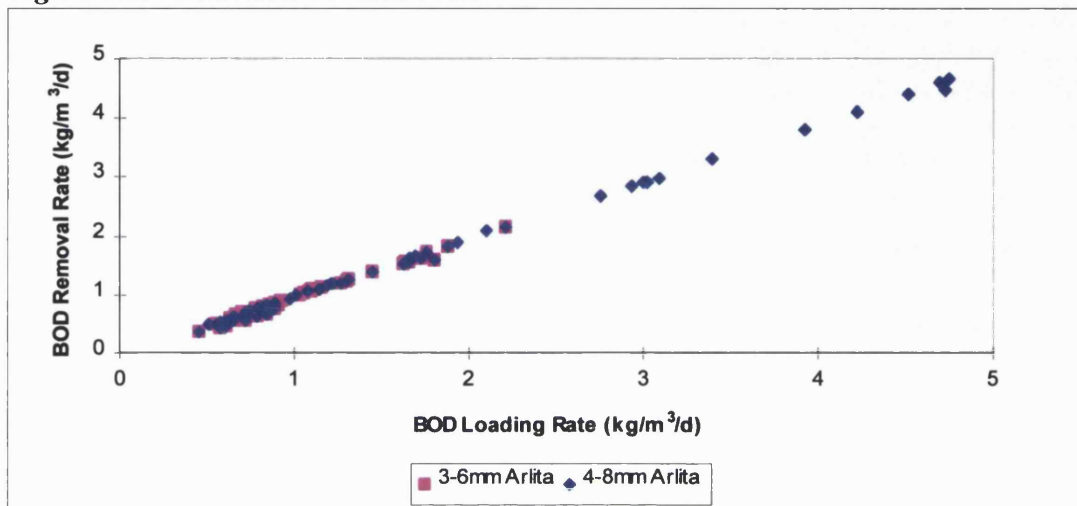


Figure 5.14: Diurnal COD Removals

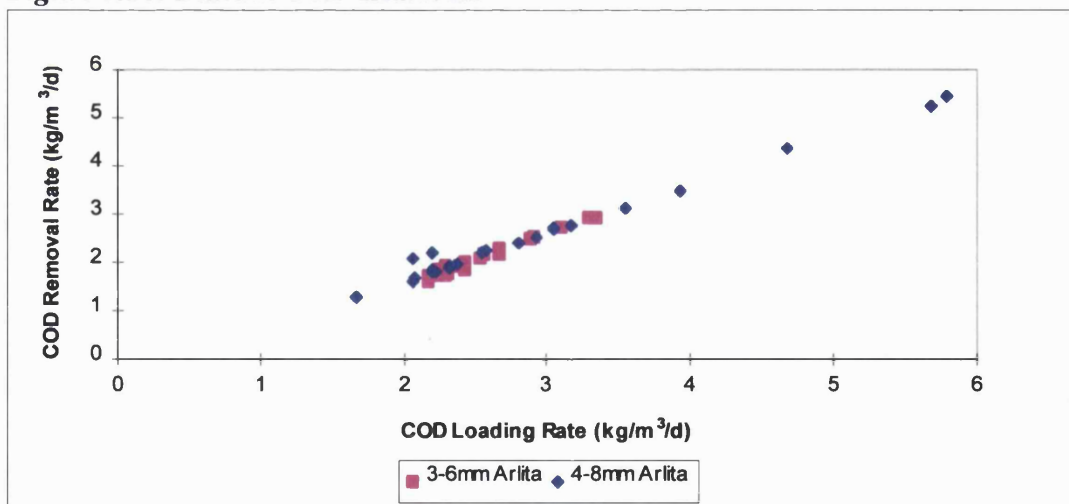


Figure 5.15: Diurnal SS Removals

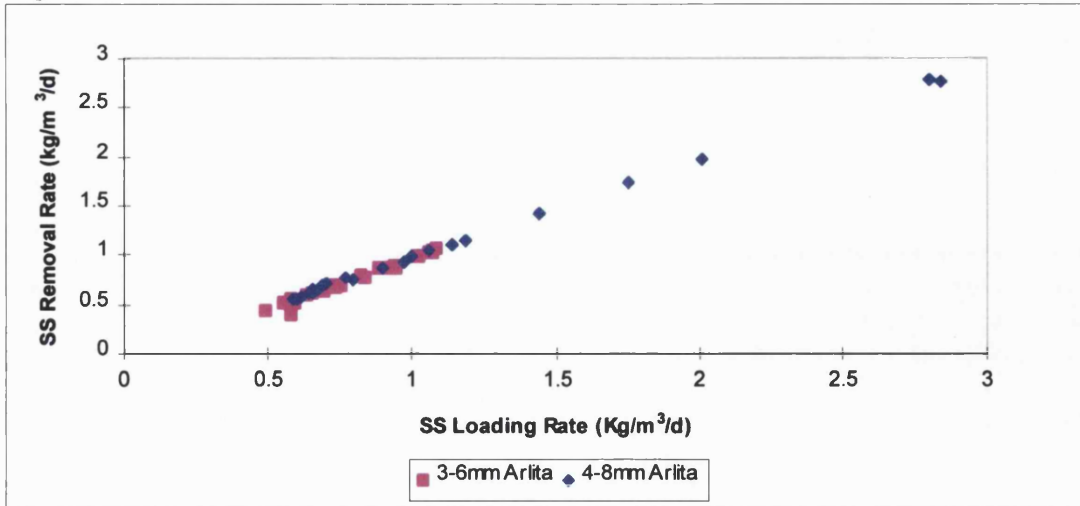


Figure 5.16: Diurnal NH₄-N Removals

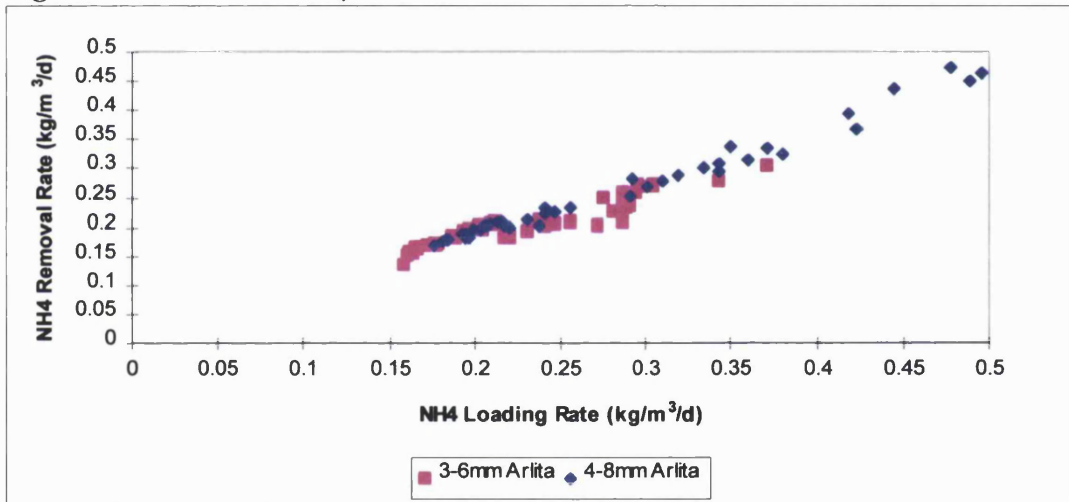
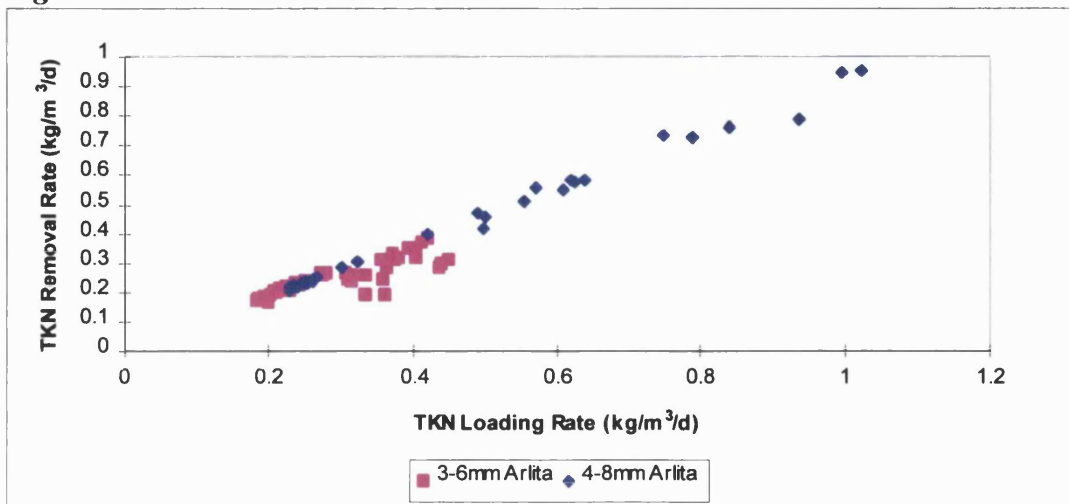


Figure 5.17: Diurnal TKN Removals



The graphs of BOD, COD and SS removal show a direct relationship between the sewage strength and removal rates. The rates of removal of $\text{NH}_4\text{-N}$ and TKN appear to have slightly less of a relationship with loading rate therefore the data was investigated in terms of the effect of backwashing on removal rates (Figures 5.30-5.31).

5.6.3 Bed Profiles

At each loading rate bed profiles of $\text{NH}_4\text{-N}$, NO_2 and SS were taken for each media size as shown by Figures 5.18 - 5.20.

Figure 5.18: $\text{NH}_4\text{-N}$ Profiles

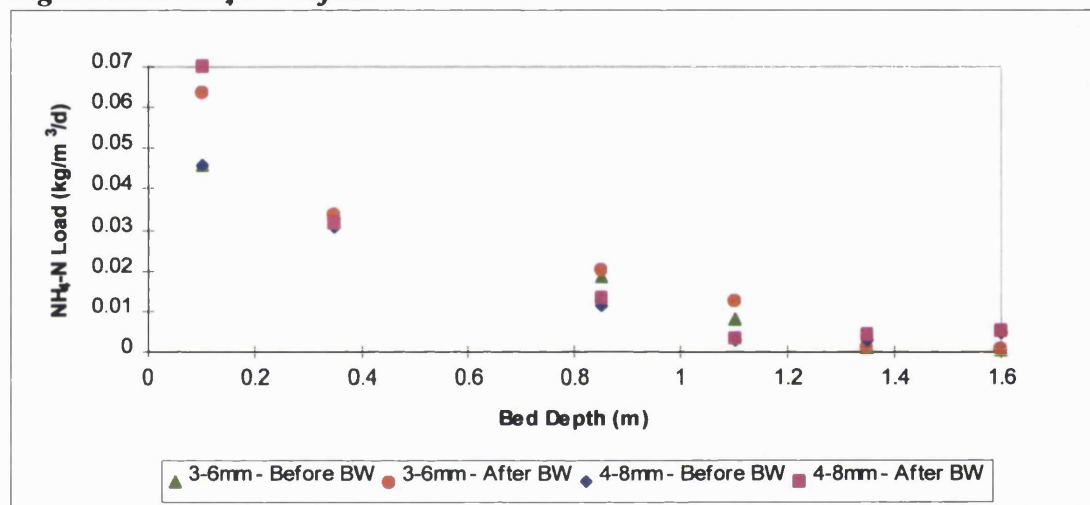


Figure 5.19: $\text{NO}_2\text{-N}$ Profiles

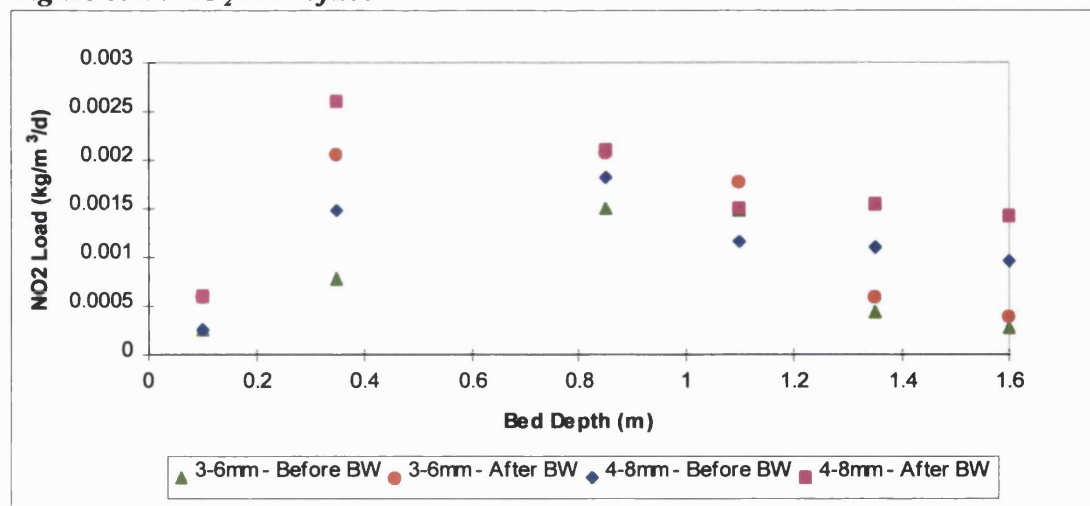
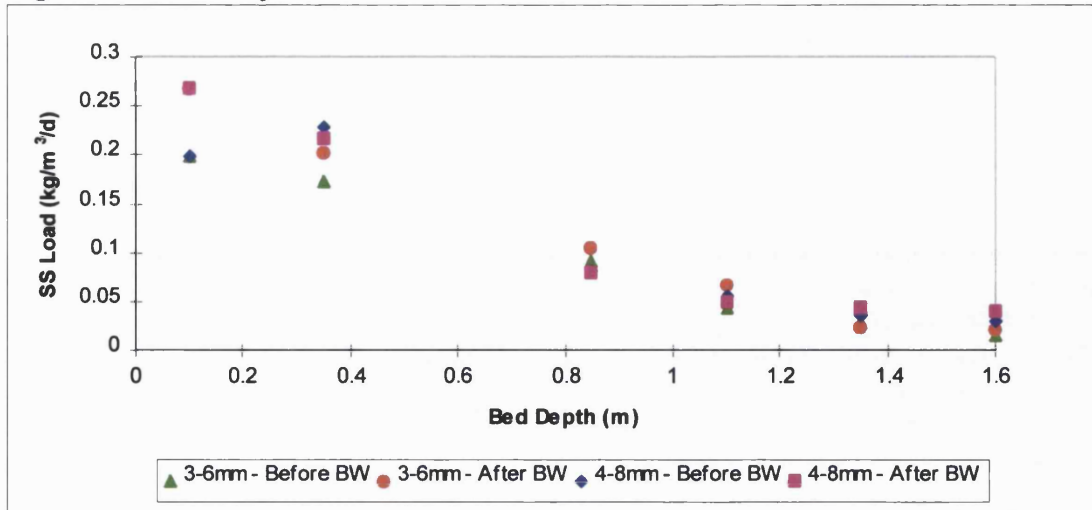


Figure 5.20: SS Profiles



5.6.4 Biomass Samples

Graphs 5.21 and 5.22 show the biomass bed profiles for each media before and after backwashing of the filters.

Figure 5.21: Biomass Profiles Before Backwashing

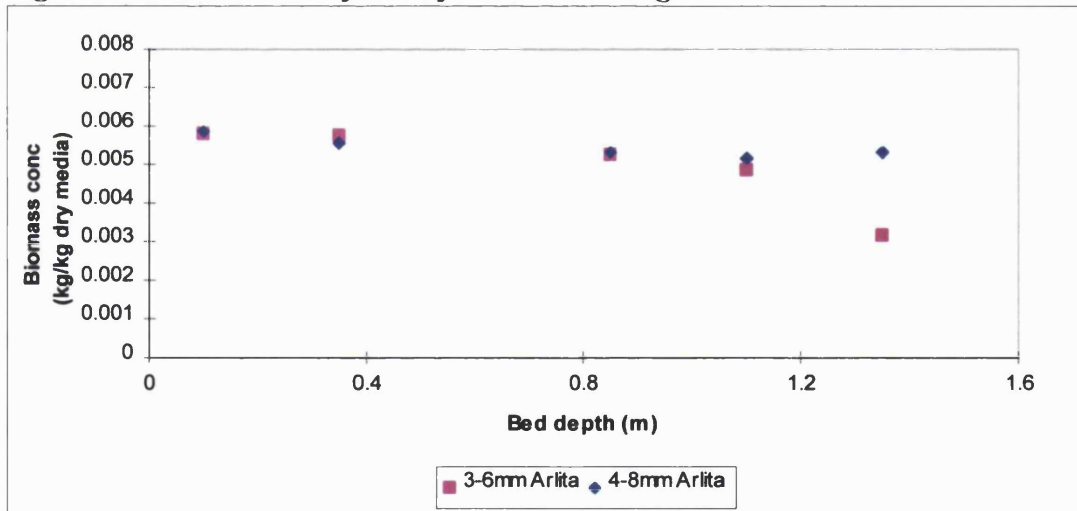
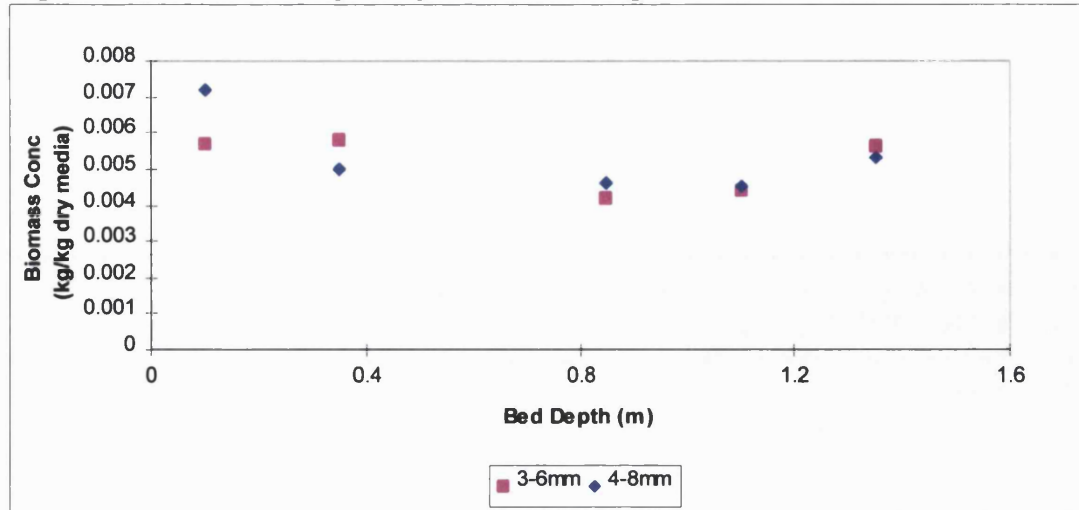


Figure 5.22: Biomass Profiles After Backwashing



5.6.5 Headloss

The head build-up for each filter was recorded at each load rate. At each load rate both filters lasted longer than 24 hours before flooding therefore there was very little head build-up between backwashes. The maximum head build-up was approximately 0.25m for 3-6mm Arlita and slightly less for 4-8mm Arlita.

5.6.6 Backwash Samples

Backwash liquors were analysed for SS and the total solids removed by backwashing were calculated as shown in Figures 5.23 and 5.24.

Figure 5.23: Backwash Profiles for Arlita Media

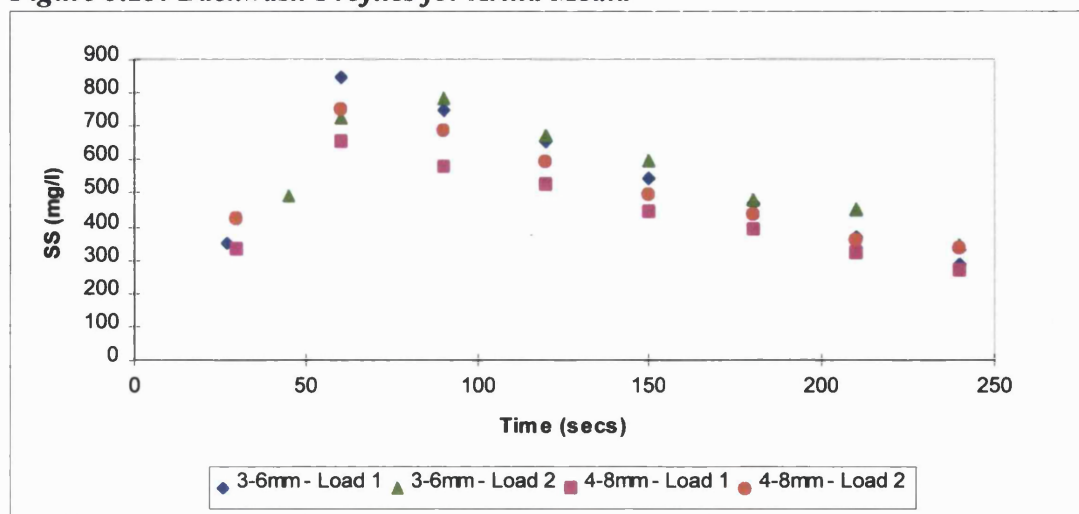
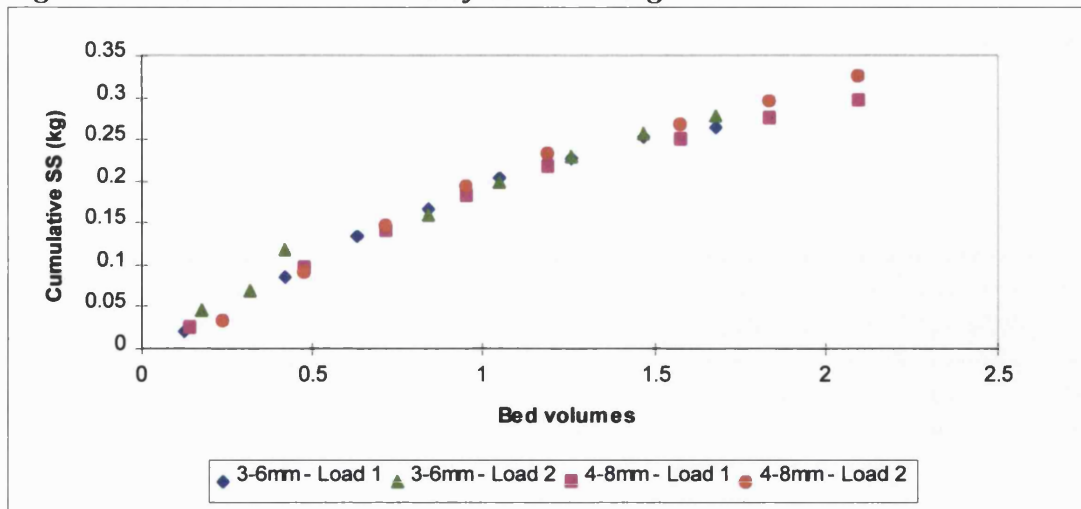


Figure 5.24: Cumulative Removal of Solids During Backwash



5.6.7 Sludge Samples

Table 5.8 shows sludge parameters for each load rate.

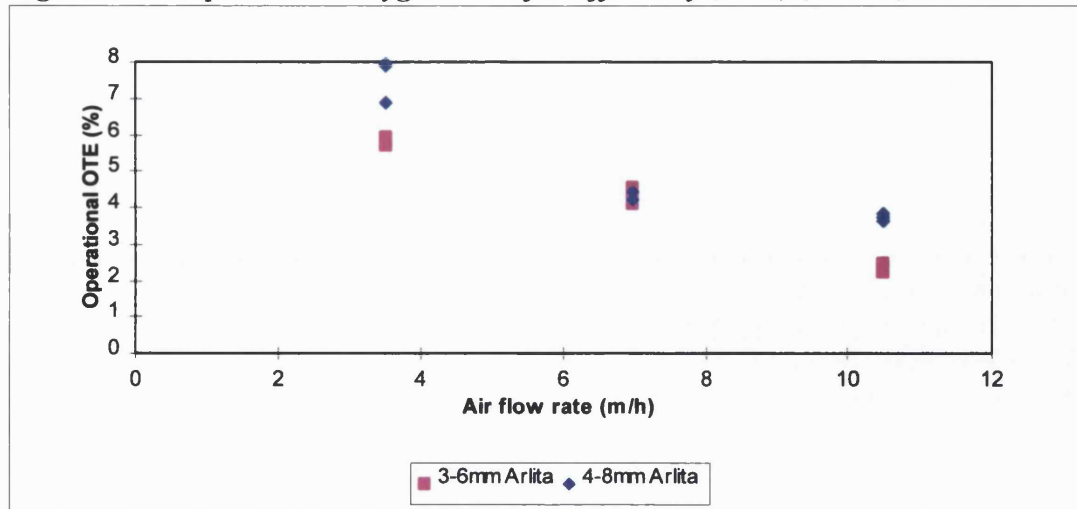
Table 5.8: Sludge Data

Media (mm)	Size	Load	BW SS (mg/l)	Sludge SS (mg/l)	Settleability (mm)	CST (s)	PFT (s)
4-8		1	452	9263		27.1	1081
3-6		1	553	8815		24.9	1217
4-8		2	453	8715	34	31.6	1027
3-6		2	622	10163	39.4	39.5	994

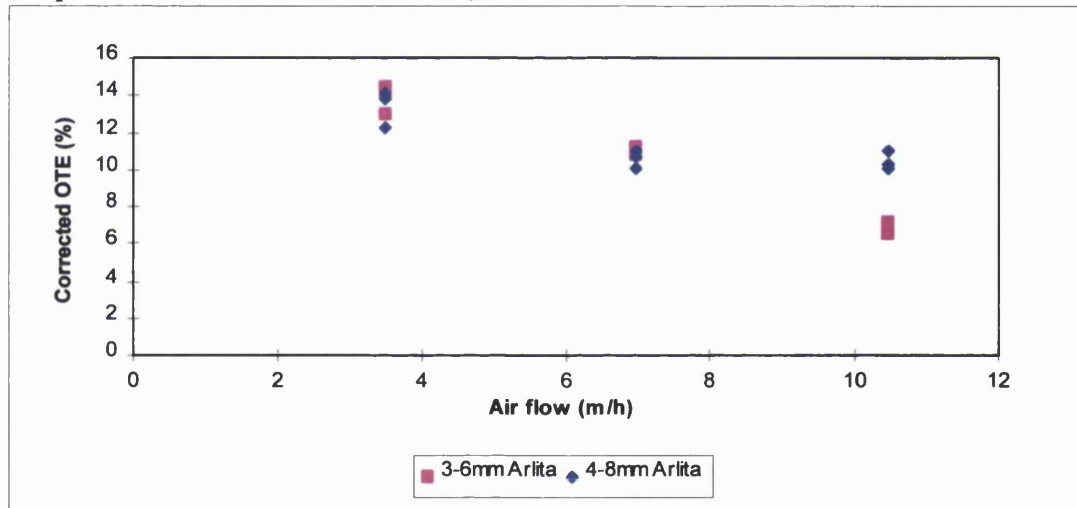
5.6.8 Off-Gas Analysis

During off-gas analysis the oxygen transfer efficiency and oxygenation capacity were determined (Figures 5.25 - 5.27) and dissolved oxygen profiles were taken (Figures 5.28 and 5.29).

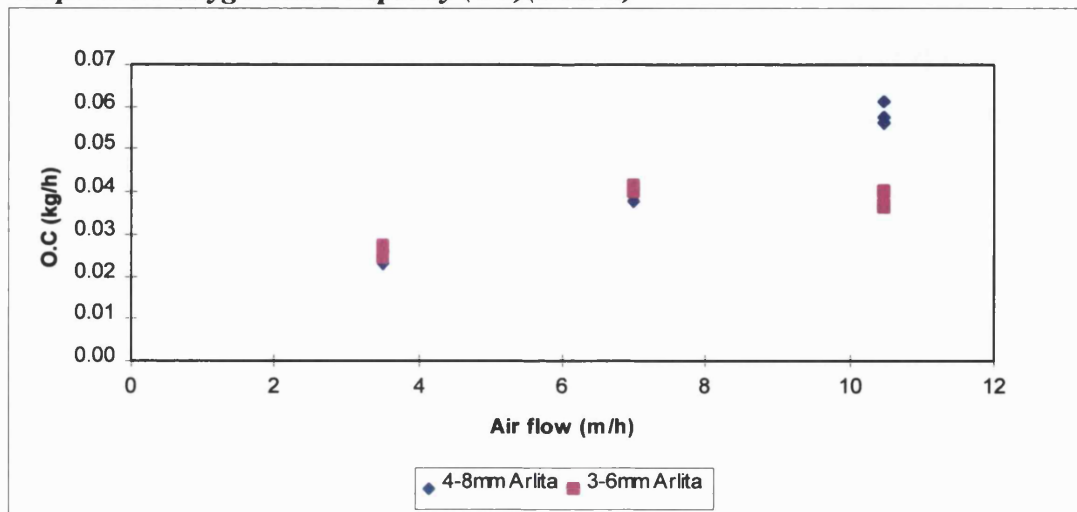
Figure 5.25: Operational Oxygen Transfer Efficiency (OTE) (HLR 2)



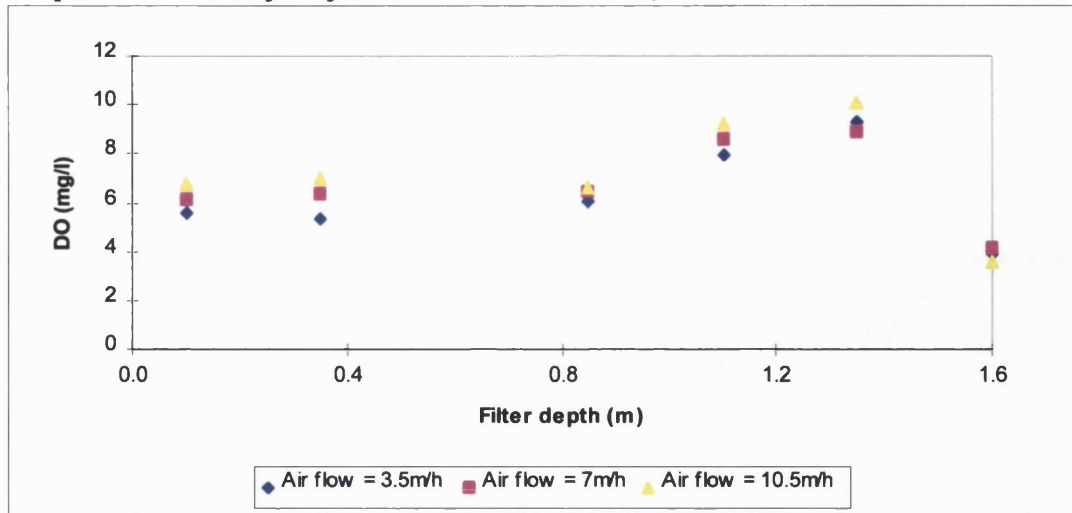
Graph 5.26: Corrected OTE (HLR 2)



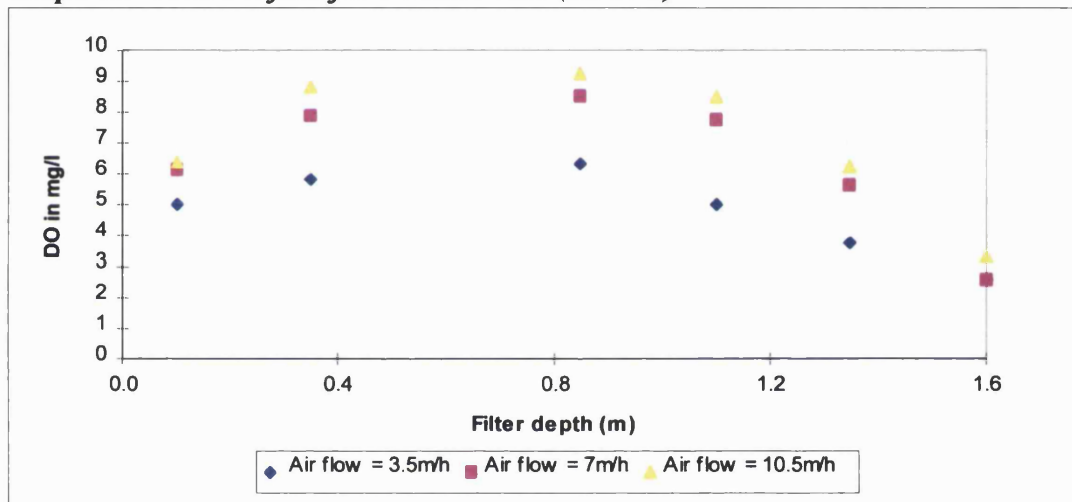
Graph 5.27: Oxygenation Capacity (OC)(HLR 2)



Graph 5.28: DO Profiles for 3-6mm Arlita (HLR 2)



Graph 5.29: DO Profiles for 4-8mm Arlita (HLR 2)



5.7 Discussion

It should be noted that the spot samples do not show a direct comparison between the settled sewage concentrations and effluent concentrations due to the time that it takes for liquid to flow throughout the filter bed. For this reason later work on Lytag media included taking composite samples of settled sewage and effluent.

5.7.1 Steady State Operation

Figures 4.5 - 4.9 show removal rates against VLR for both media sizes, combining data from the two HLRs tested. The HLRs used were very low due to the high strength of the settled sewage, with typical HLRs on BAFs being in the region of 1 - 4m/h (Stensel & Reiber, 1983). Work on upflow biofilters by Peladan *et al* (1996), found that a high

water velocity (flows up to 30m/h) had a positive effect (combined with a large bed depth) on nitrification. Pujol *et al* (1996) also showed that high water velocities improve biofilter efficiency, it may therefore have been beneficial to increase the hydraulic load by adding recycle to the system.

5.7.2 Carbonaceous Removal

Carbonaceous removal is the removal of organic carbon (often measured as BOD or COD) from wastewater by heterotrophic bacteria. From Tables 5.5 and 5.6 we can see that despite the average BOD and COD loading rates being almost the same for HLR 1 and 2 (the BOD volumetric loading rate (VLR) was approximately 1.0 kg/m³/d and COD was 2.8 kg/m³/d at both HLRs), the effluent quality in terms of both BOD and COD has deteriorated slightly for both media sizes at the higher HLR.

From Figure 5.8 showing BOD removals calculated from daily spot samples we can see that over a loading rate of 0.5 - 2.5kg BOD/m³/d there is a high BOD removal rate for both media sizes (93 - 98%) and very little difference between the two sizes. A similar relationship can be seen for COD removal over VLRs of 1 - 5kg COD/m³/d but with lower percentage removals of 74 - 85%.

In terms of actual effluent quality the BOD for 3-6mm Arlita is 5.2mg/l at HLR 1 and 5.4mg/l at HLR 2. The 4-8mm BODs are 6.9mg/l and 9.1mg/l. These values are all within the consent for Manor Farm STW of 20mg/l BOD and compare to the work of Smith & Hardy (1992) where an effluent BOD of 6mg/l was found with an HLR of 1m/h, 0.83kg BOD/m³/d and 0.19kg NH₄-N/m³/d. The BOD values gained also agree with work by Stensel *et al* (1988) who produced an effluent BOD of 8.7mg/l with a HLR of 0.5m/h and 1kg BOD/m³/d using a vitrified clay media (Effective size 3.4mm).

Figures 5.13 and 5.14 show BOD and COD removal over a period of twenty four hours. The two media sizes had diurnal profiles taken on different days therefore there was a higher settled sewage strength when 4-8mm Arlita was tested. Again the two media sizes show high removal rates and are similar in their performance. Despite the diurnal variation in sewage strength there appears to be little effect on the performance of the Arlita media.

5.7.3 Suspended Solids Removal

The removal of SS over VLRs of 0.5 - 2kg SS/m³/d is shown in Figure 5.10. There is a straight-line relationship between SS removal and VLR for both media sizes. Looking at Table 5.6 we can see that the effluent SS have improved at HLR 2 compared to HLR 1 despite the increase in SS loading rate from 0.77 to 1.08 kg/m³/d. The removal of SS is dependent on the filtration rate through the filters as well as the biological activity occurring within the filter. This may explain the improvement in solids removal at HLR 2 where there is a slightly increased HLR leading to penetration of solids further down the filter bed, combined with the increased solids load. At both loading rates the 3-6mm Arlita has slightly better percentage removals (94% compared to 92%) which is due to higher entrapment rates in the smaller pore spaces between grains (Stevenson, 1995).

The average effluent qualities for 3-6mm Arlita media are 8mg/l SS (HLR 1) and 6.8mg/l SS, these increase to 10.1mg/l and 9.2mg/l SS for 4-8mm Arlita. These values are again within the consent for Manor Farm STW. The work of Smith & Hardy (1992) produced better quality effluents in terms of SS probably due to the higher HLR leading to deeper penetration of the filter bed.

The SS diurnal profiles (Figure 5.15) show that over a period of twenty four hours there are similar removals for both media sizes again following a straight-line relationship, these appear not to be affected by fluctuations in sewage strength..

The filter bed profiles (Figure 5.20) show a decrease in SS concentration down the bed. The highest proportion of solids appears to be removed at the top of the bed but there is still high removal further down the bed, suggesting that depth filtration is occurring rather than straining. The 4-8mm media has a higher solids concentration at 0.1m than is present in the settled sewage. This could be due to the presence of broken down media or from biofilm sloughing (which could indicate underwashing of the filter). Final solids concentrations are reached at about 1.1 - 1.35m down the filter bed. The pattern shown in all four cases follows a classical filtration curve from filtration theory (Ives, 1982). Both media sizes show slightly better final removals before backwashing,

this may be due to ripening of the filters where previously captured particles act as collectors for further particles (Amirtharajah, 1988).

5.7.4 Nitrification

Rates of ammoniacal nitrogen and TKN removal are shown in Figures 5.11 and 5.12 - there are straight-line removals up to $0.35\text{kg NH}_4\text{-N/m}^3\text{/d}$ for 3-6mm Arlita and $0.3\text{kg NH}_4\text{-N/m}^3\text{/d}$ for 4-8mm, at this point there appears to be some decrease in removal. At both HLRs the smaller media shows a better effluent quality in terms of $\text{NH}_4\text{-N}$ than the larger media. At HLR 1 the 3-6mm Arlita has effluent $\text{NH}_4\text{-N}$ generally less than 1 mg/l (98% removal), this changes at HLR 2 to $2.2\text{mg/l NH}_4\text{-N}$ (94% removal). The 4-8mm Arlita shows lower removal at 95 % and 86% and approximately double the effluent concentrations. The consent $\text{NH}_4\text{-N}$ level for Manor Farm STW is 5mg/l therefore Arlita media produces effluent levels within the consent level at low HLR and OLRs. Again looking at work by Smith & Hardy (1992) we can see that their effluent $\text{NH}_4\text{-N}$ of 2.7mg/l is higher than those for both Arlita sizes at HLR 1. The Arlita media shows better nitrification than that found by Stensel *et al* (1988) for the same $\text{NH}_4\text{-N}$ load but they had a higher BOD load.

Nitrification is dependent on the OLR as well as the $\text{NH}_4\text{-N/TKN}$ loading rate. Lacamp & Bourbigot (1989) found that nitrogen oxidation rates start to decrease when the COD loading rate is $> 4\text{kg COD/m}^3\text{/d}$. The COD loads applied to the Arlita media are below this implying that nitrification should not be inhibited. Paffoni *et al* (1990) found that there was complete ammonia removal below a loading rate of $0.6\text{kg N/m}^3\text{/d}$. BAFs used for nitrification only can remove much higher loads of ammonia. For an upflow Biofor® BAF using Biolite® Pujol *et al* (1996) applied $2.3\text{kg NH}_4\text{-N/m}^3\text{/d}$ at an HLR of $9\text{-}11\text{m/h}$ and found 90% removal.

Diurnal variation of $\text{NH}_4\text{-N}$ removal was investigated for both media sizes. There was again a straight line relationship between ammoniacal nitrogen load and removals. The effect of backwash on nitrification was investigated but there didn't appear to be a relationship between backwash time and nitrification. (Figures 5.30 - 5.31).

Figure 5.30: Effect of Backwash on $\text{NH}_4\text{-N}$ Removal in 3-6mm Arlita (HLR 1)

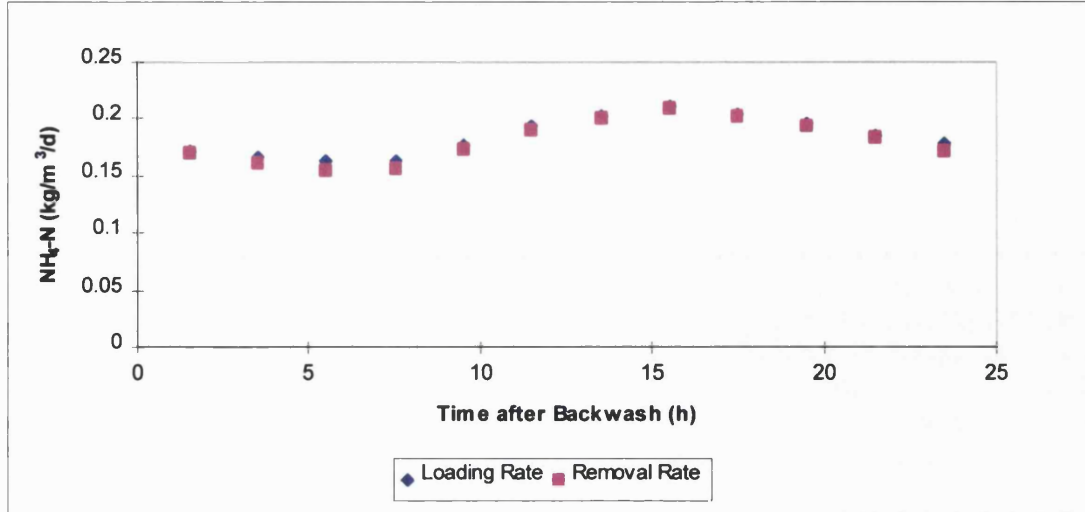
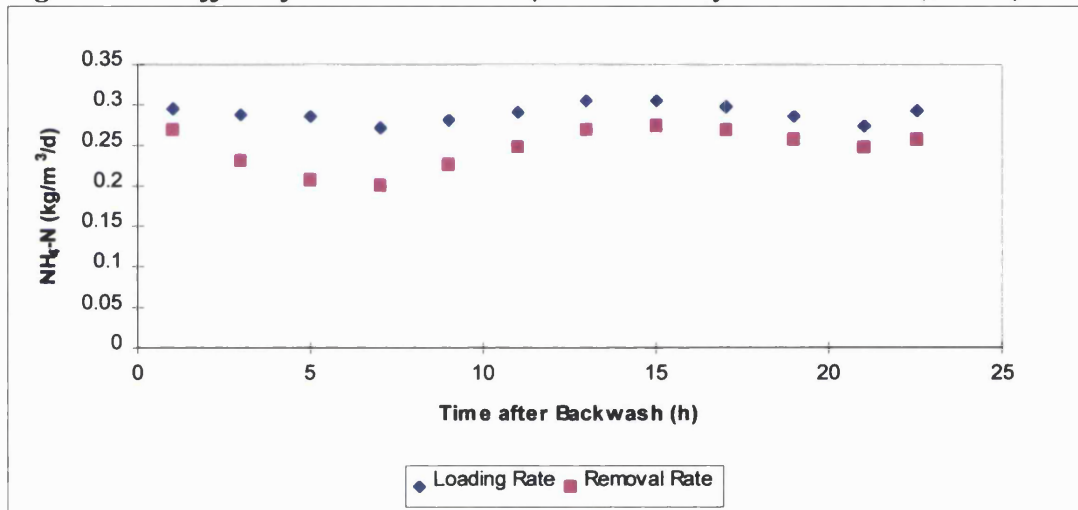


Figure 5.31: Effect of Backwash on $\text{NH}_4\text{-N}$ Removal by 3-6mm Arlita (HLR 2)



Bed profiles of $\text{NH}_4\text{-N}$ and $\text{NO}_2\text{-N}$ were taken at each loading rate for both media sizes, before and after backwashing. There is a general decrease in $\text{NH}_4\text{-N}$ down the depth of the bed for both media sizes before and after backwash. There is high nitrification at the top of the filter bed where it would be expected that nitrifying organisms would be outcompeted by heterotrophs. There is a low OLR however so nitrifying organisms are not oxygen limited. The 4-8mm Arlita shows that before the filter is backwashed nitrification is occurring by a depth of 0.85m but there is a slight increase in ammonia levels after 1.35m. This pattern also occurs after backwash but nitrification does not occur until slightly deeper than 0.85m. The same end point effluent concentration is reached before and after backwashing. The 3-6mm media shows a similar pattern

except that there is no increase in ammonia levels at the bottom of the filter bed, it also has better overall ammonia removals than the 4-8mm media.

The decreasing ammonia concentration down the bed for both media sizes corresponds with an increased proportion of nitrifiers in the biomass. There is slightly less nitrification after backwashing suggesting that the backwashing regime could be removing more nitrifiers than would be considered optimal (or this could simply be a result of the higher sewage concentrations found at this point).

The profiles actually show a similar pattern to that found in purely nitrifying systems where at the top of the bed (in downflow filters) the process of nitrification is oxygen limited whilst towards the bottom of the bed there is ammonia limitation.

The levels of nitrite in sewage was low in all cases (although again average concentrations were higher in samples taken after backwashing). Nitrite profiles (Figure 5.19) show that in both cases before backwashing nitrite increased until a depth of 0.85m due to increased nitrification, before a decrease of the $\text{NO}_2\text{-N}$ caused by conversion of $\text{NO}_2\text{-N}$ to $\text{NO}_3\text{-N}$. Values were again higher after backwashing suggesting a decrease in the conversion of $\text{NO}_2\text{-N}$ to $\text{NO}_3\text{-N}$ caused by removal of nitrifying organisms.

5.7.5 Overall Effluent Quality

In all cases the 3-6mm media shows better effluent quality than the 4-8mm media. This agrees with work by Stensel *et al* (1988) who found that 'lower average hydraulic application rates and loadings had to be used to achieve similar effluent quality with the larger media'. Also Paffoni *et al* (1990) found better nitrification in 2-4mm media compared to 3-6mm media.

Overall results are comparable to the full-scale SAFE process (Smith & Hardy, 1992) as well as other BAF processes (eg: Colox BAF, Fergusson, 1992).

5.7.6 Biofilm Growth

The biomass profiles (Figures 5.21 - 5.22) show that there is approximately 0.006kg biomass/kg media before backwashing. The pattern after backwashing suggests that solids are slightly lower throughout the bed but there is a slight increase at the top of the 4-8mm filter. This suggests that some of the solids are not being washed out of the bed properly. The values are fairly low but this may simply be due to the low loading rates being investigated combined with frequent backwashing. There are no obvious patterns between media size, bed depth and biomass concentration. This could be due to the method of sampling where the bed is fluidised in order to use the auger leading to media being mixed between the different depths.

Scanning electron micrographs of media taken from different bed depths for each media size show the presence of biofilm on the media. It was very difficult to see differences due to bed depth, media size or in relation to backwashing. Figures 5.32 and 5.33 show biofilm coverage and a species of ciliated protozoan which was found on most samples.

Figure 5.32: Biofilm Coverage on Arlita Media

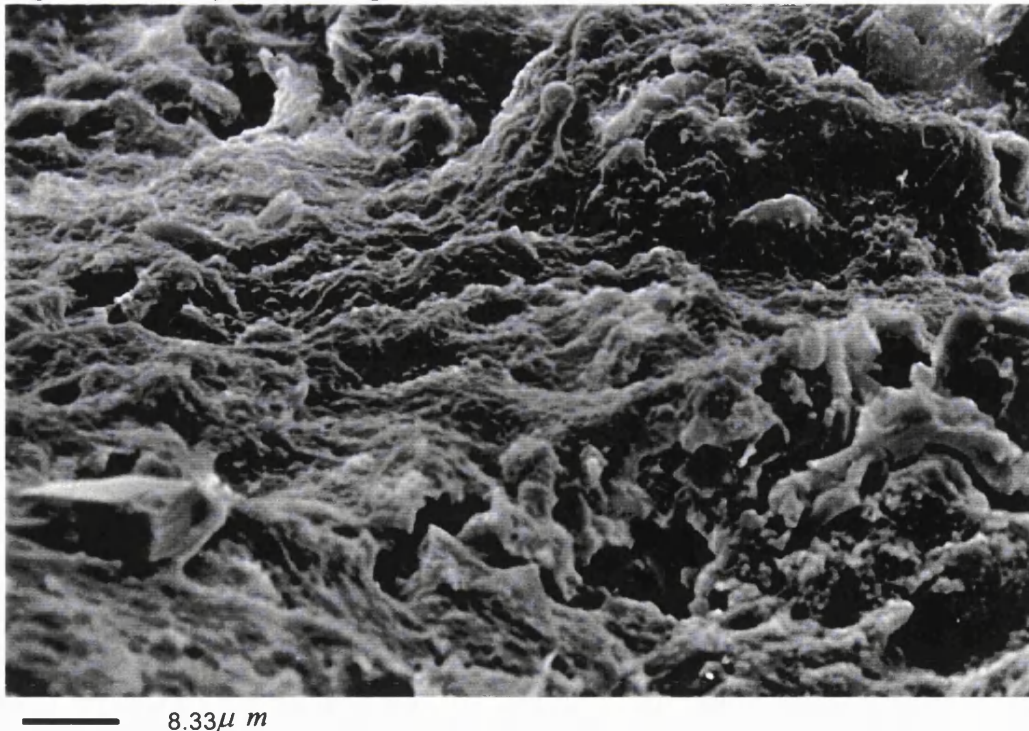


Figure 5.33: Species of ciliated protozoan on Arlita Media



5.7.7 Headloss Development

Measurements of water head development were taken down the filter beds at different times after backwashing. After twenty four hours the filters were not flooded with head height being approximately 0.25m. This could have been allowed to increase even further but the columns were washed on time (i.e. every 24 hours) rather than head build-up due to the lack of automated backwash. The head build-up was slightly higher for the smaller media (0.25m) than the larger media (0.22m) at HLR 1 (not measured at HLR 2), this was expected as the smaller media has smaller pores which therefore become clogged more quickly than large pores (Stevenson, 1995).

There were some problems with the data for HLR 2, for instance the head was higher at a depth of 0.35m than at 0.1m for both sizes of media. This could be due to air bubbles in the manometer tubing or from media blocking the sample port rather than being an actual measure. This means the headloss throughout the bed has not been calculated as there would appear to be a negative value. There did appear to be a gradual decrease in head down the bed, this again corroborates the suggestion from the SS profiles that depth filtration is occurring rather than straining.

5.7.8 Backwashing and Sludges

During backwashing at both loading rates the backwash liquors were collected from both media sizes. The backwash SS profiles (Figure 5.23) in all cases show a peak solids removal after 60 seconds of combined air and water wash. This is followed by a gradual decrease in solids removal until the end of the rinse phase. In Figure 5.24 we can see the cumulative solids removal. In all cases at the end of backwashing we can see that the solids curve has not completely leveled off so a longer rinse phase may have been appropriate to ensure thorough solids removal. This graph also shows that a larger volume of water was used for backwashing the filters at the higher HLR. The 3-6mm Arlita was washed with a water rate of 40m/h with the total volume used being equivalent to 1.7 filter bed volumes. The cumulative amount of solids removed by backwashing was approximately 0.25kg and 0.28kg (Figure 5.24). A water volume equivalent to 2.1 bed volumes was used to wash the 4-8mm Arlita with a water rate of 50m/h. The total solids removed were 0.28kg and 0.33kg. It can therefore be seen that a higher proportion of solids was removed from the larger media than the smaller media at both loading rates - this is opposite to what was expected. The higher removal rate could just be a function of the higher wash rate being used for the larger media or could possibly be due to there being higher solids accumulation/biomass growth on the larger media. Looking back at the biomass profiles there was a slightly higher proportion of biomass on the larger media at HLR 1 before and after backwash but at HLR 2 the biomass values were fairly similar for both media sizes. The smaller media was probably underwashed and would become clogged in time, therefore both media sizes should have been washed using the same backwash rates.

Smith & Hardy (1992) found that 1kg of solids were removed during backwash for every kg of BOD removed during filter operation. A similar value of 0.8 - 1.0 kg solids was found by Pujol *et al* (1996). The values for Arlita are similar, between 0.71 - 1.1kg SS removed/kg BOD removed.

As well as the amount of solids removed by backwashing the volume of water used is an important consideration. Stensel *et al* (1988) used 7-10% of the treated effluent for backwashing BAFs at similar loading rates to those in this study. In this study high effluent volumes were used during backwashing, these were between 20 and 34%. The

reason for these high percentages was that fairly high water rates were used to induce collapse-pulsing of the media during backwashing but the filters were not left until there was high head build-up before the next backwash. The filters could probably have been left for three days in between washes and this would have decreased the percentage of effluent used.

Stensel *et al* (1988) found that backwash requirements were significantly reduced by a change to a large media size. If the two sizes of Arlita media were washed on a head basis rather than time the 4-8mm media should need less backwashes than the 3-6mm media.

When the backwash liquors were settled out there were problems with floating sludges after 30 minutes settling time so a couple of co-settling tests were carried out (using sewage and backwash liquors). These showed that when mixed with settled sewage the sludge settling characteristics were good enough that there would be no problems in treating the backwash liquors. The work of Upton & Churchley (1996) found that BAFs had sludge typical of high rate sludges with a volatile proportion in the order of 80%. It was shown that this provided no particular operational problem for treatment of the sludges. The percentage volatile solids for Arlita were also found to be in the region of 80%.

The sludge data for BAF sludge on its own does not show anything conclusive with all the data having fairly high standard errors (Table 5.8). Any change in organic loading rate, hydraulic loading rate, temperature, timing of backwash etc can affect the quality of sludge produced. The suspended solids for backwash liquors and sludge appear to be similar for HLRs 1 and 2 for each media, with the larger media having a lower average backwash SS than the small media. This shows that the higher cumulative solids removal for the 4-8mm Arlita is just a function of the larger volume of washwater used.

5.7.9 Oxygen Transfer

Off-gas analysis was carried out at HLR 2 for both media sizes in order to determine the efficiency of oxygen transfer to the biofilm. The operational oxygen transfer

efficiency (OTE) is shown in Figure 5.25 for three different air flow rates. Clean bed tests were not carried out but it has been shown that the presence of media alone will increase the OTE (Fujie *et al*, 1992). The smaller media size appears to have lower efficiencies (3-6%) than the large media size (4-8%). The opposite would be expected as smaller media should have higher biomass available to take up oxygen due to the large surface area to volume ratio. The smaller void spaces should also cause bubble size to decrease leading to a large interfacial area for the volume present and a slower rise rate or gas hold-up, they will also provide a more tortuous path for air bubbles to travel through allowing more contact time between the biofilm and air and therefore more oxygen uptake.

The values of oxygen transfer found in Arlita are comparable to those found by Harris *et al* (1995) for expanded shale running at a low OLR. (At higher organic loading rates a general increase in operational OTE would be expected at all air flow rates, but this was not investigated for the Arlita media). Stensel *et al* (1984) also observed oxygen transfer efficiencies of up to 9.2% for a vitrified clay media and concluded that granular media BAFs provide a tortuous path for air bubbles and therefore hinder the free upward flow of bubbles leading to an increased transfer efficiency. In this study the efficiencies of both media decreased at higher air flow rates. The pattern of improving operational OTE with decreasing air flow has also been shown in other work (Lee & Stensel, 1986; Harris *et al*, 1995). At a low air flow rate the biofilm becomes partially oxygen depleted and therefore makes better use of any available oxygen, any gas held within the bed is also replenished less frequently and the oxygen is utilised more fully. The longer residence time of air bubbles also improves OTE. Reiber & Stensel (1985) found that there was little further response to increasing air flows above a flow of 23m/h.

The OTE's corrected to zero dissolved oxygen are used to compare different systems, corrected OTEs are higher than operational OTE's (Figure 5.26). It can be seen that when corrected the smaller media has higher efficiencies at the first two air flow rates than the large media but at the highest air flow rate the larger media appears to have the higher efficiency. This pattern is reflected in the oxygenation capacity of the media with the small media having higher values at the first two air flow rates and the large

media having higher values at the last air flow rate. The operational oxygenation capacity observed for 4-8mm Arlita is close to those seen for expanded shale (Harris, 1994). Table 5.9 shows the estimated oxygen demand and actual demand for both sizes of media. The stoichiometric methods used for estimating oxygen quantities suggest that wastewater treatment requires 1kg O₂/ kg total BOD (tBOD) applied and 4.2kg O₂/ kg NH₄-N removed. Work by Stensel *et al* (1988) showed a requirement of only 0.5kg O₂/ kg tBOD applied, this has been used in this case to estimate oxygen demand. The work of Harris (1994) used a value of 4.5kg O₂/ kg NH₄-N removed, therefore biomass assimilation of nitrogen was not accounted for.

Table 5.9: Oxygen Demand (Load 1.0kg BOD/m³/d 0.27kg NH₄-N/m³/d)

Media Size (mm)	Ammonia Reduction (%)	Estimated Demand (kg O ₂ /h)	Actual Demand (kg O ₂ /h)
3-6	94.2	0.025	0.013
4-8	92.3	0.024	0.021

The 4-8mm Arlita shows an actual oxygen demand that is close to the estimated demand. The 3-6mm Arlita has an actual demand that is half of that estimated, this suggests filter blockage or channelling of air. Some of the difference between estimated and experimental oxygen demand could be due to denitrification occurring but this has not been calculated.

Dissolved oxygen profiles were also taken of the filter beds during off-gas analysis. The 3-6mm Arlita had values of approximately 6mg/l DO at ports 1-3 , this increased up to 10 mg/l at port 5 before decreasing in the effluent to 4 mg/l. The 4-8mm Arlita increased from 6 mg/l up to 10 mg/l at port 3 and then gradually decreased again to a value of 3 mg/l in the effluent. These values are high enough for oxygen transfer to the biomass. The DO profile for 4-8mm Arlita shows the expected relationship with bed depth (See Harris, 1994) but the 3-6mm Arlita does not. This could again indicate a blockage of the process air grid or channeling through the filter bed which could explain why the OTE is lower than expected.

5.8: Conclusion - Overall Comparison of Arlita Media

The general effluent data for filter operation at low HLR and OLRs show that both sizes of Arlita media have good performance and are comparable to other media used

for the BAF process. At these low loading rates the two sizes of media produce comparable effluent qualities in terms of BOD, COD and SS but there is better nitrification in the smaller media. An increase in loading rates would probably lead to a deterioration in performance for both media sizes with the 4-8mm media expected to show much poorer effluent quality than 3-6mm media especially for $\text{NH}_4\text{-N}$ and TKN.

The two media sizes show similar concentrations of biomass, headloss development and sludge production. The backwashing regimes were carried out on a time basis rather than according to headloss of the filters therefore the benefits of larger media have not been seen in this instance. If the filters were left to flood before backwashing, the larger media would be expected to need fewer washes in a week and would use less effluent and energy for backwash requirements.

The oxygen transfer rates are slightly better in the 4-8mm media than the 3-6mm media which is opposite to expected. The most feasible explanation is that the 3-6mm media had a clogged bed or problems with the process air grid.

Overall at the low HLR and OLRs investigated and with the backwash regimes used in this study for Arlita media there appeared to be little difference between the two media sizes. An increase in loading rates would probably show any differences between the 3-6mm and 4-8mm media.

6.0 PILOT SCALE PERFORMANCE OF LYTAG MEDIA

Methodology

6.1: Introduction

A second media was chosen for use at pilot scale due to the problems involved in supply of different size gradings of the Arlita media. The Lytag media was chosen for its low attrition/ friability and high porosity which help counterbalance the high fluidisation velocities required for backwashing. Also important was the fact that it was possible to gain a number of specially requested media size gradings from the suppliers.

6.2: Methodology

Most of the experimental work completed for Arlita media was repeated or slightly modified for the pilot scale use of Lytag. The pilot rig was only different in that four columns were used instead of two columns and the sampling ports at a depth of 1.35m were modified with solenoid valves attached to timers to enable composite samples to be taken.

6.2.1: Media Utilised

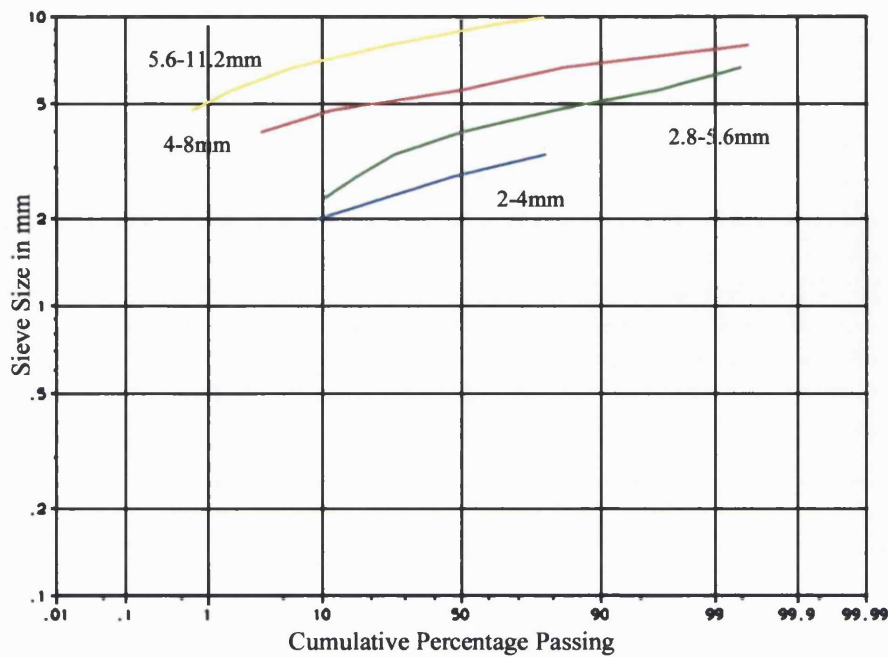
Again each column had a supporting layer of gravel filling the support section of the column. The media utilised was a pulverised fuel ash - Lytag, supplied by Boral Lytag. Each column had media of a different size range (2-4mm, 2.8-5.6mm, 4-8mm and 5.6-11.2mm) filled to approximately 1.6m from the top of the gravel layer. The size range of the four different media were chosen based on British Standard sieve sizes and each had a size range of five sieve sizes.

6.2.2: Sieve Size Analysis

Table 6.1: Sieve Size Analysis of Lytag

Media Size (mm)	Hydraulic Size (mm)	d₅ (mm)	Effective Size d₁₀ (mm)	d₆₀(mm)	Uniformity Coefficient	d₉₀(mm)	d₉₅ (mm)
2-4	2.74	1.9	2.1	3.1	1.48	3.5	3.55
2.8-5.6	3.67	2.3	2.4	3.8	1.58	5.1	5.5
4-8	5.63	4.2	4.7	5.8	1.23	6.9	7.2
5.6-11.2	8.75	6.4	7	9.3	1.33	10.5	11.2

Figure 6.1: Sieve Analysis of Lytag



6.2.3: Specific Surface Area and Internal Porosity

The data for SSA and porosity as calculated by Bradford University is given in Table 6.2.

Table 6.2 : Surface Area and Porosity Data

Media (mm)	Size	Pore diameter (μm)	BET SA (m ² /g)	Envelope Density (g/cm ³)	Grain Porosity (m ³ /m ³)	Total SSA/grain (m ² /m ³)
2-4		44.5	0.829	1.519	0.025	1.26
		2.3			0.156	
		0.01			0.338	
2.8-5.6		44.5	1.155	1.495	0.012	1.73
		2.4			0.155	
		0.01			0.34	
4-8		44.8	1.251	1.53	0.011	1.8
		2.4			0.143	
		0.01			0.311	
5.6-11.2		45	0.838	1.476	0.011	1.24
		2.4			0.165	
		0.01			0.333	

All media sizes have similar densities but there some are differences between media sizes, the 2-4mm and 5.6-11.2mm media have similar BET SA and SSA/media grain as do the 2.8-5.6mm and 4-8mm media. The smallest media has the highest grain porosity if all pore sizes are considered but grain porosities are all close if looking at pore sizes of < 2.4 μ m.

6.2.4: Minimum Fluidisation Velocities

Minimum fluidisation velocities (Table 6.3) for the four Lytag media samples were calculated from the Carman-Kozeny equation.

Table 6.3: Theoretical Minimum Fluidisation Velocities

Media Size (mm)	Temp °C	V_{mf} (Wen & Yu, 1966) (m/h)	V_{mf} (Coulson & Richardson, 1991) (m/h)
2-4	8	93	45
	15	97	52
	25	103	66
2.8-5.6	8	129	80
	15	133	92
	25	138	118
4-8	8	162	189
	15	165	218
	25	169	279
5.6-11.2	8	212	456
	15	214	525
	25	217	673

The two equations used to calculate fluidisation velocities give different results for the different media sizes. The Wen & Yu equation predicts higher V_{mf} s for the smallest media sizes than Coulson & Richardson, whilst the opposite is true for the largest media sizes.

6.2.5: Friability

Table 6.4: Sieve Size Analysis of Lytag After Friability Tests

Media Size (mm)	Hydraulic Size (mm)	d_{60} (mm)	d_{90} (mm)	d_{95} (mm)
2-4	2.47	2.75	3.5	3.65
2.8-5.6	3.2	3.9	4.9	5.2
4-8	5.1	5.3	6.0	6.8
5.6-11.2	6.64	7.2	9.0	9.8

After the friability test all sizes of Lytag have decreased in their particle size range. As media size increases the Lytag appears to become more friable.

6.2.6: Attrition

An extended backwash test was unfeasible as there was no available equipment with the necessary capacity for the calculated backwash rates. Instead media from each filter was resieved once testing had been completed.

6.3: Plant Operation

6.3.1: Commissioning

The HLR was increased incrementally when grab samples showed effluent NH₄-N levels to be below 1mg/l but this time NO₂-N levels were allowed to decrease to approximately 0.1mg/l. There were problems during commissioning with high effluent ammonia levels even at low HLR and OLRs, these indicated that there was very little nitrification in any of the media sizes. Investigation of bed profiles showed that in all cases there was significant nitrification but the ammonia levels actually increased between a depth of 1.35m and the final effluent depth at 1.6m. There was no obvious explanation for this so it was decided to monitor effluent from both depths throughout the experiment. For this reason the solenoid valves were fitted at a depth of 1.35m - this allowed composite samples to be run and 24 hour profiles to be taken using automatic samplers. During commissioning the filters were washed every 24 hours using regime 1 in Table 6.7.

Again there was no evidence of 'foaming' in the filter but 'sewage fungus' was present throughout commissioning (See Chapter 5).

6.3.2: Operating Conditions

The performance of Lytag was investigated at 4 different HLRs. Each increase in HLR also led to an increase in OLR. The following table shows the average OLRs for each phase of study (based on composite sewage samples).

Table 6.5: Operational Loading Rates

Load	Hydraulic Loading Rate (m/h)	BOD Loading Rate (kg/m³/d)	COD Loading Rate (kg/m³/d)	SS Loading Rate (kg/m³/d)	NH₄ Loading Rate (kg/m³/d)
1	0.5	1.15	2.6	0.76	0.2
2	1.0	2.15	4.39	1.26	0.3
3	1.5	2.71	6.35	2.85	0.48
4	2.0	4.96	10.82	2.95	0.9

At HLR 1, sewage was used from the main treatment works at Manor Farm which was settled in a tank outside the pilot hall. At HLRs 2 - 4 this settled sewage was very strong partly due to a lack of rain (but also due to the addition of brewery wastes to the main works load), therefore it was necessary to add a recycle system to decrease the

strength allowing an increase in HLR without excessively high OLRs. The recycle consisted of a floating submersible pump placed in the effluent collection tank - this pumped effluent into the sewage line via a diaphragm valve and flow meter.

The HLR was increased incrementally between each phase, again when grab samples showed effluent ammonia levels to be below 1mg/l and nitrite levels of approximately 0.1mg/l. At first increases in loading rate were instigated when all media samples showed the decrease in ammonia and nitrite levels but nitrification in the two large media sizes quickly deteriorated. After a couple of weeks the loading rates were increased based on the performance of the two small media sizes.

Although the two smaller media sizes showed some nitrification during the change in loading rate from HLR 3 to 4 the effluent ammonia values did not decrease to less than 1mg/l therefore the load rates were increased every 4-5 days until the new HLR had been reached.

At normal operation the air flow rate was set at 30 l/min to ensure that oxygen was not a limiting factor for biofilm growth.

6.3.3: Backwashing

The original media testing (Chapter 4) indicated that Lytag of 2.8-5.6mm needs fluidisation rates in the realms of 100m/h and therefore backwashing rates in the realms of 40-60m/h when combined with high air rates. The theoretical fluidisation velocities (Table 6.6) are much higher than this for the two large media sizes. If collapse-pulsing was to be determined from the theoretical values the following wash rates would be needed.

Table 6.6: Theoretical Collapse-Pulsing Rates for Lytag Media (at 15°C from Wen & Yu, 1966)

Media Size (mm)	Theoretical V_{mf} (m/h)	CP Rates (m/h)
2-4	97	39-58
2.8-5.6	133	53-80
4-8	165	66-99
5.6-11.2	214	86-128

The theoretical V_{mf} for 2-4mm Lytag is approximately the same as the experimental value for 2.8-5.6mm Lytag and the other media sizes have higher V_{mf} s. These higher water rates require large inputs of energy and would probably lead to high media attrition therefore it was decided that lower rates would be more appropriate.

Whilst commissioning the Lytag media a video was made of each column using an endoscope through Port 5 to see the behaviour of each media size during backwashing. This was to ensure that the problems during commissioning were not due to underwashing of the filter media. The video was made of backwash regime 1 shown in Table 6.7.

Table 6.7: Backwash Rates Investigated

Media Size (mm)	Regime 1			Regime 2			Final Regime		
	Air Rate (m/h)	Combined Rates (m/h)	Rinse Rate (m/h)	Air Rate (m/h)	Combined Rates (m/h)	Rinse Rate (m/h)	Air Rate (m/h)	Combined Rates (m/h)	Rinse Rate (m/h)
2-4 and 2.8-5.6	100	Air - 100 Water - 50	50	75	Air - 75 Water - 40	40	75	Air - 75 Water - 50	50
4-8 and 5.6-11.2	100	Air - 100 Water - 60	60	75	Air - 75 Water - 50	50	75	Air - 75 Water - 60	60

1 - All regimes consisted of 1 min air + 2 mins combined + 2 mins rinse

The video showed that the two smaller media sizes were collapse-pulsing but the two larger ones showed less movement. The media is generally clean but in places large clumps of biofilm could be seen. The lack of collapse-pulsing didn't therefore appear to have too adverse an effect on the two larger media sizes.

It was decided that a slightly lower backwashing rate would still produce enough movement to clean the two smaller media and would produce a greater benefit in terms of preventing attrition of the media and loss of media during backwashing. The rates were therefore decreased in all four columns for HLR 1 as shown in Table 6.7 - regime 2. The columns were also washed less frequently than during commissioning - Monday 9.00, Tuesday 16.00, Thursday 9.00 and Friday 16.00.

After a week of these backwash rates it could be seen that the three smallest media sizes could not last without flooding between the washes on Tuesday afternoon and

Thursday morning so a compromise was reached using an air rate of 75m/h for all media and water rates of 50m/h for the two smallest media and 60m/h for the larger two media (Table 6.7 - final regime). This almost doubled the theoretical run times of the filters.

The columns were backwashed every 32 - 40 hours to prevent solids build-up and subsequent breakthrough in the effluent.

These backwashing rates were again used at HLR 2 . The 2-4mm Lytag was found to have run times of approximately 20 hours but it was not feasible to wash the filters every 20 hours, all filters were washed every 24 hours.

At HLR 3 all filters were washed every 12 hours with the same backwashing rates as used at HLR 1 except that the two large media sizes had their combined and rinse phases decreased to 1.5 minutes each. This was to try and prevent overwashing of the larger media which had much longer run times than the small media.

The same backwashing rates were used at HLR 4 as in Phase 3. Again all filters were washed every 12 hours, although the 2-4mm Lytag was flooding after approximately 10 hours.

6.4:Data

6.4.1: Effluent Quality

Effluent spot samples were taken before backwashing and compared with spot samples from a depth of 1.35m, composite samples were also taken from 1.35m. These were tested for the same determinands as previously investigated for Arlita media (Chapter 5). Bed profiles and 24 hour profiles were also taken - soluble BOD was added to the list of determinands investigated in the bed profiles.

6.4.2: Biomass Samples

Biomass samples were taken using an auger on two different occasions both before and after backwashing, again concentrations were calculated, SEM micrographs were prepared in one instance and microbiology samples were analysed in the other.

6.4.3: Headloss

Data from manometers set at the same depths as the sample ports were recorded in order to determine headloss throughout the filter bed.

A Warren Jones Flow Monitor (WJ460) was used to record the total head of water for each filter. The height of the first backwash overflow pipe was taken to be zero metres of head, with the maximum head being 0.5m at the top backwash overflow pipe. The height of water was measured by the sensors every five seconds and automatically averaged every five.

6.4.4: Backwash Sludge Samples

Once steady-state performance had been reached by the pilot columns the backwash liquors were tested for suspended solids, settleability, and capillary suction time (CST) to see if they are affected by media size. A PFT analysis was not carried out (See Chapter 5) due to variability in results gained from Arlita media and the long wait for results.

6.4.5: Off-Gas Analysis

Off-gas analyses were carried out in the same manner as that used for Arlita media over a range of air flows, covering 1 - 15m/h to see how oxygen transfer is affected by air flow and media size.

6.4.6 Hydraulic Regime

The retention times of each filter were calculated before and after backwashing. To carry out the tests approximately 60g of salt were added to a litre of settled sewage and fed into the top of the column as a pulse input. A conductivity probe attached to a Squirrel logger was used to measure the conductivity of the effluent which was trickling out of the effluent port at the same rate as sewage entering the filter. Readings were logged every 15 seconds and this data was plotted to give residence time distribution (RTD) curves and the peak residence time. The data for twice the theoretical residence time (based on flow rates and filter volume) was analysed to determine mean retention times and the dispersion number (from Levenspiel, 1972).

6.5: Data Analysis

Effluent analyses were carried out by Thames Water laboratories (Chapter 4).

Additional analysis:

Soluble BOD: Samples are first filtered to remove suspended solids followed by Method outlined in "5 day biochemical oxygen demand (BOD₅) 91988", printed by HMSO (ISBN 011 752212-0).

All other samples (biomass, backwash solids, sludge, off-gas analysis) were analysed as for Arlita media (see Chapter 5).

7.0 PILOT SCALE PERFORMANCE OF LYTAG MEDIA

Results: 2-4mm Lytag

7.1: Introduction

The 2-4mm Lytag was the smallest media size investigated in this study. Traditionally small media sizes have been used for nitrification in BAFs, especially in cases where there is no carbonaceous removal allowing removal of ammoniacal nitrogen at high loading rates. The Biocarbhone® process often uses 2-4mm media for nitrification only systems (Paffoni *et al*, 1990; Dillon & Thomas, 1990).

7.2: Steady State Results

7.2.1: Settled Sewage

Tables 7.1 and 7.2 show the concentrations of settled sewage at each HLR and the calculated OLR onto the filter. As has already been mentioned, effluent recycle was used in HLRs 2-4 in order to decrease the strength of the settled sewage, samples were taken at a point after the settled sewage and recycled effluent had been mixed. The use of a recycle meant that any non-biodegradable COD and BOD was being put back onto the filters and therefore the proportion of untreatable COD and BOD was increasing with increasing loading rate.

Table 7.1: Composite Settled Sewage Concentrations

Load	BOD (mg/l)	COD (mg/l)	SS (mg/l)	NH ₄ -N (mg/l)	TKN (mg/l)
1	154.3	346.3	102	26.8	34.2
2	145.6	297.4	84.8	19.9	26.2
3	119	278.8	125.1	20.9	31.9
4	159.6	349.9	99	29.1	38.4

Table 7.2: Loading Rates for Composite Samples

Load	Hydraulic Load (m/h)	BOD Load (kg/m ³ /d)	COD Load (kg/m ³ /d)	SS Load (kg/m ³ /d)	NH ₄ -N Load (kg/m ³ /d)	TKN Load (kg/m ³ /d)
1	0.5	1.17	2.62	0.77	0.2	0.26
2	1.0	2.18	4.43	1.26	0.3	0.39
3	1.5	2.68	6.28	2.81	0.47	0.72
4	2.0	4.81	10.55	2.99	0.88	1.1

The filters were run at four constant HLRs, with VLRs differing according to the strength of the settled sewage. The ideal average OLRs would have been 1.0, 2.0, 3.0 and 4.0 kg BOD/m³/d but there was a large difference between HLRs 3 and 4.

7.2.2: Effluent Quality

Table 7.3 shows the percentage removals of BOD, COD, SS and NH₄-N for each HLR. There is a general decrease in percentage removals for all determinands, with increasing HLR and VLR. The removals of BOD, COD and SS are high at all HLRS but there is a large decrease in the removal of NH₄-N and TKN at HLR 4.

Table 7.3: Percentage Removals by 2-4mm Lytag

Load	BOD Removal (%)	COD Removal (%)	SS Removal (%)	NH ₄ -N Removal (%)	TKN Removal (%)
1	97.5	89.9	94	99	95.9
2	96.6	84.2	85	98.2	92.6
3	94	78.4	79.4	89.9	88.3
4	91.1	79.8	76.5	34.7	42.2

Figures 7.1 - 7.5 show the removals of different determinands for composite samples at a depth of 1.35m. All data from HLR 1 - 4 have been combined to show removals over a range of VLRs.

Figure 7.1: Composite BOD Removals

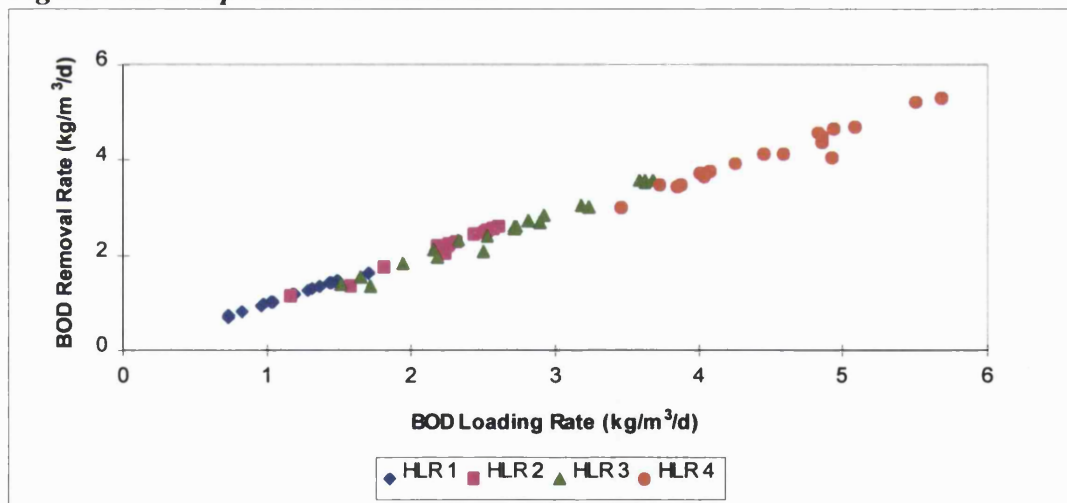


Figure 7.2: Composite COD Removals

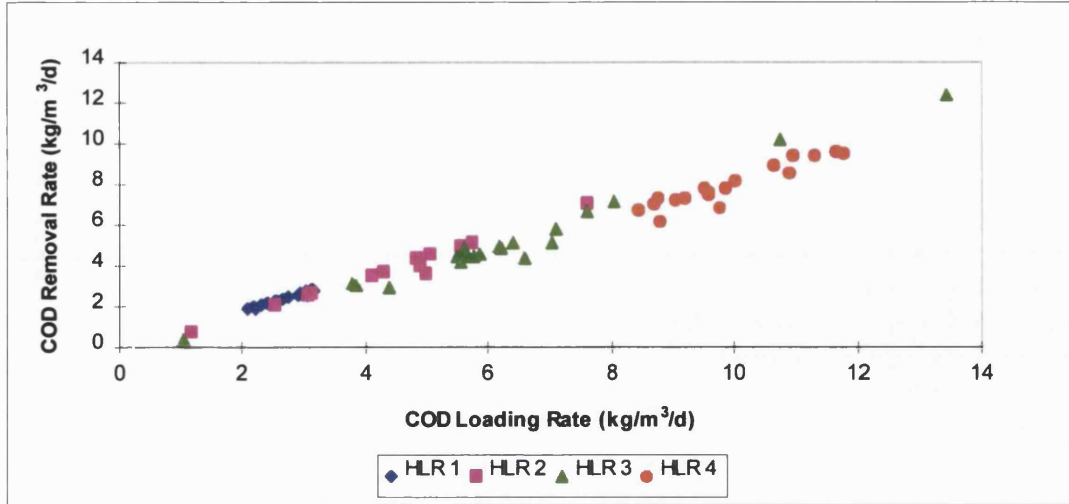


Figure 7.3: Composite SS Removals

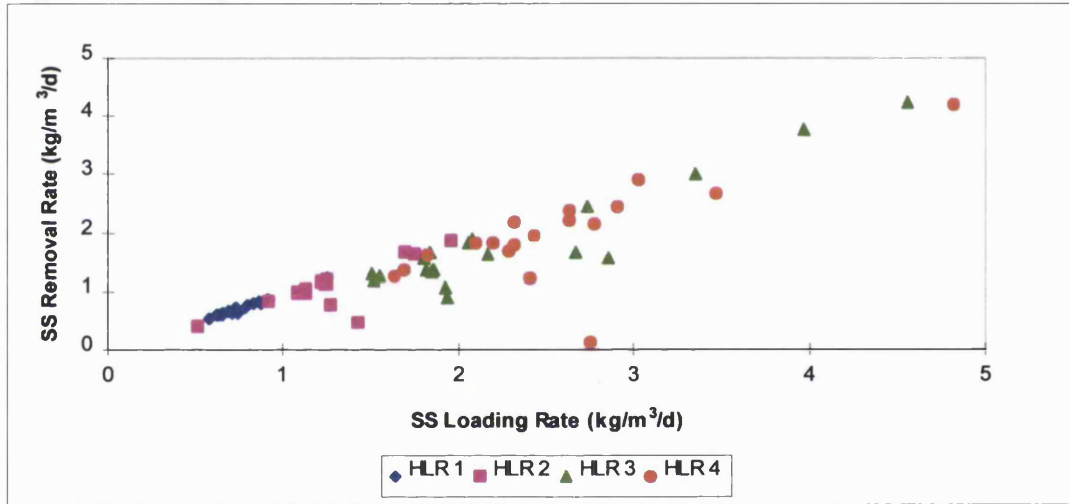


Figure 7.4: Composite NH₄-N Removals

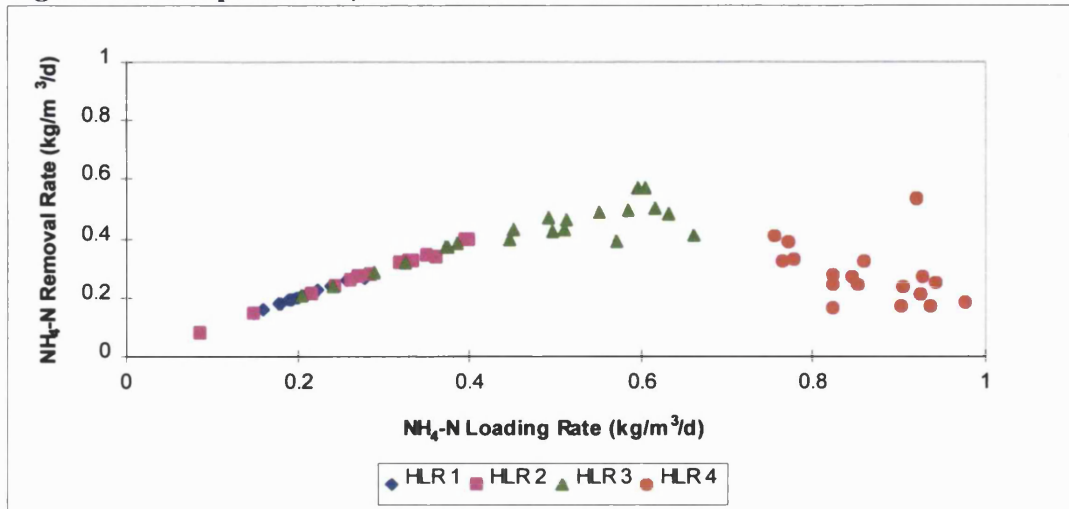
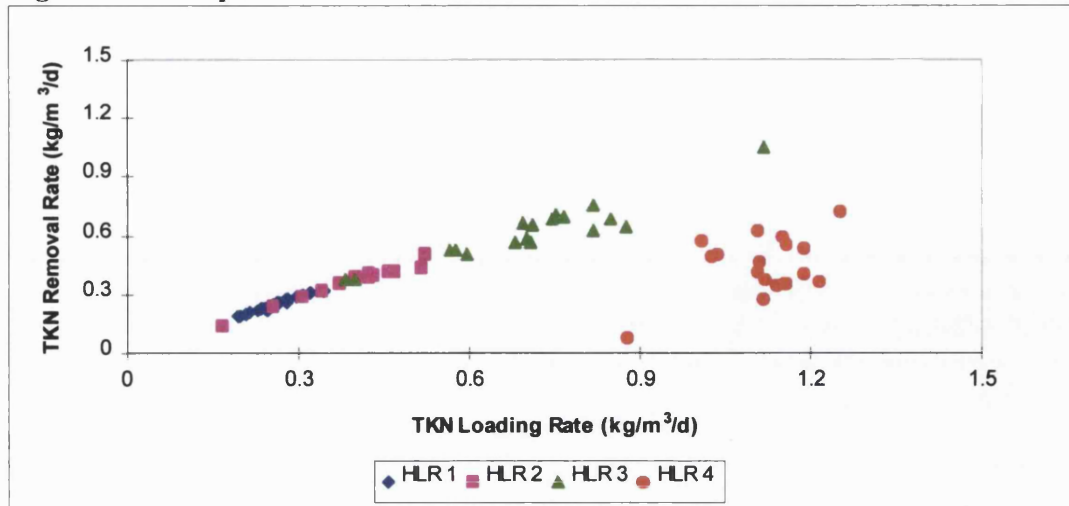


Figure 7.5: Composite TKN Removals



There is a positive linear relationship between loading rate and removal for BOD, COD and SS for the VLRs investigated. The ammoniacal nitrogen removal graph shows straight-line removals to a loading rate of approximately 0.6 kg NH₄-N/m³/d and then removal decreases at HLR 4, (a similar pattern is seen with TKN after 0.9 kg TKN/m³/d). The average effluent results in mg/l are given in Table 7.4.

Table 7.4: Effluent Concentrations for 2-4mm Lytag (Port 5 Composites)

Load	BOD (mg/l)	COD (mg/l)	SS (mg/l)	NH ₄ -N (mg/l)	TKN (mg/l)	TON (mg/l)	NO ₃ (mg/l)
1	4 (3.5)	35 (8.4)	6 (2.9)	0.4 (0.6)	1.5 (0.9)	18.4 (3.8)	18.3 (3.3)
2	4.4 (4.9)	40.6 (17.3)	13 (16.3)	0.3 (0.4)	1.9 (1.2)	15.5 (2.3)	15.2 (2.2)
3	6.4 (4.5)	50.8 (16.5)	20.8 (13.9)	2.5 (2.9)	3.8 (2.7)	13.5 (2.3)	13.1 (2.2)
4	14.2 (7.3)	71.1 (28.9)	25.2 (31.9)	18.9 (4.4)	21.8 (4.2)	3.1 (3.6)	2 (2)

Note: Standard deviations in brackets

The effluent concentrations for BOD, COD, SS, TKN and NH₄-N increase with increasing HLR/VLR whilst TON decreases. There is good effluent quality for HLRs 1 - 3 with SS:BOD:NH₄-N of less than 30:20:5. At HLR 4 the removal of ammoniacal nitrogen is poor (effluent NH₄-N 19mg/l) although SS and BOD removals are still high.

As mentioned previously there were problems with effluent deterioration between sample port 5 and the effluent port. Figures 7.6 and 7.7 compare effluent quality with samples from a depth of 1.35m. There is very little difference in BOD removals but there appear to be slightly poorer effluent NH₄-N removals at 1.6m.

Figure 7.6: Comparison of BOD Removal at 1.35m and 1.6m (Spot Samples)

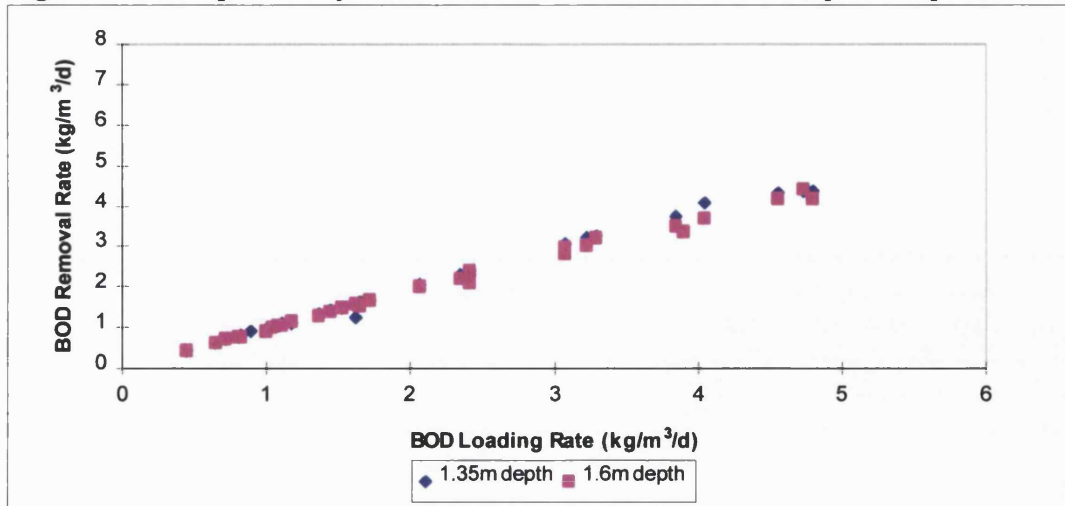
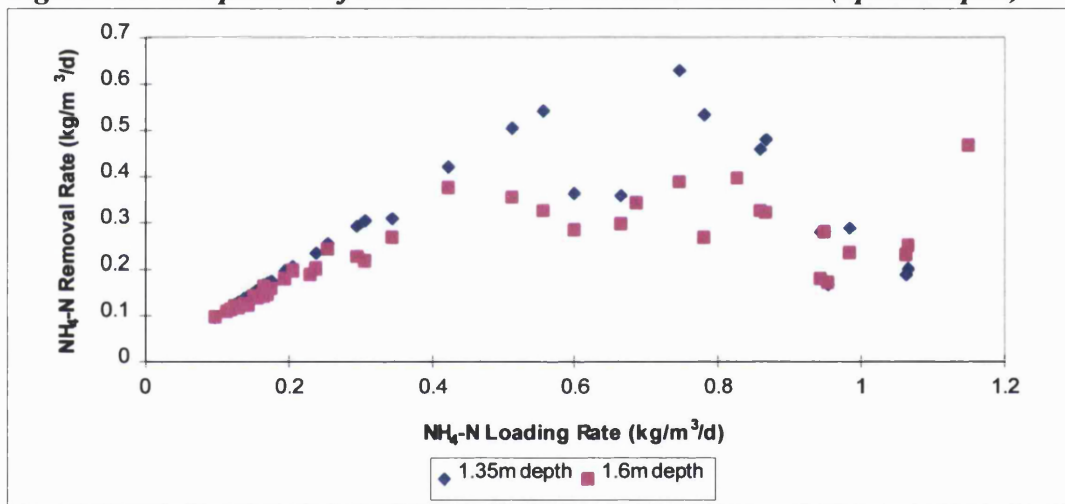


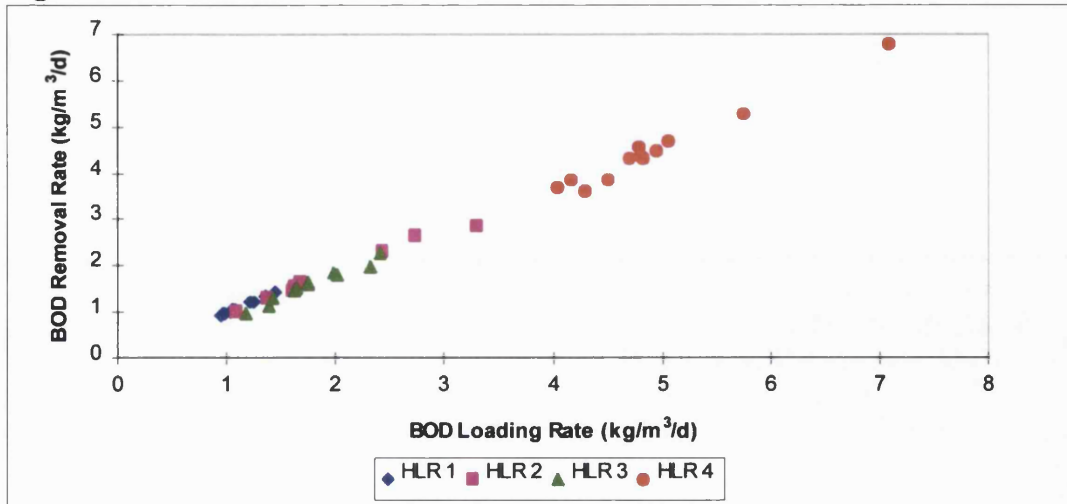
Figure 7.7: Comparison of NH₄-N Removal at 1.35m and 1.6m (Spot Samples)



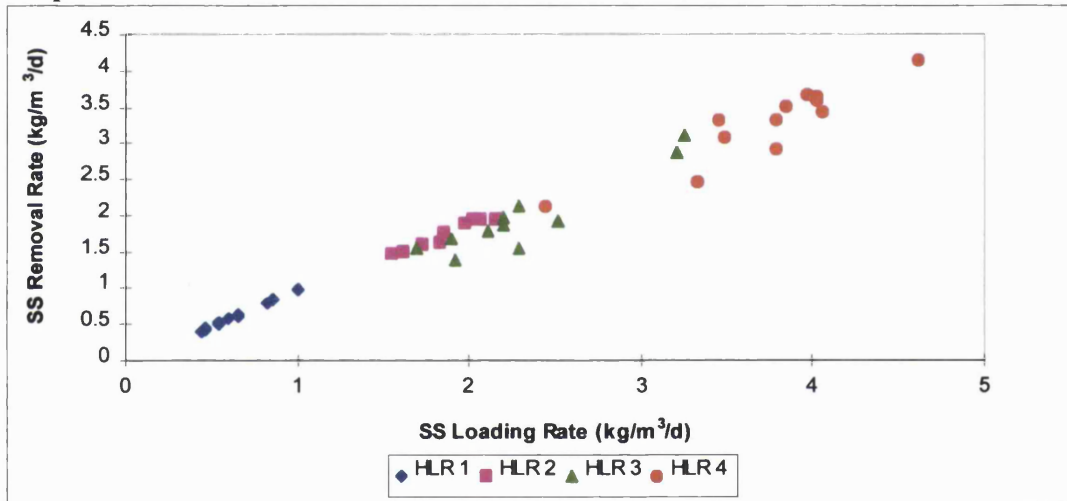
7.2.3: Diurnal Variation

Figures 7.8 - 7.10 show BOD, SS and NH₄-N removals against VLR for samples taken over 24 hour periods. The patterns of removal are similar to those for the composite samples with BOD and SS following straight line removals whilst NH₄-N removals decrease after 0.6kg NH₄-N/m³/d.

Figure 7.8: Diurnal BOD Removals



Graph 7.9: Diurnal SS Removals



Graph 7.10: Diurnal NH₄-N Removal

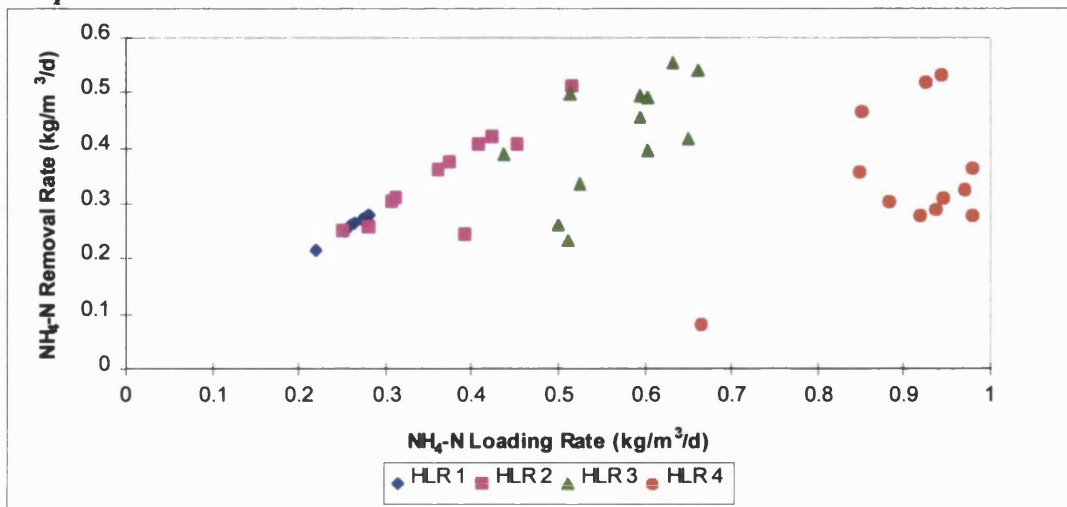


Figure 7.11: Diurnal SS Removal (HLR 1)

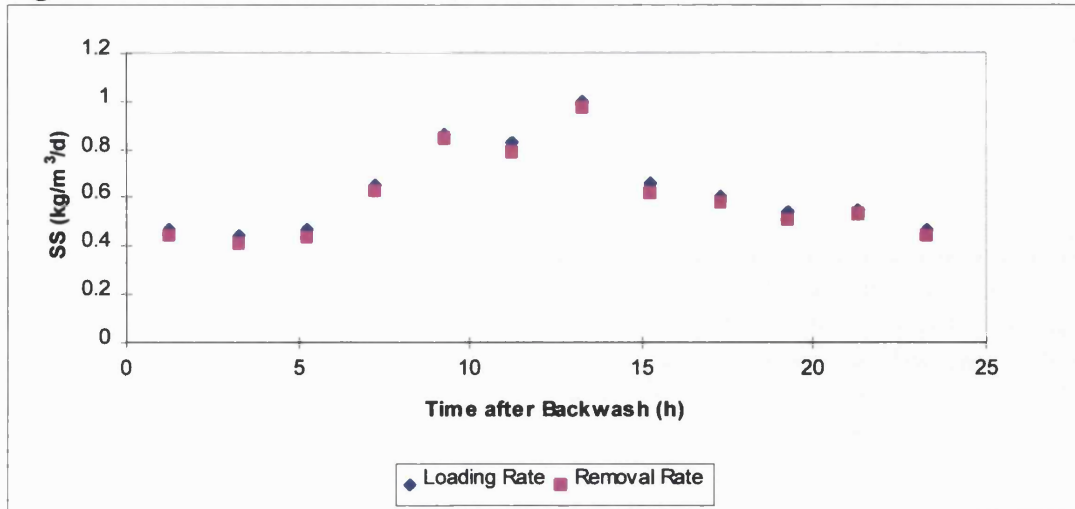
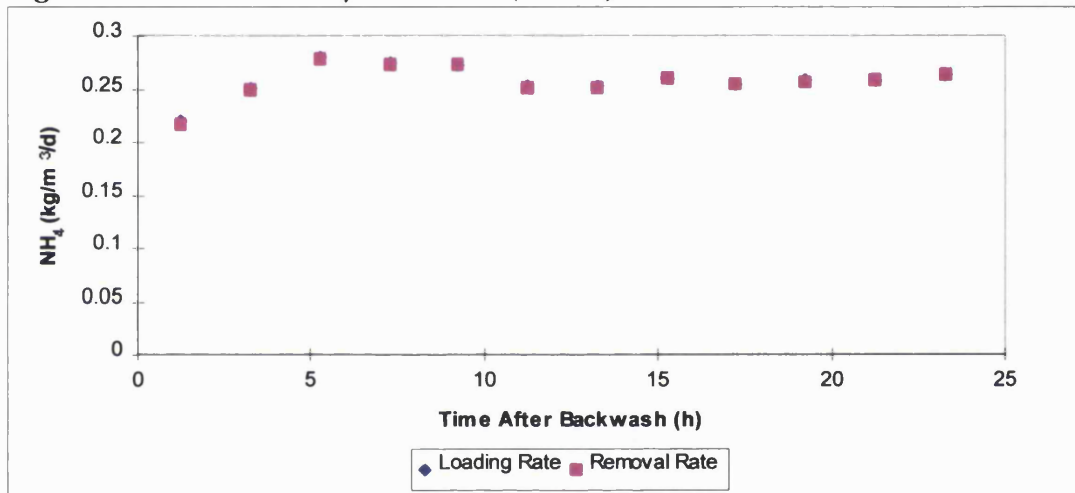


Figure 7.12 : Diurnal NH₄-N Removal (HLR 1)



The effect of backwashing on removal of solids and NH₄-N is shown in Figures 7.11 and 7.12 for HLR 1. The removals appear to follow VLR and therefore appear not to be affected by backwashing at any of the HLRs.

7.2.4: Bed Profiles

Bed profiles were taken for each HLR as shown by Figures 7.13 - 7.18.

The BOD and COD profiles have similar patterns with removal mostly occurring at the top 0.85m of the filter bed except at HLR 4 where the whole bed depth is used for carbonaceous removal. The same relationship is seen for SS removal although at HLR 4 there is a large increase in SS concentration at Port 2 (0.35m depth).

Figure 7.13: BOD Profiles

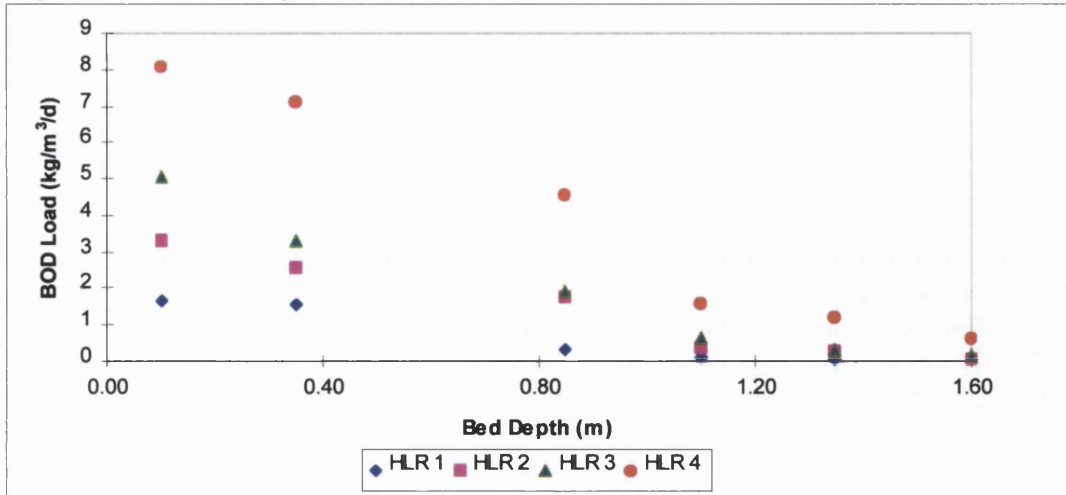


Figure 7.14: COD Profiles

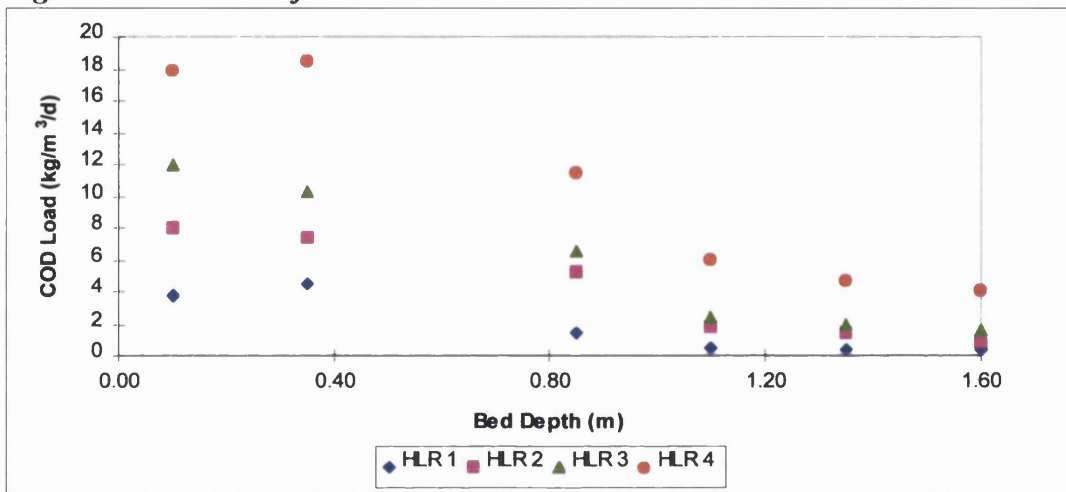


Figure 7.15: Suspended Solids Profiles

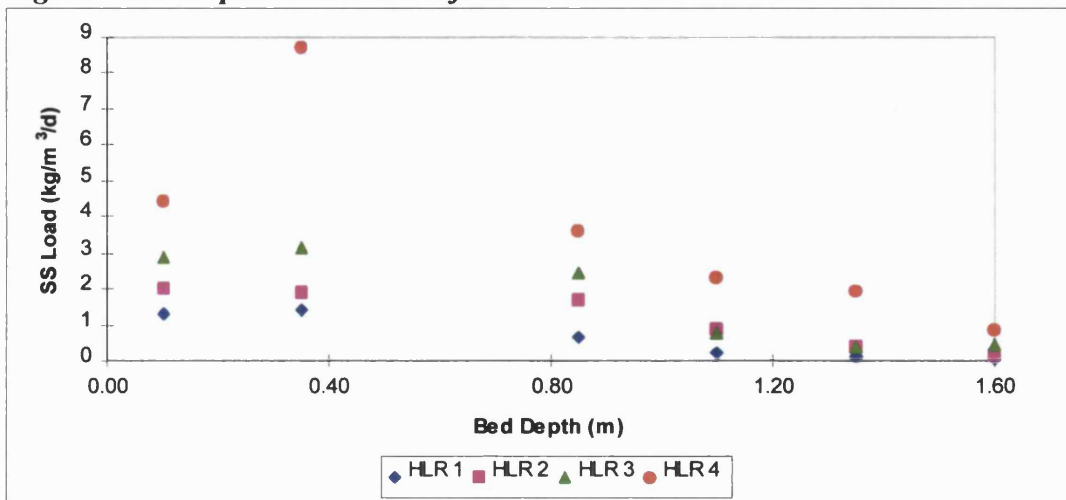


Figure 7.16: NH₄-N Profiles

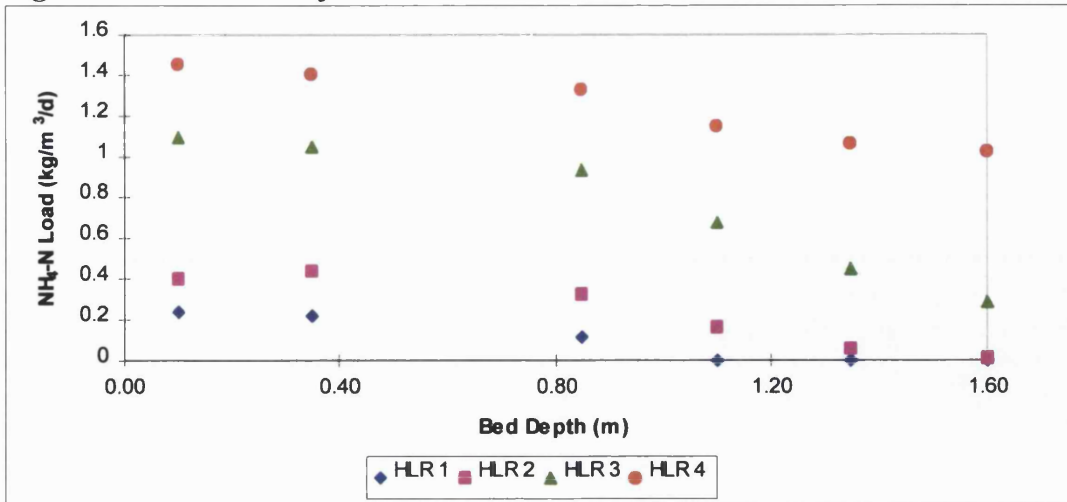


Figure 7.17: TON Profiles

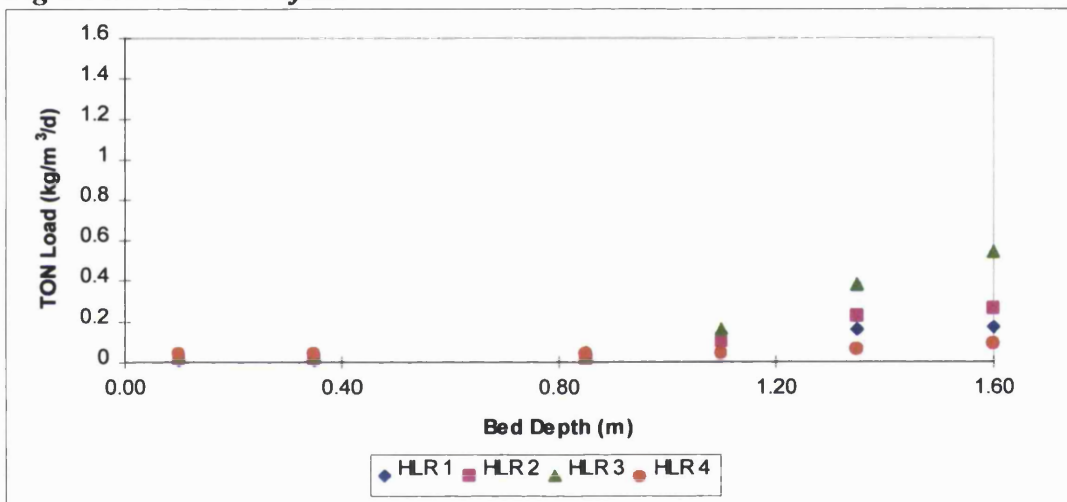
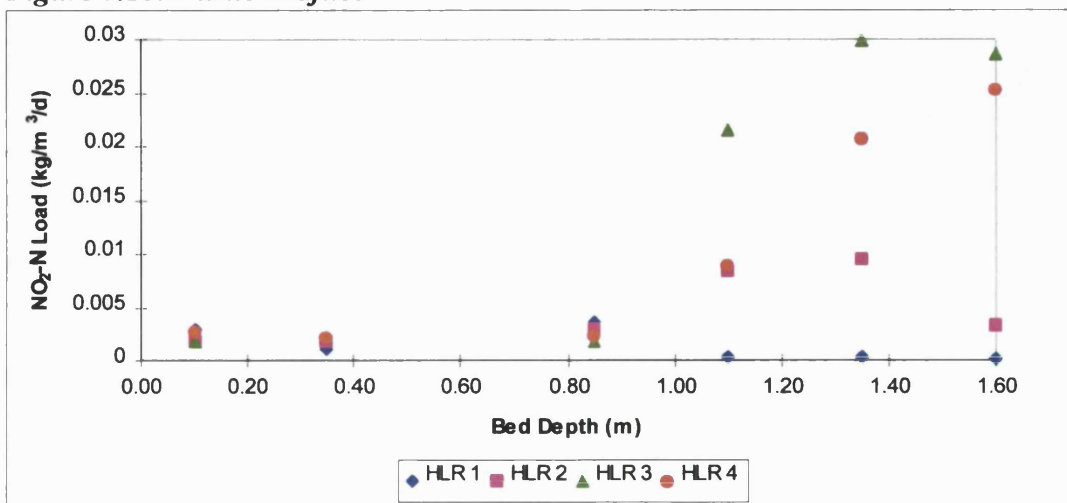


Figure 7.18: Nitrite Profiles



The profiles of NH₄-N removal (and TKN removal) show some removal in the top of the bed where carbonaceous removals are occurring. The bulk of ammoniacal nitrogen removal is at 0.85 - 1.1m depth, this pattern is mirrored in the profile of TON with TON first present at a depth of approximately 1.1m. At HLR 4 there is very little TON in the effluent. Figure 7.18 shows NO₂-N profiles at all HLRs, at HLR 1 most NO₂-N is converted to NO₃-N, but as loading rate increases NO₂-N also increases except at HLR 4 which has lower NO₂-N than HLR 3.

Data from composites was used to gain an idea of the amount of denitrification occurring (Table 7.5) based on removals of TKN, production of TON and assimilation of nitrogen into the biofilm, which was assumed to be approximately 5% of BOD removed. It can be seen that at HLRs 1 - 3 there is a low percentage denitrification occurring. At HLR 4 the percentage denitrification increases significantly to 75% of TON removed from the filter. These are approximate values, an accurate measure could only be gained if nitrogen gas released from the filters was measured.

Table 7.5: Denitrification (Denite)

HLR	TKN VLR	TKN Removed	BOD Removed	N Assimilation	TON Expected	TON Produced	Denite	Denite (%)
1	0.26	0.25	1.14	0.06	0.19	0.13	0.06	32
2	0.39	0.36	2.13	0.11	0.25	0.22	0.03	12
3	0.72	0.62	2.54	0.13	0.49	0.28	0.11	22
4	1.11	0.45	4.12	0.21	0.24	0.06	0.06	75

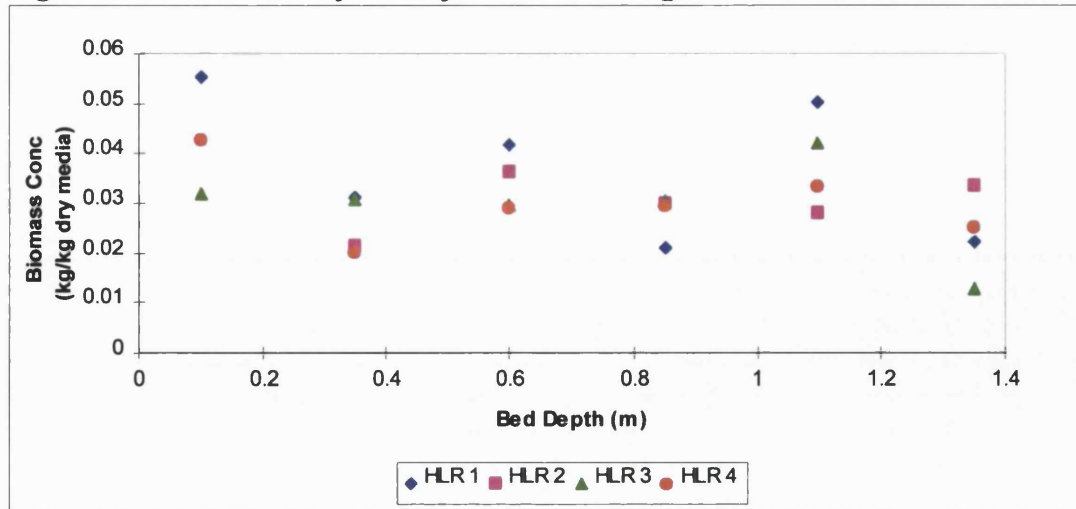
All expressed in kg/m³/d except % denitrification

7.3: Biofilm Growth

7.3.1: Biomass Samples

Figure 7.19 shows the biomass bed profiles for each HLR before backwashing of the filters. The concentrations of biomass are between 0.02 - 0.06kg biomass/kg dry media, there appears to be no relationship between biomass concentration and bed depth or HLR.

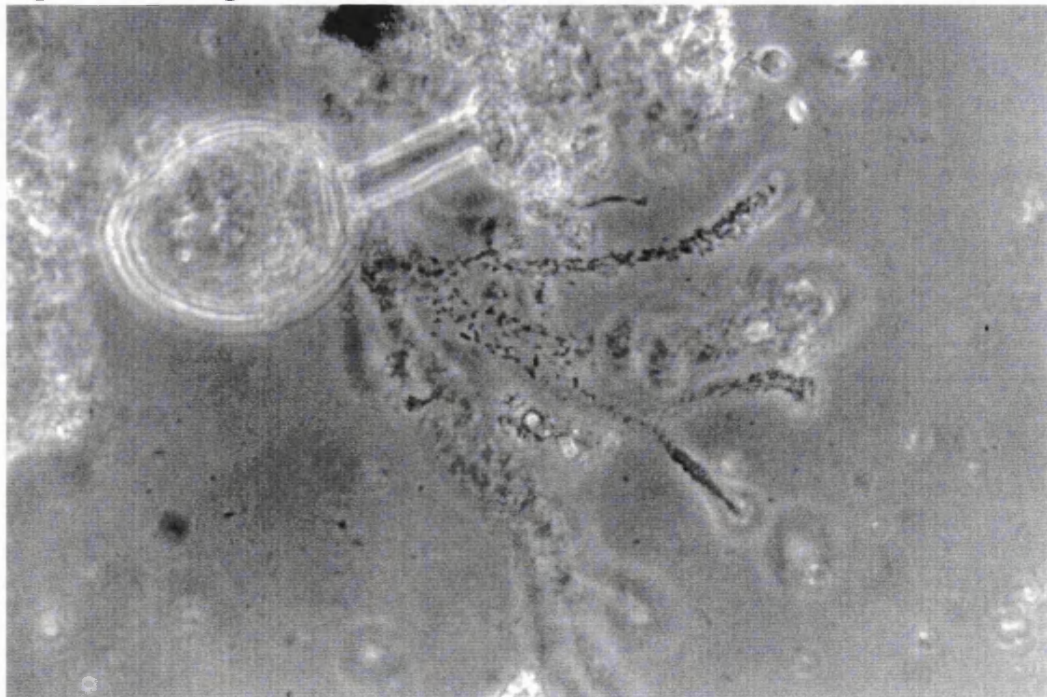
Figure 7.19: Biomass Profiles (Before Backwashing)



7.3.2: Microbiological Analyses

Analyses were taken at each loading rate from the top, middle and bottom of the filter bed. No real difference could be seen between the different samples. Micro-organisms present were *Sphaerotilus natans*, *N.limicola*, Type 021N, Type 1701, Type 0041 and Type 0092 (Eikelboom & van Buijgen, 1981). In all cases slime forming Zoogloea were also present in small amounts.

Figure 7.20: Zooglea [1cm = 0.007mm]



7.3.3: 'Slime' Growth on Media Particles

Photographs were taken of media particles at three different bed depths for each loading rate. The particles appear to be fairly clean with some patches of biofilm present. There were no obvious signs of 'slime' presence or excessive biofilm growth even at the highest loading rate.

Figure 7.21: 2-4mm Media Particles From Middle of Filter Bed (HLR 1)



Figure 7.22: 2-4mm Media Particles From Middle of Filter Bed (HLR 4)



7.3.4: Scanning Electron Micrographs

Again it was difficult to see differences between samples from different bed depths and loading rates. It was possible to see biofilm across the media particles and in most cases there were colonies of a ciliated protozoan species present.

Figure 7.23: Biofilm Coverage on Media Particle [1cm = 5 μ m]

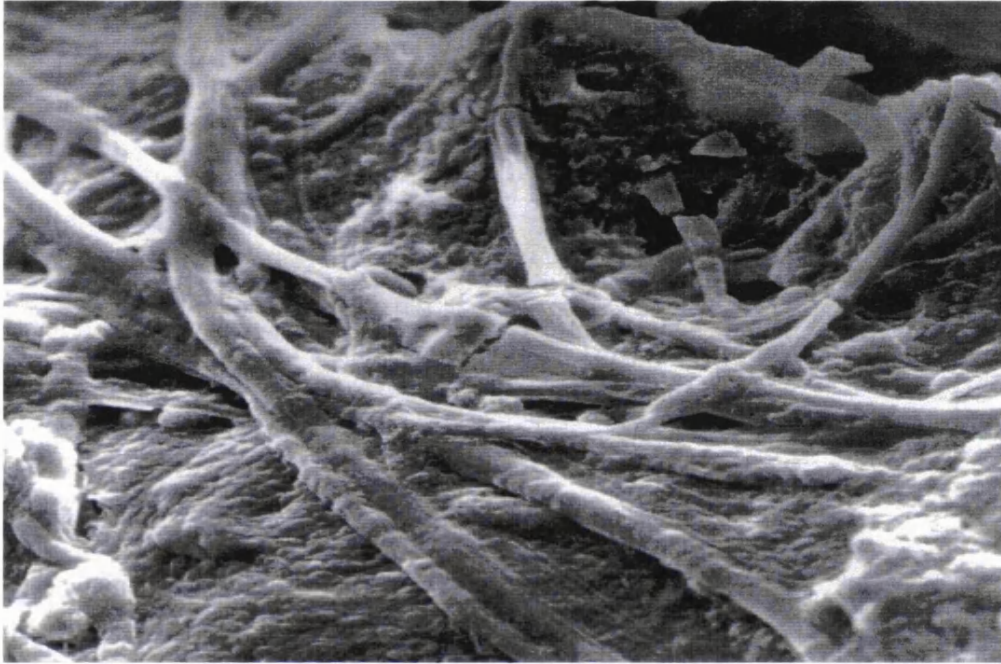
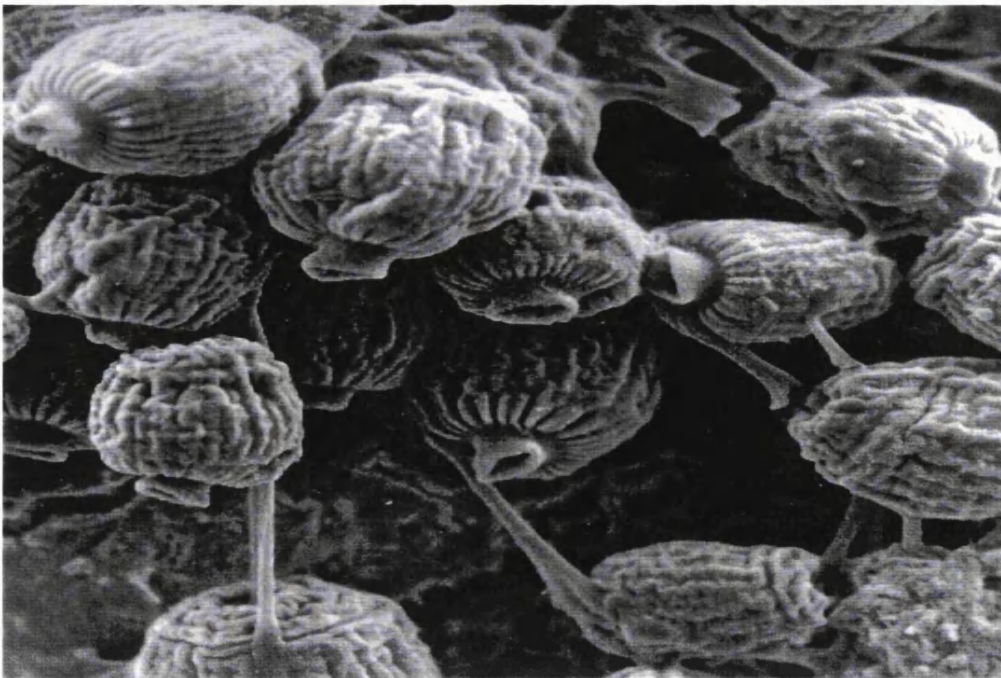


Figure 7.24: Ciliated Protozoan Species on Media Particle [1cm = 10 μ m]



7.4: Headloss

The head build-up for each loading rate was recorded at each manometer point as shown in Figures 7.25 - 7.26 for HLRs 1 and 4. At HLR 1 the filter does not flood until approximately 45 hours of normal operation. From the ranger data we can see there is a low level of head (0.15m) throughout the filter run, after 20 hours there is a gradual development of head which then increases more rapidly after 30 hours. At HLR 4 there is an immediately high level of head (0.3m), due to the higher HLR and gas hold-up, this rapidly increases with the filter flooding after only 12 hours.

Figure 7.25: Head Profile (HLR 1)

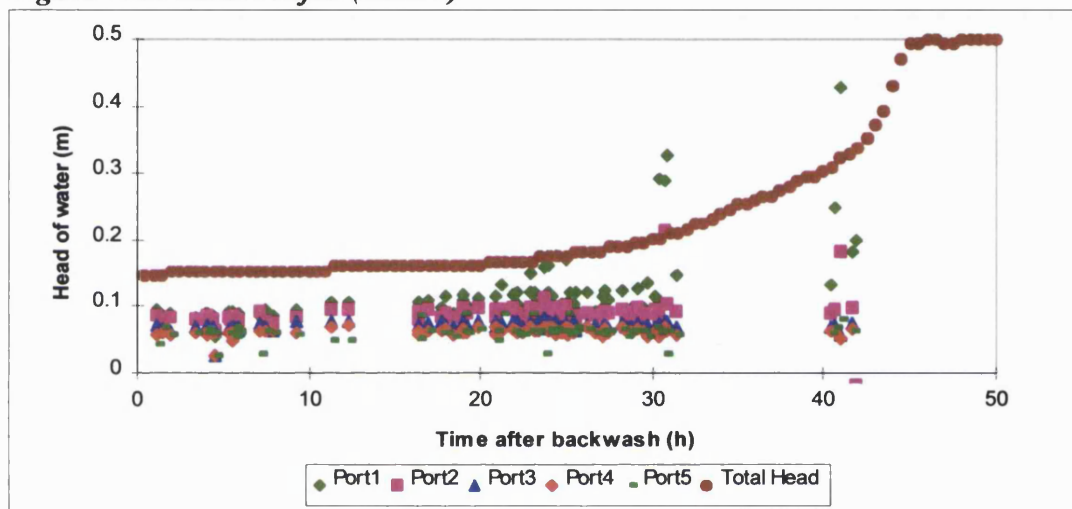
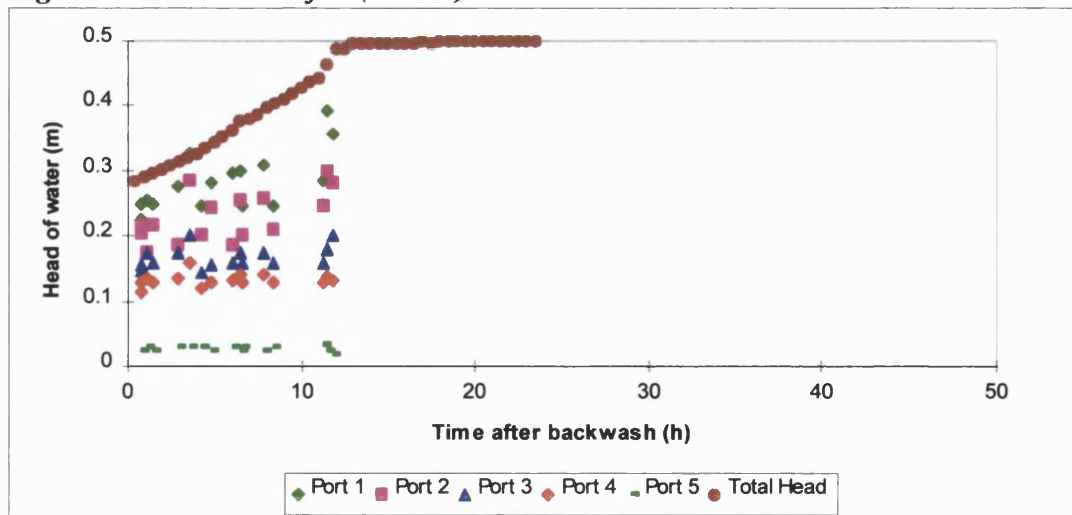


Figure 7.26: Head Profile (HLR 4)



The flood times as given in Table 7.6 show that filter run times decrease with increasing hydraulic and organic loading rates.

Table 7.6: Flood Times from Ranger Data

Load	HLR (m/h)	Flood Time (hours)
1	0.5	30 - 40
2	1.0	20 - 25
3	1.5	16 - 22
4	2.0	6 -10

7.5: Backwash Samples

Backwash liquors were analysed for SS in mg/l and the total solids removed by backwashing were calculated as shown in Figures 7.27 and 7.28. The pattern is the same as that seen previously with the Arlita media with a peak in solids removal (1200 mg/l) after 90 seconds of combined air and water wash, followed by a gradual decrease in solids removal with the water rinse until the solids concentration removed was approximately 200mg/l. At each loading rate there was an average solids removal of 0.4 - 0.55kg per backwash

Figure 7.27: Backwash Profiles

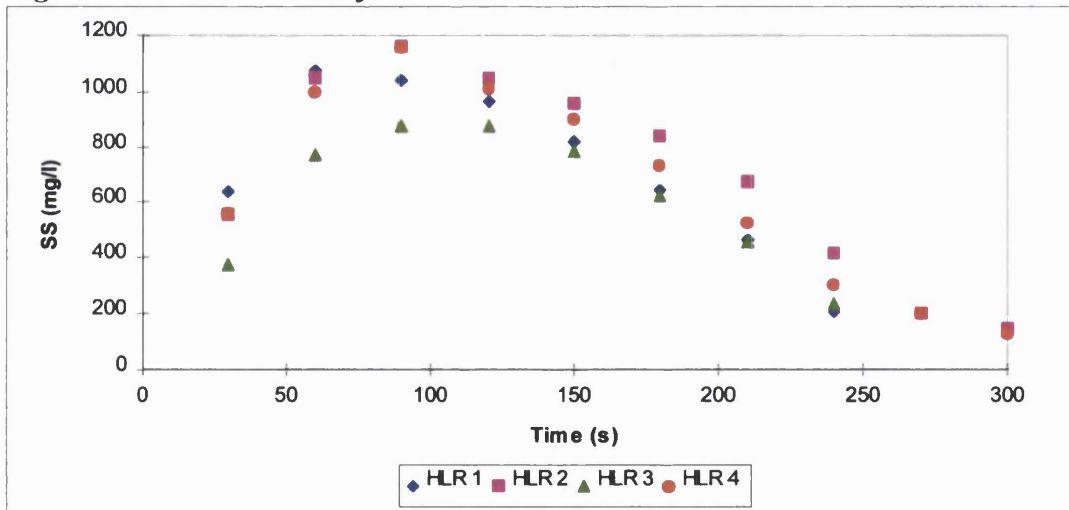
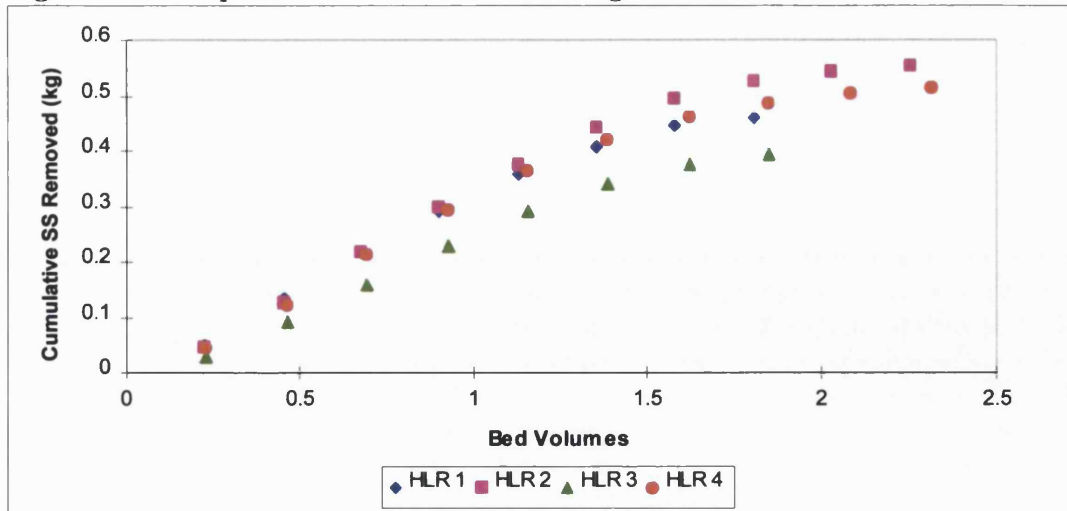


Figure 7.28: Suspended Solids Removed During Backwash



Calculations of total solids removed and effluent reuse during backwashing are given in Tables 7.7 and 7.8. There is an obvious increase in the amount of solids removed by backwash with the increase in solids load to the filter.

Table 7.7: Total Suspended Solids Removed During Backwash

Load	Total SS Load (kg/week)	Total SS Removed (kg) ¹	Total SS Removed (kg/week) ²	Effluent SS (kg/week)
1	1.63	0.46	1.84	0.10
2	2.67	0.55	3.88	0.40
3	5.94	0.39	5.50	1.00
4	6.32	0.52	7.21	1.61

1 - Average for each backwash 2 - Actual removals when washed on time basis

The volume of treated effluent needed to wash the filter each week was also calculated based on actual numbers of washes each week, in all cases there was a very high percentage of effluent reuse for backwashing (16 - 19%). This should decrease if the filter was washed according to head build-up.

Table 7.8: Percentage of Treated Effluent Used For Backwash

Load	Backwash water volume (l)	Total vol/week	Percentage of weekly effluent produced
1	630	2520	15.7
2	787.5	5513	17.5
3	630	8820	18.5
4	787.5	11025	17.4

7.6: Sludge Samples

The different sludge parameters investigated for each loading rate are shown in Table 7.9. One way ANOVA tests show that there is no significant difference between sludges produced at different HLRs in terms of solids present. The CST values indicate that the filterability of the sludge is similar at HLR 3 and 4 but not at the other HLRs. There may be inaccuracies in the CST measurements as sludge may be significantly altered by age, temperature or pH.

Table 7.9: Sludge Data

Load	BW SS (mg/l)	Sludge SS (mg/l)	Sludge Dry Solids (%)	Volatile Solids (%)	CST (seconds)
1	635	5644	65	74.6	38
2	733	6922	71	79.3	100
3	566	7166	83	74	62
4	738	5859	71	85.3	50

7.7: Off-Gas Analysis

During off-gas analysis the oxygen transfer efficiency and oxygenation capacity were determined (Figures 7.29 - 7.31). The operational oxygen transfer of 2-4mm Lytag shows an increasing percentage efficiency with decreasing air flows to the filter for all loading rates. The percentage transfers are in the region of 3-8% at an air flow of 10m/h (equivalent to 30l/min air which was used to prevent oxygen limitation). At an air flow of 2m/h this increased significantly to 25% oxygen transfer. There is a general increase in transfer rate with increasing HLR/OLR until HLR 4 is reached, at which point the oxygen transfer rate is similar to that of HLR 3. The graph of oxygen transfer corrected to zero DO produces higher oxygen transfer values and also shows an increase in efficiency with increased HLR/OLR except that in this case the OTE at HLR 4 is even lower than that at HLR 2. The operational OTE is of greater significance as it portrays the actual transfer in a respiring system.

Oxygenation capacity of the filter increases at low air flows before gradually dropping at high air flows. There is a general increase with increasing loading rate to the filter apart from with HLR 4 where OC is lower than that at HLR 3. The maximum oxygenation capacity occurs at an air rate of approximately 8-10m/h.

Figure 7.29: Operational Oxygen Transfer Efficiency (OTE)

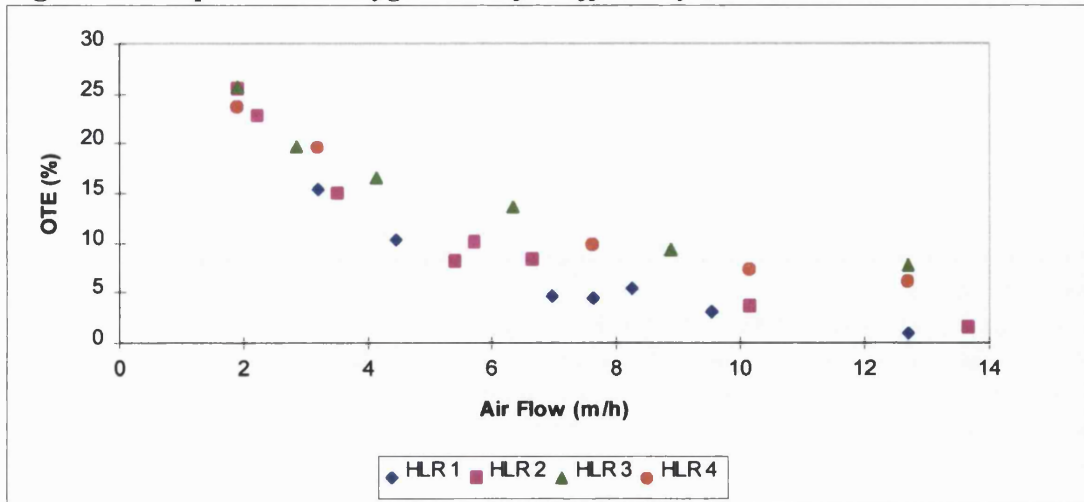


Figure 7.30: Corrected OTE

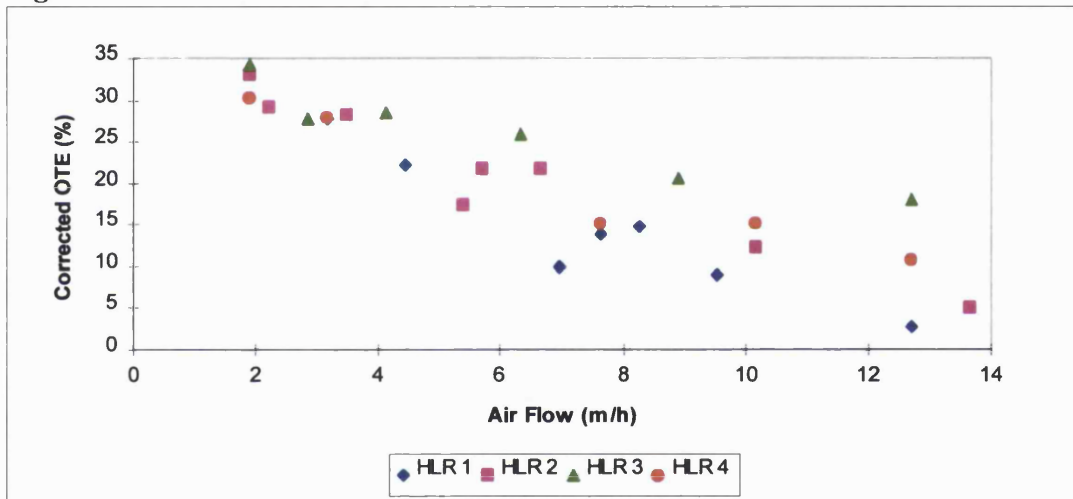
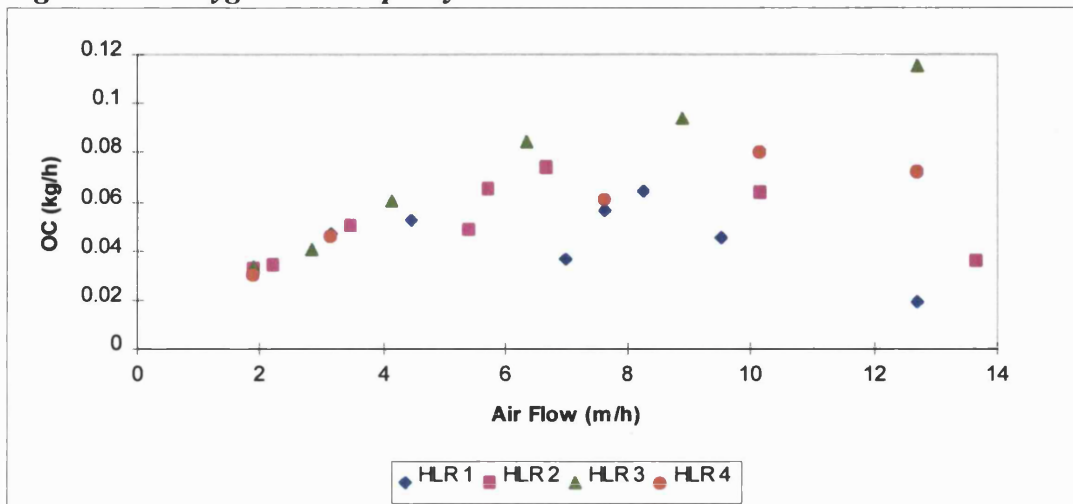
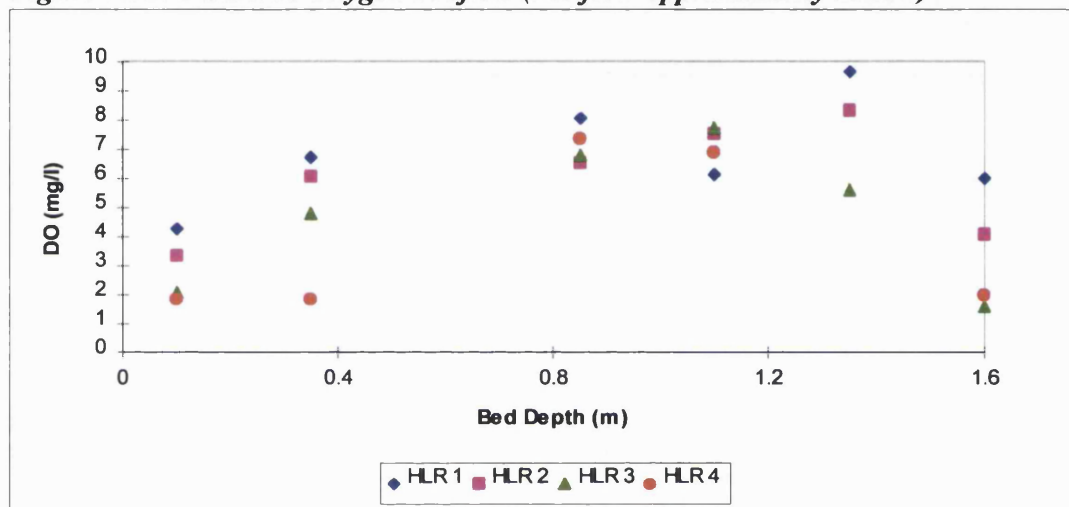


Figure 7.31: Oxygenation Capacity



Profiles of bed DO were taken for a number of different process air rates at each HLR, Figure 7.32 shows a DO profile for the highest air rate investigated. Again the profiles of bed DO show the same pattern as that found with 4-8mm Arlita with a peak at 1.35m depth (above the process air grid) followed by a gradual decrease up the filter as well as a low effluent DO. The same pattern can be seen at all HLRs and air flows, with DO concentrations decreasing with increasing HLR/VLR. The effluent DOs are constantly greater than 2 mg/l.

Figure 7.32: Dissolved Oxygen Profiles (Air flow approximately 13m/h)



The theoretical oxygen demand for each loading rate was calculated (See Chapter 5) and compared with the experimental oxygen demand (Table 7.10). The calculated denitrification has been taken into account in the estimates for Lytag. The actual oxygen demand increases with increasing HLR/VLR until HLR 4 where there is a slight decrease in oxygen demand.

Table 7.10: Oxygen Demand For 2-4mm Lytag Media

Load	Loading (kg/m ³ /d)	Ammonia Oxidation (%)	Estimated Demand (kg O ₂ /h)	Actual Demand (kg O ₂ /h)
1	BOD - 1.17			
1	NH4-N - 0.2	99	0.017	0.016
2	BOD - 2.18			
2	NH4-N - 0.3	98	0.031	0.021
3	BOD - 2.68			
3	NH4-N - 0.47	90	0.038	0.044
4	BOD - 4.81			
4	NH4-N - 0.88	35	0.037	0.04

7.8: Hydraulic Regime

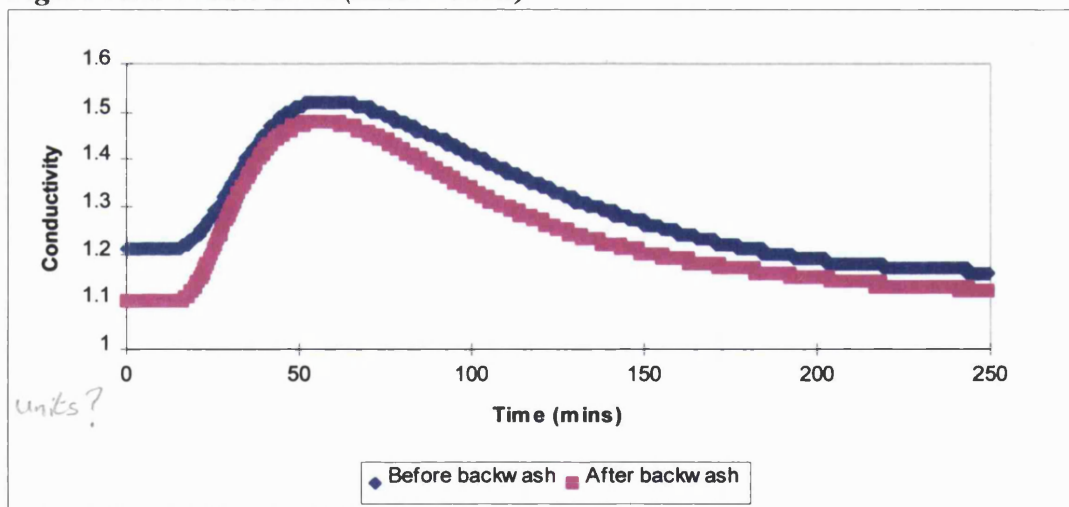
Tracer tests were used to calculate the retention time (RT) in the filter bed at each HLR. Figure 7.33 shows an example of a residence time distribution (RTD) curve before and after backwashing for HLR 2. It can be seen that the flow regime tends more to plug flow after backwash. Calculations of residence time (RT) are given in Table 7.11, the retention time decreases with increasing HLR as does the dispersion number indicating that there are better plug flow conditions with increasing HLR.

Table 7.11: Clean Bed Retention Times for 2-4mm Lytag (After Backwash)

Load	Theoretical Retention Time (mins) ¹	TRT (mins) ²	D/uL ³	Peak RT (mins)	Mean RT (mins)
1	190	59	0.1725	90	147.1
2	97	30	0.274	55	85.9
3	64	20	0.1163	35	52.9
4	48	15	0.0819	30	38.8

1 - Empty Bed 2 - Assuming experimental voidage of 0.31 3 - Dispersion number

Figure 7.33: Tracer Tests (HLR = 1m/h)



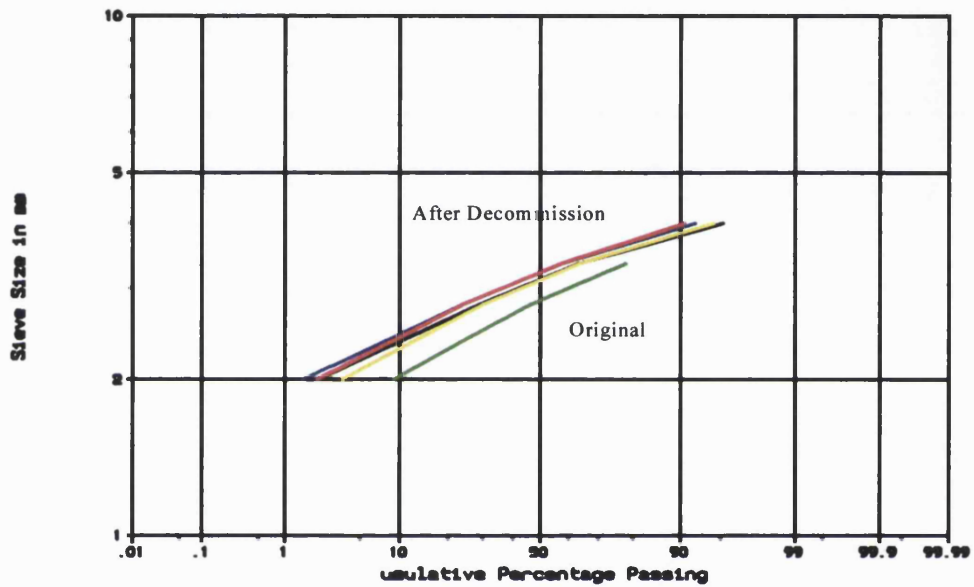
7.9: Decommissioning

At the end of the study auger samples were taken of media from the filter. Samples taken from the top, middle and bottom of the filter bed were resieved as was a sample from the bed as a whole. Analysis of the data (Table 7.12) was then used to see if the samples had changed from their original size ranges.

Table 7.12: Sieve Analysis of 2-4mm Lytag After Filter Operation

Media Sample	Hydraulic Size (mm)	d ₅ (mm)	d ₁₀ (mm)	d ₆₀ (mm)	UC	d ₉₅ (mm)	d ₉₀ (mm)
Original	2.74	1.9	2.05	3	1.46	3.55	3.5
Overall	3.04	2.2	2.4	3.3	1.38	4.0	3.8
Top	3.01	2.15	2.3	3.3	1.44	4.0	3.8
Middle	3.13	2.3	2.45	3.4	1.39	4.05	3.95
Bottom	3.13	2.2	2.45	3.4	1.39	4.1	4.0

Figure 7.34: Sieve Analysis of 2-4mm Lytag After Decommissioning



From Figure 7.34 we can see that all samples sieved after filter operation have similar particles size ranges and this is considerably different to the original size range. There appears to be an increase in size distribution after filter operation.

8.0 PILOT SCALE PERFORMANCE OF LYTAG MEDIA

Results: 2.8-5.6mm Lytag

8.1: Introduction

The 2.8-5.6mm Lytag used in this study is similar to the media size range normally used for carbonaceous treatment, eg: in the Biocarbhone® process 3- 6mm media is used (Dillon & Thomas, 1990).

8.2: Steady State Results

8.2.1: Settled Sewage

The concentrations of the settled sewage at each HLR were the same as those for settled sewage onto the 2-4mm Lytag (Chapter 7, Table 7.1), the calculated VLRs are slightly different due to slight differences in flow rate onto the filter (Table 8.1).

Table 8.1: Loading Rates for Composite Samples

Load	Hydraulic Load (m/h)	BOD Load (kg/m³/d)	COD Load (kg/m³/d)	SS Load (kg/m³/d)	NH₄-N Load (kg/m³/d)	TKN Load (kg/m³/d)
1	0.5	1.16	2.59	0.76	0.2	0.26
2	1.0	2.15	4.39	1.26	0.3	0.39
3	1.5	2.71	6.35	2.85	0.48	0.73
4	2.0	4.96	10.82	2.95	0.89	1.17

8.2.2: Effluent Quality

Table 8.2 shows the percentage removals for each loading rate. There is a general decrease in percentage removals for all determinands, with increasing HLR and VLR.

Table 8.2: Percentage Removals by 2.8-5.6mm Lytag

Load	BOD Removal (%)	COD Removal (%)	SS Removal (%)	NH₄-N Removal (%)	TKN Removal (%)
1	96.1	87.3	92.1	97	92.6
2	95.5	79.6	86	91.5	87.2
3	93.4	80.2	88.7	78.5	78.9
4	90.3	79.3	85.9	63.4	62.5

Figures 8.1 - 8.5 show the removals of different determinands for composite samples at a depth of 1.35m. The data for 3-6mm Arlita has also been included for a comparison between two different media types of similar size.

Figure 8.1: Composite BOD Removals

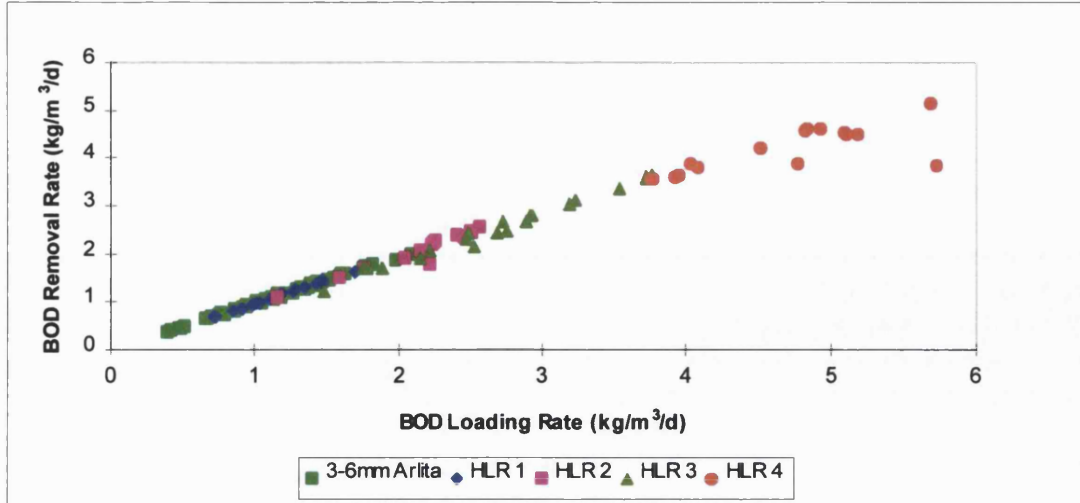


Figure 8.2: Composite COD Removals

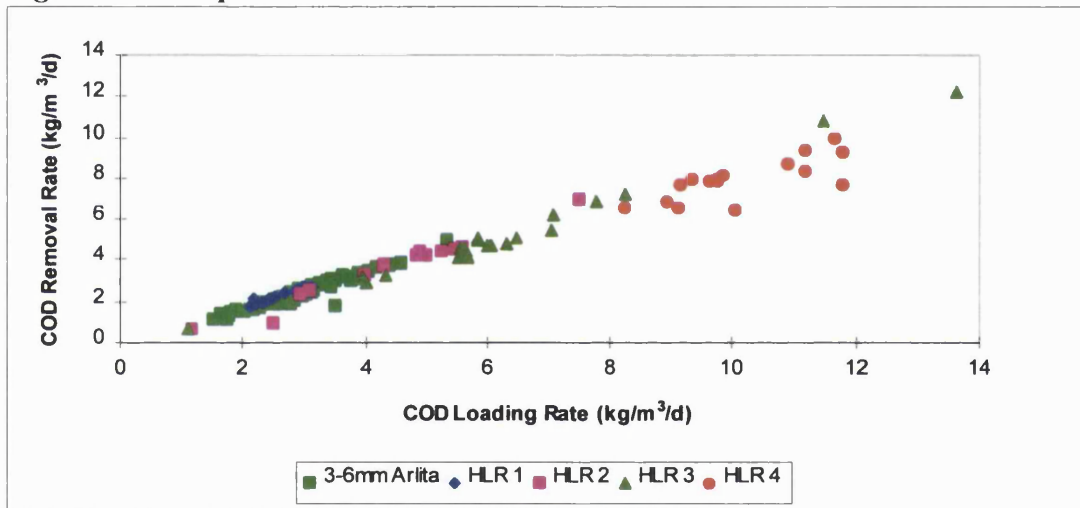


Figure 8.3: Composite SS Removals

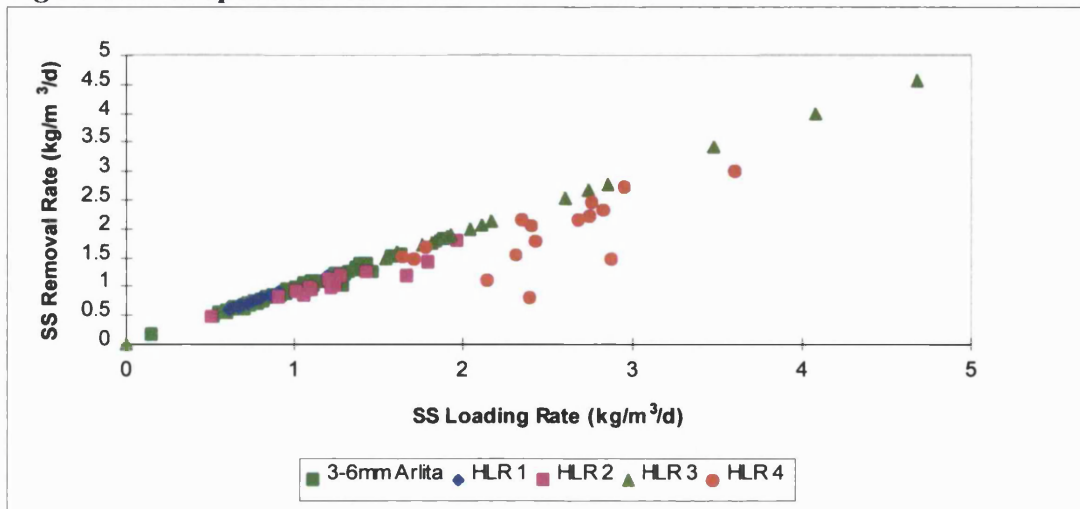


Figure 8.4: Composite NH_4-N Removals

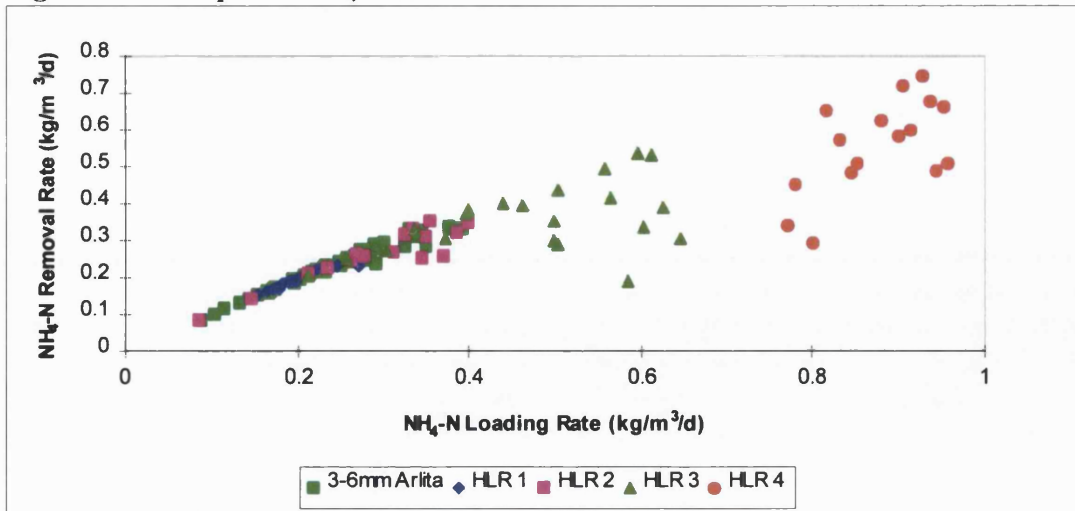
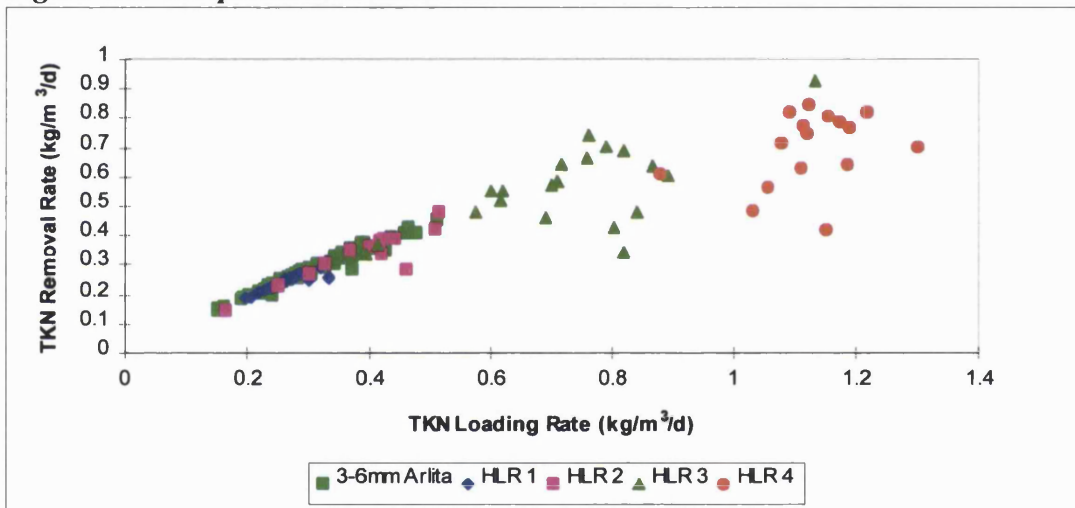


Figure 8.5: Composite TKN Removals



The graphs of BOD, COD and SS removal show a positive linear relationship between loading rate and removal. The NH_4-N removal graph shows increasing removals with increasing VLR but there is a high degree of scatter in the results after 0.4kg $NH_4-N/m^3/d$. The actual effluent results in mg/l are given in Table 8.3. Data for 3-6mm Arlita is only available for the lower loading rates but it appears to have similar removal rates to those of the 2.8-5.6mm Lytag.

Table 8.3: Effluent Concentrations for 2.8-5.6mm Lytag

Load	BOD (mg/l)	COD (mg/l)	SS (mg/l)	NH ₄ -N (mg/l)	TKN (mg/l)	TON (mg/l)	NO ₃ (mg/l)
1	5.8 (2.4)	43.7 (5.9)	7.8 (3.4)	0.9 (1.1)	2.7 (2.4)	12.1 (3.2)	11.1 (3.4)
2	6.7 (7.1)	73 (19.8)	12 (7.5)	1.9 (2.4)	3.6 (2.8)	7.4 (2.3)	6.8 (2.3)
3	7.2 (3.8)	48.6 (14.1)	11.3 (6.1)	5.2 (5.1)	7.1 (5.6)	6.1 (3.1)	5.5 (3.1)
4	16.5 (13.4)	72.8 (23.9)	20.4 (14.7)	10.6 (3.2)	14.3 (4.3)	4.1 (2.3)	2.7 (1.6)

Note: Standard deviations in brackets

There are increasing effluent BOD, COD, SS, TKN and NH₄-N with increasing HLR/VLR, whilst TON decreases. Effluent is of a good quality for HLRs 1- 3 but deteriorates at HLR 4 especially with reference to NH₄-N and TKN.

A comparison of spot samples at a depth of 1.35m and 1.6m are shown in Figures 8.6 and 8.7. At OLRs above 3kg BOD/m³/d BOD removal rates are much better at 1.35m than at 1.6m. This is also the case for ammoniacal nitrogen removals above loading rates of 0.2kg NH₄-N/m³/d.

Figure 8.6: Comparison of BOD Removal at 1.35m and 1.6m (Spot Samples)

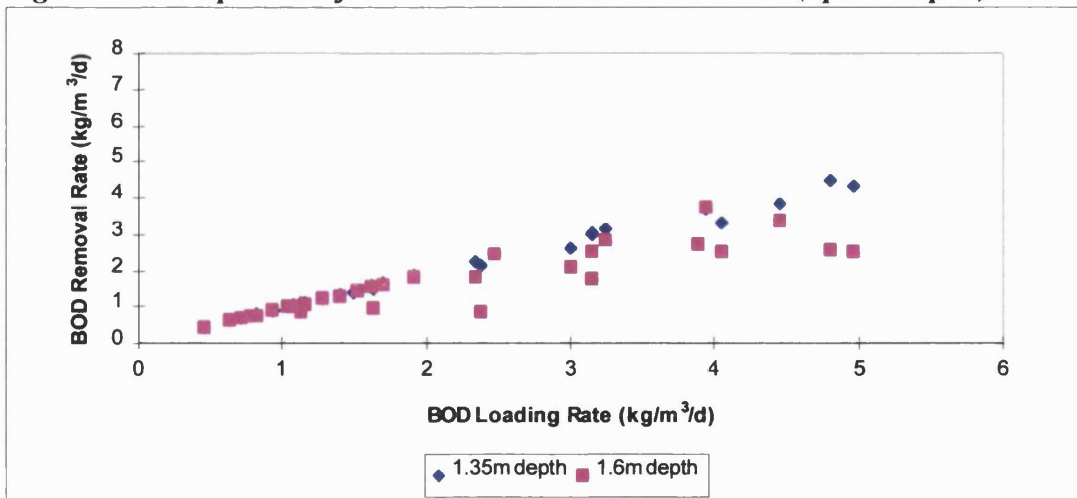
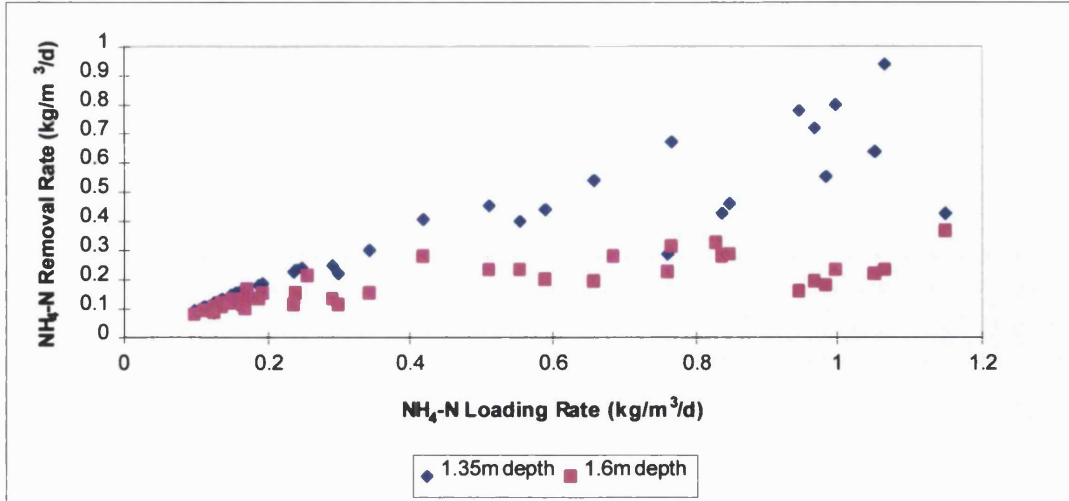


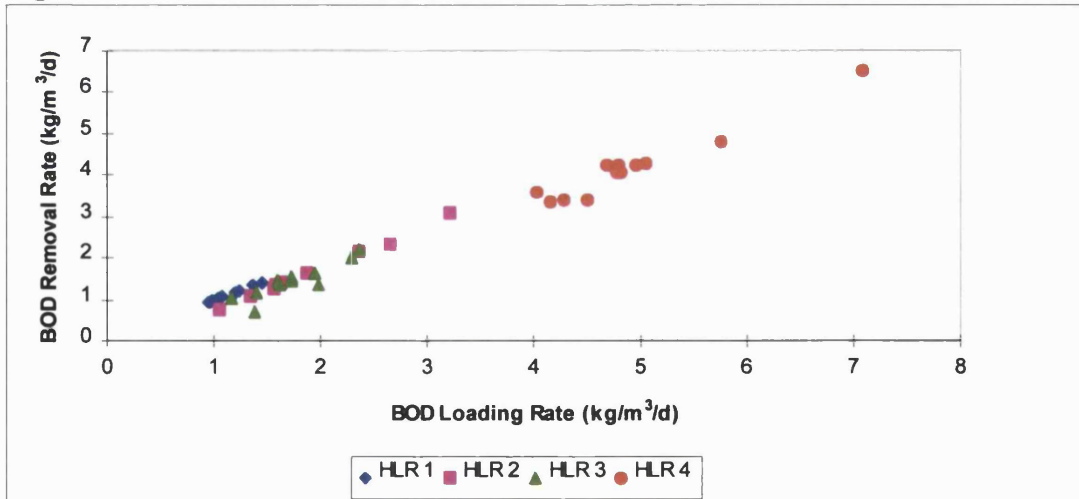
Figure 8.7: Comparison of NH₄-N Removal at 1.35m and 1.6m (Spot Samples)



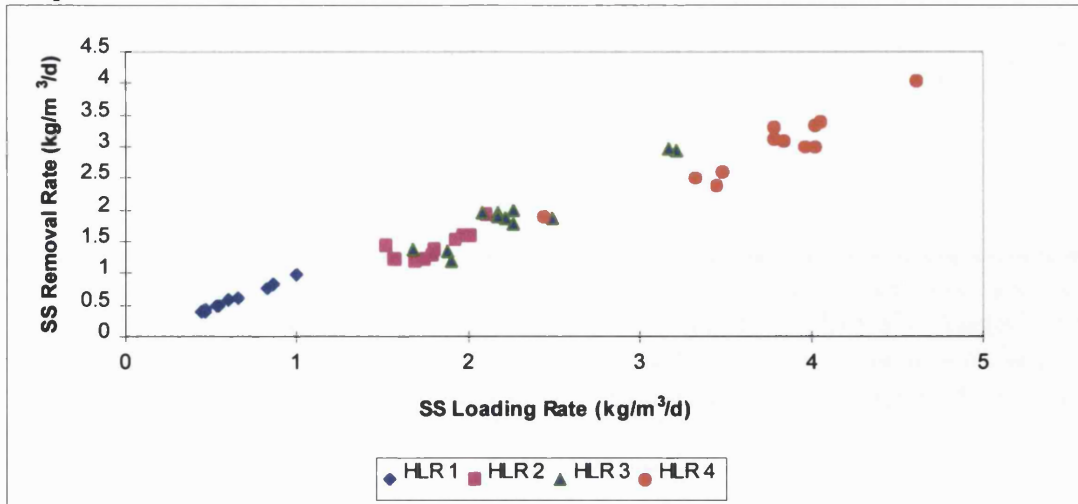
8.2.3: Diurnal Variation

Figures 8.8 - 8.10 show BOD, SS and NH₄-N removals against VLR for samples taken over a 24 hour period. The patterns for removal are similar to those from composite samples with positive relationships between removal and VLR. There is again a high degree of scatter for the graph of NH₄-N removal against VLR.

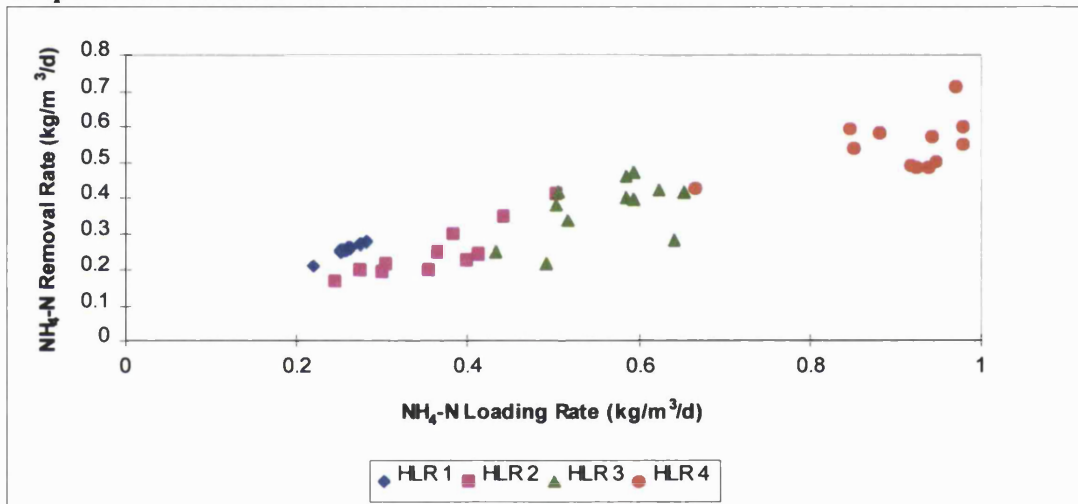
Figure 8.8: Diurnal BOD Removals



Graph 8.9: Diurnal SS Removals



Graph 8.10: Diurnal NH₄-N Removals



Again graphs of SS and NH₄-N removals and loading rate against time from backwash showed that backwash did not affect removals.

8.2.4: Bed Profiles

Bed profiles are shown for each HLR (Figures 8.11 - 8.15). The removal of BOD and COD is very high in the top 0.85m of the filter bed, at this point the final effluent concentrations have been reached. The profiles of SS removal are similar except that at HLR 1 and 2 there is an increase in concentration at Port 2 (0.35m) before concentrations again decrease with high removals still occurring by a depth of 0.85m. At HLR 4 there is still a high concentration of SS at 0.85m and this does not decrease any further.

Figure 8.11: BOD Profiles

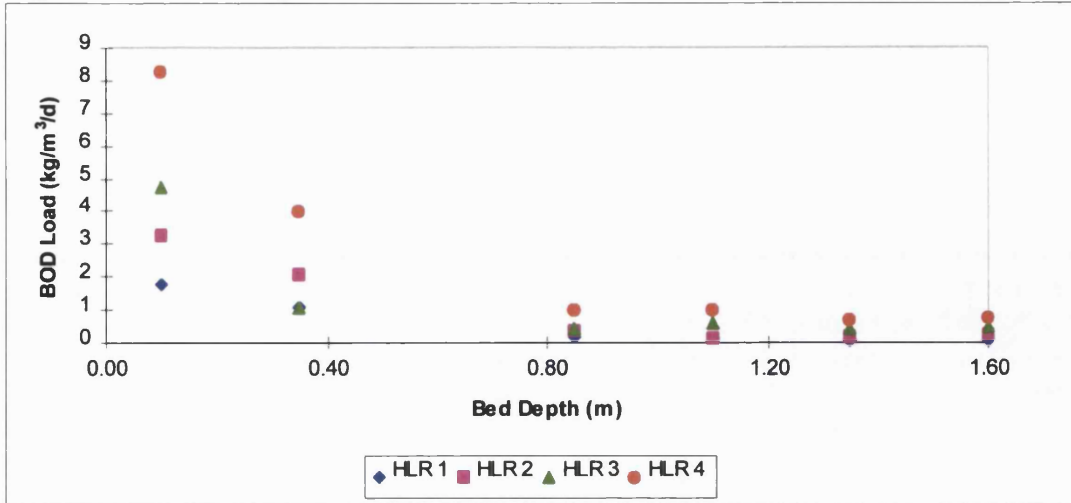


Figure 8.12: COD Profiles

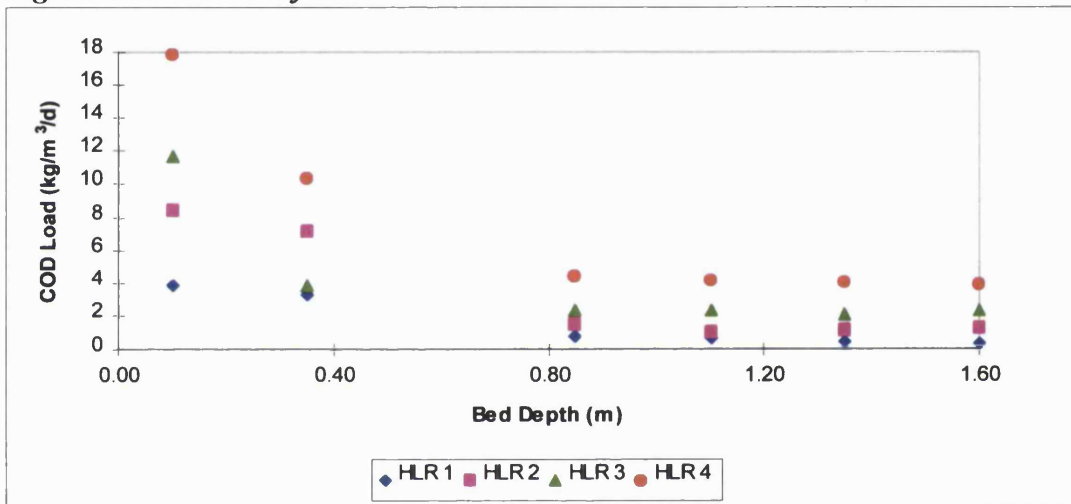


Figure 8.13: Suspended Solids Profiles

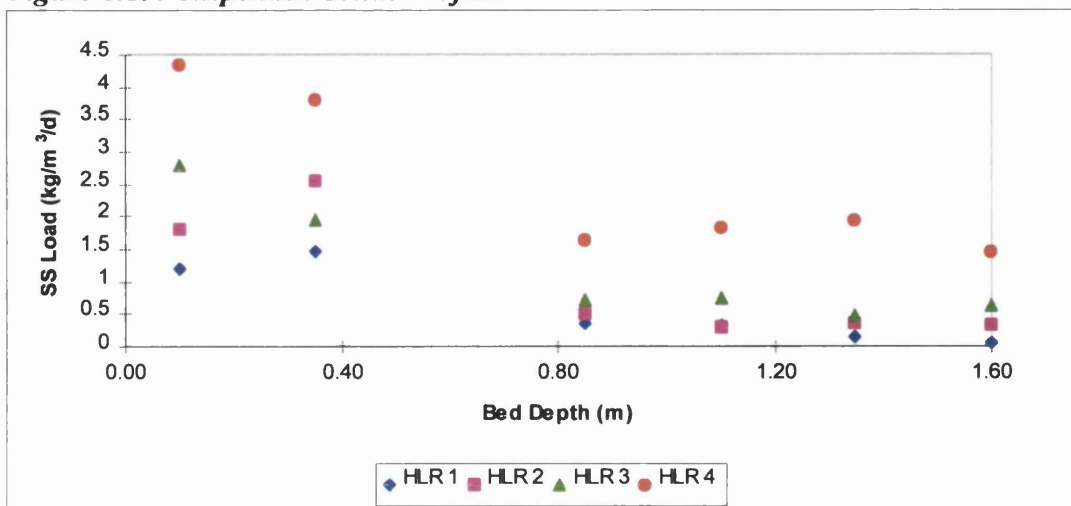


Figure 8.14: NH₄-N Profiles

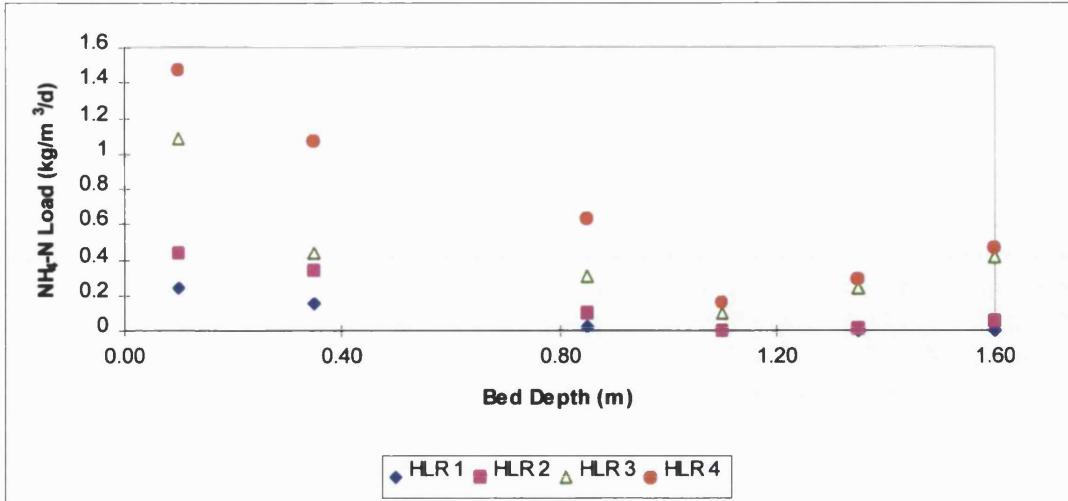


Figure 8.15: TON Profiles

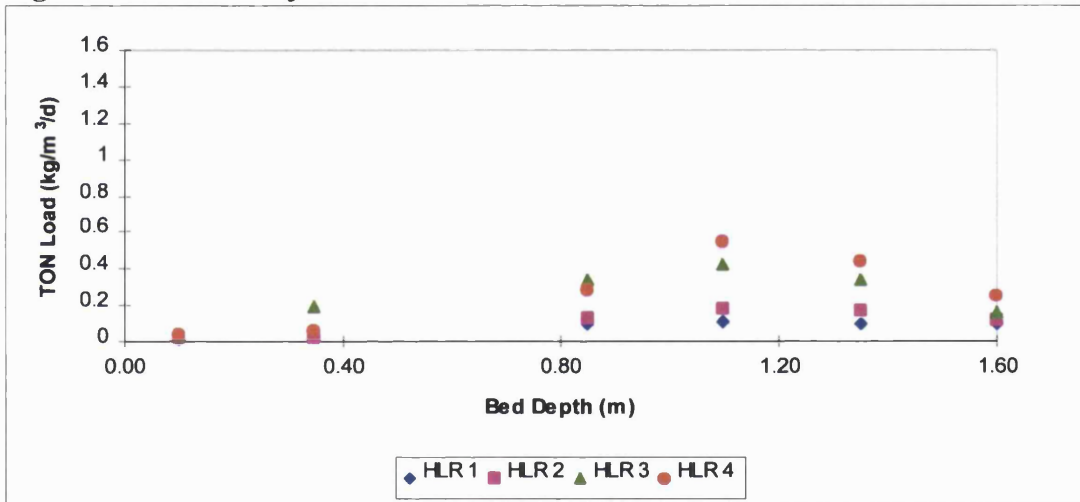
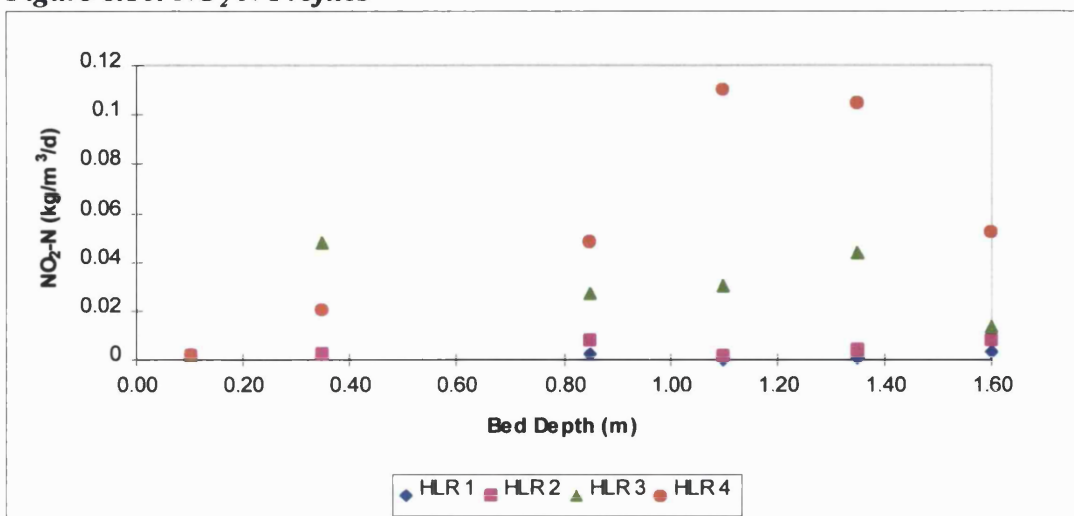


Figure 8.16: NO₂-N Profiles



The NH₄-N profile shows fairly high removals at the top of the bed where carbonaceous treatment is occurring. At HLR 3 and 4 the NH₄-N increases again after 1.1m of filter bed, this is mirrored in the profile of TON with production occurring up to a filter depth of 1.1m and then decreasing. The NO₂-N profiles show that at HLR 1 and 2 all NO₂-N is converted to NO₃-N, at HLR 3 and 4 we can see increased NO₂-N with increased loading rate.

Values of denitrification were calculated from bed profile data as described in Chapter 7 and are given in Table 8.4. There is an obvious increase in the percentage denitrification with increasing loading rate.

Table 8.4: Denitrification

HLR	TKN VLR	TKN Removed	BOD Removed	N Assimilation	TON Expected	TON Produced	Denite	Denite (%)
1	0.26	0.24	1.11	0.06	0.18	0.08	0.1	54
2	0.39	0.34	2.07	0.1	0.24	0.1	0.14	59
3	0.73	0.57	2.54	0.13	0.44	0.12	0.32	74
4	1.11	0.62	4.15	0.21	0.41	0.1	0.31	76

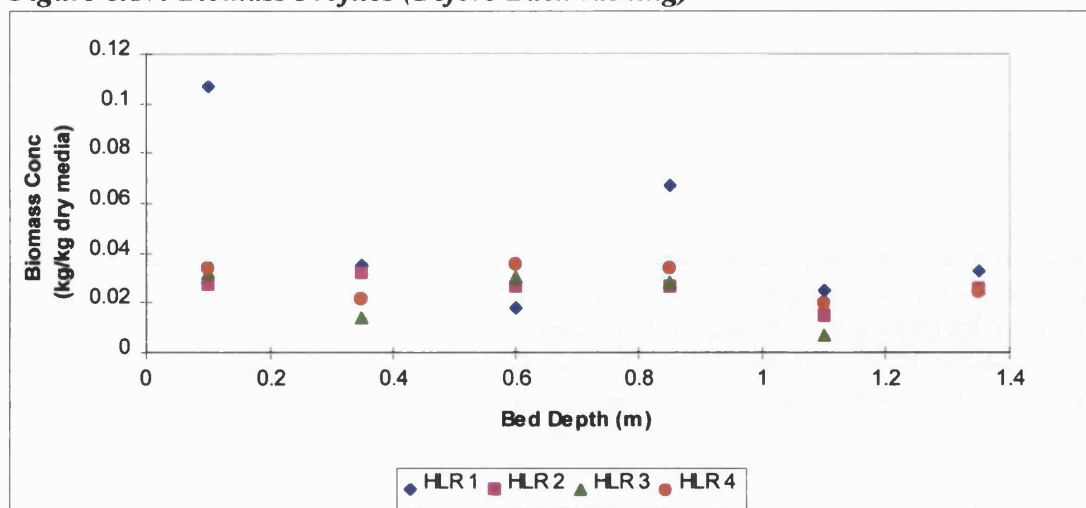
All expressed in kg/m³/d except % denitrification

8.3: Biofilm Growth

8.3.1: Biomass Samples

Figure 8.17 shows the biomass bed profiles for each media before backwashing of the filters. Biomass concentrations are generally 0.02 - 0.04kg biomass/kg dry media for all bed depths and all HLRs.

Figure 8.17: Biomass Profiles (Before Backwashing)



8.3.2: Microbiological Analyses and Scanning Electron Micrographs

The microbiological analysis showed similar microorganisms to those found on 2-4mm Lytag at all depths, SEMs also showed similar biofilm coverage and ciliate presence as found for 2-4mm Lytag (Chapter 7).

8.3.3: 'Slime' Growth on Media Particles

The particles again appear to be fairly clean with some patches of biofilm present but no excessive biofilm coverage.

Figure 8.18: 2.8-5.6mm Media Particles From Middle of Filter Bed (HLR 1)



Figure 8.19: 2.8-5.6mm Media Particles From Middle of Filter Bed (HLR 4)



8.4: Headloss

The head build-up for each loading rate was recorded at each manometer point as shown in Figures 8.20 -8.21 for HLR 1 and 4. The time for filter flooding is given in Table 8.5, there is a decrease in filter run time with increased HLR.

Figure 8.20: Head Profile (HLR 1)

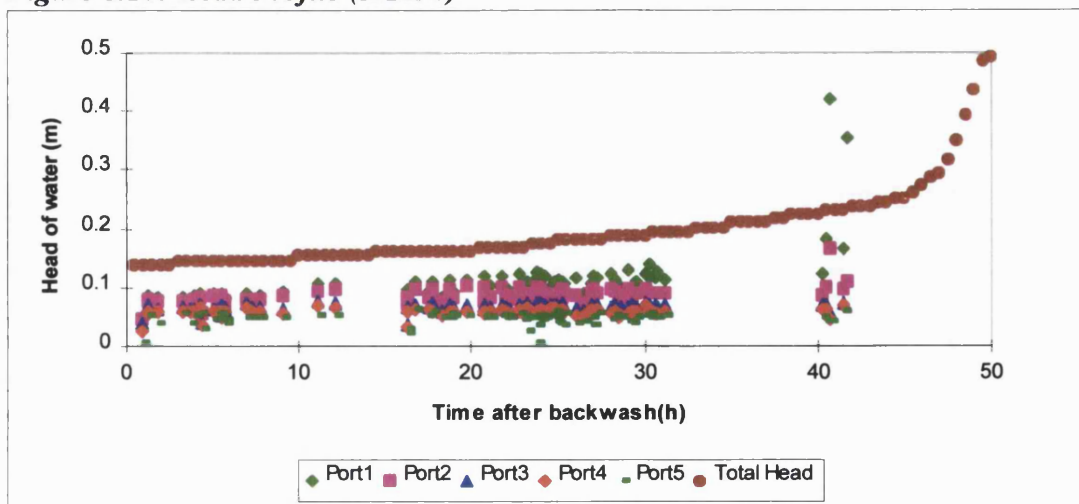
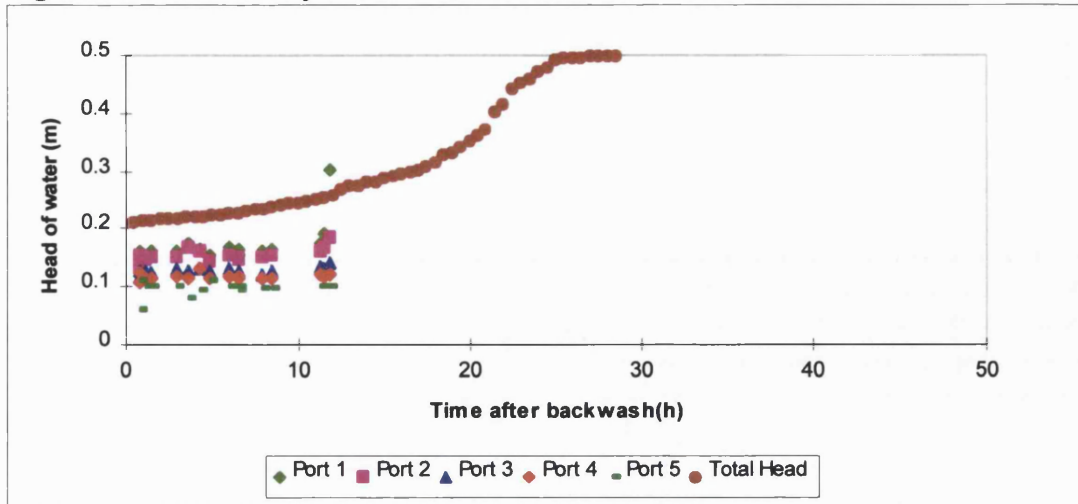


Figure 8.20: Head Profile (HLR 4)



At HLR 1 the 2.8-5.6mm Lytag shows a gradual head build-up from 0.1m of head, with a sudden increase to a flooded state after 50 hours. Head build-up appears to be similar at all bed depths. At HLR 4 the head level immediately jumps to 0.2m and then rapidly rises with the filter being fully flooded after approximately 25 hours.

Table 8.5: Flood Times from Ranger Data

Load	HLR (m/h)	Flood Time (hours)
1	0.5	50 - 62
2	1.0	33 - 36
3	1.5	28 - 32
4	2.0	27 - 30

8.5: Backwash Samples

Backwash solids removal is shown in Figures 8.22 and 8.23. The peak removal of solids (1200mg/l) occurs after 60 seconds of combined air and water wash, this decreases to approximately 200mg/l SS removed at the end of the backwash rinse phase. In total 0.3 - 0.5kg SS were removed at every backwash.

Figure 8.22: Backwash Profiles

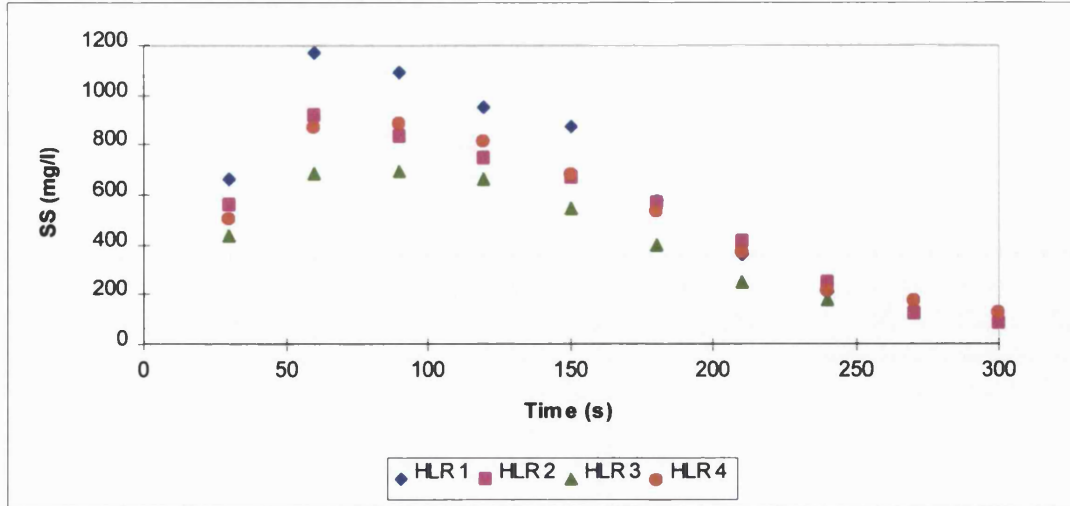
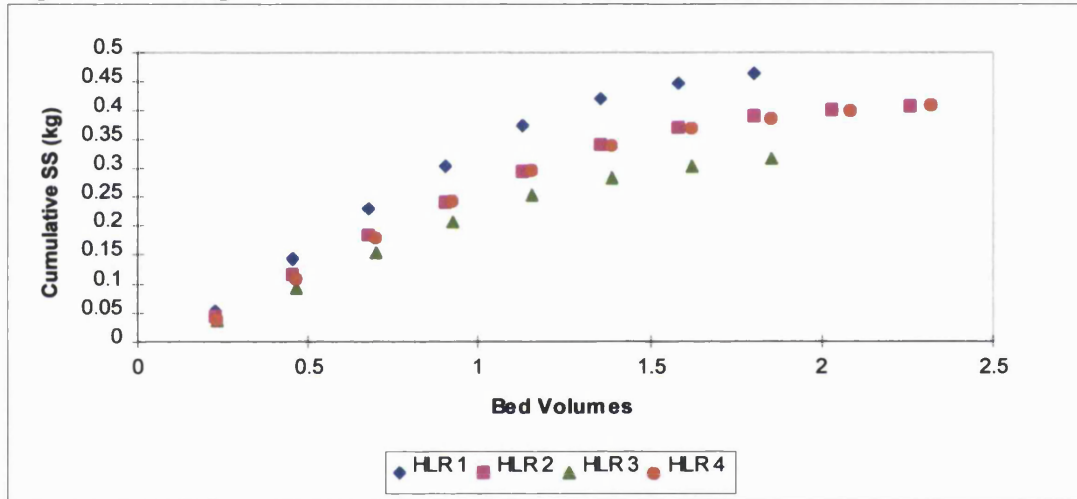


Figure 8.23: Suspended Solids Removed During Backwash



Calculations of total solids removed each week are given in Table 8.6, there is an increase in solids removed with increased loading rate.

Table 8.6: Total Suspended Solids Removed During Backwash

Load	Total SS Load (kg/week)	Total SS Removed (kg) ¹	Total SS Removed (kg/week) ²	Effluent SS (kg/week)
1	1.61	0.46	1.84	0.01
2	2.67	0.41	2.87	0.43
3	6.02	0.32	4.48	0.55
4	6.24	0.41	5.74	1.31

1 - Average for each backwash 2 - Actual removals when washed on time basis

The volume of treated effluent used for filter backwashing is given in Table 8.7. The percentage reuse is fairly high at 16 - 18% but would be lower if the filter was washed according to head build-up rather than on a time basis.

Table 8.7: Percentage of Treated Effluent Used For Backwash

Load	Backwash water volume (l)	Total vol/week	Percentage of weekly effluent produced
1	630	2520	15.9
2	787.5	5513	17.6
3	630	8820	18.4
4	787.5	11025	17.1

8.6 Sludge Samples

Table 8.8 shows the different sludge parameters investigated at each HLR. One-way ANOVA tests show sludges produced at different HLRs are similar despite backwash solids differing between HLRs. At HLR 2 there was also a high SS content.

Table 8.8: Sludge Data

Load	BW SS (mg/l)	Sludge SS (mg/l)	Sludge Dry Solids (%)	Volatile Solids (%)	CST (seconds)
1	680	6259	0.81	73	58
2	487	7227	0.73	74.7	99
3	461	6163	0.75	72.7	51
4	592	6320	0.72	85.4	58

8.7 Off-Gas Analysis

During off-gas analysis the oxygen transfer efficiency and oxygenation capacity were determined (Figures 8.24 - 8.26). Profiles of bed DO were taken for a number of different process air rates at each HLR. Figure 8.27 shows a DO profile for the highest air rate investigated.

The operational OTE appears to be similar at all HLRs, with OTE increasing with decreasing air flow rate. When the OTE is corrected to zero DO there appears to be a slight decrease in OTE with increasing HLR.

Figure 8.24: Operational Oxygen Transfer Efficiency (OTE)

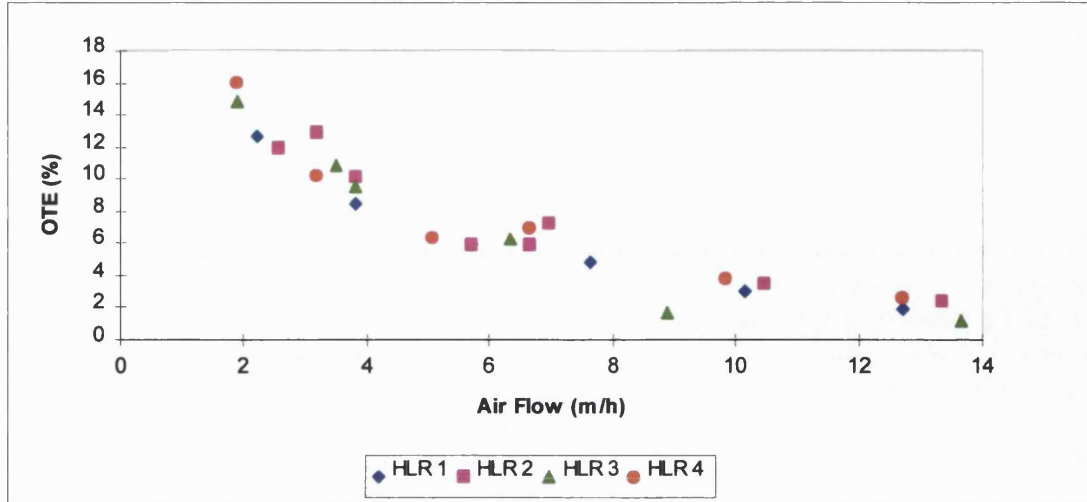


Figure 8.25: Corrected OTE

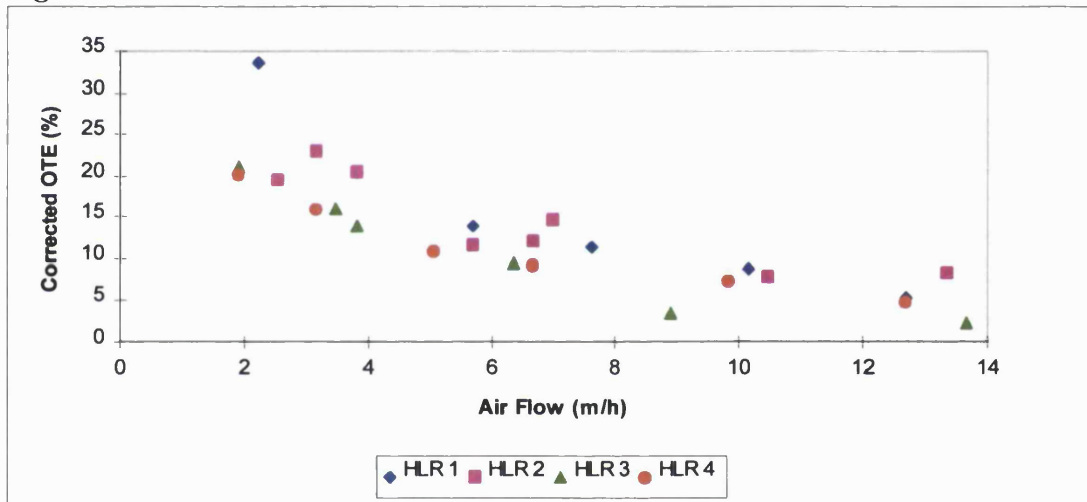
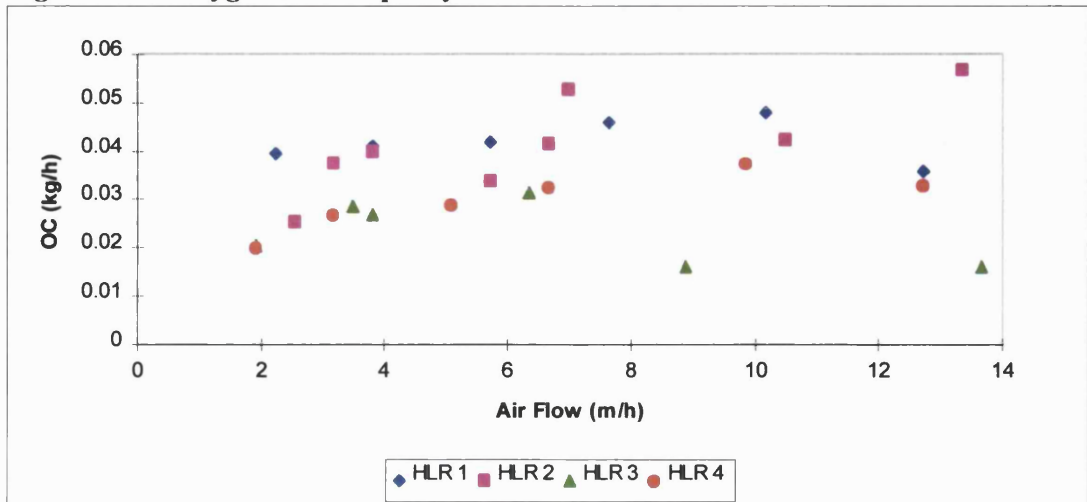
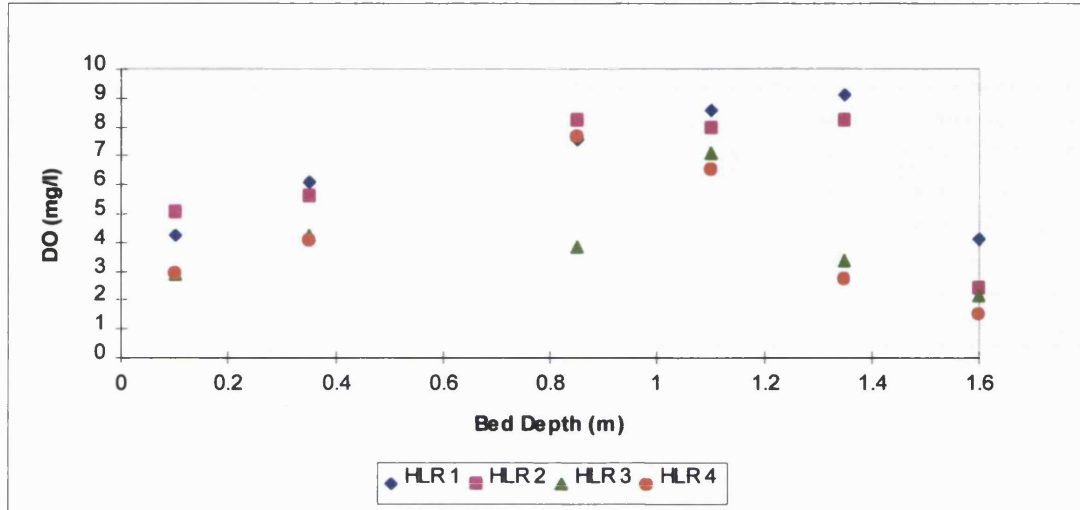


Figure 8.26: Oxygenation Capacity



The OC appears to be higher at HLR 1 and 2 than HLR 3 and 4, there is also no obvious point where air flow becomes optimum for each HLR.

Figure 8.27: Dissolved Oxygen Profiles (Air flow approximately 13m/h)



The DO profile shows a peak DO at a bed depth of 1.35m. This gradually decreases up the filter bed and is lowest in the effluent. The DO is consistently greater than 2 mg/l.

The theoretical oxygen demand for each loading rate was calculated and compared with the experimental oxygen demand (Table 8.9)

Table 8.9: Oxygen Demand For 2.8-5.6mm Lytag Media

Load	Loading (kg/m ³ /d)	Ammonia Oxidation (%)	Estimated Demand (kg O ₂ /h)	Actual Demand (kg O ₂ /h)
1	BOD - 1.16			
1	NH ₄ -N - 0.2	97	0.015	0.016
2	BOD - 2.15			
2	NH ₄ -N - 0.3	92	0.024	0.019
3	BOD - 2.71			
3	NH ₄ -N - 0.48	79	0.025	0.01
4	BOD - 4.96			
4	NH ₄ -N - 0.89	63	0.048	0.02

The estimated oxygen demand increases with increasing loading rate, this is followed by the experimental oxygen demand for the first two loading rates but demand falls off at HLR 3 and 4. This suggests there may be a blockage of the process air grid.

8.8: Hydraulic Regime

Tracer tests were used to calculate the retention time of the filter bed at each HLR.

Figure 8.28 shows an example of a RTD curve before and after backwashing for HLR

2, plug flow conditions are more obvious after backwashing. Calculations of RT are given in Table 8.9.

Figure 8.28: Tracer Tests (Hydraulic Load = 1m/h)

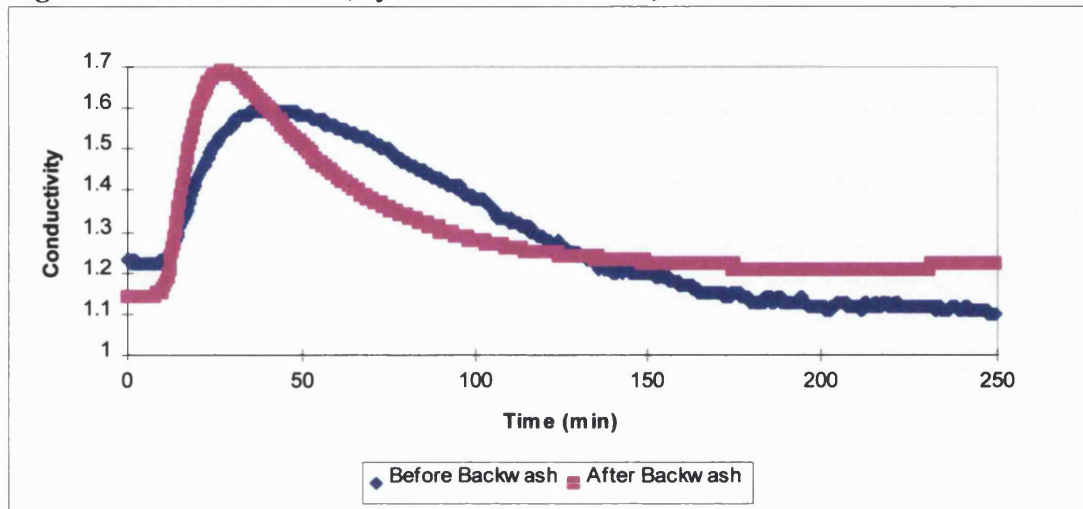


Table 8.9: Retention Times (After Backwash)

Load	Theoretical Retention Time (mins) ¹	TRT (mins) ²	D/uL ³	Peak RT (mins)	Mean RT (mins)
1	193	59	0.2521	50	166
2	96	30	0.312	30	69
3	63	20	0.2539	20	42
4	47	15	0.1883	15	26

1 - Empty Bed 2 - Assuming experimental voidage of 0.31 3 - Dispersion number

The retention times decrease with increasing HLR as does the dispersion number indicating more plug flow with increasing HLR.

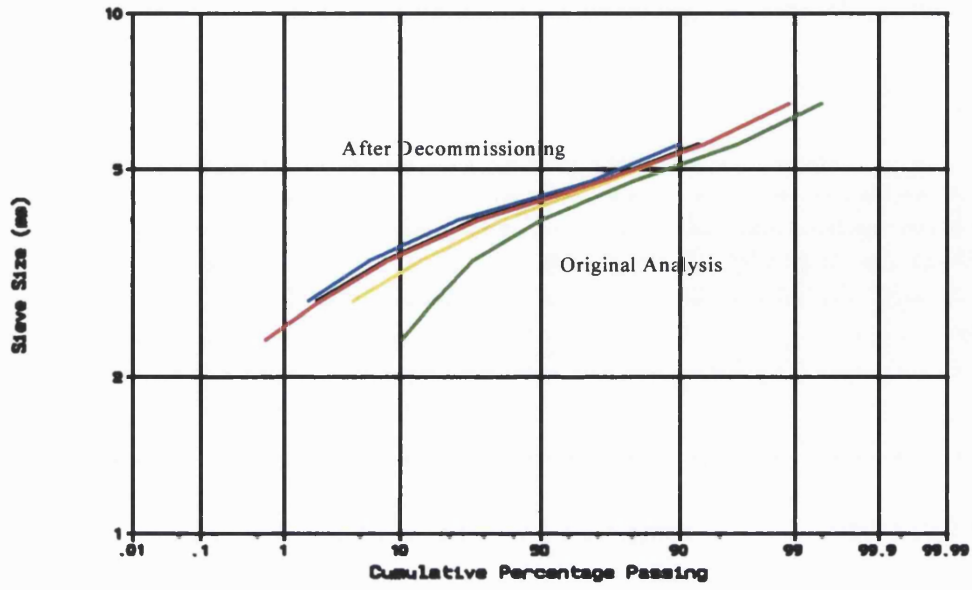
8.9: Decommissioning

The particle size range of 2.8-5.6mm Lytag after filter operation is shown in Figure 8.29 and Table 8.10. Again the media appears to have increased in size after a period of filter operation.

Table 8.10: Sieve Analysis of 2.8-5.6mm Lytag After Filter Operation

Media Sample	Hydraulic Size (mm)	d ₅ (mm)	d ₁₀ (mm)	d ₆₀ (mm)	UC	d ₉₀ (mm)	d ₉₅ (mm)
Original	3.67	2.3	2.4	3.0	1.25	5.1	5.5
Overall	4.29	3.1	3.5	4.5	1.29	5.4	5.7
Top	4.03	2.85	3.2	4.4	1.38	5.4	5.7
Middle	4.31	3.1	3.5	4.5	1.29	5.4	5.7
Bottom	4.41	3.3	3.6	4.6	1.28	5.6	5.8

Figure 8.29: Sieve Analysis of 2.8-5.6mm Lytag After Decommissioning



9.0: PILOT SCALE PERFORMANCE OF LYTAG MEDIA

Results: 4-8mm Lytag

9.1: Introduction

The 4-8mm Lytag has a slightly larger particle size range than that normally found in BAFs.

9.2: Steady State Results

The results for HLR 1 have not been included for 4-8mm Lytag as problems were encountered with the peristaltic pump used to feed settled sewage to the filter.

9.2.1: Settled Sewage

Table 9.1 shows the calculated VLRs onto the filter.

Table 9.1: Loading Rates for Composite Samples

Load	Hydraulic Load (m/h)	BOD Load (kg/m³/d)	COD Load (kg/m³/d)	SS Load (kg/m³/d)	NH₄-N Load (kg/m³/d)	TKN Load (kg/m³/d)
2	1.0	2.17	4.4	1.23	0.29	0.39
3	1.5	2.63	6.43	2.92	0.46	0.71
4	2.0	4.78	10.48	2.97	0.87	1.15

9.2.2: Effluent Quality

Table 9.2 shows percentage removals for each loading rate. There is a general decrease in percentage removals for all determinands, with increasing HLR and VLR, with a large decrease at HLR 4.

Table 9.2 Percentage Removals by 4-8mm Lytag

Load	BOD Removal (%)	COD Removal (%)	SS Removal (%)	NH₄-N Removal (%)	TKN Removal (%)
2	94.1	80.3	81.8	80.5	78.3
3	90.4	75	80.4	64.7	67.8
4	78	66.6	52	30.3	33.9

Figures 9.1 - 9.5 show the removals of different determinands for composite samples at a depth of 1.35m. The data for 4-8mm Arlita has been included so that a comparison can be made between the same size of two different media types.

Figure 9.1: Composite BOD Removals

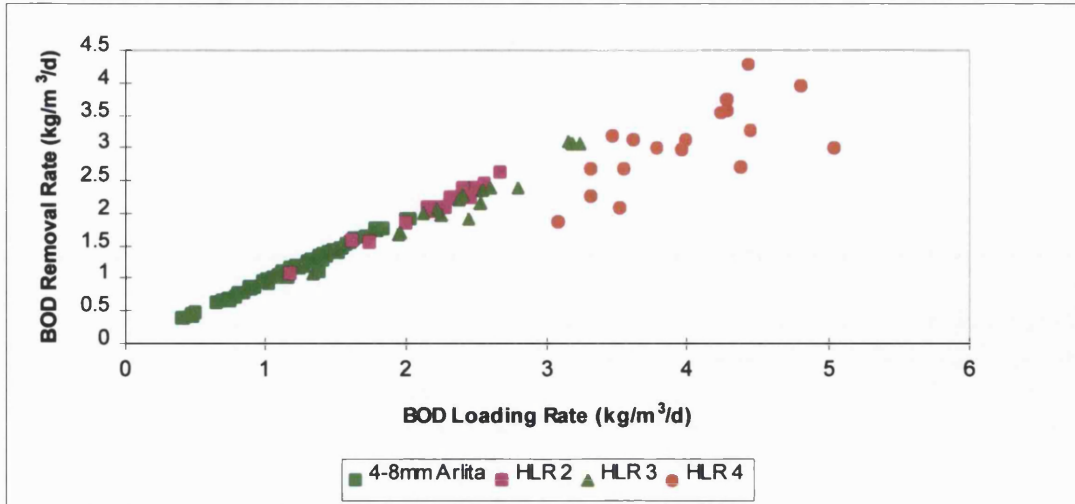


Figure 9.2: Composite COD Removals

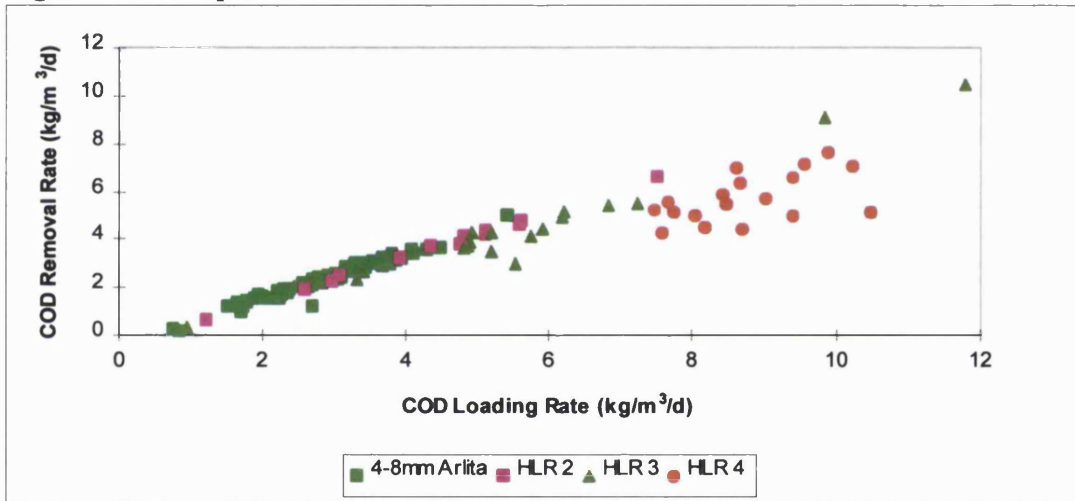


Figure 9.3: Composite SS Removals

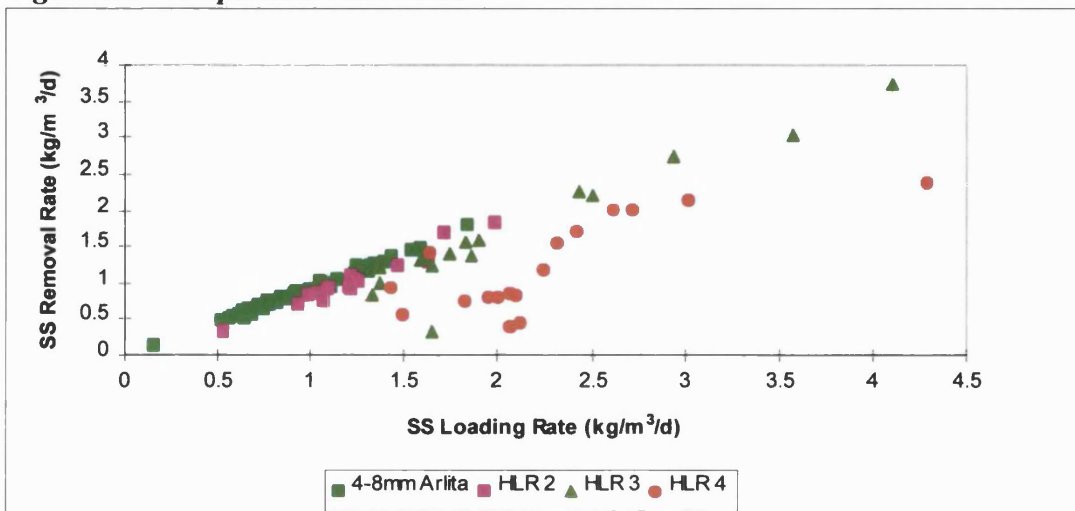


Figure 9.4: Composite NH₄-N Removals

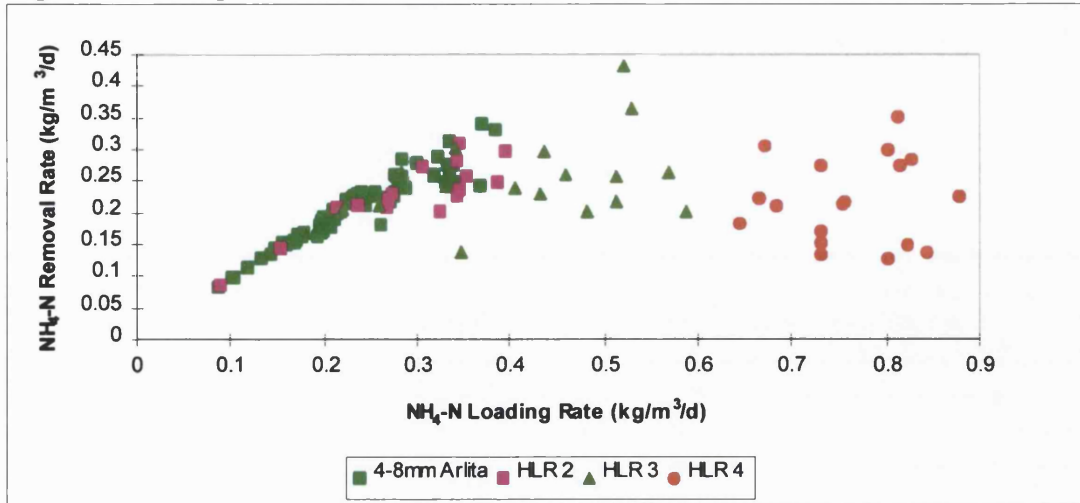
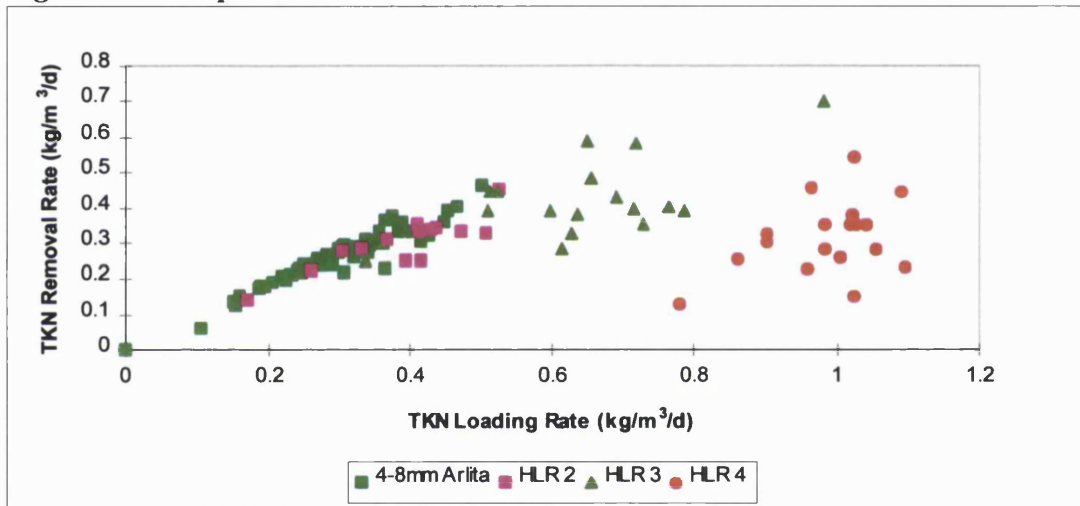


Figure 9.5: Composite TKN Removals



The graphs of BOD, COD and SS removal show a positive straight line relationship between VLR and removal but there is a high degree of scatter. The NH₄-N removal graph shows the same relationship to a loading rate of approximately 0.4 kg NH₄-N/m³/d and then removal decreases (a similar pattern is seen with TKN after 0.7 kg TKN/m³/d). Data for 4-8mm Arlita is only available at the lower loading rates but it appears to have similar removals as the 4-8mm Lytag.

Table 9.4: Effluent Concentrations for 4-8mm Lytag

Load	BOD (mg/l)	COD (mg/l)	SS (mg/l)	NH ₄ -N (mg/l)	TKN (mg/l)	TON (mg/l)	NO ₃ (mg/l)
2	8.9 (5)	58.6 (30)	13.7 (5.4)	4.1 (3)	6 (3.5)	5.5 (2.2)	4.8 (2.1)
3	10.7 (6.4)	61.4 (22.7)	18.9 (12.7)	8 (5.6)	10.6 (5.9)	3.9 (2.7)	3.4 (2.6)
4	33.9 (16.8)	113.8 (32.4)	43.3 (20.4)	20.2 (3)	25.2 (33)	1.5 (1)	1.1 (0.7)

The effluent quality in terms of SS and BOD is good for HLR 2 and 3 but poor at HLR 4. The concentration of $\text{NH}_4\text{-N}$ in the effluent is $< 5\text{mg/l}$ at HLR 2 but is too high at HLR 3 and 4. There is low effluent TON at all loading rates.

Figures 9.6 and 9.7 show the comparison between effluent spot samples at 1.35m and 1.6m. The removal of BOD and $\text{NH}_4\text{-N}$ are slightly better at 1.35m for all VLRs.

Figure 9.6: Comparison of BOD Removal at 1.35m and 1.6m (Spot Samples)

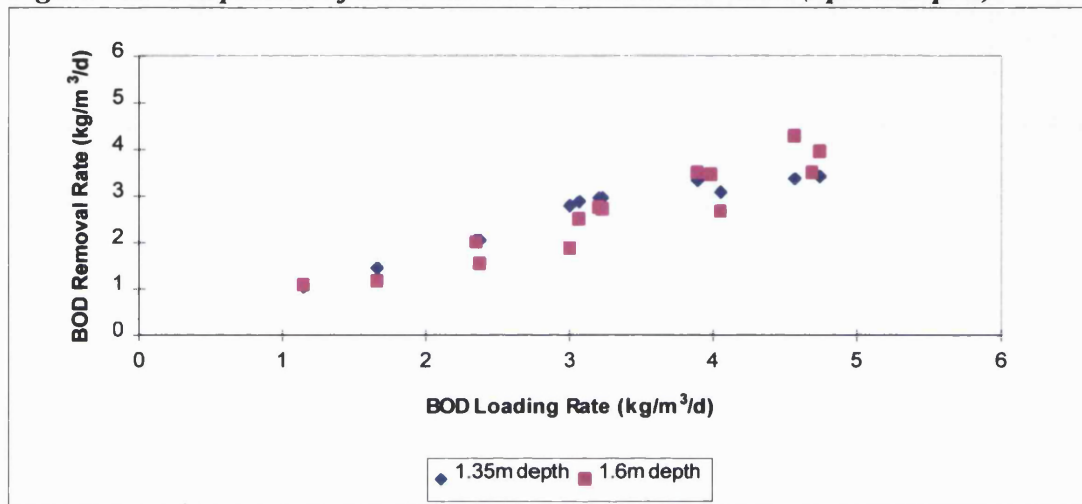
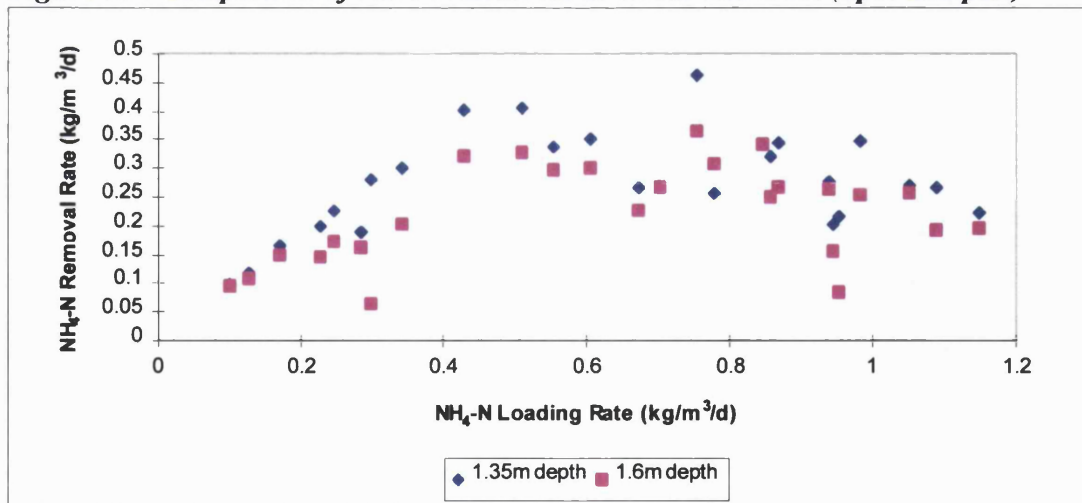


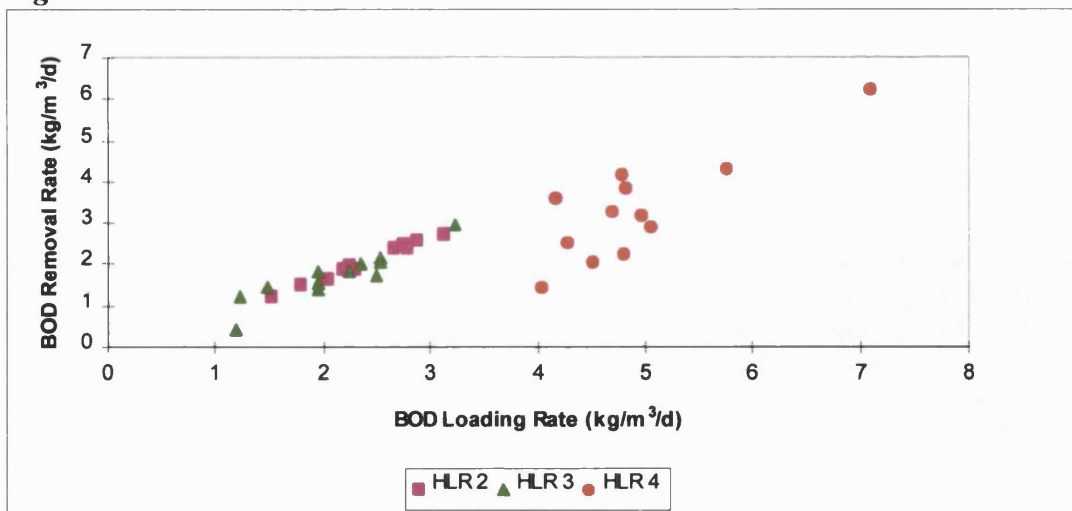
Figure 9.7: Comparison of $\text{NH}_4\text{-N}$ Removal at 1.35m and 1.6m (Spot Samples)



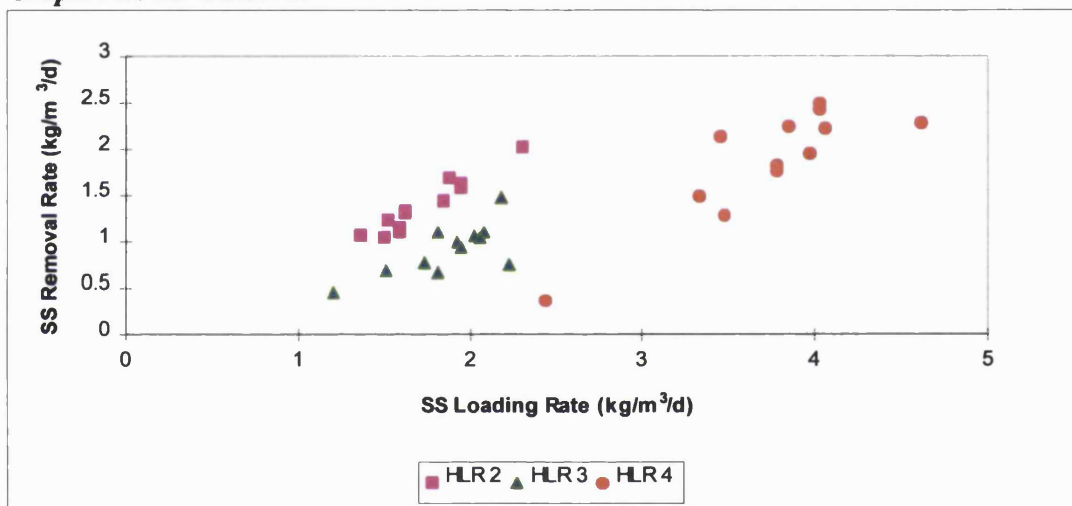
9.2.3: Diurnal Variation

Figures 9.8 - 9.10 show BOD, SS and $\text{NH}_4\text{-N}$ removals over twenty four hours. The patterns of removal are similar to those seen with composite samples.

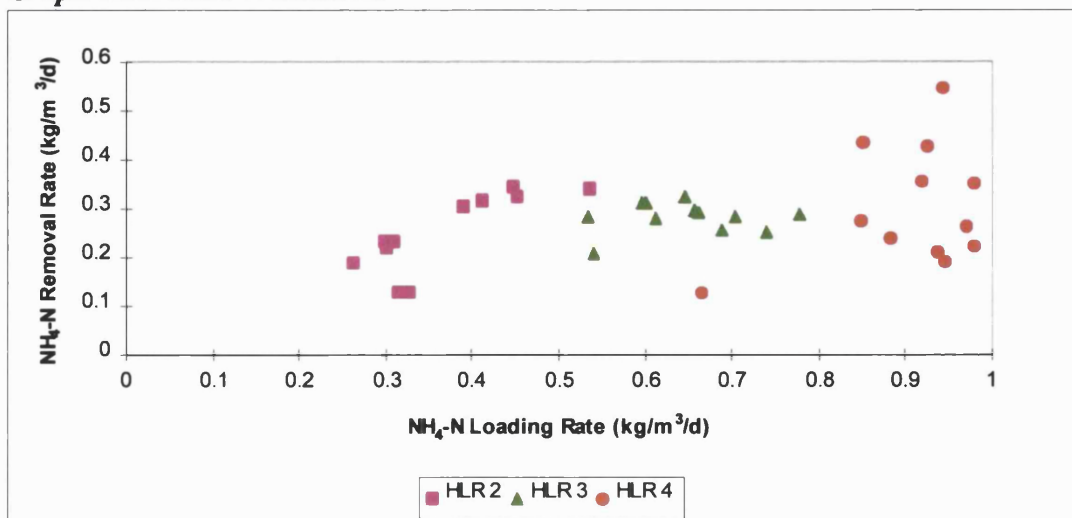
Figure 9.8: BOD Removal



Graph 9.9: SS Removal



Graph 9.10: NH₄-N Removal



Again SS and NH₄-N removals follow loading rate rather than being affected by backwashing.

9.2.4: Bed Profiles

Bed profiles were taken for each HLR as shown by Figures 9.11 - 9.15. The BOD and COD profiles show very high removals in the top 0.35m of the filter bed, with removal continuing to a depth of approximately 1.1m. There is removal of SS throughout the top 1.1m of the filter bed but removals are fairly low at HLR 4.

The bed profiles of NH₄-N removal show there is some removal in the top 0.85m of the bed but very little removal at the bottom of the bed. This corresponds to the low TON production shown throughout the filter bed at all HLRs.

Figure 9.11: BOD Profiles

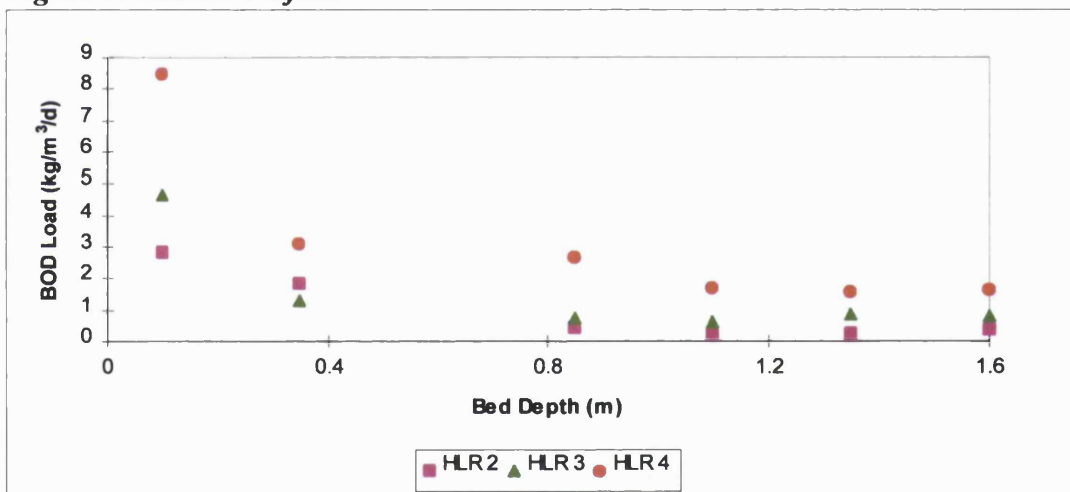


Figure 9.12: COD Profiles

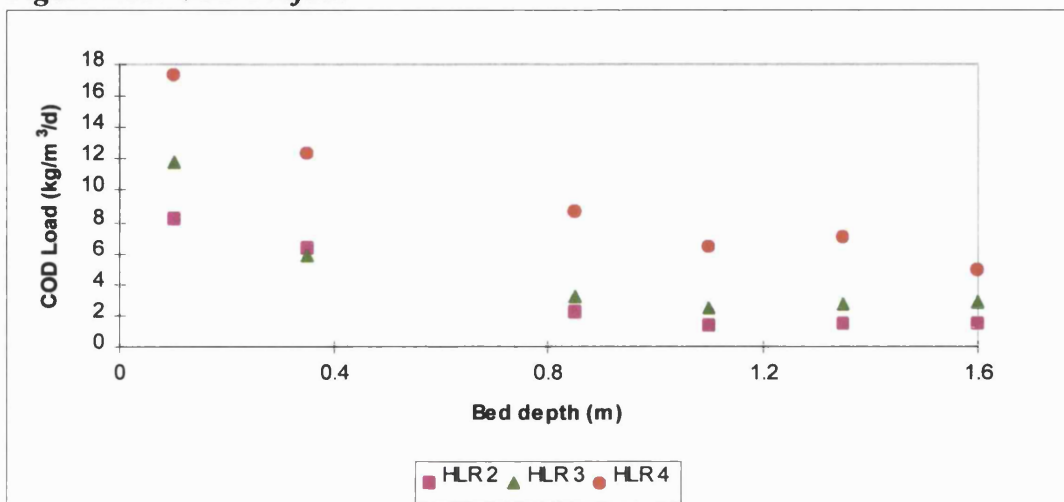


Figure 9.13: SS Profiles

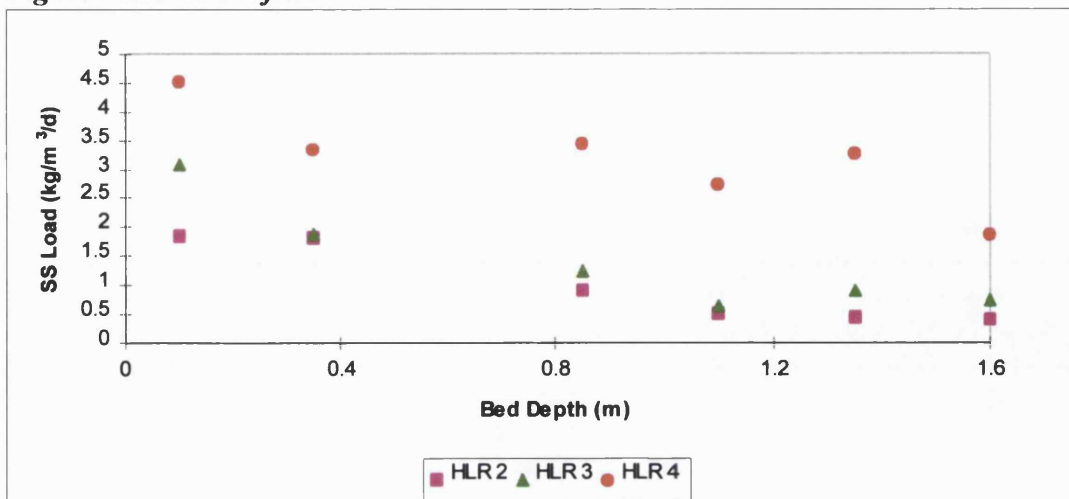


Figure 9.14: NH₄-N Profiles

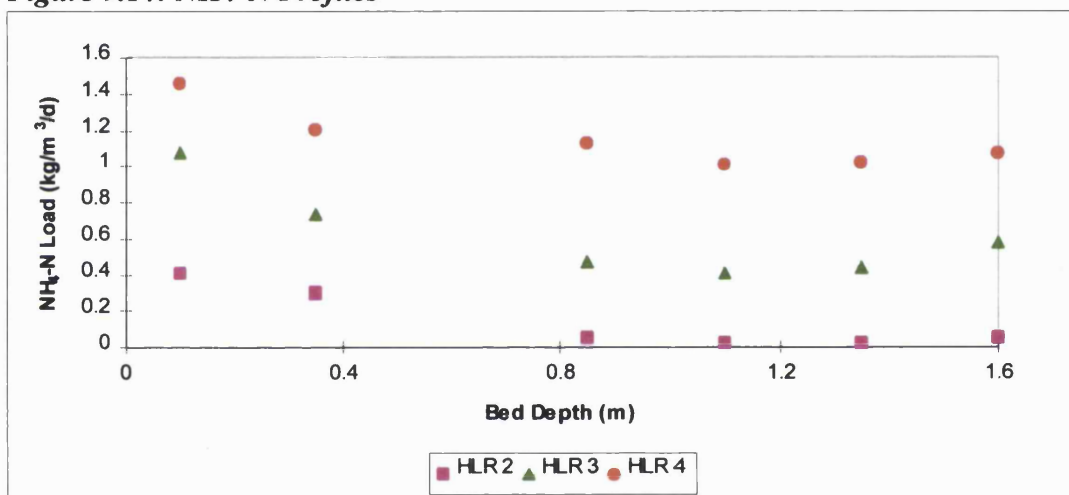


Figure 9.15: TON Profiles

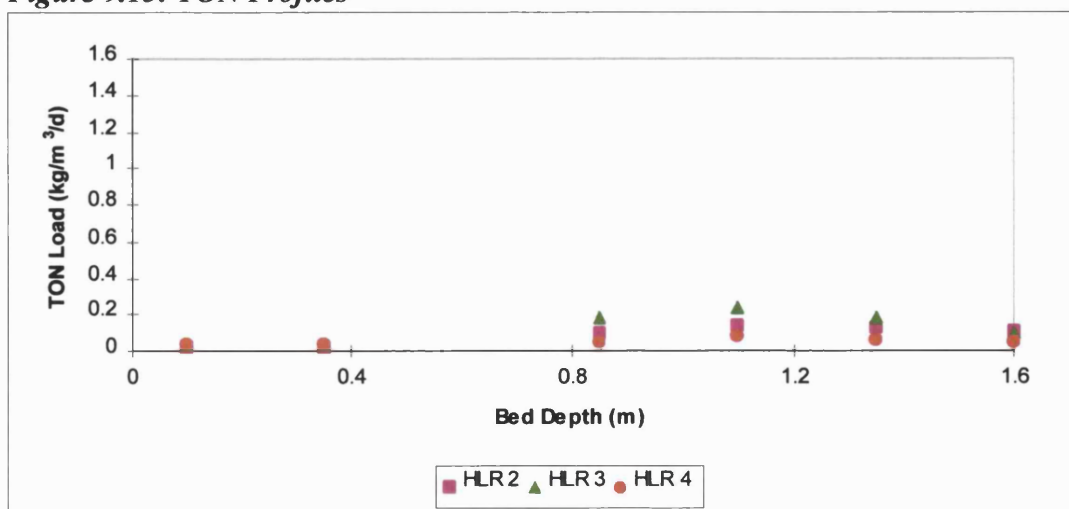
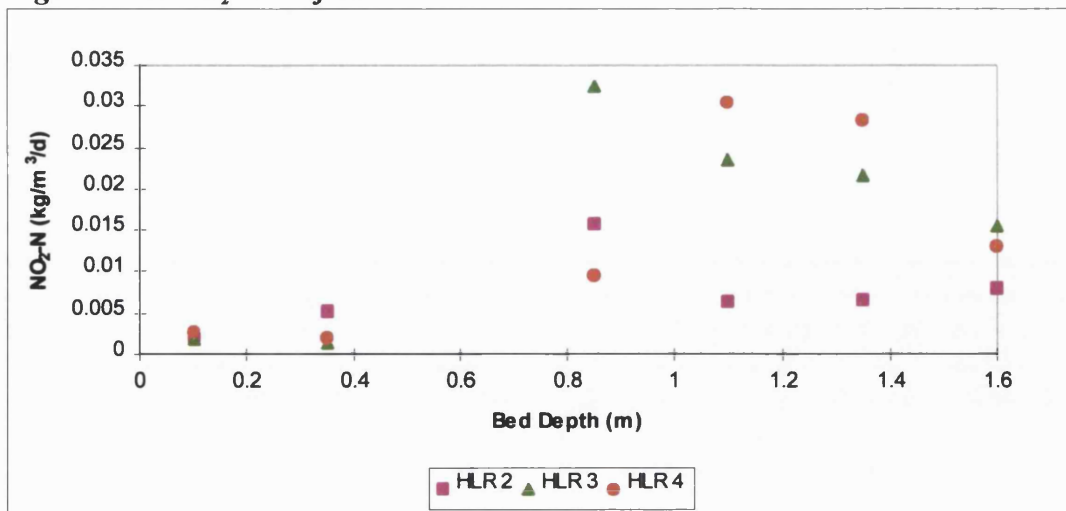


Figure 9.16: NO₂-N Profiles



There are high values of denitrification at all HLRs (Table 9.5) and there is an obvious increase in the percentage denitrification with an increase in HLR/VLR.

Table 9.5: Denitrification

HLR	TKN VLR	TKN Removed	BOD Removed	N Assimilation	TON Expected	TON Produced	Denite	Denite (%)
2	0.39	0.27	2.05	0.1	0.17	0.07	0.1	60
3	0.71	0.47	2.39	0.12	0.35	0.06	0.29	82
4	1.1	0.36	3.45	0.17	0.19	0.02	0.17	90

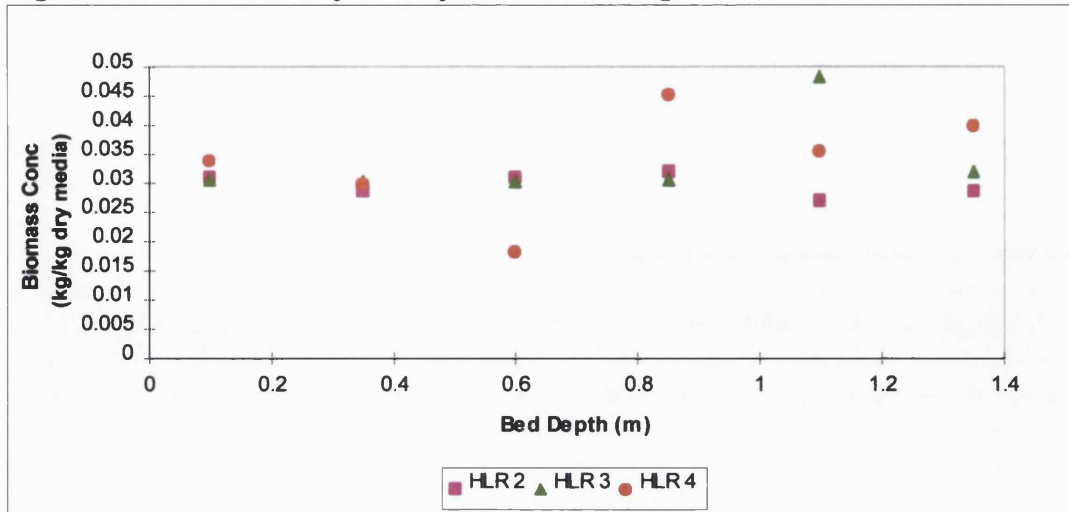
All expressed in kg/m³/d except % denitrification

9.3: Biofilm Growth

9.3.1: Biomass Samples

Figure 9.17 shows the biomass bed profiles for each media before backwashing of the filters. The concentration of biomass is 0.02 - 0.05kg biomass/kg dry media with no obvious pattern relating to bed depth or HLR.

Figure 9.17: Biomass Profiles (Before Backwashing)



9.3.2: Microbiological Analyses and SEMs

The microbiological analysis showed similar microorganisms to those found on 2-4mm Lytag at all depths, SEMs also showed similar biofilm coverage and ciliate presence as found for 2-4mm Lytag (Chapter 7).

9.3.3: 'Slime' Growth on Media Particles

The particles appear to be fairly clean with some patches of biofilm present.

Figure 9.18: 4-8mm Media Particles From Middle of Filter Bed (HLR 2)

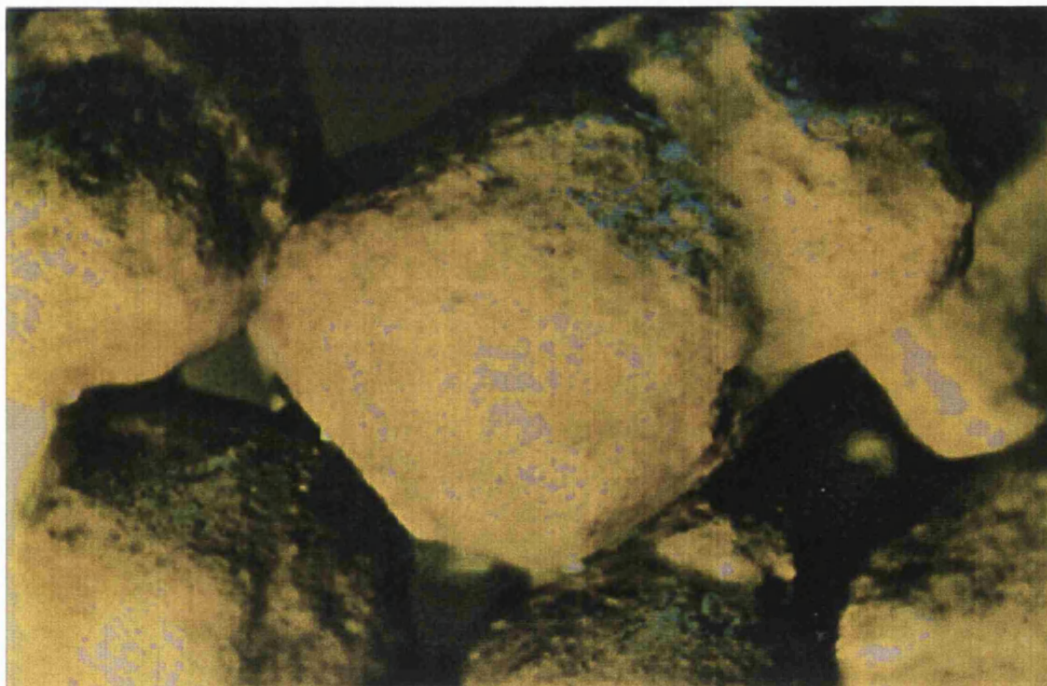


Figure 9.19: 4-8mm Media Particles From Middle of Filter Bed (HLR 4)



9.4: Headloss

The head build-up for each loading rate was recorded at each manometer point as shown in Figure 9.20 for HLR 4. There is a gradual build-up of head until the filter floods at approximately 45 hours. Table 9.5 shows flood times at each HLR, the filter run times decrease as HLR increases.

Figure 9.20: Head Profile (HLR 4)

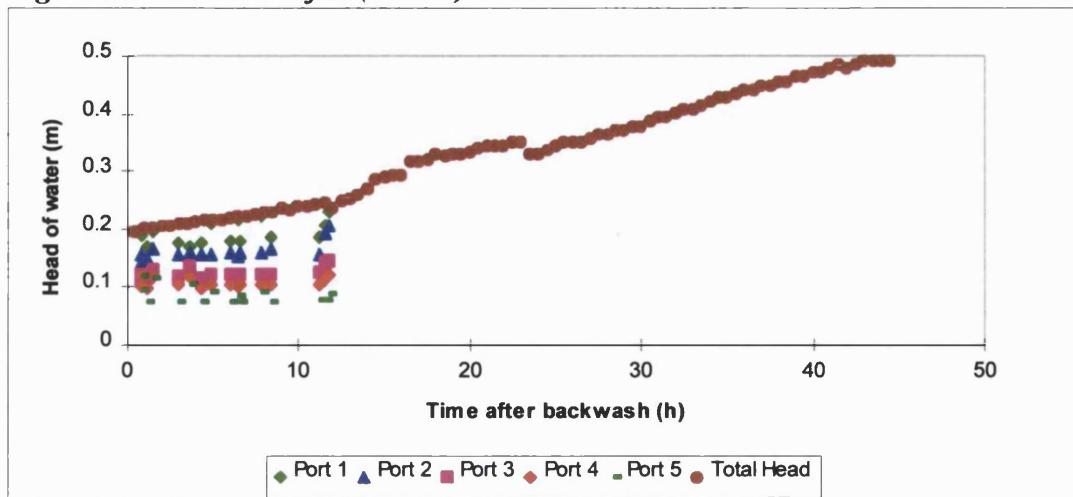


Table 9.5: Flood Times from Ranger Data

Load	HLR (m/h)	Flood Time (hours)
2	1.0	36 - 40
3	1.5	33 - 38
4	2.0	30 - 32

9.5: Backwash Samples

The pattern of suspended solids removal by backwashing is shown in Figures 9.21 and 9.22. There is a peak removal of SS (1000mg/l) after 60 seconds of combined water and air wash, this decreases to less than 200mg SS/l at the end of the rinse phase. At all HLRs there is a total of 0.4kg SS removed at each backwash.

Figure 9.21: Backwash Profiles

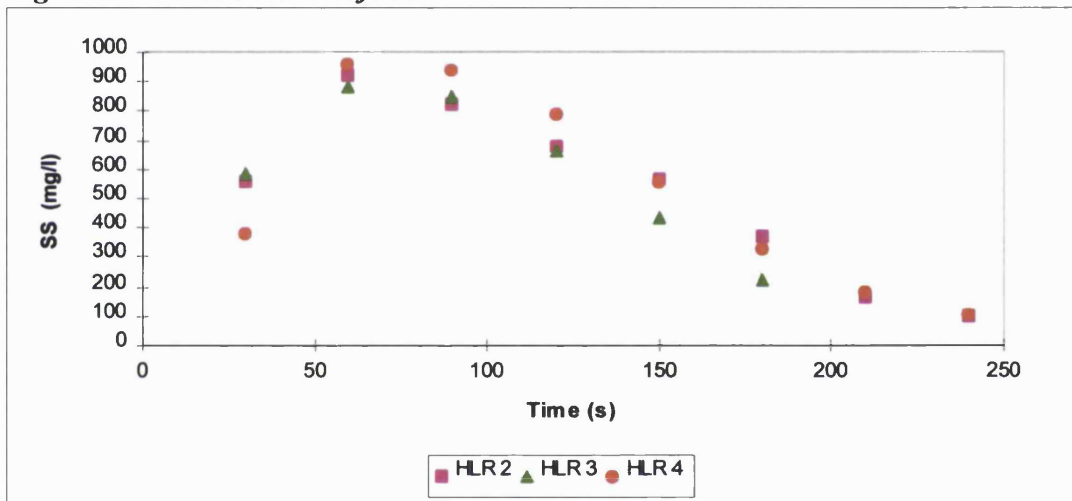
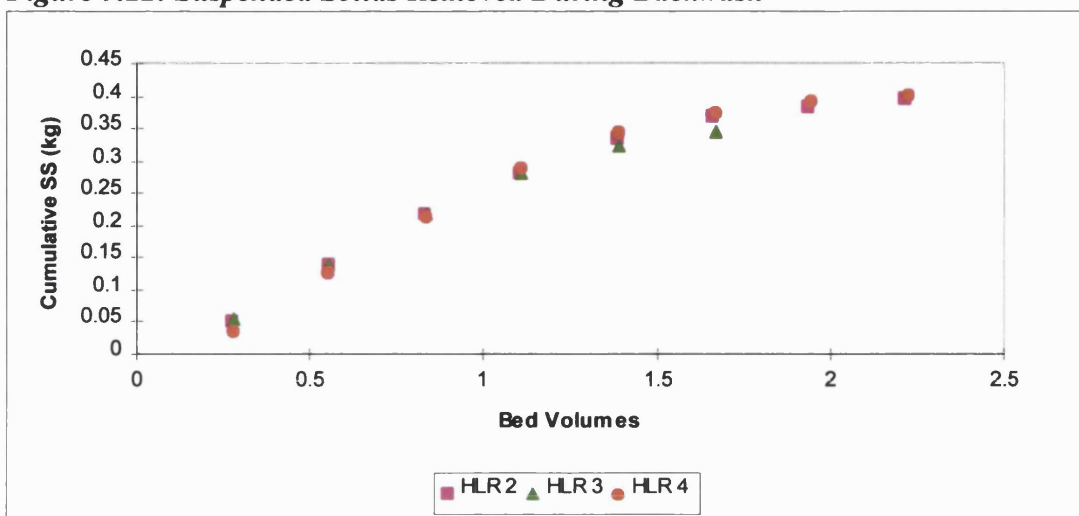


Figure 9.22: Suspended Solids Removed During Backwash



Calculations of total solids removed each week and effluent reused for backwashing each week are given in Tables 9.6 and 9.7. The amount of solids removed by backwashing increases as solids load to the filter increases. The percentage effluent reuse for backwashing is high at approximately 16-17 % for backwashing on time, but if filters were washed according to head build-up there would be a much lower percentage effluent reuse.

Table 9.6: Total Suspended Solids Removed During Backwash

Load	Total SS Load (kg/week)	Total SS Removed (kg) ¹	Total SS Removed (kg/week) ²	Effluent SS
2	2.6	0.39	2.73	0.43
3	6.17	0.34	4.76	0.9
4	6.28	0.31	5.6	2.65

1 - Average for each backwash 2 - Washed on time basis

Table 9.7: Percentage of Treated Effluent Used For Backwash

Load	Backwash water volume (l)	Total vol/week	Percentage of weekly effluent produced
2	756	5292	16.8
3	567	7938	16.3
4	756	10584	16.5

9.6: Sludge Samples

Table 9.8 shows parameters investigated for sludge samples at all HLRs. One-way ANOVA tests show that differences occur in the CST tests and the sludge solids content in HLR 2 is different to at the other HLRs.

Table 9.8: Sludge Data

Load	BW SS (mg/l)	Sludge SS (mg/l)	Sludge Dry Solids (%)	Volatile Solids (%)	CST (seconds)
2	508	4198	0.82	72	59
3	540	5088	0.67	78.6	35
4	647	4774	0.55	86.6	29

9.7: Off-Gas Analysis

During off-gas analysis the oxygen transfer efficiency and oxygenation capacity were determined (Figures 9.23 - 9.25) and dissolved oxygen profiles were taken (Figure 9.26). There is a slight increase in operational OTE with increasing HLR and with decreased air flow. When the OTE is corrected to zero DO it decreases slightly with

increased HLR. The OC for 4-8mm Lytag increases with increased air flow and appears to be maximum at an air flow of 9 - 11m/h for HLR 2 and 3 , whilst OC is still increasing for HLR 4 at air flows above 13m/h.

Figure 9.23: Operational Oxygen Transfer Efficiency (OTE)

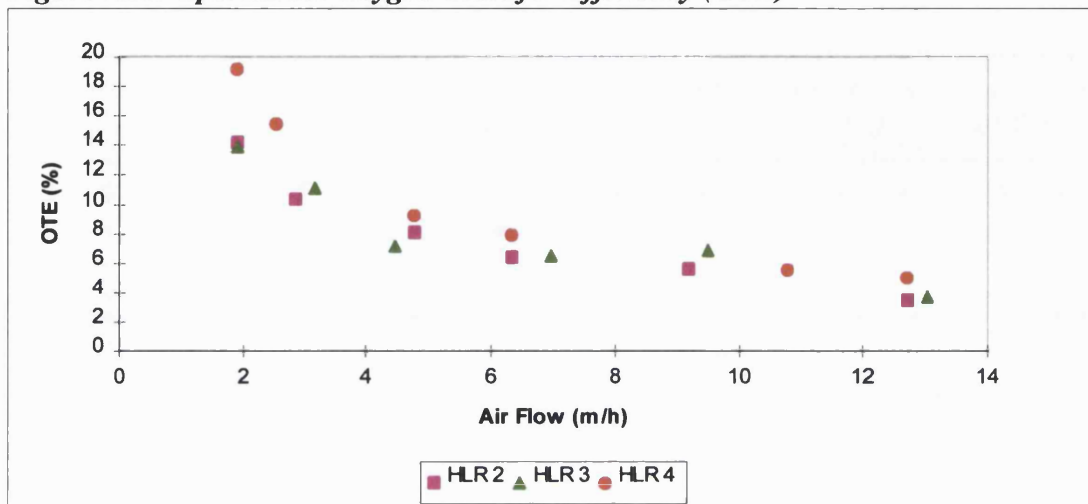


Figure 9.24: Corrected OTE

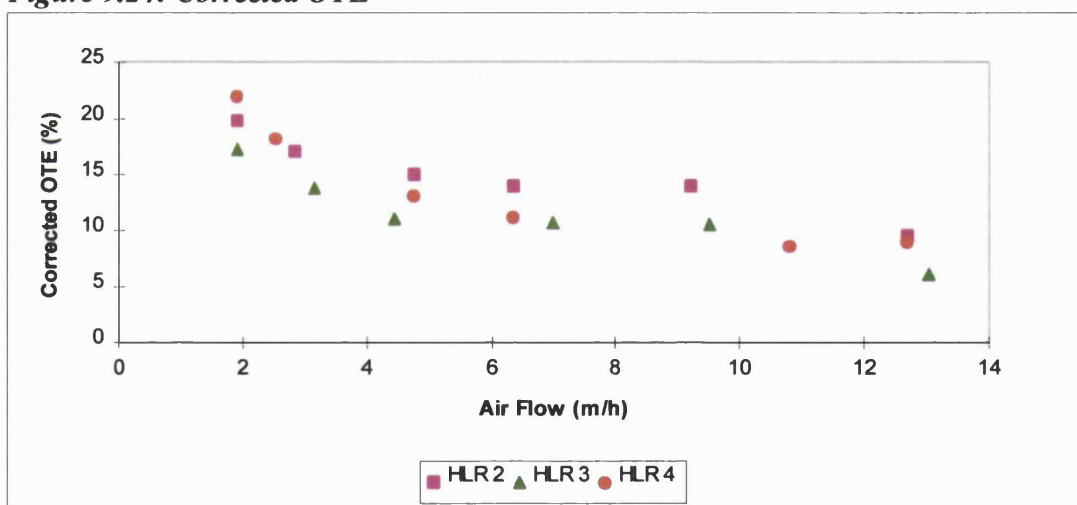


Figure 9.25: Oxygenation Capacity

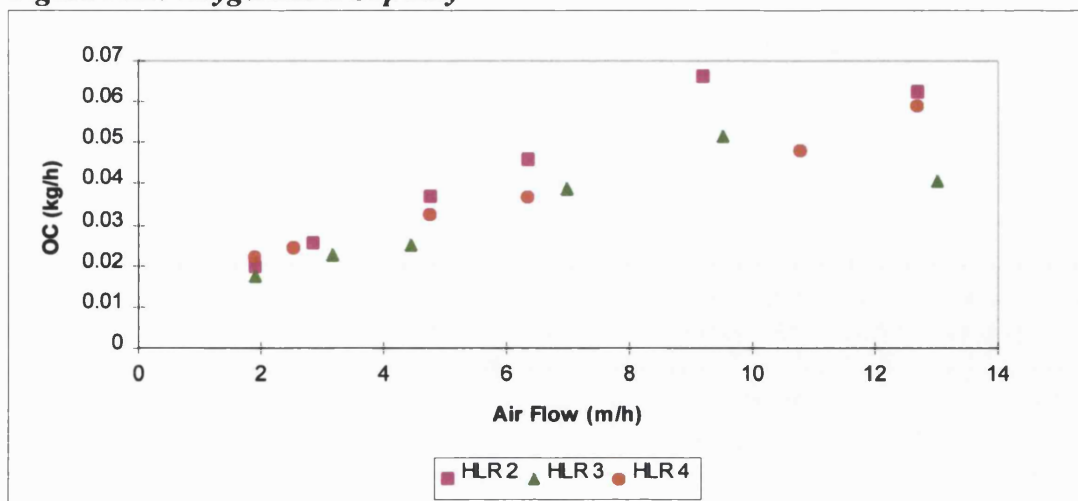
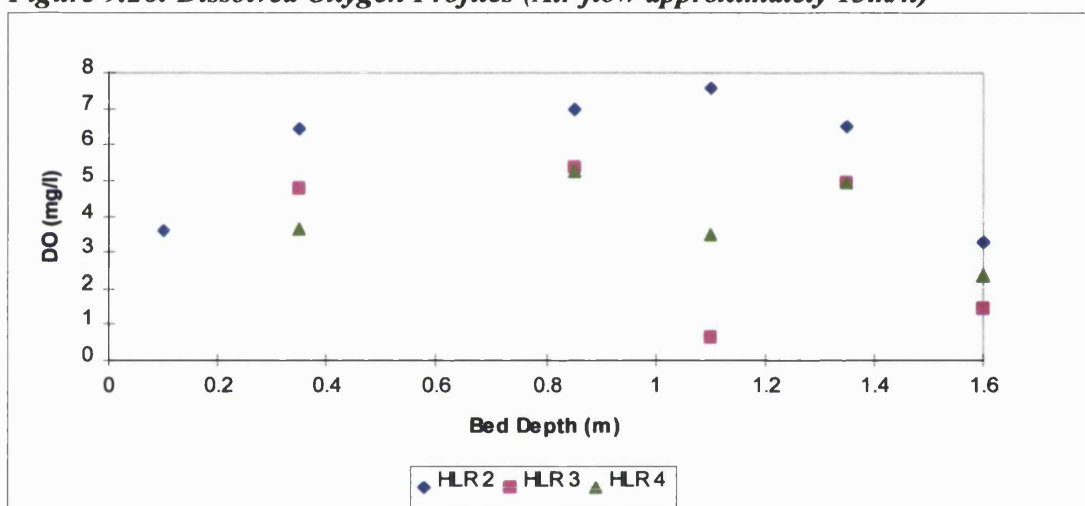


Figure 9.26: Dissolved Oxygen Profiles (Air flow approximately 13m/h)



The DO profile for 4-8mm Lytag shows a decreased DO with increasing HLR.

The theoretical oxygen demand for each loading rate was calculated and compared with the experimental oxygen demand (Table 9.9). The demand increases with increased HLR/VLR with a slight decrease at HLR 4.

Table 9.9: Oxygen Demand For 4-8mm Lytag Media

Load	Loading (kg/m ³ /d)	Ammonia Oxidation (%)	Estimated Demand (kg O ₂ /h)	Actual Demand (kg O ₂ /h)
2	BOD - 2.17			
2	NH ₄ -N - 0.29	81	0.028	0.027
3	BOD - 2.63			
3	NH ₄ -N - 0.46	65	0.033	0.035
4	BOD - 4.78			
4	NH ₄ -N - 0.87	30	0.039	0.032

9.8: Hydraulic Regime

Figure 9.27 shows an example of a residence time distribution (RTD) curve before and after backwashing for HLR 2. Calculations of RT are given in Table 9.10.

Figure 9.27: Tracer Tests (Hydraulic Load = 1m/h)

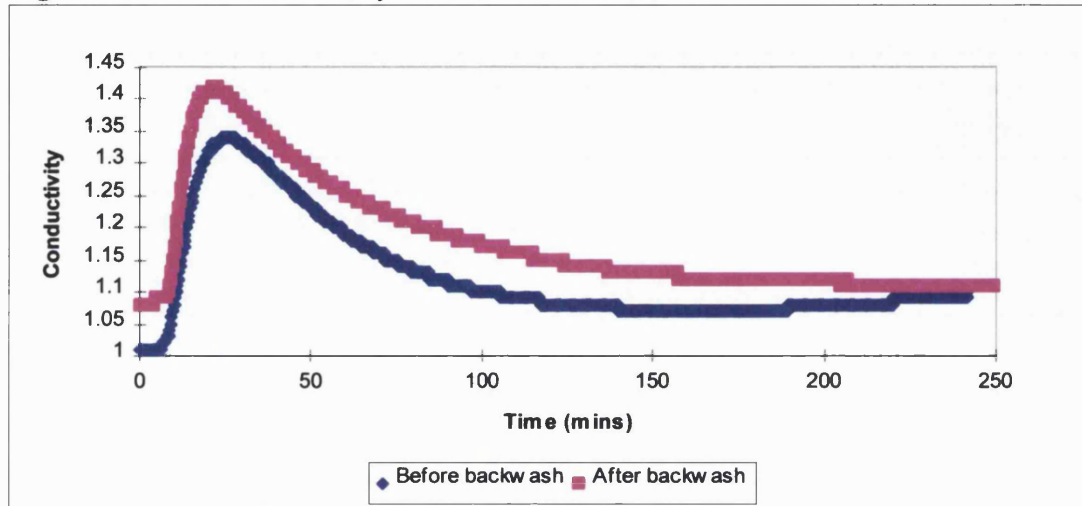


Table 9.10: Retention Times (After Backwash)

Load	Theoretical Retention Time (mins) ¹	TRT (mins) ²	D/uL ³	Peak RT (mins)	Mean RT (mins)
2	96	30	0.3571	25	66
3	63	20	0.267	17	49
4	47	15	0.1619	20.5	39

1 - Empty Bed 2 - Assuming experimental voidage of 0.31 3 - Dispersion number

The retention times decrease with increasing HLR, whilst flow regimes tend more towards plug flow (as shown by the decreasing dispersion number).

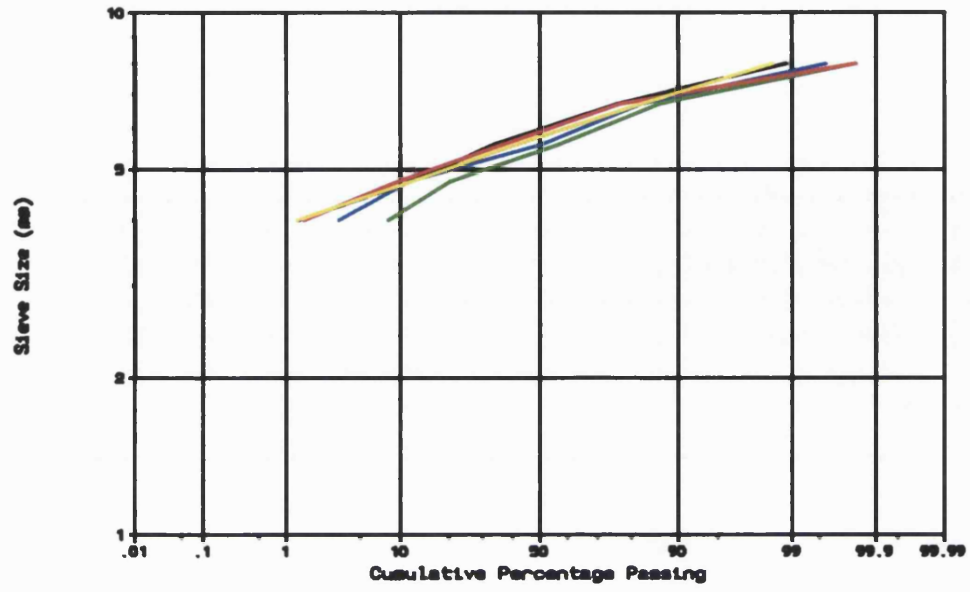
9.9: Decommissioning

The particle size range after filter operation is shown in Figure 9.28 and Table 9.11. There appears to be very little difference from the original size range of 4-8mm Lytag.

Table 9.11: Sieve Analysis of 4-8mm Lytag After Filter Operation

Media Sample	Hydraulic Size (mm)	d ₅ (mm)	d ₁₀ (mm)	d ₆₀ (mm)	UC	d ₉₀ (mm)	d ₉₅ (mm)
Original	5.63	4.2	4.7	5.8	1.23	6.9	7.2
Overall	5.74	4.4	4.7	6.0	1.28	7.0	7.4
Top	5.37	3.9	4.1	5.6	1.37	6.8	7.0
Middle	5.87	4.4	4.7	6.2	1.32	7.0	7.4
Bottom	5.63	4.4	4.8	6.0	1.25	7.0	7.2

Figure 9.28: Sieve Analysis of 4-8mm Lytag After Decommissioning



10.0 PILOT SCALE PERFORMANCE OF LYTAG MEDIA

Results: 5.6-11.2mm Lytag

10.1: Introduction

The 5.6-11.2mm Lytag is larger than normal for BAF media. It was included in this study to see whether it could compare to the more usual BAF media and if there were any benefits to using media that needed a low frequency of backwashes.

10.2: Steady State Results

10.2.1: Settled Sewage

Table 10.1 gives calculated VLRs onto the filter.

Table 10.1: Loading Rates for Composite Samples

Load	Hydraulic Load (m/h)	BOD Load (kg/m³/d)	COD Load (kg/m³/d)	SS Load (kg/m³/d)	NH₄-N Load (kg/m³/d)	TKN Load (kg/m³/d)
1	0.5	1.17	2.62	0.77	0.2	0.26
2	1.0	2.19	4.47	1.28	0.3	0.4
3	1.5	2.68	6.29	2.81	0.47	0.72
4	2.0	4.86	10.65	3.02	0.89	1.17

10.2.2: Effluent Quality

Table 10.2 shows the percentage removals of BOD, COD, SS and NH₄-N for each loading rate. There is a general decrease in percentage removals for all determinands, with increasing HLR and VLR, with low removals at HLR 4.

Table 10.2: Percentage Removals by 5.6-11.2mm Lytag

Load	BOD Removal (%)	COD Removal (%)	SS Removal (%)	NH₄-N Removal (%)	TKN Removal (%)
1	93.8	83.2	84.4	91.6	86
2	85.9	69.4	61.6	62.7	65.1
3	76.5	60.2	65.1	36.1	41.6
4	48.5	43.1	26	13.3	14.4

Figures 10.1 - 10.5 show the removals of different determinands for composite samples at a depth of 1.35m.

Figure 10.1: Composite BOD Removals

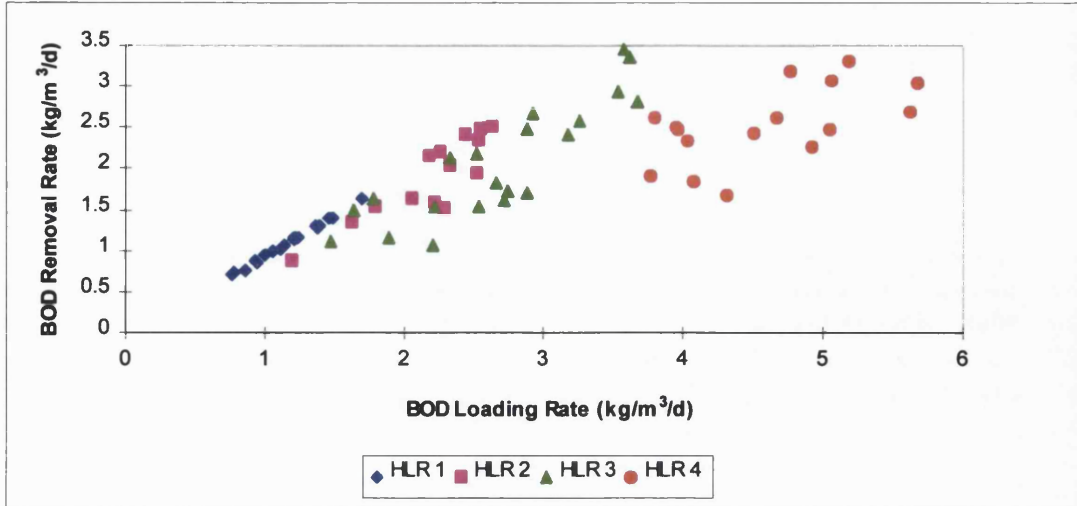


Figure 10.2: Composite COD Removals

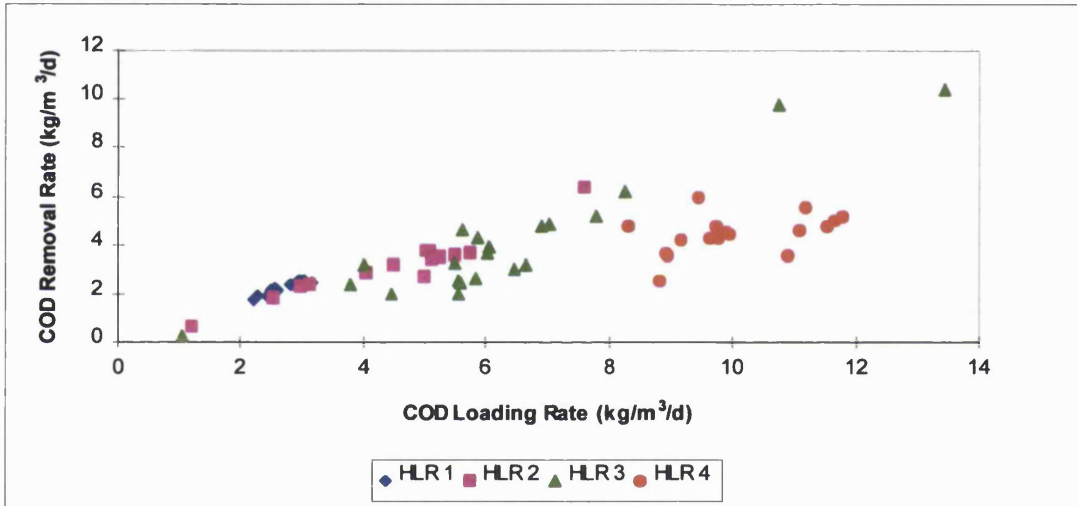


Figure 10.3: Composite SS Removals

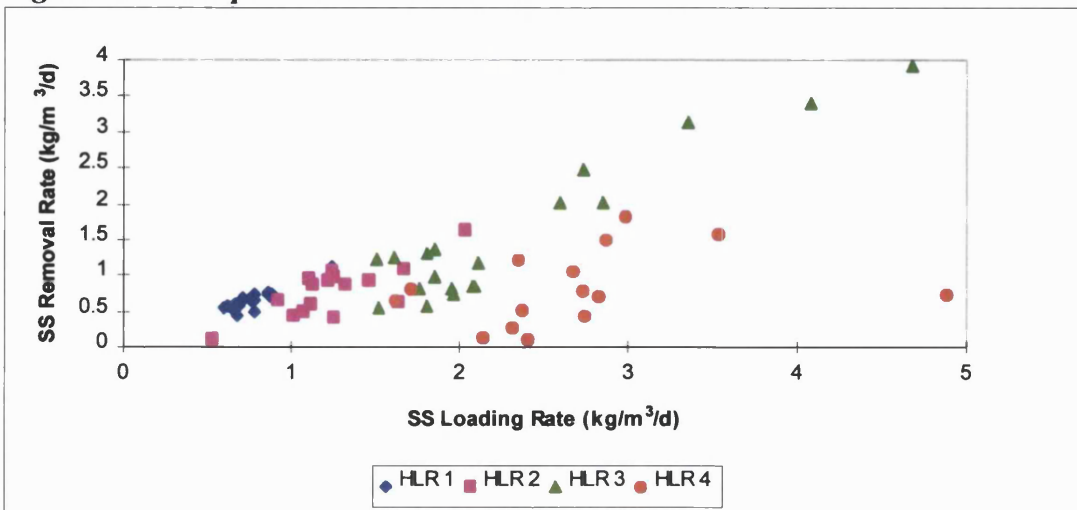


Figure 10.4: Composite NH₄-N Removals

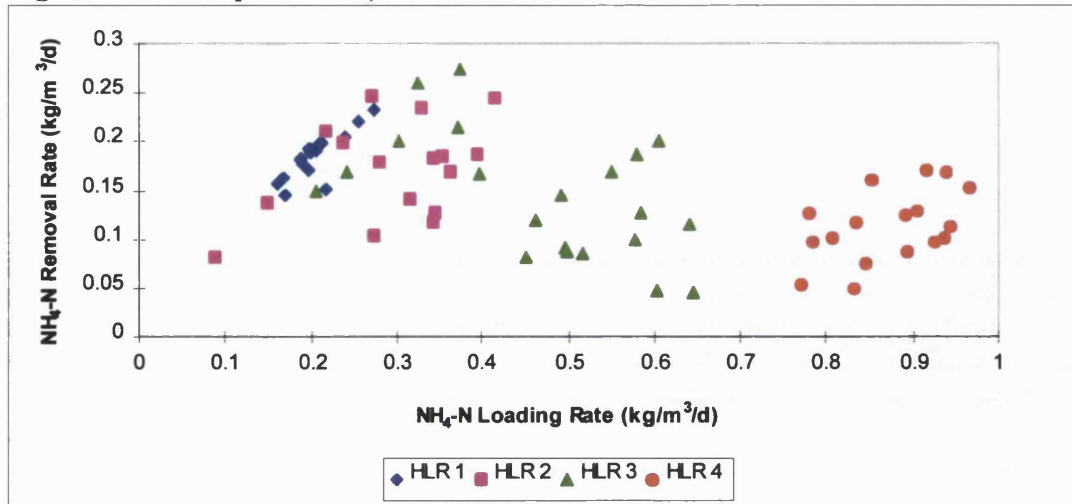
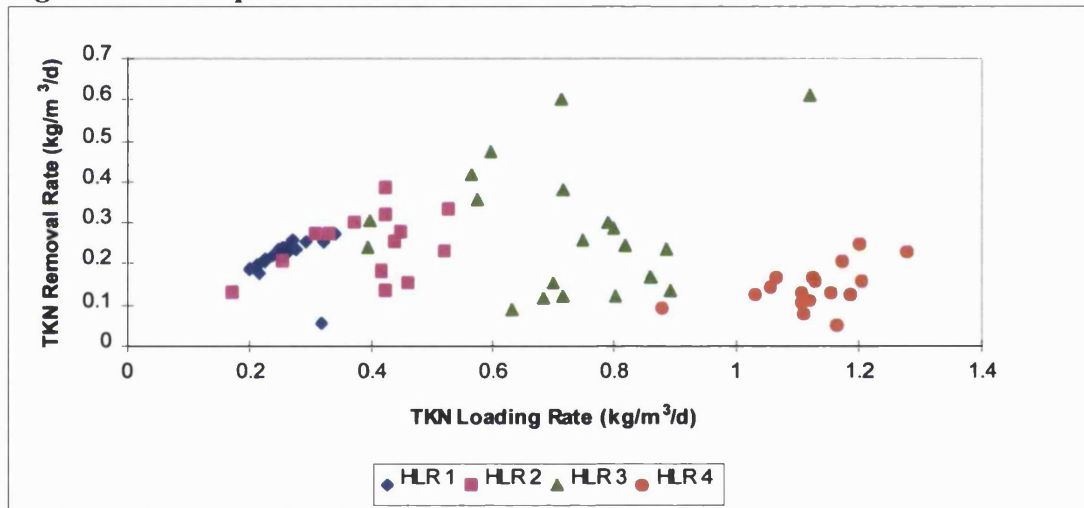


Figure 10.5: Composite TKN Removals



There is a high degree of scatter for removals of all determinands against VLR. The graphs of BOD, COD and SS show positive relationships between removal and VLR. The graphs of NH₄-N and TKN show high removals at HLR 1 but this decreases at HLR 2 - 4 where there is very little removal. Actual effluent concentrations are shown in Table 10.3.

Table 10.3: Effluent Concentrations for 5.6-11.2mm Lytag

Load	BOD (mg/l)	COD (mg/l)	SS (mg/l)	NH ₄ -N (mg/l)	TKN (mg/l)	TON (mg/l)	NO ₃ (mg/l)
1	9.8 (2.9)	58.8 (12.1)	16 (8.1)	2.8 (2.7)	5.5 (7.2)	9.9 (5.1)	9 (5.1)
2	18.2 (15)	84.1 (36.8)	29.5 (15.3)	8.2 (5.5)	10.2 (6.8)	3.4 (2.6)	2.9 (2.2)
3	27 (15.7)	100 (38.9)	34 (15.5)	14.4 (7.5)	19.3 (9.5)	1.8 (1.4)	1.5 (1.2)
4	79.9 (42)	195.3 (45)	67.5 (26.5)	25.1 (1.8)	32.8 (3.7)	1 (0)	0.9 (0.1)

Note: Standard deviations in brackets

Effluent concentrations are low for all determinands at HLR 1, at HLR 2 - 4 the $\text{NH}_4\text{-N}$ levels are high as are BOD and SS at HLR 4. A comparison of removals at depths of 1.35m and 1.6m is shown in Figures 10.6 and 10.7. There appear to be similar removals at these depths for both BOD and $\text{NH}_4\text{-N}$.

Figure 10.6: Comparison of BOD Removal at 1.35m and 1.6m (Spot Samples)

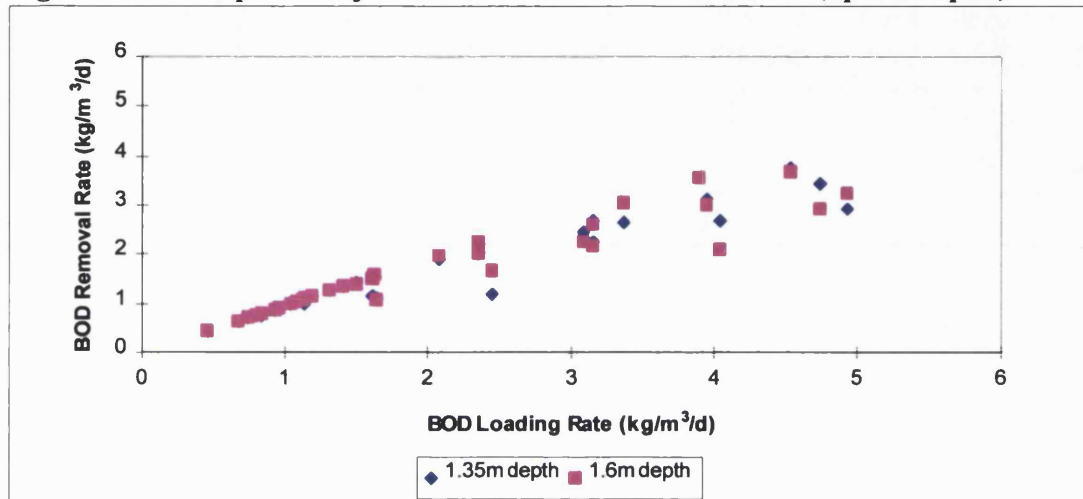
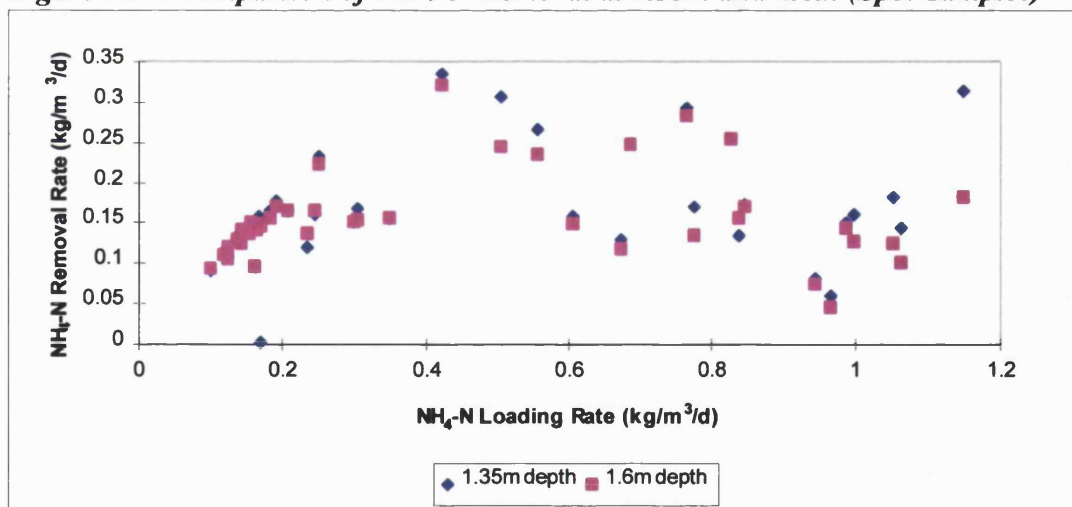


Figure 10.7: Comparison of $\text{NH}_4\text{-N}$ Removal at 1.35m and 1.6m (Spot Samples)

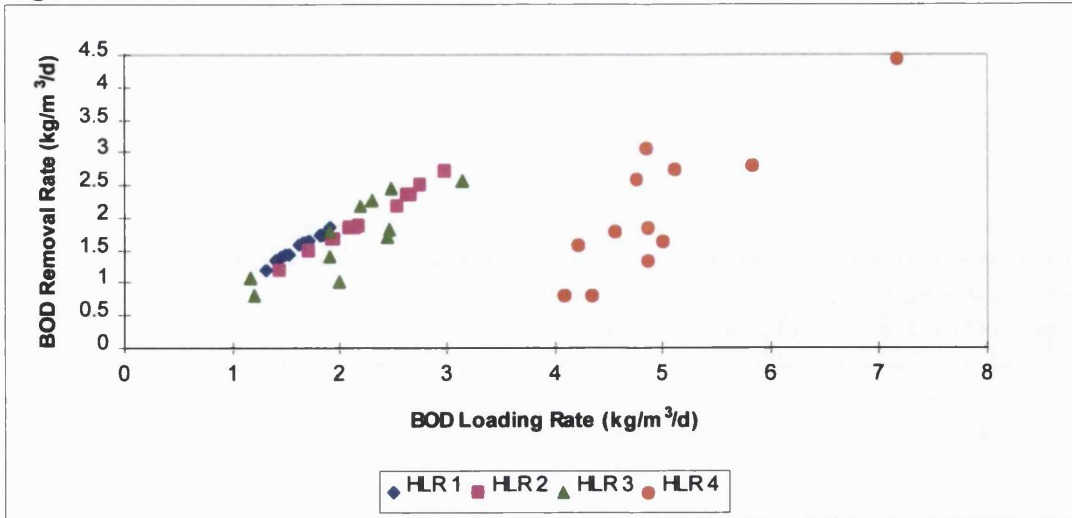


10.2.3: Diurnal Variation

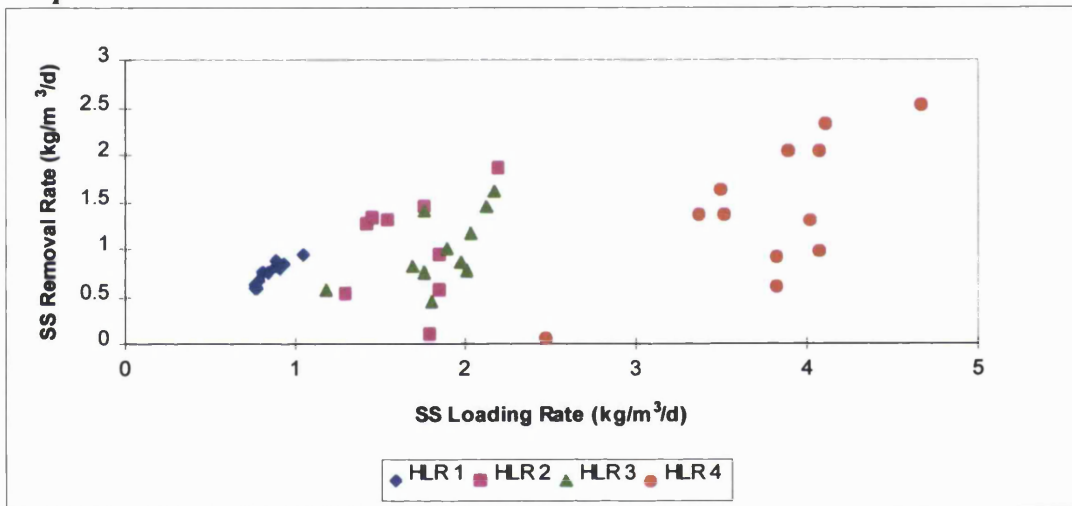
Figures 10.8 - 10.10 show BOD, SS and $\text{NH}_4\text{-N}$ removals over 24 hours. Similar relationships can be seen to those for composite samples.

The SS and $\text{NH}_4\text{-N}$ removals are affected more by VLR than backwash time.

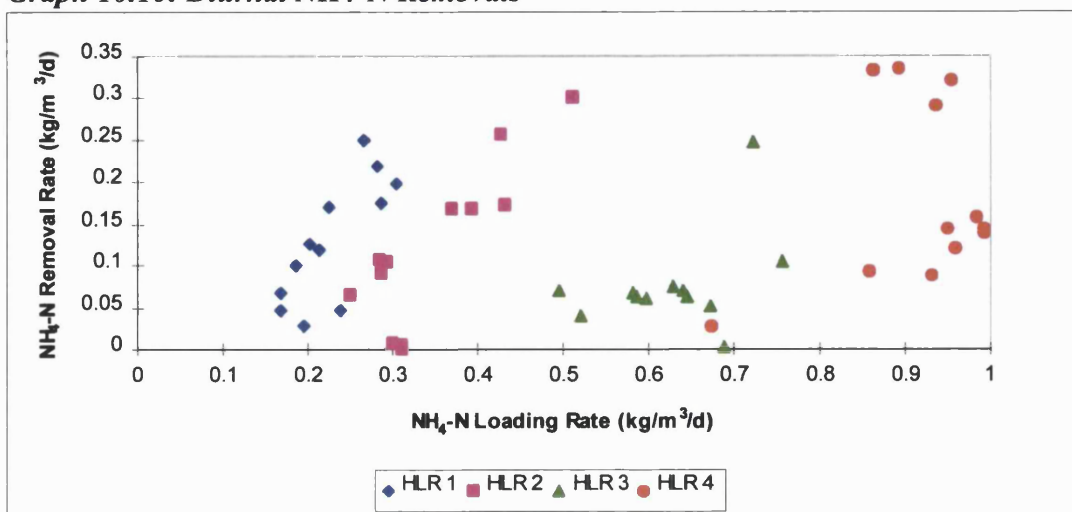
Figure 10.8: Diurnal BOD Removals



Graph 10.9: Diurnal SS Removals



Graph 10.10: Diurnal NH₄-N Removals



10.2.4: Bed Profiles

Bed profiles are shown by Figures 10.11 - 10.15. The profiles of BOD, COD and SS show highest removals in the top 0.35m of the bed, this then gradually decreases to effluent concentrations. There are very low levels of NH_4 removal and there appears to be low production of TON throughout the filter bed.

Figure 10.11: BOD Profiles

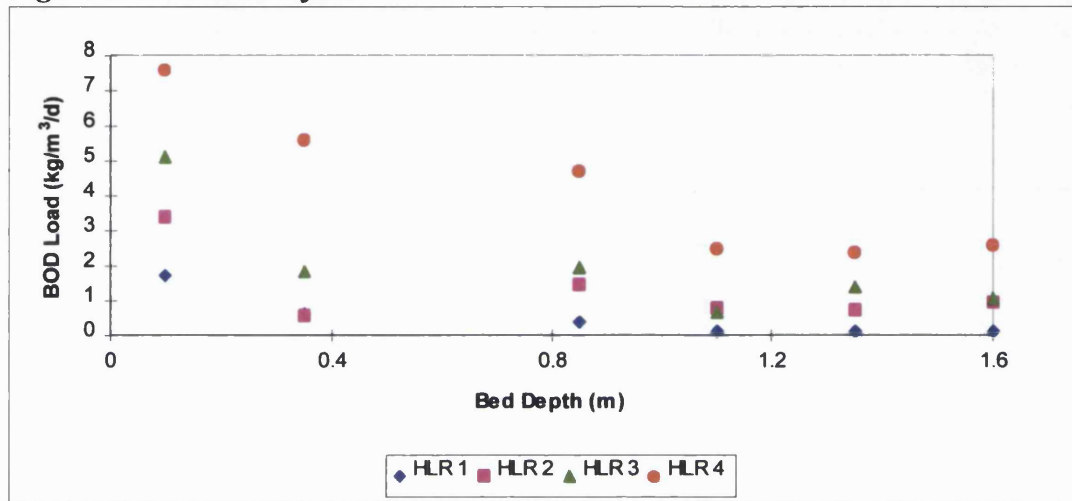


Figure 10.12: COD Profiles

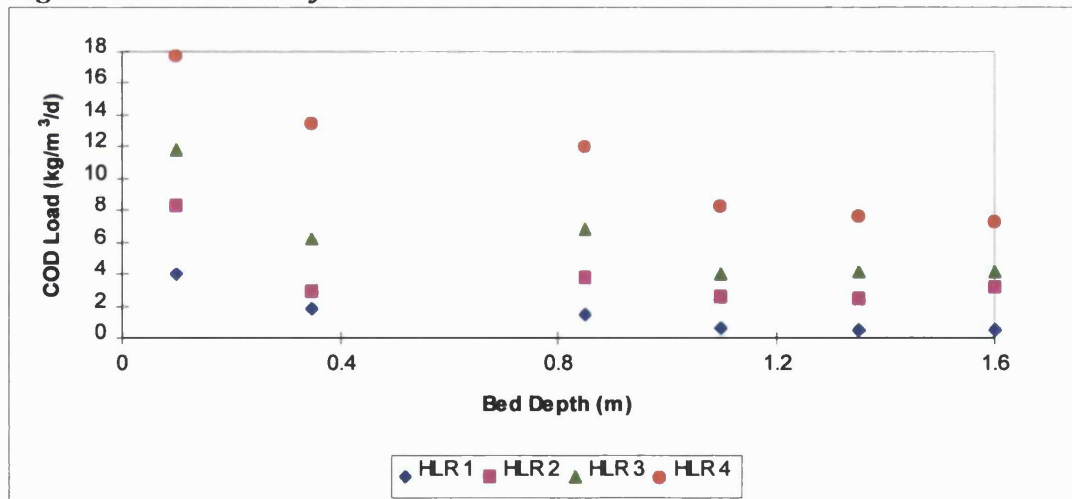


Figure 10.13: Suspended Solids Profiles

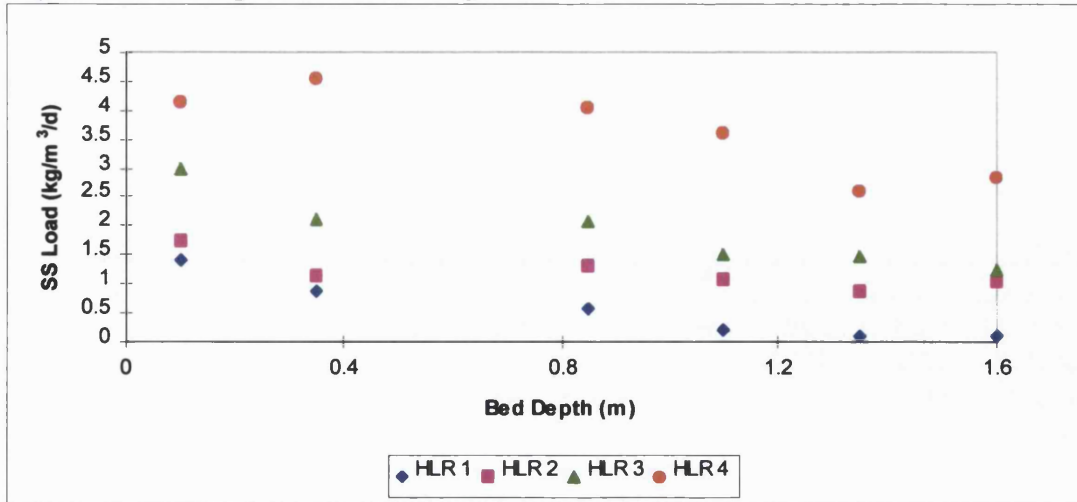


Figure 10.14: NH₄-N Profiles

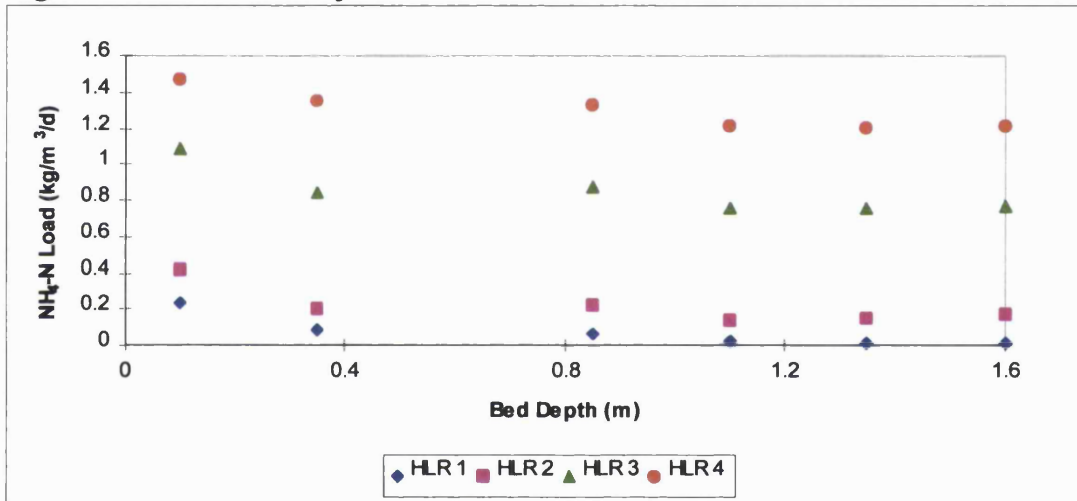


Figure 10.15: TON Profiles

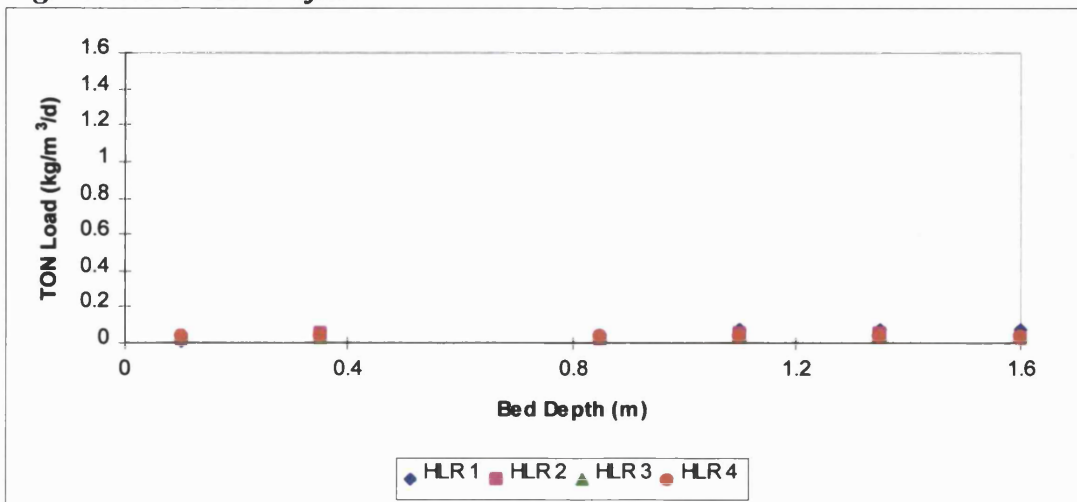
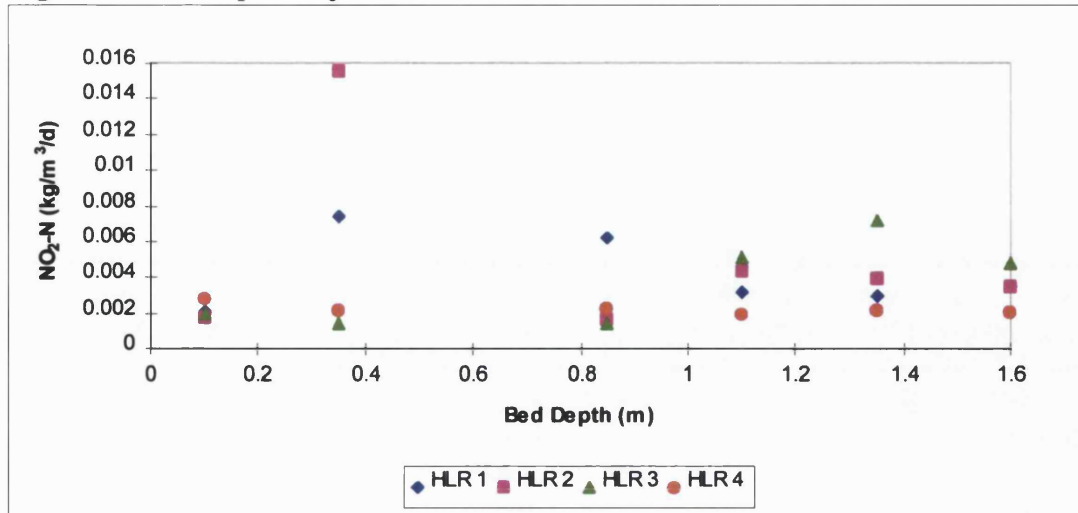


Figure 10.16: NO₂-N Profiles



Values of denitrification are given in Table 10.4. There is increasing denitrification with increasing load up to HLR 4, at which point the low concentrations of NH₄-N removed are converted straight to biomass and there is no NO₃-N available for denitrification.

Table 10.4: Denitrification

HLR	TKN VLR	TKN Removed	BOD Removed	N Assimilation	TON Expected	TON Produced	Denite	Denite (%)
1	0.26	0.22	1.1	0.05	0.17	0.07	0.1	54
2	0.39	0.25	1.9	0.1	0.15	0.04	0.14	59
3	0.72	0.28	2.07	0.1	0.18	0.02	0.32	74
4	1.11	0.11	2.12	0.11	0	0	0	0

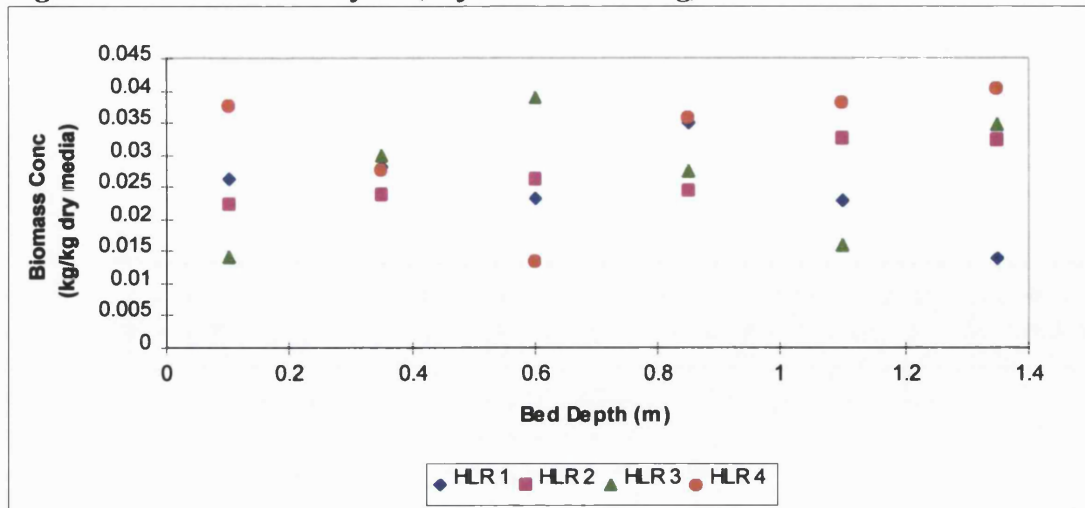
All expressed in kg/m³/d except % denitrification

10.3: Biofilm Growth

10.3.1: Biomass Samples

Figure 10.17 shows the biomass bed profiles for each media before backwashing of the filters. The concentration is approximately 0.02 - 0.04kg biomass/kg dry media, with no obvious pattern between concentration and bed depth or HLR.

Figure 10.17: Biomass Profiles (Before Backwashing)



10.3.2: Microbiological Analyses and SEMs

The microbiological analysis showed similar microorganisms to those found on 2-4mm Lytag at all depths, SEMs also showed similar biofilm coverage and ciliate presence as found for 2-4mm Lytag (Chapter 7).

10.3.3: 'Slime' Growth on Media Particles

Media particles appear to be fairly clean with some patches of biofilm present. There were no obvious signs of 'slime' presence or excessive biofilm growth even at the highest loading rate.

Figure 10.18: 5.6-11.2mm Media Particles From Middle of Filter Bed (HLR 1)

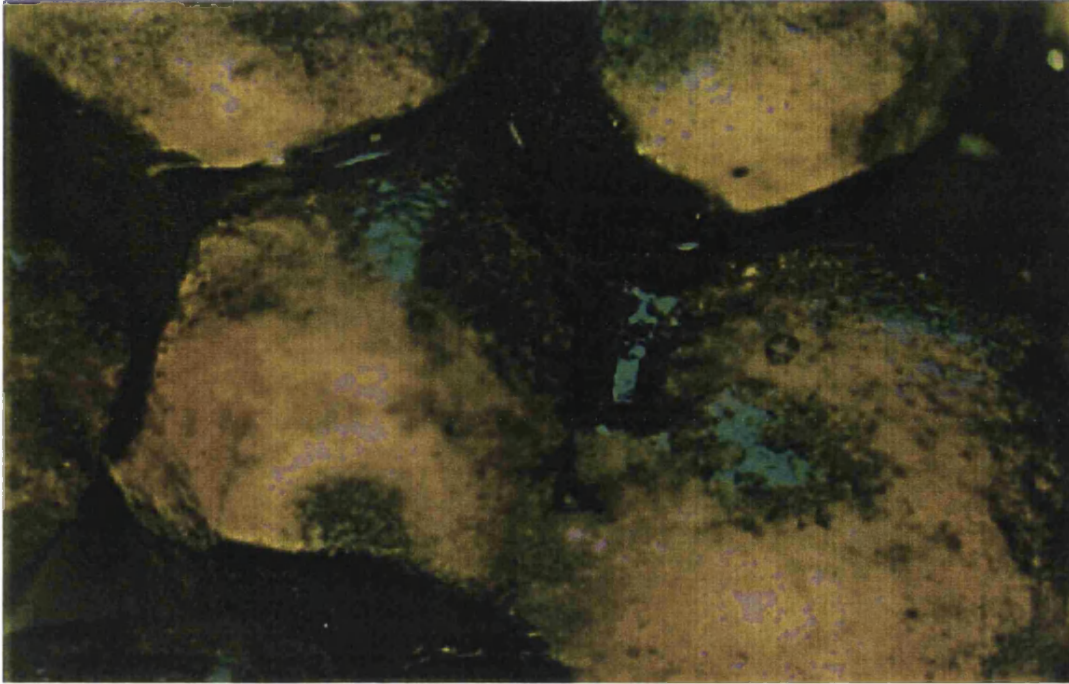
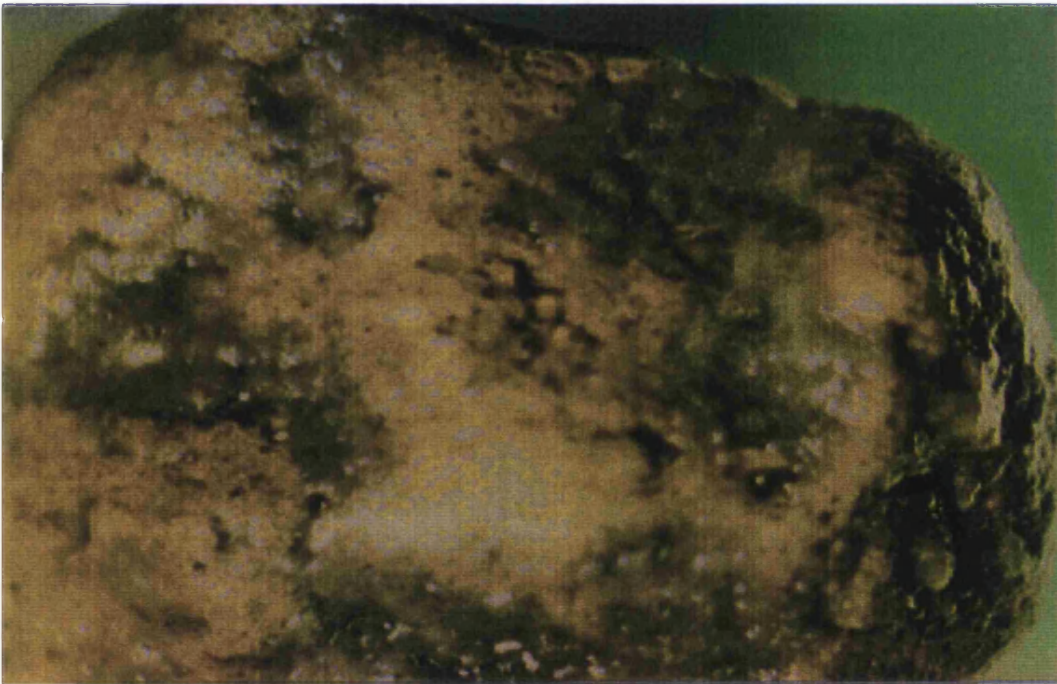


Figure 10.19: 5.6-11.2mm Media Particles From Middle of Filter Bed (Load 4)



10.4: Headloss

The head build-up for each loading rate was recorded at each manometer point as shown in Figures 10.20 -10.21 for HLR 1 and 4. There is very little increase in head and at all investigated HLRs the filter could have had run times of > 50 hours if they were not washed on a time basis.

Figure 10.20: Head Profile (HLR 1)

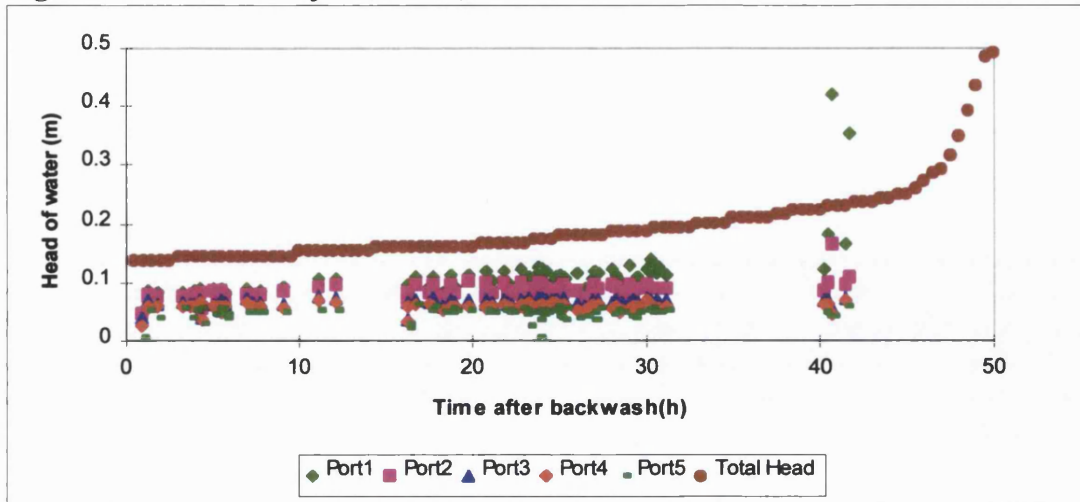


Figure 10.21: Head Profile (HLR 4)

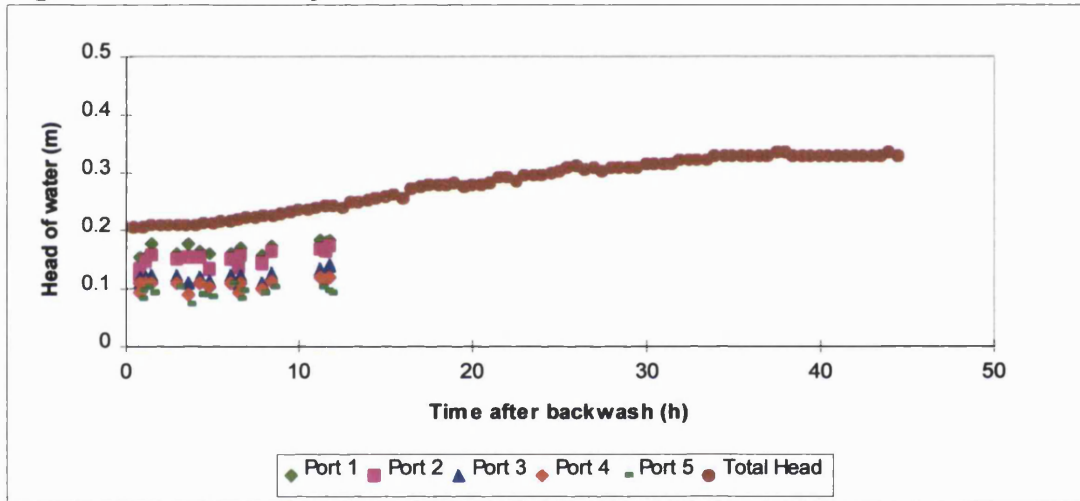


Table 10.5: Flood Times from Ranger Data

Load	Flood Time (hours)
1	> 65
2	56 - 60
3	57 - 60
4	54 - 56

10.5: Backwash Samples

The removal of SS by backwashing is shown in Figures 10.22 and 10.23. The backwash profile shows that peak removals of 1100 mg/l are found after 60 seconds combined air and water wash, this decreases to less than 200 mg/l at the end of the

rinse phase. Total solids removed decreases with increased HLR and is 0.3 - 0.5 kg/backwash.

Figure 10.22: Backwash Profiles

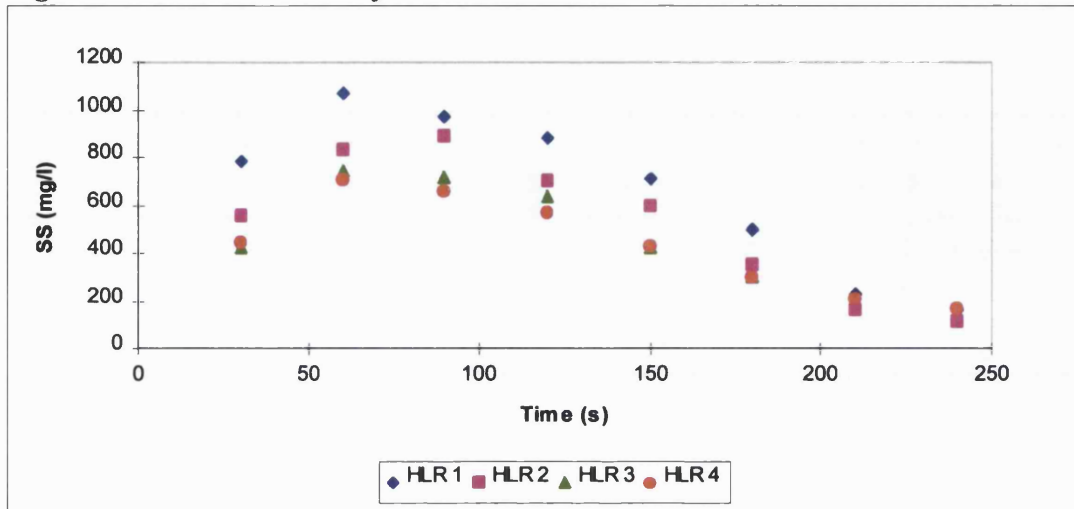
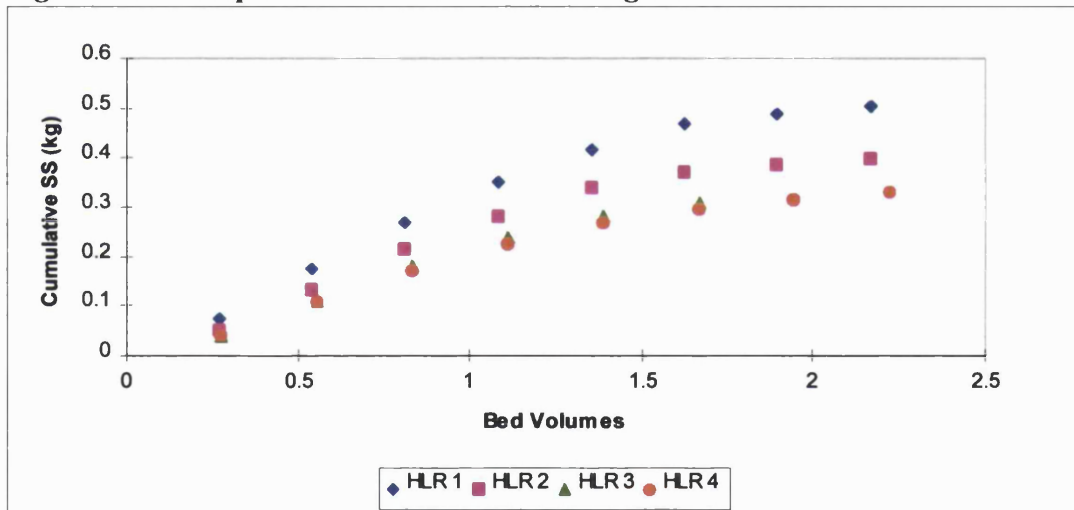


Figure 10.23: Suspended Solids Removed During Backwash



Calculations of total solids removed each week and effluent reused for backwashing each week are given in Tables 10.6 and 10.7. The SS removed increases with increased solids load.

Table 10.6: Total Suspended Solids Removed During Backwash

Load	Total SS Load (kg/week)	Total SS Removed (kg) ¹	Total SS Removed (kg/week) ²	Effluent SS (kg/week)
1	1.63	0.5	2	0.25
2	2.71	0.4	2.8	1.03
3	5.94	0.31	4.34	1.63
4	6.38	0.33	4.62	4.34

1 - Average for each backwash 2 - Washed on time basis

Table 10.7: Percentage of Treated Effluent Used For Backwash

Load	Backwash water volume (l)	Total vol/week	Percentage of weekly effluent produced
1	756	3024	18.9
2	756	5292	16.7
3	567	7938	16.5
4	756	10584	16.4

Effluent reuse for backwash is high at all HLRs when the filter is washed on a time basis. If the filter was left and washed according to head build-up the effluent reuse could be down to 4% at HLR 3 and 4.

10.6: Sludge Samples

Table 10.8 shows sludge parameters investigated at all HLRs. T-tests show that differences between HLRs are only seen in the CST tests.

Table 10.8: Sludge Data

Load	BW SS (mg/l)	Sludge SS (mg/l)	Sludge Dry Solids (%)	Volatile Solids (%)	CST (seconds)
1	632	4857	0.57	71	33
2	479	4779	0.68	72.8	41
3	498	4409	0.58	77.4	29
4	500	4763	0.64	84.4	41

10.7: Off-Gas Analysis

During off-gas analysis the oxygen transfer efficiency and oxygenation capacity were determined (Figures 10.24 - 10.26) and dissolved oxygen profiles were taken (Figure 10.27). There is some increase in operational OTE with increasing HLR/VLR and with decreasing air flow. This is also seen for the graph of OTE corrected to zero against air flow. The oxygenation capacity of 5.6-11.2mm Lytag increases with loading rate and shows that a higher air flow is needed for maximum OC at higher loading rates.

Figure 10.24: Operational Oxygen Transfer Efficiency (OTE)

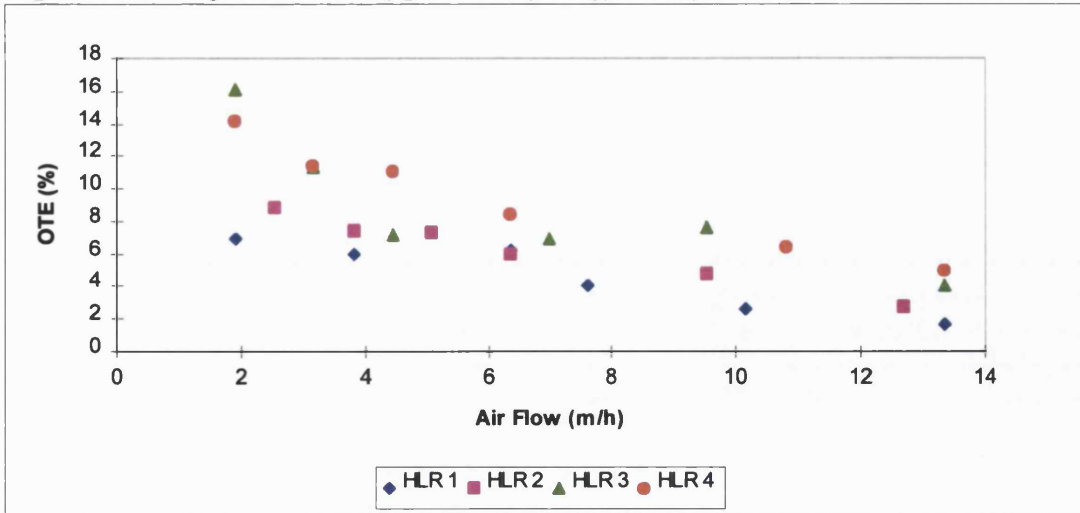


Figure 10.24: Corrected OTE

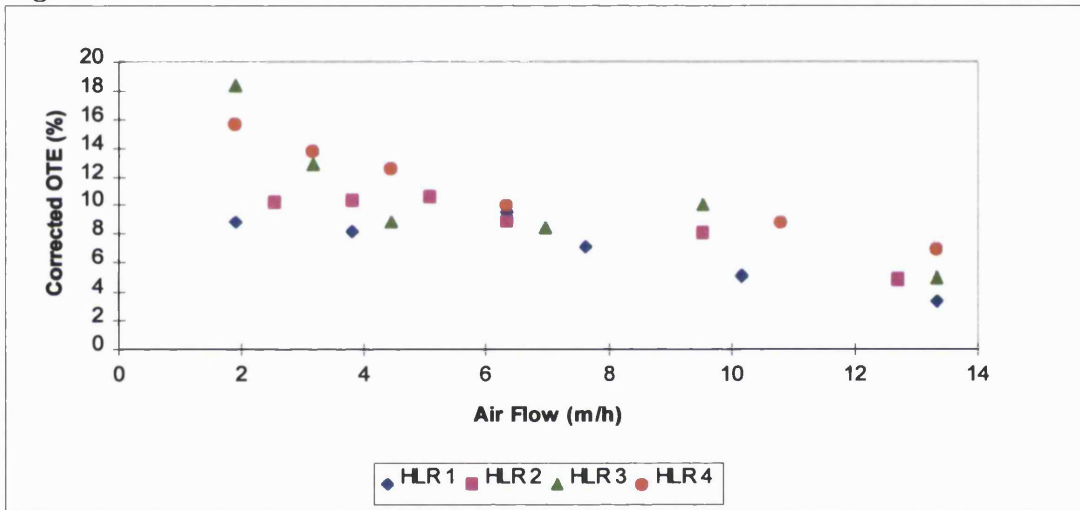


Figure 10.26: Oxygenation Capacity

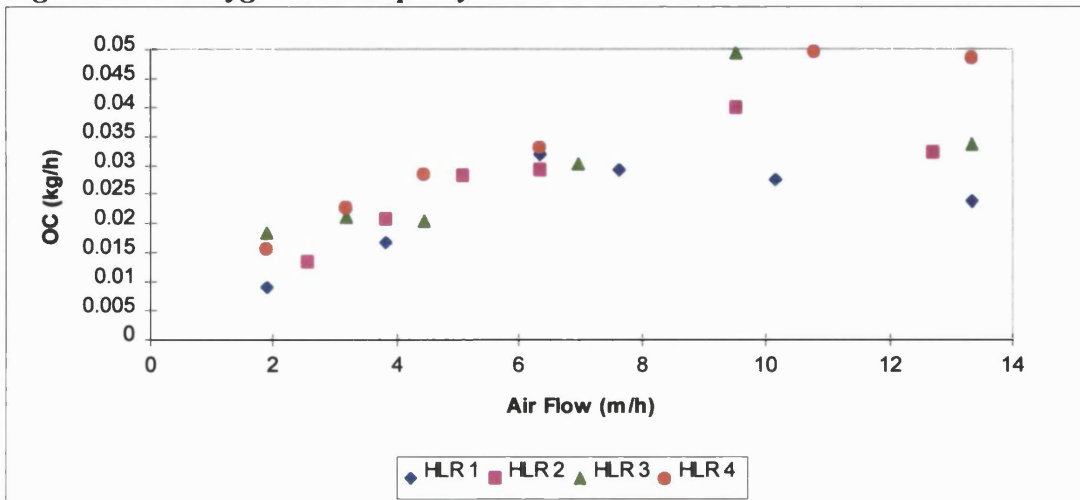
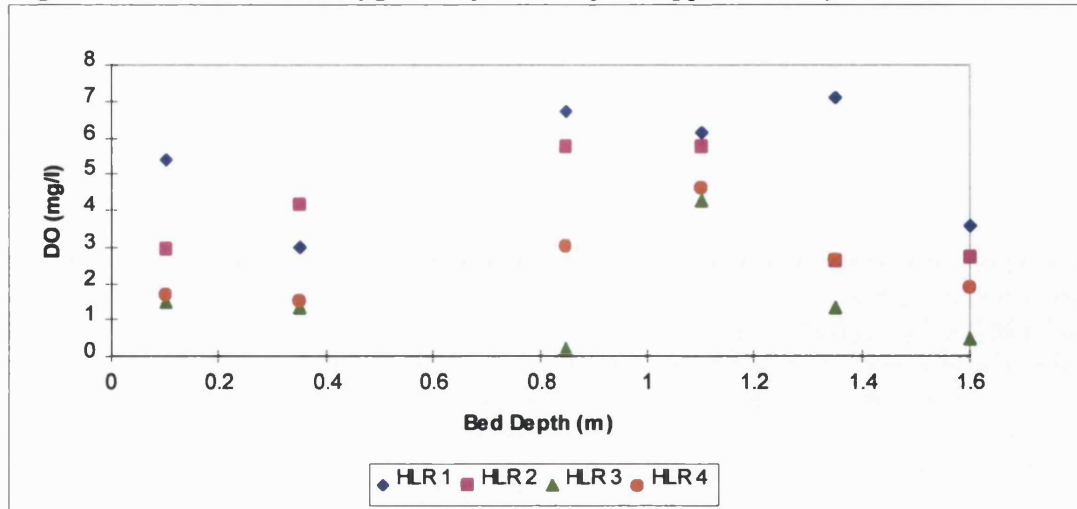


Figure 10.27: Dissolved Oxygen Profiles (Air flow approximately 13m/h)



The profile of DO shows decreasing DO with increasing HLR. The theoretical oxygen demand for each loading rate was calculated and compared with the experimental oxygen demand (Table 10.9). The oxygen demand increases with HLR but is similar at HLR 3 and 4.

Table 10.9: Oxygen Demand For 5.6-11.2mm Lytag Media

Load	Loading (kg/m ³ /d)	Ammonia Reduction (%)	Estimated Demand (kg O ₂ /h)	Actual Demand (kg O ₂ /h)
1	BOD - 1.17			
1	NH ₄ -N - 0.2	92	0.02	0.014
2	BOD - 2.19			
2	NH ₄ -N - 0.3	63	0.024	0.024
3	BOD - 2.68			
3	NH ₄ -N - 0.47	36	0.023	0.038
4	BOD - 4.86			
4	NH ₄ -N - 0.89	13	0.021	0.037

10.8: Hydraulic Regime

An example of an RTD curve is shown in Figure 10.28 and retention times are shown in Table 10.10. The retention times decrease with increased HLR but plug flow conditions were similar at all HLRs.

Figure 10.27: Tracer Tests (Hydraulic Load = 1m/h)

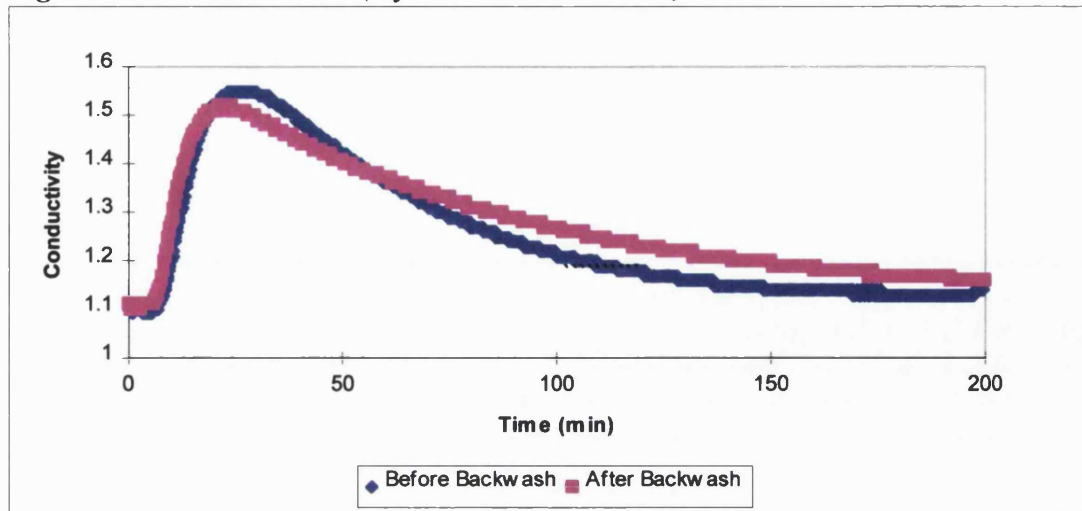


Table 10.10: Retention Times (After Backwash)

Load	Theoretical Retention Time (mins) ¹	TRT (mins) ²	D/uL ³	Peak RT (mins)	Mean RT (mins)
1	193	59	0.3355	25	126
2	96	30	0.3041	25	72
3	63	20	0.4224	12	44
4	47	15	0.341	12	32

1 - Empty Bed 2 - Assuming experimental voidage of 0.31 3 - Dispersion number

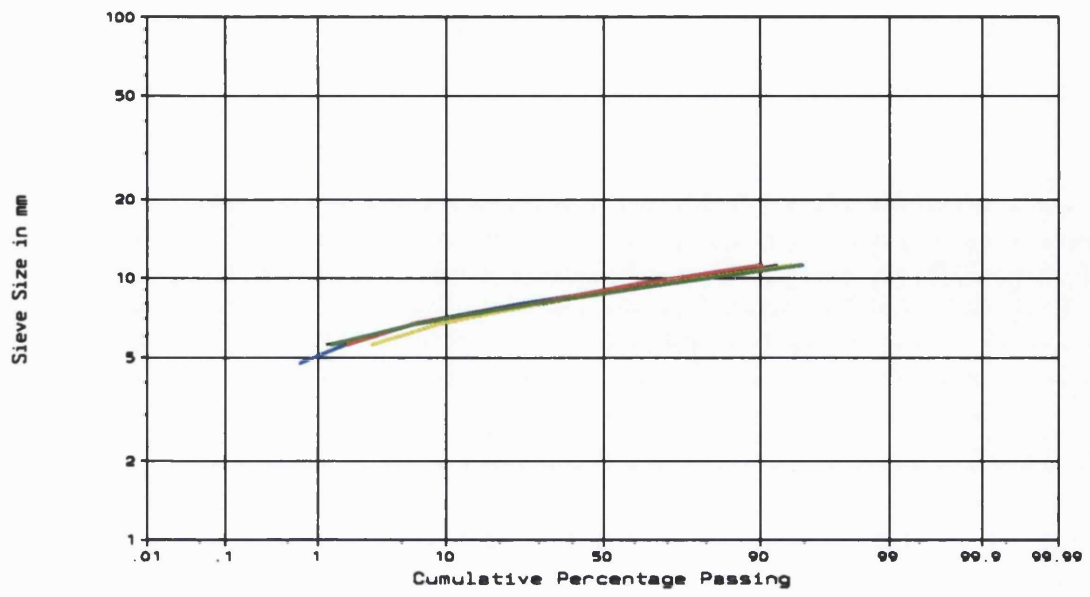
10.9: Decommissioning

The particle size range of media after filter operation is given in Table 10.11 and Figure 10.29. There appears to be little difference from the original particle size range.

Table 10.11: Sieve Analysis of 5.6mm-11.2 Lytag After Filter Operation

Media Sample	Hydraulic Size (mm)	d ₅ (mm)	d ₁₀ (mm)	d ₆₀ (mm)	UC	d ₉₀ (mm)	d ₉₅ (mm)
Original	8.75	6.4	7.0	9.3	1.33	10.5	11.2
Overall	8.64	6.5	7.0	9.0	1.29	10.8	11.3
Top	8.55	6.0	6.7	9.0	1.34	10.6	11.2
Middle	8.82	6.4	7.0	9.4	1.34	10.8	11.1
Bottom	8.65	6.5	7.0	9.0	1.29	10.8	11.3

Figure 10.29: Sieve Analysis of 5.6-11.2mm Lytag After Decommissioning



11.0 PILOT SCALE PERFORMANCE OF LYTAG MEDIA

Discussion: The Effect of Media Size on BAF Performance

11.1: Introduction

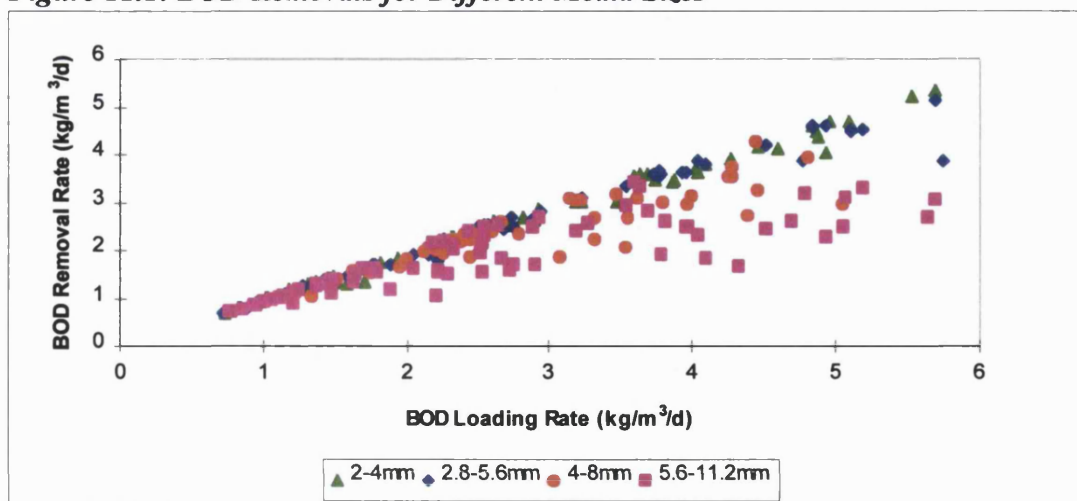
A comparison was made of the four different media sizes over all HLR/VLRs in order to determine which size range is most suitable for the BAF process and in which situations.

11.2: Carbonaceous Removal

Carbonaceous removal is shown by the removal of BOD and COD. The removal of BOD over a range of OLRs is shown in Figure 11.1. The 2-4mm and 2.8-5.6mm Lytag show a positive linear relationship between removal and VLR with over 90% removal for all HLRs. The 4-8mm Lytag also shows this pattern but there is slightly more scatter. The removals by 5.6-11.2mm Lytag tend to level off above a VLR of approximately 3.5kg BOD/m³/d, with removals dropping to 50% at HLR 4. The same pattern is found for COD removals but with more scatter in the data.

At each successive loading rate the effluent recycle leads to the presence of slightly more unbiodegradable sCOD and sBOD present which is untreatable, this contributes to the decreasing percentage removals with increasing COD/BOD load.

Figure 11.1: BOD Removals for Different Media Sizes



The graphs of BOD removal over 24 hours have similar relationships to those found in composite samples showing that removals are not affected by diurnal variations in

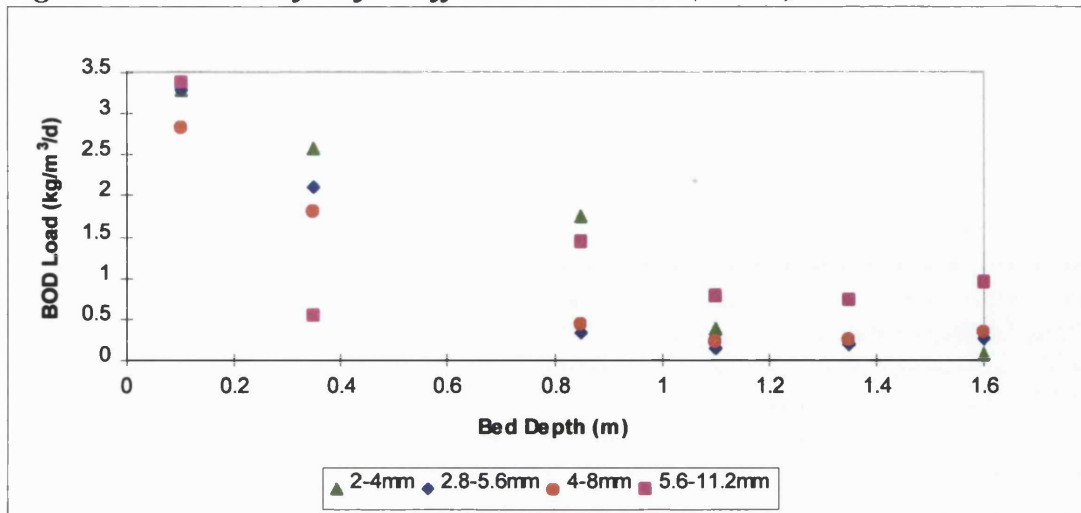
sewage strength. Work by Smith & Hardy (1997) found diurnal BOD removals of >85% even at shock loading rates, with fast growing heterotrophs quickly adapting to any variations in sewage strength.

The bed profiles of BOD at HLR 2 show that for the three smallest media sizes there is a roughly first order decrease in BOD to a depth of 1.1m, this indicates high heterotroph growth at the top of the filter. The largest media size shows a rapid decrease in BOD in the top 0.25m of the bed but this increases at 0.85m before decreasing again. At the depth where most BOD has been removed the heterotrophic bacteria become substrate limited. At HLR 4 a similar pattern occurs for all media sizes but with a much higher BOD load at the bottom of the filter. At HLR 4 there is also a greater penetration of sewage due to the higher HLR and therefore a larger proportion of the bed supports heterotroph growth.

A similar pattern is found with the COD profiles. Lacamp & Bourbigot (1989) reported 60 - 70% COD removal in the first quarter of the reactor with a total of 90% removal. With 2-4mm and 2.8-5.6mm Lytag there was very little removal in the first quarter of the reactor and approximately 2/3 of the reactor was used for 60 - 70% COD removal. The 4-8mm media uses the whole filter bed for COD removal and the largest media size does not reach 60% removal. In COD profiles of 2-4mm Lytag there appears to be an increase in COD concentration at a depth of 0.35m for 3 of the HLRs. This could be a sampling error from taking spot samples, with build-up of solids in the sample port or an analysis error.

The higher COD and BOD concentration at the bottom of the filter beds at HLR 4 may consist of unbiodegradable sCOD and sBOD from the effluent recycle.

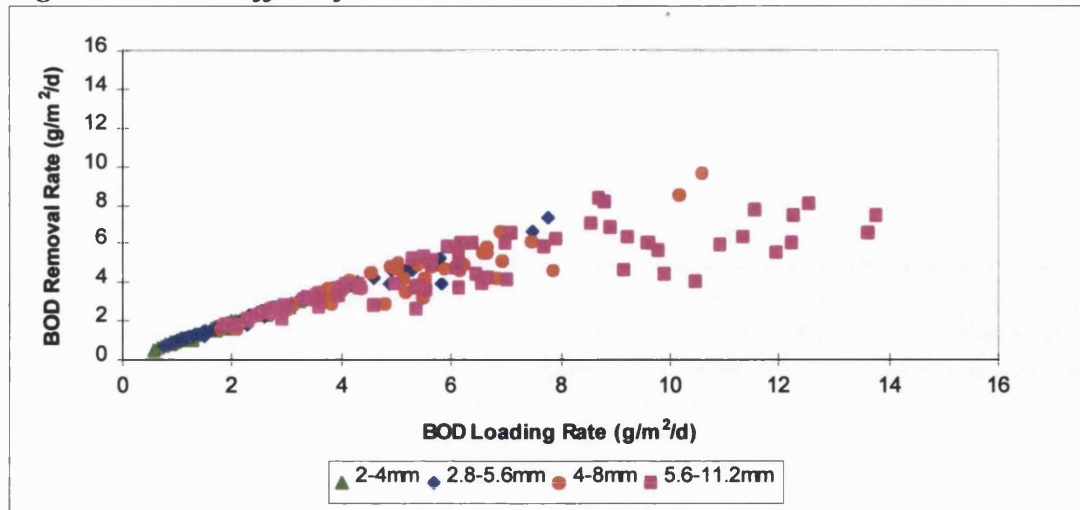
Figure 11.2: BOD Profiles for Different Media Sizes (HLR 2)



The effluent BOD concentrations of <14 mg/l and <17 mg/l for 2-4mm and 2.8-5.6mm Lytag are as good as those found by Stensel *et al* (1988) for combined BOD removal and nitrification. The 4-8mm Lytag has poor effluent levels at HLR 4 (34 mg/l) and the largest media size has poor effluents at HLR 3 and 4. Effluent BODs of <30mg/l have been seen for loads of 4- 8kg BOD/m³/d (Stensel & Reiber, 1983; Amar *et al*, 1986) but these have been carbonaceous removal processes without nitrification.

The higher removals of BOD and COD could be due to higher capture of particulate BOD/COD and higher assimilation of soluble BOD/COD into biomass. Higher biomass assimilation is expected in small media due to high surface area to volume ratio for biomass growth but biofilm concentrations appear to be similar in all media sizes. The higher removals of BOD/COD in small media are probably due to the capture of particulates in the small pore spaces. The particulates are also eventually broken down for assimilation into biofilm but first must be adsorbed onto the biofilm surface and hydrolysed before being transported into the biofilm (Särner, 1986). Figure 11.3 shows the effect of SSA on BOD removals, the pattern of removal is similar to that seen in Figure 11.1 suggesting that capture of particles in small pore spaces is responsible for the better removals by small media sizes.

Figure 11.3: The Effect of SSA on BOD Removals

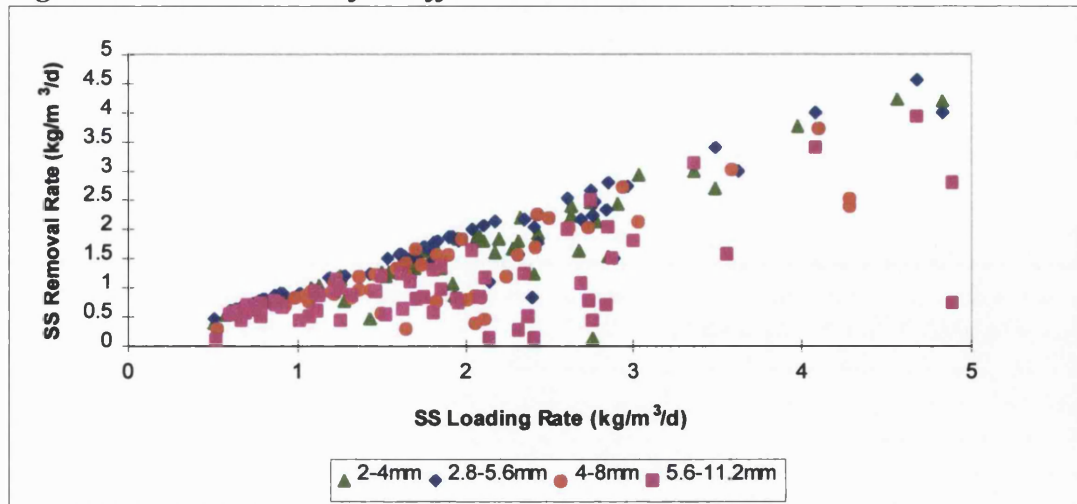


11.3:Suspended Solids Removal

The pattern of suspended solids removal for the two smallest media sizes is similar, they show a positive linear relationship between VLR and removal. There doesn't appear to be any improvement with increasing HLR as predicted by Pujol *et al* (1996) but this may be because the HLRs are still low (0.5 - 2m/h). The large media sizes also show this relationship for HLR 1 - 3 but at HLR 4 there is a significant decrease in removals.

The low solids removals by the two large media sizes at HLR 3 and 4 could be due to the high frequency of backwashing. This prevents ripening of the filters so that there is always a 'clean' bed rather than a build-up of particles within pores which would improve the capture of further particles. Filtration theory also predicts that small media will be more efficient at particle capture as there are smaller pore diameters between media particles and therefore better ripening capabilities. It is possible that larger media sizes are also more prone to breakthrough of biomass which adds to the effluent solids.

Figure 11.4: SS Removals for Different Media Sizes



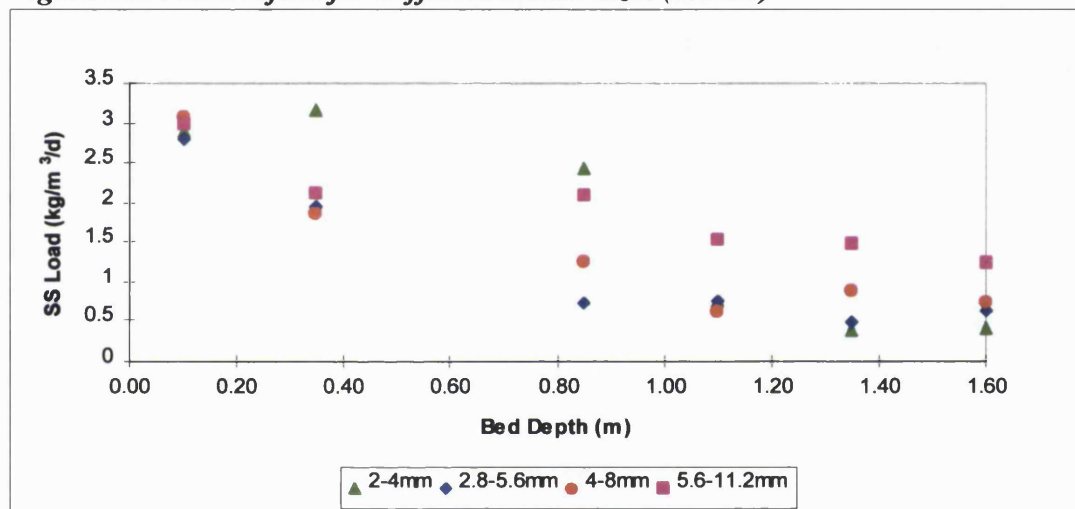
A similar pattern of removals against VLR is seen in 24 hour profiles. Smith *et al* (1990) found that effluent quality deteriorated immediately after backwashing in a BAF plant with effluent solids reaching a high of 60mg/l before dropping back to 20mg/l after 45 minutes. An initial poor effluent quality after backwashing is also predicted by filtration models which assume that backwash remnants remain in the filter system (Amirtharajah & Wetstein, 1980). Boller *et al* (1997) also found that removal efficiency especially of small particles improved during the filter run in aerated biofilters due to ripening. A solids peak was not seen after backwash of the Lytag media but more frequent sampling may have detected one immediately after backwashing.

The bed profiles of SS removal for all sizes at HLR 3 show a pattern typical of all HLRs. The 2-4mm Lytag has low removals in the top 0.35m. Possible explanations for this include sloughing of biomass as found by Harris (1994) in the same pilot columns or media loss during backwashing leading to a smaller bed volume for treatment. The other three media sizes have much higher removals in this portion of the bed. Over the next 0.5m of the bed there is increasing removal with decreasing media size (except for the 2-4mm Lytag) so that effluent concentrations have been reached by 0.85m depth. In all cases except the smallest media size there is very low filtration occurring in the bottom portion of the bed. At HLR 4 there was very little solids removal throughout the bed for all media sizes. These patterns of removal agree with filtration theory (Ives, 1982).

In some instances the small media have an increase in solids at 0.35m depth. There could be a number of reasons leading to errors, for instance the smaller media had high attrition so media fines may have built up within the sample port. There may also have been biofilm growth and breakthrough from the sample port. The small media would be expected to have the highest removals at the top of the bed due to the small pore sizes allowing high particle capture.

As HLR increases there should be more depth filtration by the filter beds rather than straining - this is in agreement with the SS profiles found.

Figure 11.5: SS Profiles for Different Media Sizes (HLR 3)



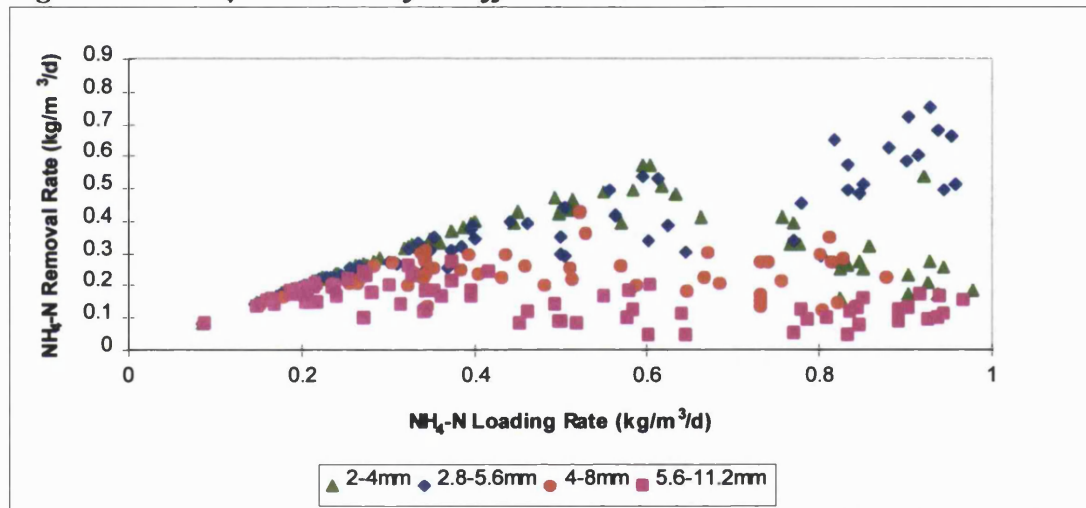
The concentrations of effluent SS can be seen to increase with increasing SS load despite the high variability of data within HLRs. The 2-4mm Lytag has effluent values below 25 mg/l for all HLRs this is slightly higher than effluent from 2.8-5.6mm Lytag, probably due to the fact that the small media ran to flooding at two of the HLRs and this affected the quality of the effluent. Again the 4-8mm media had high effluent qualities except at HLR 4 whilst the largest media size had poor effluent at HLR 3 and 4.

11.4: Nitrification

Ammoniacal nitrogen removal can be seen in Figure 11.6. The relationship between loading rate and removals for NH₄-N is different for each media size. The 2-4mm Lytag shows a positive linear relationship until a maximum of 0.6kg NH₄-N/m³/d at

which point there is a dramatic decrease in $\text{NH}_4\text{-N}$ removal. This corresponds to average percentage removals of 90 - 99% for VLRs of 0.2 - 0.5 $\text{kg NH}_4\text{-N/m}^3/\text{d}$ which drop to just 35% at 0.9 $\text{kg NH}_4\text{-N/m}^3/\text{d}$. This pattern is also shown for TKN removal with the drop in removals occurring at 0.9 $\text{kg TKN/m}^3/\text{d}$. The 2.8-5.6mm media shows a positive relationship at all VLRs in this study (0.1 - 1.2 $\text{kg NH}_4\text{-N/m}^3/\text{d}$) but above 0.4 $\text{kg NH}_4\text{-N/m}^3/\text{d}$ there is a high degree of scatter in the data. The removals may have reached a plateau at approximately 1 $\text{kg NH}_4\text{-N/m}^3/\text{d}$ or there may be decreased removals above this point. The 4-8mm and 5.6-11.2mm media have decreased removals at less than 0.4 $\text{kg NH}_4\text{-N/m}^3/\text{d}$. Paffoni *et al* (1990) found complete removal of ammoniacal nitrogen at loads $<0.6 \text{ kgN/m}^3/\text{d}$ which is lower than the point of full nitrification found in this study for the 2-4mm Lytag.

Figure 11.6: $\text{NH}_4\text{-N}$ Removals for Different Media Sizes



A fully nitrifying system would have shown an increase in $\text{NH}_4\text{-N}$ removal with increasing load until the system became oxygen limited, at this point a plateau would have been reached linked to the SSA of the media, as seen in Le Tallec *et al*, (1996). This is close to the pattern shown by the middle media sizes, but there is a drop in nitrification which is easily seen in the 2-4mm media. This is probably due to nitrifying organisms being outcompeted by heterotrophic organisms at high BOD and $\text{NH}_4\text{-N}$. The work of LaCamp & Bourbigot (1989) suggested that nitrogen oxidation rates start to decrease when COD loads were $>4 \text{ kg/m}^3/\text{d}$ but in this study there was still high nitrogen oxidation up to a COD load of $6.3 \text{ kg/m}^3/\text{d}$ for smaller media. This could be due to the effluent recycle which adds soluble COD that is unavailable for assimilation

indicating that the available COD load could be close to $4\text{kg}/\text{m}^3/\text{d}$. There is no data available for $\text{NH}_4\text{-N}$ removals above loading rates of $1\text{kg } \text{NH}_4\text{-N}/\text{m}^3/\text{d}$, the 2.8-5.6mm media could either reach a plateau or have a decrease in removal above this load.

Effluent $\text{NH}_4\text{-N}$ concentrations for 2-4mm Lytag were very good at 0.4 - 2.5mg/l at HLRs 1- 3 but at the final load there was a very high concentration of 18.9mg/l. With similar $\text{NH}_4\text{-N}$ and TKN loads as those found in HLR 1- 3 but lower BOD loads Stensel *et al* (1988) had higher effluent $\text{NH}_4\text{-Ns}$ of 3.7 - 7.5mg/l, their media however had an effective size of 3.4mm compared to 2.1mm for the 2-4mm Lytag. The 2.8-5.6mm Lytag had effluent $\text{NH}_4\text{-N}$ of < 5mg/l which increased to 11mg/l at HLR 4, this is better than 2-4mm media effluents. As media size increases the effluent quality deteriorates at lower HLRs.

The TON concentrations at HLRs 1 - 3 for 2-4mm Lytag were fairly high in this study (13 - 18mg/l) but dropped to only 2mg/l at HLR 4. Again as media size increases the TON concentration decreases until at HLR 4 the 5.6-11.2mm Lytag has effluent concentrations of 1mg/l which is the same as sewage TON concentrations.

Looking at diurnal variations we can see a similar pattern between loading rate and removals. The work of Smith & Hardy (1997) found that peak to average load variations of 1.6:1 led to a decrease in the efficiency of nitrification with an increased BOD load inhibiting nitrification and decreasing the rate of recovery. This is due to the low growth rate of nitrifying organisms in comparison to heterotrophs therefore heterotrophs quickly recover and outcompete nitrifying organisms.

Smith & Hardy (1992) found that effluent $\text{NH}_4\text{-N}$ concentrations deteriorated after backwashing. In this study it looks as though removals are not affected by backwash at HLR 1 they simply follow VLR. If samples had been taken more regularly after backwash it may have been possible to see an effluent $\text{NH}_4\text{-N}$ deterioration. At HLR 3 there are obviously lower removals but again the backwash does not appear to have affected removals. In this case it looks as though there is more response to changes in loading rate. At HLR 2 and 4 for 2-4mm media, when the filter has flooded and needs backwashing, ammoniacal nitrogen removals are very low.

The bed profiles of $\text{NH}_4\text{-N}$ show that at all HLRs there is removal in the top 0.85m of the bed for all media sizes. This is mainly due to nitrogen assimilation into the biomass but also indicates that some nitrification is occurring alongside carbonaceous treatment suggesting that there is no oxygen limitation. The $\text{NH}_4\text{-N}$ oxidation would be expected to occur further down the bed where there is a low BOD load as is found in RBCs where at low or moderate loading rates the first contactor is used for BOD removal and there is inhibition of nitrification, nitrification occurs in later contactors (Figueroa & Silverstein, 1992). Boller *et al* (1997) found that biofilters with granular media had biomass and nitrification activity distributed equally over the whole filter depth due to the mixing of filter grains during backwashing.

The higher nitrification in large media at the top of the bed at low HLRs could be due to the high removal of BOD and therefore high nitrogen assimilation into biofilm. It could also be due to higher penetration of effluent through the large media pores. The poor removals by 2-4mm Lytag at the top of the bed could again be due to media loss by backwashing and the subsequent poor removals of BOD leading to low nitrogen assimilation.

At HLR 4 there is lower removal of $\text{NH}_4\text{-N}$ throughout the filter than at HLR 3 for all media sizes (except 2.8-5.6mm) due to the high BOD load. The nitrifying organisms are probably oxygen limited throughout the filter bed as the biofilm will have become too thick for oxygen penetration to the inner layers despite effluent DO concentrations above 2mg/l throughout the filter bed. A larger proportion of the bed will be needed by heterotrophs to treat the high BOD load therefore theoretically there is less bed available for nitrification, a larger bed depth could possibly lead to increased nitrification. The removals of $\text{NH}_4\text{-N}$ throughout the bed at HLR 4 are mainly due to assimilation into biomass. The 2.8-5.6mm Lytag does have high removals at the top of the bed at HLR 4 (with only 1/3 of removal being due to assimilation), but is probably oxygen limited at the bottom of the bed. Similar bed profiles are seen for TKN removal.

Figure 11.7: $\text{NH}_4\text{-N}$ Profiles for Different Media Sizes (HLR 2)

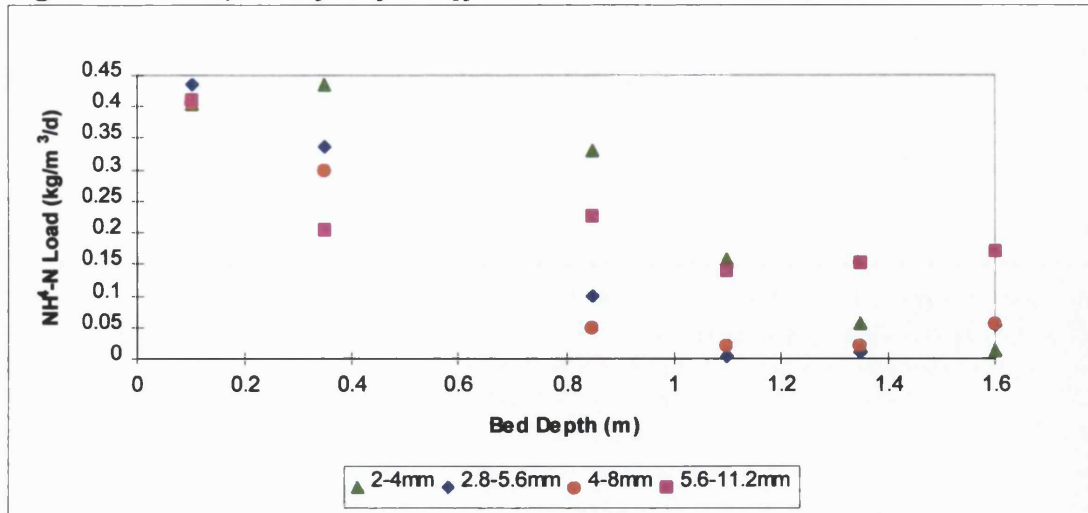
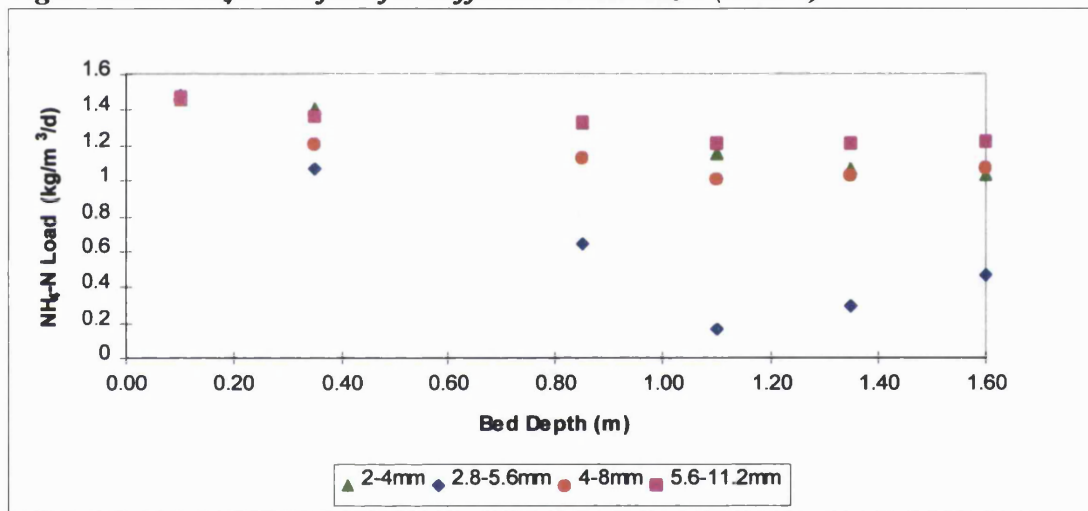


Figure 11.8: $\text{NH}_4\text{-N}$ Profiles for Different Media Sizes (HLR 4)



The TON profiles for HLR 2 show low TON until a depth of 0.85m. Any TON production from nitrification at the top of the filter has been removed and will have been taken up by biofilm assimilation by heterotrophs. There is a pattern of increased TON production with decreasing media size although the 2-4mm media takes a larger proportion of bed for TON production to increase, it is still increasing at the bottom of the bed whilst the other sizes have decreased TON concentrations at the bottom of the bed. A larger bed depth may therefore allow more ammoniacal nitrogen removal by 2-4mm Lytag. There is actually lower TON production in the 2.8-5.6mm Lytag than 2-4mm Lytag despite there being higher $\text{NH}_4\text{-N}$ removal by the 2.8-5.6mm media. This suggests that there is higher denitrification occurring in the 2.8-5.6mm Lytag.

At HLR 4 all media sizes except 2.8-5.6mm media show very little TON production throughout the bed due to nitrogen assimilation into the biomass. The 2.8-5.6mm Lytag has high TON production with peak levels at a depth of 1.1m.

Figure 11.9: TON Profiles for Different Media Sizes (HLR 2)

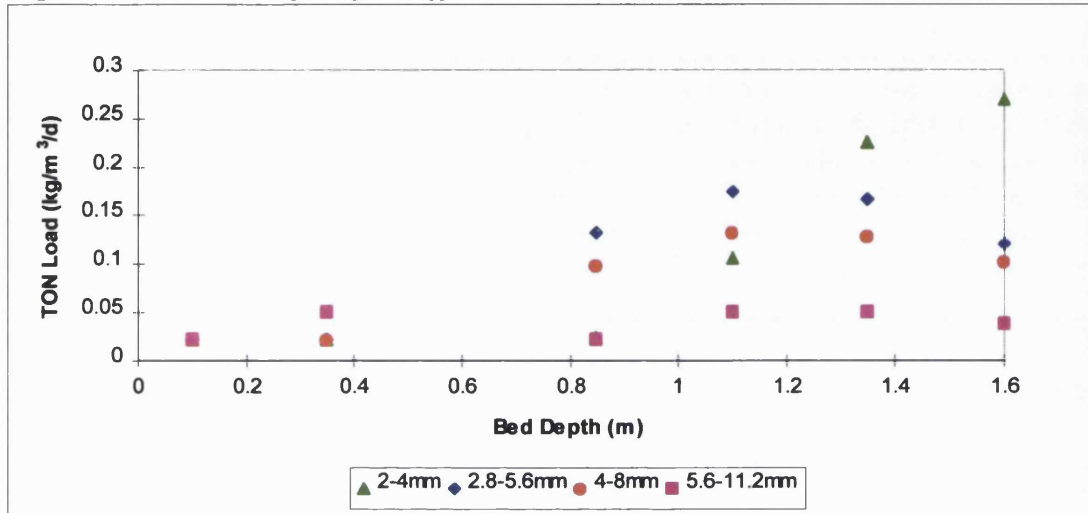
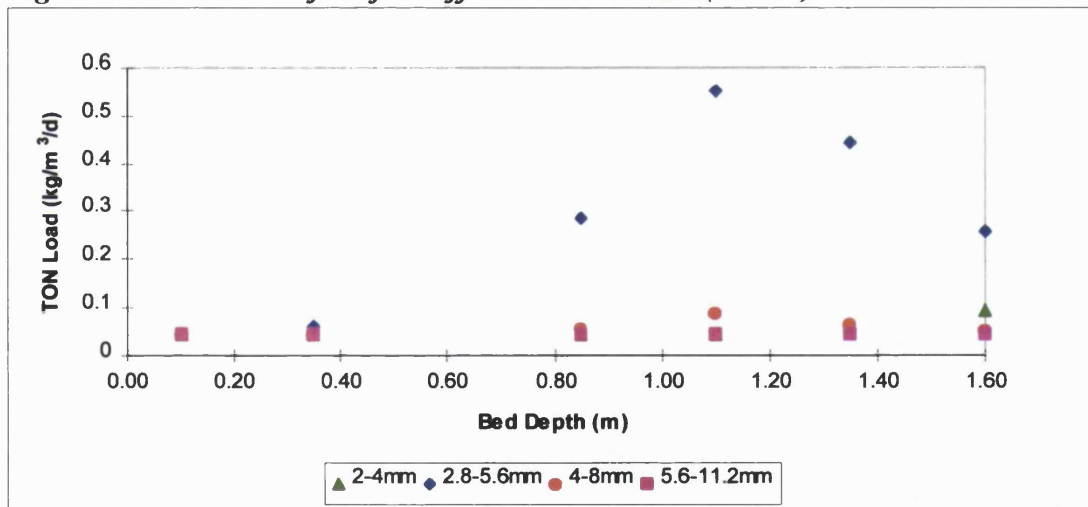


Figure 11.10: TON Profiles for Different Media Sizes (HLR 4)



The rate limiting step in nitrification is the first stage ie: $\text{NH}_4\text{-N}$ oxidation to $\text{NO}_2\text{-N}$, therefore the concentration of nitrite indicates whether nitrifying organisms have become stressed. At HLR 1 the highest $\text{NO}_2\text{-N}$ levels are found in the 5.6-11.2mm Lytag with maximum levels occurring between 0.35 - 0.85m. This suggests that the $\text{NO}_2\text{-N}$ is not converted to $\text{NO}_3\text{-N}$ until the bottom of the filter and that Nitrobacter species are oxygen limited at the top of the bed. The smaller media has higher conversion of $\text{NO}_2\text{-N}$ to $\text{NO}_3\text{-N}$ throughout the bed and is therefore not oxygen limited. The profile of nitrite nitrogen at HLR 4 shows very low levels in 2-4mm media and

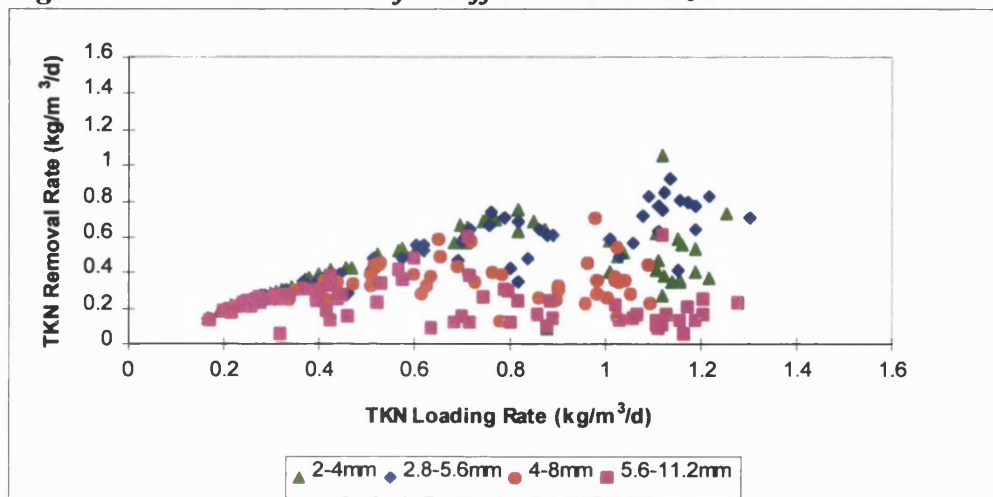
5.6-11.2mm media due to low $\text{NH}_4\text{-N}$ oxidation, high levels are still found with 2.8-5.6mm Lytag but most of the TON consists of $\text{NO}_3\text{-N}$ and it is therefore not oxygen limited.

A number of factors can affect the nitrification rate including:

1. $\text{NH}_4\text{-N}$ /TKN load
2. BOD/COD load
3. Hydraulic load
4. pH
5. Temperature
6. Toxic substances
7. Oxygen transfer
8. SSA of media

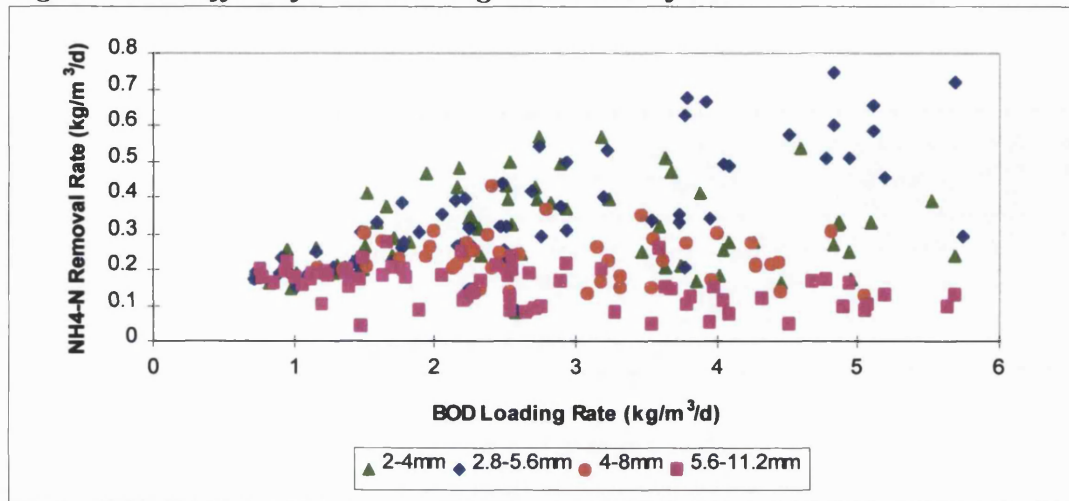
The relationship between $\text{NH}_4\text{-N}$ load and nitrification has already been shown in Figure 11.6. We can also look at nitrification in terms of TKN removal according to the TKN load available for nitrification, Figure 11.11 shows the TKN loading rate once the TKN removed by biomass assimilation has been accounted for (ie: 5% of the BOD load removed). This graph appears to show an optimum point of removal followed by a slight decrease in all media sizes except the 2-4mm media which again shows a rapid decrease in removals above a point of $0.7\text{kg available TKN/m}^3/\text{d}$. In this instance all media sizes appear to act in the same manner for nitrification except the smallest media size.

Figure 11.11: TKN Removals for Different Media Sizes



The BOD loading rates do not appear to have a large effect on nitrification over the whole filter bed

Figure 11.12: Effect of BOD Loading Rate on Nitrification



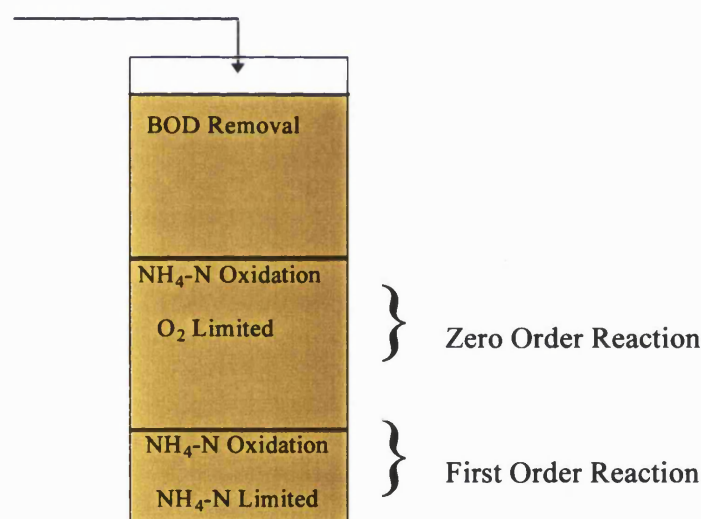
An increase in organic loading rate is expected to negatively affect nitrification. Figure 11.12 shows that nitrification is poor in both of the large media sizes at all BOD loading rates in this study. The 2-4mm media has decreasing nitrification at loading rates above 3.5kg BOD/m³/d but 2.8-5.6mm media is still nitrifying at loading rates of 5kg BOD/m₃/d.

The BOD loading rates were the same for all media sizes but it is possible that the difference between media sizes is due to the differences in BOD removal throughout the bed depth and therefore differences in heterotroph growth and competition with nitrifying organisms for oxygen. The organic concentration may reach a value at which the concentration of oxygen is so low that the heterotrophs with higher growth rates, near the biofilm support surface, displace slow growing nitrifying organisms (Parker & Richards, 1986). As the total organic load increases a high concentration of BOD is pushed further down the filter bed theoretically leading to less available surface area for nitrifying organisms and therefore less nitrification. In trickling filters the absence of a continuous supply of NH₄-N leads to patchy biofilm development and therefore declining nitrification rates with depth (Parker *et al*, 1989).

The theory for combined carbonaceous treatment and nitrification predicts that removals occur in different sections of the filter bed as shown by Figure 11.12. In this

study carbonaceous treatment and low levels of nitrification appear to occur alongside each other in the filter bed. The theory can therefore be adapted to apply to treatment in different sections of biofilm on a single media particle. Biofilms will not be of a uniform thickness therefore different parts may be fully penetrated by $\text{NH}_4\text{-N}$ and O_2 allowing nitrification whilst other sections may be anoxic preventing nitrification. Thick heterotroph growth will inhibit nitrification by successfully competing for any limited oxygen. Slow growing nitrifying organisms may form a small proportion of the outer layer of biofilm but their growth rate must be sufficient to maintain population numbers. The heterotroph and nitrifying organisms growth rate will only be equal if oxygen fully penetrates the biofilm (Parker & Richards, 1986).

Figure 11.13: Wastewater Treatment According To Filter Depth



The model of treatment within biofilm layers on media particles is complicated by air flows and water velocities which will be different in different sections of the filter bed due to channelling and stagnant areas. Areas of denitrification may be present in the layers of biofilms where $\text{NH}_4\text{-N}$ oxidation occurs but oxygen is limited leading to heterotrophic use of $\text{NO}_3\text{-N}$. It is also possible for anaerobic areas to develop, here biofilm will break down leading to sloughing.

The presence of particulates in the settled sewage could also have affected nitrification in that they adsorb readily onto the biofilm surface leading to thicker biofilms with higher fractions of non-nitrifying solids. The adsorbed particles lead to oxygen shortages inside the biofilm due to degradation activity, this cannot be shown by the oxygen concentration in the bulk liquid. Any effect from particulates should again have been the same for all the media sizes but there may have been a difference in removals at different depths.

In nitrification only upflow biofilters (Peladan *et al*, 1996), an increased hydraulic load had a positive effect on the maximum nitrified loading rate (with non-limiting air). The increase in water velocity allowed an improved substrate bulk/biofilm transfer due to bed expansion leading to more effective bed use. This was also found by Pujol *et al* (1996). In this study the hydraulic loading rates were not increased above 2m/h and the regression models of ammoniacal nitrogen removal do not appear to be greatly affected when hydraulic load is included. The downflow configuration would not show bed expansion in the same way as the upflow filter therefore hydraulic load should not have such a large effect on nitrification.

Nitrification may be inhibited by a low pH if it is not neutralised. This may be occurring in the 2-4mm Lytag at loading rates above 0.6kg NH₄-N/m³/d but pH values were not taken in this study. It is unlikely that the pH in 2-4mm Lytag would differ greatly from that in the other media sizes. A change in temperature may also affect nitrification, *Nitrosomonas* has a maximum activity at 28-29°C (Fdz-Polanco *et al*, 1996) and therefore maximum nitrification should occur at this temperature. All filters in this study were fed with settled sewage of the same temperature so despite any temperature change with season there should have been the same effect for all media sizes, a similar situation would have been found for toxic materials.

Oxygen transfer rates can affect nitrification in that there is a high oxygen demand for NH₄-N oxidation. Oxygen is consumed and replaced by oxygen from the edge of the biofilm leading to a concentration gradient between the edge of the biofilm and the minimum concentration within the biofilm. A low oxygen transfer rate may therefore indicate that there is not enough oxygen passing into the biofilm for use by nitrifying

organisms. In this study though the highest OTE at all HLRs is found in 2-4mm Lytag (Section 11.10). The OTE was calculated after backwashing when there was a 'clean' bed, transfers may have decreased later in the filter run due to clogging of the filter bed especially in the 2-4mm Lytag which had short run times at HLR 4.

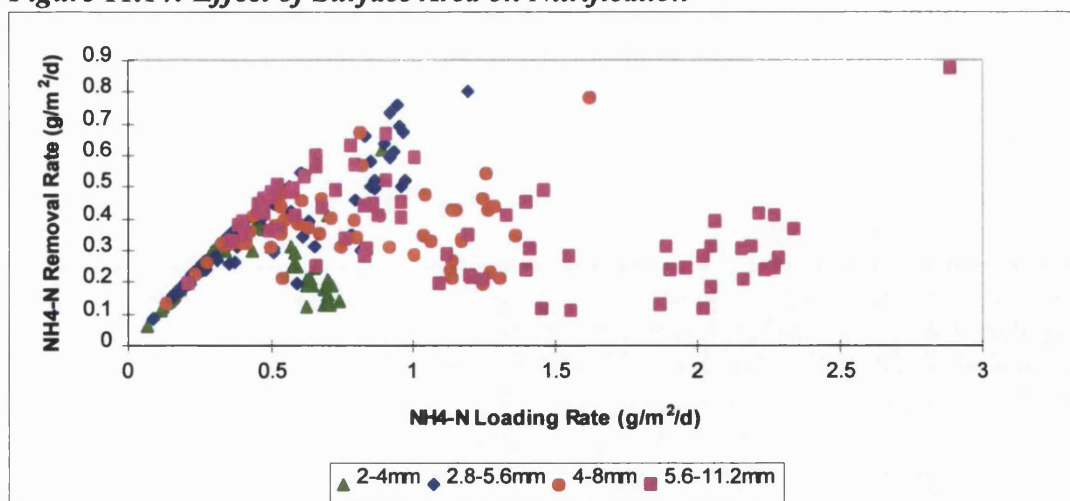
Different media sizes have different SSA with the smallest size having the largest SSA: Volume. The 4-8 and 5.6-11.2mm Lytag have low removals above 0.2 and 0.4 kg NH₄-N/m³/d respectively, this is probably due to their low surface areas which do not allow for sufficient enough nitrifier growth to treat high NH₄-N loads. The data for NH₄-N removals was investigated in terms of SSA using a value calculated from the numbers of equivalent spheres. The SSA used are given in Table 11.1.

Table 11.1: Theoretical SSA

Media Size (mm)	SSA (m ² /m ³)
2-4	1319
2.8-5.6	984
4-8	642
5.6-11.2	413

The graph of NH₄-N removal against loading rate in g/m²/d show a more obvious decrease in removals at higher loading rates for all media sizes except the 2.8-5.6mm Lytag. The 2.8-5.6mm Lytag shows some decrease in removals between 0.5 - 1g NH₄-N/m²/d. This suggests that there may be a surface area which is optimum for nitrification .

Figure 11.14: Effect of Surface Area on Nitrification



In nitrifying trickling filters Upton & Cartwright (1984) found that effective ammoniacal nitrogen removal/m³/d was related to the SSA of the media but an expanded slate was more effective than granite of higher SSA. They concluded that the surface texture also had an effect on nitrification. Boon *et al* (1997) found that for trickling filters the higher the available surface area the greater the rate of nitrification per volume of media - provided the interstices between media did not block with solids. The different Lytag media sizes will also have different voidages during filter runs as captured solids and biofilm growth begins to clog the pores. There may be the same amount of biofilm present in the filters but the smaller pores spaces of the 2-4mm media will clog quicker than the larger available pore space of the larger media sizes. The 2-4mm media has the shortest filter run times and therefore the lowest voidage during the filter run, with voidage increasing with increasing media size.

An optimum combination of SSA and voidage may therefore be necessary to maintain optimum nitrification.

The results suggest that the smallest media size in this study is optimum for nitrification (when in combination with carbonaceous treatment) at low NH₄-N loading rates up to 0.6kg/m³/d. Above this loading rate there is a rapid decrease in nitrification but the 2.8-5.6mm media continues to have good nitrification, at least until a loading rate of 1kg/m³/d. The larger media sizes show low nitrification due to low SSA and in the 5.6-11.2mm Lytag NH₄-N removal is mainly in the form of biomass assimilation.

11.5: Denitrification

It is possible for denitrification to occur in a BAF even when there is no specific anoxic zone within the reactor. There may be oxygen limitation in the depths of thick biofilm layers that are produced at high OLRs, so nitrate will be used as an electron acceptor by heterotrophs leading to reduction of $\text{NO}_3\text{-N}$ to nitrogen gas.

The percentage denitrification is similar for the three larger media sizes and increases with increasing HLR. At HLR 4 there is no denitrification in the 5.6-11.2mm Lytag due to there being no nitrification and therefore no available $\text{NO}_3\text{-N}$ at this loading rate. The 2-4mm media has lower denitrification than the other media sizes at low HLRs (which is opposite to expected) but there is a large increase at HLR 4 to 75%. The increase in denitrification at HLR 4 for the three smaller media sizes is probably due to an increase in BOD removal with increasing HLR and therefore an increase in biofilm thickness. This leads to anoxic zones and the subsequent limitation of oxygen to inner layers of biofilm which encourages denitrification. There appears to be a combination of heterotrophs and nitrifying organisms throughout the bed depth and at HLR 4 there was a larger proportion of bed available to heterotrophic organisms, alongside nitrifying organisms. The large numbers of heterotrophs already present in the biofilm were able to use nitrate nitrogen instead of oxygen as an electron donor breaking up the $\text{NO}_2\text{-N}$ to N_2 throughout the filter bed. The lower levels of denitrification in the 2-4mm media suggests that it is not oxygen limited at HLR 1- 3 and this is shown by the high oxygen transfer in this media size (See Section 11.10).

Recycle of effluent into the reactor may also lead to denitrification due to addition of nitrate to the reactor. In this instance though the combined sewage and effluent feed to the BAF showed TON concentrations of <1 mg/l so there appeared to be no additional nitrate introduced to the reactor. It is possible that TON was being quickly converted in the effluent tank or before analysis by the laboratories.

The actual value of denitrification occurring could only have been calculated if a complete nitrogen balance was carried out on the process, this would have included measuring nitrogen gas emissions from the filters.

11.6: Overall Effluent Quality

The effluent quality produced by Lytag media can be seen to deteriorate with increasing media size. All the media sizes tested show good effluent quality at a VLR of 1kg BOD/m³/d but as loading rate increases the larger media begin to lose performance.

The data from the two different sizes of Arlita used at the beginning of this study at a VLR of 1kg BOD/m³/d, 0.77kg SS/m³/d and 0.2kg NH₄-N/m³/d can be compared to data for Lytag at HLR 1 (1.2kg BOD/m³/d, 0.77kg SS/m³/d and 0.2kg NH₄-N/m³/d). The 3-6mm Arlita has a similar effluent quality to the 2.8-5.6mm Lytag with 5.2mg/l BOD compared to 5.8mg/l, 8mg/l SS compared to 7.8mg/l and 0.7mg/l NH₄-N compared to 0.9mg/l. The 4-8mm Arlita has slightly poorer effluent quality than 3-6mm Arlita, unfortunately there is no data available for 4-8mm Lytag at HLR 1 so a direct comparison cannot be made.

Diurnal sewage variations appear to have little effect on the performance of all sizes of Lytag and Arlita, it is possible that this would be different if the HLR as well as the VLR was varied over 24 hours as is generally the case on STWs.

In this study the performance of Arlita and Lytag media did not appear to be greatly affected by backwashing although more frequent sampling may have picked up differences in effluent quality immediately after backwashing.

All the effluent qualities quoted in this study are only appropriate for this media type and in these conditions ie: with these sewage concentrations, effluent recycle and backwash regimes. In this study the Arlita and Lytag have similar performances at low loading rates but different types of media may produce different results despite being the same size. It also should be noted that at HLRs 2 and 4 the 2-4mm Lytag was allowed to flood in between washes as there was no automatic backwash system. This probably affected effluent quality by decreasing the load actually reaching the filter, and solids removed during backwashing due to a solids build-up at the top of the filter.

The decrease in quality between Port 5 and the effluent port could be related to the lower DO at the effluent port - this in turn may be related to problems with the process air grids. Further investigation is necessary to determine the exact cause of this deterioration in effluent quality.

11.7: Biofilm Growth

The biomass profiles at different HLRs and bed depths do not show any clear difference between media sizes, with concentrations in all cases for Lytag being 0.02 - 0.04kg biomass/kg media. This may be due to the difficulty in gaining a representative media sample. The easiest way to take a sample was to fluidise the filter bed when positioning the auger, this meant the bed was disturbed leading to mixing of media from different depths. It is possible that there is a similar overall growth of biofilm on the different media sizes but this might mean that the biofilm layer occupies a greater proportion of the bed in 2-4mm Lytag than on larger media and thicker biofilm would be expected at the top of the filter where the highest carbonaceous treatment occurs. The Arlita media appeared to have 1/5th of the biomass concentration found for Lytag, this is probably due to low loading rates combined with frequent backwashing.

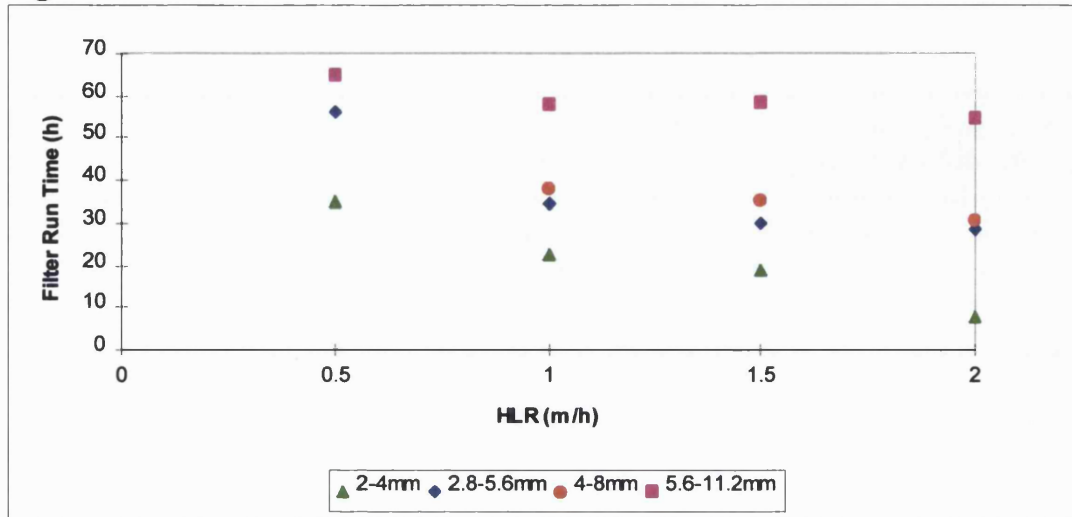
The media samples from the auger were also investigated for 'slime' growth to see whether the bed was being cleaned sufficiently. At all loading rates all media sizes appeared to be free of excessive growth of filamentous organisms. This was confirmed by microbiological analyses which showed the presence of slime-forming zoogaea but only in small amounts.

11.8: Headloss Development

The headloss development over the depth of a BAF is due to solids retention, biomass growth and gas hold-up. The filter run times for each media size at each HLR are given in Figure 11.15 based on the time taken to reach the maximum head height of 0.5m. There is an obvious increase in run time with increasing media size and a decrease in HLR (and therefore VLR), although there is not a completely linear relationship between media hydraulic size and run time. The largest media size had similar run times at all HLRs and would be able to run at even higher HLRs although there would be poor performance in terms of effluent quality. If the loading rate were increased

further the 2-4mm Lytag would have very short run times and it would be unfeasible to operate due to excessive backwashing requirements.

Figure 11.15: Filter Run Times



The short filter run times of the small media are due to high solids retention and biomass growth leading to lower voidage in the bed, this in turn leads to further solids capture but it will also lead to increased gas hold-up within the bed.

The ‘clean bed’ headloss in BAFs is the amount of head present immediately after backwashing although in BAFs the bed is never completely clean due to residual biofilm on the media particles. The Carman-Kozeny equation was used to predict a theoretical clean bed headloss which could be compared with experimental headloss (Table 11.2).

Table 11.2: Predicted Headloss (in m at 15°C)

HLR (m/h)	Media Size (mm)			
	2-4	2.8-5.6	4-8	5.6-11.2
0.5	0.008	0.005	0.002	0.001
1.0	0.016	0.009	0.004	0.002
1.5	0.024	0.014	0.006	0.002
2.0	0.032	0.019	0.008	0.003

The theoretical headloss predicts that there will be higher headloss with small media and headloss will increase with loading rate, agreeing with experimental findings. In all media sizes the theoretical headloss is at least $1/10^{\text{th}}$ that of the experimental headloss. The discrepancy is mainly because the Carman-Kozeny equation was developed for clean water filters where the filter bed is kept very clean, in wastewater filters the presence of biofilm leads to decreases in the voidage of the bed and therefore increased headloss. The theoretical headloss does not take into account the presence of process air which will be held-up in the bed leading to higher headloss. There may also be errors in the calculations of media size and sphericity used in the Carman-Kozeny equation.

The manometer profiles show that there is a higher headloss at the top of the filter bed at low HLRs and this is more obvious with decreasing media size. This indicates straining of solids at the top of the filter as found by Tchobanoglous & Eliassen (1970). Boller *et al*, (1997) also found that solids accumulation in the top layers of the filter caused the main headloss and led to gas entrapment which produced a sudden increase in headloss and terminated the filter run. The smallest media also had the highest initial headloss after backwashing at all HLRs, the problem with high initial headloss is most obvious at HLR 4 where there is 0.3m of headloss in the 2-4mm media - with the maximum available being only 0.5m. This pattern was again seen by Tchobanoglous & Eliassen (1970) for much smaller media (0.49mm, 0.68mm and 0.98mm). They hypothesized that with large media the material removed at the beginning of the filter run accumulated in void spaces that did not enter into the primary flow pattern through the filter, as the dead spaces began to fill the flow channels began to constrict leading eventually to headloss development. The higher starting headloss at high HLRs will be a function of the higher flows through the filter as well as due to high gas hold-up.

With an increased HLR there is deeper solids penetration through the filter bed leading to less straining of solids at the top of the bed and therefore headloss development (as seen by manometer profiles) becomes more evenly spread throughout the filter bed.

11.9: Backwashing and Sludge Production

The profiles of suspended solids removed by backwashing are similar for all media sizes with a peak in removals after 60 - 90 seconds of combined air and water wash followed by a decrease in removals as the rinse phase proceeds. Total solids removed per backwash ranged from 0.3 - 0.55kg depending on media size and HLR, with highest removals for all media sizes being at HLR 3. Smith & Hardy (1992) found that 1kg solids were removed during backwash for every 1kg BOD during filter operation and a value of 0.8-1kg solids was found by Pujol *et al* (1990), this is similar to values found in this study for Lytag as shown by Table 11.4 and compares to solids removals of nitrifying activated sludge plants. The values for solids removed/kg BOD removed do not show a clear pattern according to media size or HLR probably because the backwash was based on time rather than head build-up.

Table 11.3: Removal of Suspended Solids (kg SS Removed in Backwash/kg BOD Removed)

HLR (m/h)	Media Size (mm)			
	2-4	2.8-5.6	4-8	5.6-11.2
0.5	0.76	0.78		0.86
1.0	0.86	0.66	0.63	0.65
1.5	1.03	0.83	0.94	0.99
2.0	0.78	0.61	0.71	0.9

Weekly totals (assuming that the same amount of solids were removed at each backwash) were compared with the solids load onto the filter for each loading rate (Table 11.4). The solids removed by backwashing are similar for all media sizes except the 2-4mm Lytag which has higher removals at HLR 2 and 4. At these HLRs the filter flooded and therefore solids were retained at the top of the filter rather than filtered through the bed. Apart from these instances it appears the backwashing had a similar effect on all media types with all filters having the same degree of cleaning except the 2-4mm which could have used higher backwash rates/durations. There is an increased solids removal with increased solids loading onto the filters.

It can be seen that the combined amount of solids removed from the filter by backwashing and in the effluent is larger than the total suspended solids load onto the filter for all media sizes at all HLRs. This is due to the production of biomass from the

soluble portion of BOD in the settled sewage, a high proportion of this biomass is then removed in the backwash along with captured particulate material. The total solids load onto the filter can therefore consist of actual suspended solids but also a proportion of the soluble BOD/COD. A complete solids balance has not been carried out as measures of volatile solids were not taken.

**Table 11.4: Total Solids Yield
(Solids Removed by Backwash Plus Solids Remaining in Effluent - kg/week)**

HLR (m/h)	Solids Load (kg/week)	Media Size (mm)			
		2-4	2.8-5.6	4-8	5.6-11.2
0.5	1.6	1.9 (1.84)	1.85 (1.84)		2.25 (2)
1.0	2.7	4.28 (3.88)	3.3 (3.3)	3.16 (2.73)	3.83 (2.8)
1.5	6	6.5 (5.5)	5.03 (4.48)	5.66 (4.76)	5.97 (4.34)
2.0	6.3	8.82 (7.21)	7.05 (5.74)	8.34 (5.6)	8.96 (4.62)

NOTE: Figures in brackets represent solids removed by backwashing

The volume of effluent reused for backwashing each week was similar for all media sizes and all HLRs (Table 11.5). This was due to washing the filters according to time and is high compared to general operating levels. If the filters had been allowed to run until just before flooding they would generally have required lower volumes for backwashing, with decreasing wash water volumes necessary for increasing media size. It would be expected that larger media would have lower backwash requirements than the small media, due to longer filter run times although this might be outweighed by higher backwashing rates.

Table 11.5: Actual Effluent Reuse for Backwashing (%)

HLR (m/h)	Media Size (mm)			
	2-4	2.8-5.6	4-8	5.6-11.2
0.5	16	16		19
1.0	18	18	17	17
1.5	19	18	16	17
2.0	17	17	17	16

Sludges from BAFs are derived from the growth of biomass and filtration of non-biodegradable solids which are removed during backwashing. These sludges are quoted as being high in volatile matter [>80%] (Upton & Stephenson, 1993), which agrees with the results of 71-87% found in this study. There does not appear to be any difference in sludges based on media size or HLR. At different HLRs the media sizes

only appear to show differences in the CST of the sludges. There was high variability in the values at each HLR and there may be some inaccuracies in the test itself (see Section 7.7).

Table 11.6: Sludge Volatile Solids (%)

HLR (m/h)	Media Size (mm)			
	2-4	2.8-5.6	4-8	5.6-11.2
0.5	75	73		71
1.0	80	75	72	73
1.5	74	73	79	77
2.0	85	85	87	84

A clearer relationship between backwashing/sludge parameters and media size/HLR would probably have been found if the same backwash rates and durations had been used in all instances. In a full-scale process backwashing regimes are altered according to the situation, so using the same regimes in this study would not have been representative of the ‘real’ situation.

11.10: Oxygen Transfer

When oxygen transfer rates were measured it was assumed that there was no change in the proportions of N₂ in the system. Denitrification has been seen to occur in all the media sizes, looking at the worst case where there is 0.32kg/m³/d denitrification occurring we can calculate that there is only a 0.019% change in nitrogen concentration over a day so we can assume for off-gas analysis that there is no change.

All media sizes show increased OTE with decreasing air flows at all HLRs. At low air rates there is an increased residence time in the filter bed, the held-up gas is replenished less frequently so more oxygen is utilised - this allows more efficient oxygen transfer. As air flows increase there is more chance of bubble coalescence and there is a reduced hold-up time for gas bubbles, high frequency of air replacement and low oxygen depletion leading to less efficient oxygen transfer.

The graphs of OTE show an increase in transfer with decreasing media size. The 2-4mm Lytag has a higher OTE (both operational and corrected) than any of the other

sizes. This agrees with the oxygen transfer in Arlita and with the work of Stensel *et al* (1988). The OTE at operational air flows (5-10Nm/h) are similar to those of Harris (1994) at 4 - 13%, depending on loading rate. The 2-4mm Lytag though has higher OTEs at 10 - 16%. The increased oxygen transfer in the small media is due to the smaller gas bubbles present due to smaller void spaces within the filter bed. This allows a larger interfacial area for a given volume of air, slower bubbles rise rates and larger gas volume hold-up. The large interfacial area of the gas bubbles allows a large proportion of oxygen transfer to be through the direct uptake of oxygen by the biofilm (interfacial oxygen transfer). The large media may have lower oxygen transfers due to large bubbles or bubble coalescence producing low interfacial areas. The small media will also have a higher demand for oxygen due to higher media surface area allowing higher biomass growth. This will lead to an oxygen limitation which then drives the process of oxygen transfer.

The high OTE found in 2-4mm Lytag indicates that it will not be oxygen limited and therefore oxygen will be used preferentially to NO₃-N, hence the lower rates of denitrification than the other larger media sizes.

Figure 11.16: Operational OTE for Different Media Sizes (HLR 3)

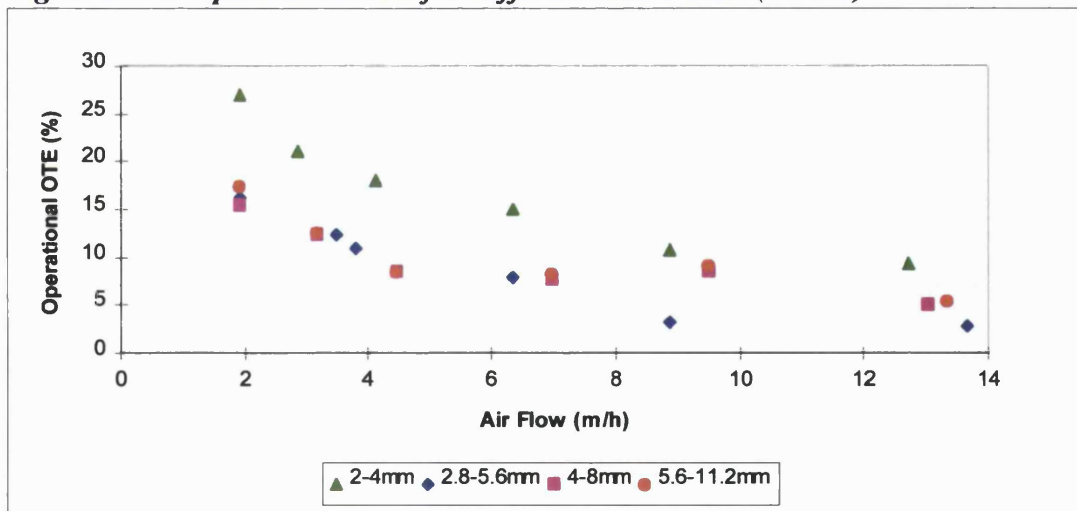
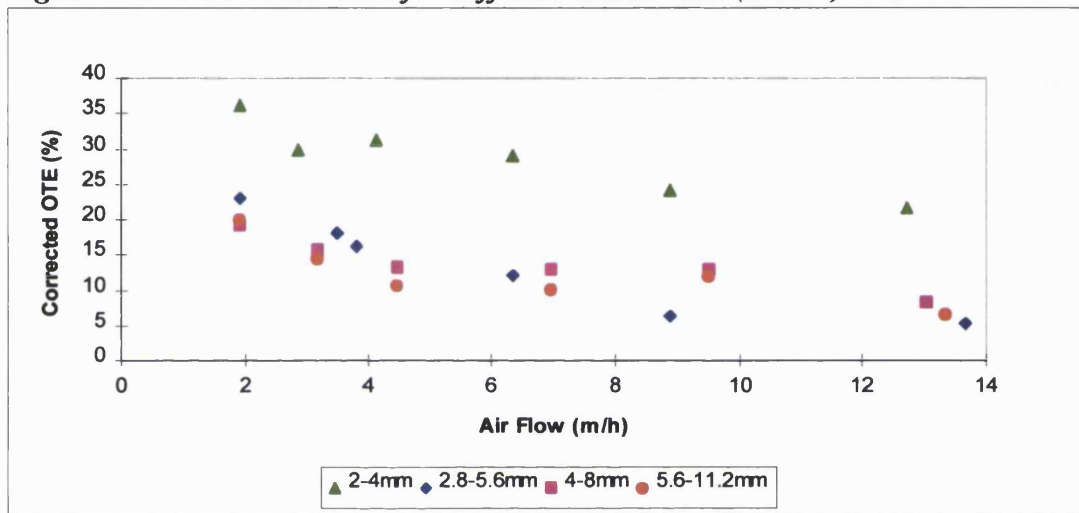


Table 11.7: Operational OTE (%)

HLR (m/h)	Media Size (mm)			
	2-4	2.8-5.6	4-8	5.6-11.2
0.5	16 (2.1)	13.6 (2.2)		7 (1.7)
1.0	25.6 (1.6)	12 (2.5)	14 (3.5)	8.8 (2.7)
1.5	25.6 (7.8)	14.9 (1.3)	14 (3.7)	16 (4.1)
2.0	23.7 (6.1)	16 (2.7)	19.3 (5)	14.2 (5)

Air flow approximately 2m/h (Air flow approximately 13m/h)

Figure 11.17 : Corrected OTE for Different Media Sizes (HLR 3)



The effluent recycle used at HLR 2- 4 could have an effect on the OTE as seen by Lessar (1993) who found a slight increase with an effluent recycle of 1m/h. The low recycle rates used in this study would probably have had very little effect on OTE.

The graph of oxygenation capacity can be used to determine optimum air flows for different media sizes and loading rates. At HLR 3 the 2-4mm media has a much higher OC than the other 3 sizes which have similar capacities. At an air flow of 13m/h the 2-4mm media has still not reached its maximum OC. The 2.8-5.6mm media has slightly lower capacities than the larger media, this may indicate that channeling may be occurring. Harris (1994) found that increasing air flow beyond 5 Nm/h did not significantly increase the quantity of oxygen transferred. This was found in all media sizes except the 2-4mm.

Figure 11.18: Oxygenation Capacity for Different Media Sizes (HLR 3)

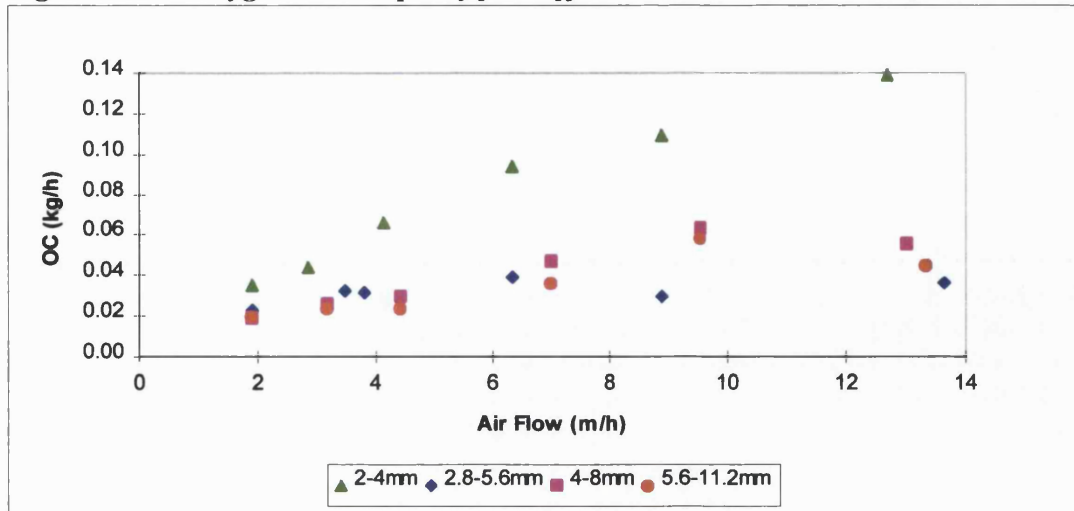


Table 11.8: Oxygen Demand (kg O₂/h)

HLR (m/h)	Media Size (mm)			
	2-4	2.8-5.6	4-8	5.6-11.2
0.5	0.016 (0.017)	0.016 (0.015)		0.014 (0.02)
1.0	0.021 (0.031)	0.019 (0.024)	0.027 (0.028)	0.024 (0.024)
1.5	0.044 (0.038)	0.01 (0.025)	0.035 (0.033)	0.038 (0.023)
2.0	0.04 (0.037)	0.02 (0.048)	0.032 (0.039)	0.037 (0.021)

NOTE: Figures in brackets are theoretical oxygen demands

The estimated oxygen demand shows an increase with increasing HLR and increasing nitrification. This generally indicates increased oxygen demand with decreasing media size. Actual oxygen demands tend to follow this pattern except in 2.8-5.6mm media at HLR 3 and 4. In these instances there is very low oxygen demand which could indicate channelling or a blockage. Discrepancies between estimated and actual oxygen demand may be due to the estimated demands being calculated using average composite data for BOD/NH₄-N removal and denitrification. Experimental oxygen demand was calculated from off-gas analysis on individual days when performance may have been different to average.

Harris *et al* (1995) found that BAFs had an increased OTE with increasing load, with a slight decrease at the highest load investigated (2.7kg BOD/m³/d). As the loading rate increases so does the microbial activity, this leads to oxygen limitation (an increased oxygen demand) and this is the driving force behind oxygen transfer. All the media sizes in this study except the 2.8-5.6mm media show an increased oxygen demand with

increasing HLR up to HLR 4 (4.8kg BOD/m³/d) where demand decreases slightly. The 2-4mm Lytag shows the highest oxygen demand but the demand in 2.8-5.6mm Lytag is very low at HLR 3 and 4 suggesting that there may be a blockage in the process air grid or in the filter bed leading to channelling of air. The slight decrease in oxygen demand at HLR 4 may be explained by the fact that denitrification has increased at load 4 and therefore the overall oxygen demand has decreased slightly. In the 2-4mm Lytag nitrification has decreased at HLR 4, this has a higher oxygen demand than BOD removal, leading to decreased OTE. The decrease in oxygen transfer with a loss of nitrification is also an indication of the presence of interfacial oxygen transfer. If all oxygen transfer was via the liquid there should be no decrease in oxygen transfer at HLR due to transfer into the liquid phase even if oxygen did not reach the biofilm. Where the actual oxygen demand is higher than predicted in the 5.6-11.2mm media the system may be oxygen limited.

A high DO level in BAFs leads to a greater level of protection against influent shock loads but may be expensive to achieve. During normal filter operation in this study the filter DOs were generally above 2mg/l even at the highest loading rate, therefore the filter as a whole should not have been oxygen limited. The 5.6-11.2mm media had DO levels slightly lower than 2mg/l which would correspond with the filter being oxygen limited at higher loading rates. There may have been oxygen limitation within biofilms due to differences in the biofilm thickness. Harris (1994) found similar DO profile patterns to those in this study with the lowest DO in the top of the reactor, increasing towards the base and lower in the effluent than at Port 5. The rise in DO was found to occur higher up the bed at lower loading rates. The high OTE at low air flows suggest that process air could be decreased, this would probably lead to poor performance due to low bulk DO levels in the filters.

11.11: Hydraulic Regime

It has been suggested that the relatively short hydraulic residence times found in BAFs make the process more susceptible to variations in flow and load (Smith, & Hardy, 1997). RTD curves for Lytag at HLR 2 can be seen in Chapters 7 -10. They show the pattern of tracer found in the filter effluent after a tracer impulse has been introduced to the filter. It can be seen that the tracer levels do not always fall to background filter

levels. This could be due to a dilution effect in the effluent recycle, adsorption of the NaCl tracer onto the biofilm/media, entrapment within pores or due to hold up in stagnant regions (Levenspiel, 1972). For this reason a time limit of 2 X theoretical retention time was used for data collection and subsequent analysis.

The theoretical empty bed retention times for HLR 1 - 4 were approximately 190, 97, 64 and 48 minutes for all media, if we use the experimental voidage of 0.31 for Lytag media we can calculate TRT of 59, 30, 20 and 15 minutes.

The literature (Levenspiel, 1972) suggests that differences between the theoretical HRT, peak and mean residence times indicate whether there is mixing or channelling/stagnant zones. For all media sizes except the 2-4mm media the peak residence time is lower than the tHRT. This indicates that there is some channelling or stagnant zones within the reactors. The peak is larger in 2-4mm media indicating the use of a large volume of the filter bed for treatment. The mean is higher than the peak and this indicates that there is some mixing occurring in all media sizes. The large mean time may be a function of adsorption of NaCl onto the biofilm. The tracer tests were carried out with process air flow to the filters, this could have led to hold up of the tracer within the filters. The work of Mendoza-Espinosa *et al* (1997) found that the mean retention time (MRT) of downflow BAFs was smaller than the tHRT indicating channelling and stagnant zones (with only 23 - 25% active volume) but this was improved when media was added to the plenum chamber to decrease entrapment of air bubbles.

Table 11.9: Retention Times

HLR	2-4mm		2.8-5.6mm		4-8mm		5.6-11.2mm	
	Peak	Mean	Peak	Mean	Peak	Mean	Peak	Mean
1	90	147	50	166			25	126
2	55	86	25	69	22	66	22	72
3	35	53	20	42	17	49	12	44
4	30	39	15	26	21	39	12	32

The flow regime of reactors can be determined from the dispersion number (Chapters 7 10). In all cases that there is plug flow through the filter with less dispersion occurring

with increasing HLRs. The smallest media appears to have the most plug flow as shown by the low dispersion numbers. In a plug flow reactor the substrate concentration decreases through the reactor (Rusten, 1984) and this can be seen from the bed profiles of all media sizes.

It could be expected that large media may have more plug flow than small media if the filter bed as a whole is considered. The large media has larger void spaces which allow channelled flow of liquid without a high degree of hold-up. There would be expected to be hold-up in smaller media with a more tortuous path through the small void spaces. Looking closer at void spaces within the filter bed there is expected to be streamline flow in small pore spaces and therefore plug flow through the pores whereas flow begins to become more turbulent as void size increases leading to more mixing within the pores (Coulson & Richardson, 1981). Looking at the Reynolds numbers for all media sizes it can be seen that there is streamline or laminar flow in all media sizes, ($Re < 5$ for all media sizes, for turbulent flow $Re > 61$ in porous media [Cunningham, 1989]), indicating that it is feasible for the smallest media to show greatest plug flow. Air flow to the reactors increases mixing with the largest media size showing the most mixing. In a granular material streamline flow is expected through pore spaces as the velocity of fluid and the width of channels is small.

The RTD curves appear to show that the 2-4mm Lytag actually has less plug flow than the larger media sizes (as opposed to dispersion numbers $[D/uL]$ which show more plug flow in 2-4mm Lytag). This may be due to the build-up of head within the filter beds affecting the volume of fluid at the top of the filter bed. In small media there is an build-up of head immediately after backwash producing a large enough volume of fluid to induce mixing of the tracer before plug flow through the bed begins this volume of fluid approximates to a mixed reactor system.

11.12: Decommissioning

When normal operation of the filters was complete they were drained and media samples were removed for sieving in order to determine how much attrition had occurred. The 2-4mm and 2.8-5.6mm Lytag appear to have increased in particle size range, this is possible as throughout filter operation there was a high percentage loss of

media and fines during backwash (especially in the 2-4mm media) so media was often 'topped up'. Over the period of filter use therefore all small particles will have been removed leaving the larger heavier particles in the filter. After filter operation the two larger media sizes have particle size ranges close to the original size range indicating that there was very low media attrition and any media fines will have been removed at the beginning of filter operation.

When filter operation was complete the pipework of the columns were also investigated for sludge/biofilm build-up. The columns containing 2.8-5.6mm and 4-8mm Lytag had some sludge build-up in the effluent pipework suggesting that this contributed to the poor effluent quality.

12.0 PILOT SCALE PERFORMANCE OF LYTAG MEDIA

Conclusions

12.1: Conclusions

A comparison of the advantages and disadvantages of the different media sizes is shown by Table 12.1.

Table 12.1: Advantages and Disadvantages of Different Media Sizes

Media Size (mm)	Advantages	Disadvantages
2-4	High carbonaceous treatment (at 6kg BOD/m ³ /d) High solids removal (at 3kg SS/m ³ /d) Good nitrification at low loads (up to 0.6kg NH ₄ /m ³ /d) High OTE	Poor nitrification at high loads (above 0.6kg NH ₄ /m ³ /d) High headloss Short filter run times High energy requirements High effluent reuse
2.8-5.6	High carbonaceous treatment (at 6kg BOD/m ³ /d) High solids removal (at 2kg SS/m ³ /d) Good nitrification (up to 1kg NH ₄ /m ³ /d)	Low OTE High headloss Short filter run times High energy requirements High effluent reuse
4-8	Low headloss Long filter run times Low energy requirements Low effluent reuse	Poor carbonaceous treatment (above 3kg BOD/m ³ /d) Poor solids removal (above 1.5kg SS/m ³ /d) Poor nitrification (above 0.3kg NH ₄ /m ³ /d) Low OTE
5.6-11.2	Low headloss Long filter run times Low energy requirements Low effluent reuse	Poor carbonaceous treatment (above 2kg BOD/m ³ /d) Poor solids removal (above 1kg SS/m ³ /d) Poor nitrification (above 0.2kg NH ₄ /m ³ /d) Low OTE

The two smaller media sizes produce good quality effluents for all parameters although it has been shown that the 2-4mm media actually has poorer performance in terms of nitrification at the highest loading rates than the 2.8-5.6mm media. Both of the smallest media sizes produce high headloss due to having small void spaces and this leads to high backwash requirements and therefore high energy requirements - with the smallest media having the shortest run time and consequently needing the most frequent backwashes. The small media does have high rates of oxygen transfer so this could decrease energy costs in relation to air supply. The smallest media would probably be uneconomical to use in most instances except if there was a strict ammoniacal nitrogen consent at low loading rates or in instances of nitrification only (tertiary filters).

The two large media sizes produce poorer effluent quality than smaller media although at low loading rates the BOD and SS values are of a high enough quality to meet consents in certain areas. The energy use for backwashing is low especially in the largest media size and this may make it more feasible to use the large media where there is no $\text{NH}_4\text{-N}$ consent or where loading rates are high and roughing filtration is needed before nitrification.

Media size has a number of different effects on the BAF process and can be used to optimise the use of BAFs in different situations. All conclusions drawn are for the four Lytag media sizes used in this study and the process conditions employed in this study.

1. Carbonaceous treatment improves with decreasing media size and decreasing HLR/OLR
2. Suspended solids removal by filtration improves with decreasing media size and HLR/OLR
3. Nitrification is more efficient with decreasing media size, up to an optimum capacity where nitrification then decreases
4. The optimum size of media for nitrification is based on surface area and voidage. In this case the 2-4mm Lytag is optimum at low loading rates but the 2.8-5.6mm is more effective at higher loading rates, probably due to slightly larger voidage

5. Denitrification occurs in aerobic BAFs due to differences in biofilm thickness and oxygen/substrate penetration through the biofilm
6. Headloss increases with HLR/OLR and with decreasing media size
7. Filter run times decrease with decreasing media size and increasing HLR/OLR
8. Similar backwash solids and sludges are produced by all media sizes (for regimes used in this study)
9. High effluent reuse (high backwash rates and long backwash durations) may be necessary for optimum washing of media - this translates as high energy use and process costs
10. Small media is more prone to being washed out of the filters during backwashing and may need replacing frequently
11. Oxygen transfer efficiencies increase with decreasing air flow and media size
12. Oxygen transfer efficiency is optimum before nitrification rates begin to decrease
13. Different media types of the same size appear to produce similar effluent qualities (at the low loading rates used for Arlita media in this study)

The different media sizes studied could all have possible uses in BAFs but for different treatment options. All process variables such as headloss and run times should be taken into account combined with effluent quality when choosing media size for use in BAFs.

The general uses for the media sizes investigated in this study could be:

- 2-4mm Lytag - tertiary nitrification where there are high effluent consents but low loading rates
- 2.8-5.6mm Lytag - general use on BAFs where there is the need for carbonaceous treatment and nitrification but consents are 30 SS:20 BOD:5 NH₄-N
- 4-8mm - use for carbonaceous treatment only
- 5.6mm Lytag - use for roughing filtration of wastewater.

12.2:Future Work

A number of different interrelated processes are used in the treatment of wastewater by BAFs. Further studies could be carried out on both large and small scales to gain a better understanding of the process as a whole.

1. Different backwash regimes could be studied with the filters washed according to head build-up rather than time
2. Different HLRs could be investigated to simulate stormwater situations and how different media sizes perform in these instances
3. Either HLR or VLR could be varied to distinguish which has the most effect on performance of different media sizes
4. Nitrification could be further investigated by using low BOD loading rates combined with high $\text{NH}_4\text{-N}$ loading rates
5. Comparison could be made between different media types of the same size to determine whether the physical characteristics have a large influence on performance
6. It would also be useful to investigate the more detailed processes occurring at the level of individual media particles in order to determine the effects of media shape/surface roughness/porosity on biofilm growth and nitrification



TESTING OF BIOLOGICAL AERATED FILTER (BAF) MEDIA

T. D. Kent*[†], C. S. B. Fitzpatrick*[†] and S. C. Williams**

* *School of Water Sciences, Cranfield University, Cranfield, Beds, MK43 0AL, UK*

** *R & D, Thames Water Utilities Ltd, Spencer House, Manor Farm Rd, Reading, Berks, RG2 0JN, UK*

ABSTRACT

The cost of filter media contributes a significant proportion of the initial capital outlay in wastewater treatment by biological aerated filters (BAFs). Media characteristics also affect day to day running costs such as those involved in backwashing. To allow an informed choice relating to filter media and their prospective uses a number of standards have been produced, most recently the British Effluent and Water Association (BEWA) standard. The aim of this study was to investigate a number of granular media using the BEWA standard in order to determine their suitability for BAFs. All the media samples investigated appear suitable for use as BAF media with one in particular having all the necessary characteristics e.g. low density, high specific surface area and resistance to attrition. Copyright © 1996 IAWQ. Published by Elsevier Science Ltd.

KEYWORDS

Backwashing; biological aerated filter (BAF); biomass; collapse-pulsing; filter media; minimum fluidisation velocity (V_{mf}).

INTRODUCTION

Many different types of filter and their associated media are in use today for potable and wastewater treatment. One such filter is the biological aerated filter or BAF which is used for secondary treatment of sewage and combines biological treatment with suspended solids capture, negating the need for a separate solids removal stage. BAFs must be cleaned by regular backwashing due to clogging of filter media by biomass and attached solids. If backwashing is ineffective it may lead to formation of mudballs, poor effluent quality during initial stages of filtration and increased headloss build-up during subsequent filter runs (Amirtharajah, 1993). Backwashing is therefore designed to remove excess biomass, allowing treatment to be resumed directly after washing (Smith & Hardy, 1992) and is carried out in downflow filters by reversing the flow of water - causing deposits to dislodge from the filter media surfaces.

The variation in filter mechanisms has led to the need to characterise media to determine their suitability for use and to help in the choice of alternative materials. In developing countries for example, there may be natural local materials that could provide cheaper alternatives to commercial filter media (Ogedengbe & Olawale 1983).

[†] Present address: Department of Civil & Environmental Engineering, UCL, Gower Street, London, WC1E 6BT, UK

The filter material represents a significant proportion of the initial capital outlay, but it can greatly affect day to day running costs such as energy costs in backwashing (Letterman, 1980). It is therefore important to choose media with appropriate characteristics e.g.: low density and fluidisation rates, as these can influence water and air flows necessary to carry out efficient backwashing. Other important characteristics include size, porosity and attrition resistance.

Media used in BAFs are usually granular in nature and have traditionally consisted of natural materials such as sand, shale and expanded clays. More recently synthetic materials have been used e.g. polystyrene which may be less prone to attrition during backwashing, (Sagberg *et al.*, 1992). There is also a certain degree of control over grain characteristics (Lacamp *et al.*, 1993) e.g. the lightweight floating 'Biostyr' beads facilitate backwashing and the furrowed 'Biobead' improves biomass attachment during the backwashing period (Cantwell and Whitaker, 1993). The production of synthetic material is usually costly though and media may not be significantly more effective than natural materials.

A number of standards for filter media have been developed including the American Water Works Association (AWWA) specification (AWWA, 1989), the Indian Standard (Anon, 1977) and the recent British Effluent and Water Association Granular Filtering Materials Standard (BEWA, 1993). The BEWA standard has been reviewed by Stevenson (1994). The aim of this study was to characterise seven different media using the BEWA standard and to determine the most appropriate for use in a BAF. The suitability of the BEWA standard for testing BAF media was also assessed.

MATERIALS AND METHODS

A number of tests were carried out on seven media types to BEWA specifications (1993) with some adaptations. Parameters determined according to the BEWA standard included grain specific gravity, bulk density, friability, attrition, acid solubility and minimum fluidisation velocity, in addition porosity and specific surface area were investigated. Media characterised are described in Table 1.

Table 1. Details of media and suppliers

Media Name	Stated Size Range	Suppliers	Description
EFG	2 - 5mm	Alpha Aggregates	Expanded fireclay grog
Experimental 'Starlight'	+ 2.8mm	ECC	Foamed cylindrical clay
Molochite	2 - 6mm	ECC	Angular calcine clay
Old Expanded Shale	2.5 - 4mm	Akdolit-Werk, GMBH	Angular shale
New Expanded Shale	3 - 6mm	Akdolit-Werk, GMBH	Angular shale
Lyttag	2.36 - 4.75mm	Lyttag Ltd	Pulverised fuel ash
Arlita	3 - 6mm	Aridos Ligeros, Spain	Expanded spherical clay

Adaptations used in the investigation are detailed below.

Sieve analysis

In this study one media sample ('Starlight' + 2.8mm), was found to produce a high volume of fines if sieved for a prolonged period. Samples were therefore sieved for two periods of five minutes to produce a sample size range against which samples subjected to friability and attrition tests could be compared.

Grain specific gravity

Biological aerated filter media are usually porous so samples were soaked overnight (as advised by BEWA, 1993) to fill pores with water and then blotted to remove excess water. From the work of Humby (1994) it

was shown that a large volumetric flask could be used to produce results approximate to those gained using a density bottle. therefore a 250ml volumetric flask was used in this study.

Settling velocity

The procedure described by Ives (1990) was followed with media grains being soaked overnight and inserted into a column of 81mm diameter, using tweezers. The time taken by each of 20 grains of each sieve size of each media type to settle through a water depth of 1m was recorded.

Minimum Fluidisation Velocity (V_{mf})

The minimum fluidisation velocity is the velocity required for the onset of fluidisation of a filter bed. This velocity was determined experimentally for each sample using a media depth of approximately 600mm and by measuring the percentage change in bed depth and the headloss in relation to increasing water velocities. The point of V_{mf} is considered to be where headloss across the depth of the media levels off and the % change in bed depth increases linearly.

Two different methods for calculating V_{mf} were used:

$$\text{Wen \& Yu (1966): } V_{mf} = \frac{(R_{mf})}{d_{eq}\rho} \quad [* \text{ in Table 2}]$$

$$\text{Where: } R_{mf} = [33.7^2 + 0.0408Ga]^{\frac{1}{2}} - 33.7 \quad \text{and: } Ga = \frac{[d_{eq}^3\rho(\rho_s - \rho)g]}{\gamma^2}$$

Carmen-Kozeny equation, described by Coulson & Richardson (1978):

$$V_{mf} = 0.0055 \left(\frac{\epsilon^3}{1-\epsilon} \right) \frac{d_h^2(\rho_s - \rho)g}{\gamma} \quad [! \text{ in Table 2}]$$

Where:

- ϵ = voidage (bed porosity)
- d = hydraulic diameter of filter media
- d_h = equivalent diameter of filter media as defined by d_{90} from sieve analysis (m)
- ρ = density of fluid (kg/m^3)
- ρ^s = density of filter media (kg/m^3)
- γ = dynamic viscosity (kg/ms)
- g = gravitational acceleration (9.81 m/s^2)

Attrition

An accelerated backwash test as suggested by Ives (1990) and BEWA (1993) was used combining air and water wash with water flow rates determined from the experimental V_{mf} . Amirtharajah (1993) has shown that air flow combined with water flows of 40-60% of the V_{mf} are needed to produce the condition of collapse-pulsing necessary for efficient backwashing. Air rates in the region of 100m/hr were necessary for all media (except for 'Starlight' which needed a rate of approximately 40m/hr in order to prevent media being lost over the overflow weir). In this study most of the media investigated tended to fluidise before a true condition of collapse-pulsing was achieved (as determined visually), therefore attrition tests were set with the bed pulsing but little sign of cavity formation and collapse.

Friability

The aim of the friability test is to reproduce the effect of transport and crushing during handling of filter media. The apparatus used was a simple ring shear tester as described by Humby *et al* (In Press). An annular sample was subjected to a normal stress load via a shoe which was then manually rotated 360° to apply a

shear force. The normal load applied was equivalent to the pressure underfoot of an average person, as calculated by Humby *et al.* (In Press).

Internal porosity and specific surface area

The powder testing and characterisation service provided by the School of Powder Technology, University of Bradford was used to gain an idea of surface area and porosity of each of the media samples. The particle porosity was determined using a Micromeritics Mercury Porosimeter and the surface area was determined using Micromeritics ASAP Adsorption Apparatus (Allen, 1981).

Voidage (external porosity)

After weighing the media, they were soaked overnight in order to fill the internal pores with water. The media were then drained through a sieve in order to remove excess water before being placed in the columns.

Fluidisation, attrition and voidage tests were carried out in a column of 15cm diameter and 2m height. The outlet stream passed through a settling tank to enable media entrapment before running to drain.

RESULTS

All media samples had similar size ranges but differed in other respects (Table 2). Generally any filter media must be chemically inert, a surrogate test for this is the acid solubility test as described in the BEWA standard. A weight loss of more than 2% is considered unsatisfactory, therefore all the media in this study can be considered acceptable for use in filters in terms of inertness.

Table 2. Summary of media data

Table 2: Summary of Media Data

Media Type	Starlight'	Molochite	EFG	Lytag	Old ES	New ES	Arlita
Size Range (mm)	2.6 - 3.4 (+2.8)	1.8 - 5 (2 - 6)	2.5 - 4.7 (2 - 5)	2.6 - 4.3 (2.36 - 4.75)	2.1 - 3.9 (2.4 - 4)	2.65 - 4.1 (3 - 6)	3.5 - 6.2 (3 - 6)
Density (kg/m ³)	1340	2600 (2700)	1720	1940 (1950)	1900	1680	1550 (1350)
Porosity (m ³ /m ³)	0.06	0.01	0.15	0.06	0.08	0.18	0.05
SSA (m ² /cm ³)	2.16	0.9	1.18	3.89	0.83	0.47	3.98
Exp ^t V _{mf} at 8°C (m/hr)	approx 28	> 140	approx 88	approx 92	60 - 80	64 - 96	72 - 80
Theoretical V _{mf} at 8°C (m/hr)	* 42 ! 41.5	* 160 ! 200	* 97 ! 132	* 110 ! 113	* 93 ! 86	* 84 ! 82	* 104 ! 69
Voidage	0.39	0.4	0.4	0.35	0.34	0.36	0.3
Friability-% undersize	45	3.5	14	6.5	6.5	22	5.5
% Attrition	45.2	1.1	6	5.5	2.3	2.8	1.5
% Acid solubility	0.15	0	0.1	0.75	0.35	0.8	1.4
Settling velocity mm/s at 22 °C	61 - 89	100 - 297	88 - 171	95 - 239	80 - 172	87 - 141	132 - 225
	at 22 °C	at 20 °C	at 20 °C	at 19 °C	at 19 °C	at 24 °C	at 19 °C

NOTE: Suppliers details, where available, are shown in brackets.

* - From Wen & Yu ! - From Carmen-Kozeny

Biomass attachment is an important consideration when choosing BAF media, this is mainly affected by the specific surface area (SSA) and surface characteristics of media. Porosimetry data was calculated for pores of 2.5 μm and above to allow for maximum reproduction of bacteria by fission (Messing, 1988). This data shows that media samples in this study all have high porosities, except for molochite which has a low porosity of $13.6\text{m}^3/\text{m}^3$ of media. From scanning electron (SEM) micrographs it was noted that each media type has a range of porosities and although the molochite did not appear very porous it does have a high degree of surface roughness to allow biomass attachment. The data and observation therefore suggest that all media in this study are suitable for biomass growth but further investigation is necessary. The Arlita and Lytag have the highest specific surface areas of all the media investigated allowing for a high degree of biomass colonisation.

The behaviour of filter media during backwashing is an important consideration for filter operation. The minimum fluidisation rate (V_{mf}) dictates water flows used and is greatly affected by media density. From Table 1 it can be seen that Molochite has a high density of $2600\text{kg}/\text{m}^3$ and 'Starlight' has a low density of $1340\text{kg}/\text{m}^3$ with the remaining media in the study having densities in the range of $1600\text{--}1900\text{kg}/\text{m}^3$. The relationship between density and V_{mf} for similar-sized media can be seen with all media having V_{mf} s in the region of $80\text{--}90\text{m}/\text{hr}$ except 'Starlight' and Molochite. Headloss in cm of water and change in bed depth vs water velocity for Lytag is shown in Figure 1.

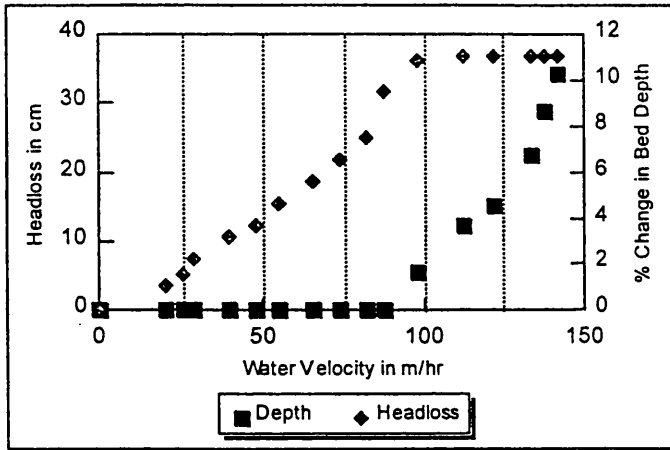


Figure 1. Fluidisation of Lytag at 7.5-8°C.

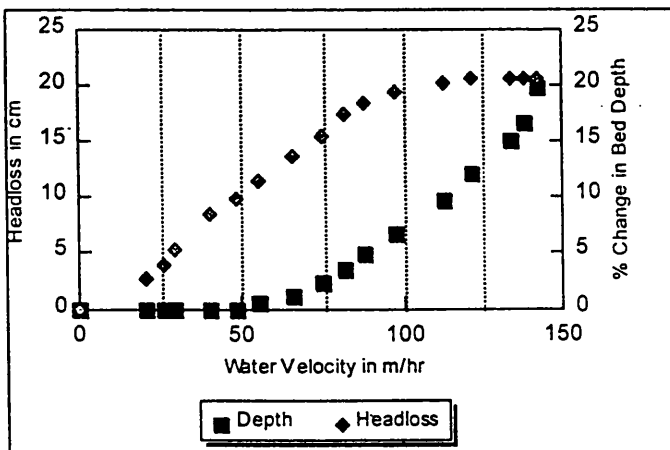


Figure 2. Fluidisation of New Expanded Shale at 8°C.

The high water flows necessary for backwashing molochite make it unsuitable as a filter medium. Although both shales have V_{mf} s of 80-90m/hr, it was seen from fluidisation graphs (Figure 2) and observation that neither had a clear fluidisation point with low density/small particles fluidising first leading to stratification. If high flows are applied to backwash these media there is the possibility of considerable media loss; on the other hand if only low flows are used it is possible that a large proportion of the media will not be sufficiently cleaned.

The experimental V_{mf} s at 8°C are all significantly lower than the theoretical value from the Wen & Yu equation (1966), apart from the New Expanded Shale. The difference in values could be due to the lack of sphericity and voidage terms in the Wen & Yu equation. The Carmen-Kozeny equation incorporates voidage and corresponds more closely to the experimental data for Old Expanded Shale and Arlita than the Wen & Yu equation but is still inaccurate for the other media. It assumes that flow conditions within the bed are streamline and that particles are spherical - this would explain why it gives a V_{mf} that is close to the experimental value for the spherical Arlita media.

During the attrition tests it was found that a high percentage of 'Starlight' (Figure 3), was lost due to production of fines, this makes 'Starlight' unsuitable for use in filters as these fines would quickly build up and lead to clogging of the filter. The molochite and Arlita (Figure 4) proved to be most resistant to attrition with 1.1 and 1.5% loss of media respectively, these values and those of the shales are within the BEWA standard's 1-3% doubtful category. All other media had more than 5% weight loss which is termed unsatisfactory by the standard.

Starlight was easily worn down in the friability test with 45% production of fines (again indicating its unsuitability as a filter medium). The media most resistant to wear were molochite, Arlita, Lytag and Old Expanded Shale but they still had high values of fine production.

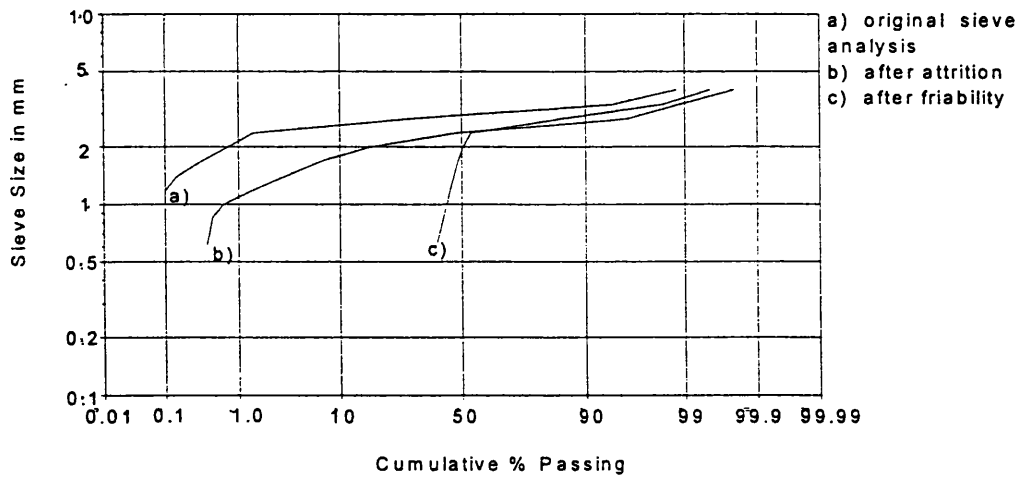


Figure 3. Sieve analysis of 'Starlight' (including analyses after friability and attrition tests).

REFERENCES

- Allen, T. (1981). Mercury porosimetry. In: *Particle Size Measurement*, 3rd ed. Chapman and Hall, pp. 564-582.
- Amirtharajah, A. (1993). Optimum backwashing of filters with air scour: A review. *Wat. Sci. Tech.*, **27**(10), 195-211.
- AWWA Standards Committee on Filtering Material. (1989). Standard for filtering material. A.W.W.A.
- British Effluent and Water Association (BEWA) (1993). Standard for the specification, approval and testing of granular filtering materials.
- Cantwell, A. D. C. and Whitaker, J. (1993). The development and application of the Biobead™ system. *SCI - Wastewater treatment by BAFs - Latest developments seminar, Cranfield*. (Abstract).
- Coulson, J. M. and Richardson, J. F. (1978). In: *Chemical Engineering*, 3rd ed. Pergamon Press.
- Dillon, G. R. and Thomas, V. K. (1990). A pilot-scale evaluation of the 'Biocarbone Process' for the treatment of settled sewage and for tertiary nitrification of secondary effluent. *Wat. Sci. Tech.*, **22**(1/2), 305-316.
- Humby, M. S. (1994). Attrition of granular filter media. *MSc Thesis*, School of Water Sciences, Cranfield University, England.
- Humby, M. S., Fitzpatrick, C. S. B. and Stevenson, D. G. (1995). Development of a friability test for granular filter media. *J. I.W.E.M.* (In Press).
- Indian Standards Institute. (1977). Requirements for filtration equipment. *Indian Standard - IS 8419* (Part 1).
- Ives, K. J. (1990). Testing of filter media. *J. Wat. SRT - Aqua.*, **39**(3), 144-151.
- Lacamp, B., Hansen, F., Penillard, P. and Rogalla, F. (1993). Wastewater nutrient removal with advanced biofilm reactors. *Wat. Sci. Tech.*, **27**(5/6), 263-276.
- Letterman, R. D. (1980). Economic analysis of granular bed filtration. *J. Env. Eng (ASCE)*, **106** (EE2), 279-291.
- Messing, R. A. (1988). Immobilized cells in anaerobic waste treatment. In: *Bioreactor Immobilized Enzymes and Cells - Fundamentals and Applications*, M. Moo-Young (Ed.). Elsevier Press, pp. 311-316.
- Ogedengbe, O. (1982). Water filtration using locally available sand. *Wat (Australia)*, **9**(6), 20-23.
- Ogedengbe, O. and Olawale, O. (1983). Palm kernel shells as filter media. *Filtration and Separation*, **20**(2), 138 and 140.
- Sagberg, P., Dauthville, P. and Hamon, M. (1992). Biofilm reactors: A compact solution for the upgrading of wastewater treatment plants. *Wat. Sci. Tech.*, **26**(3/4), 733-742.
- Smith, A. J. and Hardy, P. J. (1992). High rate sewage treatment using biological aerated filters. *J. I.W.E.M.*, **6** (October), 179-193.
- Stevenson, D. G. (1994). The specification of filtering materials for rapid-gravity filtration. *J. I.W.E.M.*, **8** (April), 527-533.
- Wen, C. Y. and Yu, Y..H. (1966). *Mechanics of fluidization*. Chem. Eng. Prog. Symp. Series no.62. New York: AIChE.

REFERENCES

- Adachi, S & Fuchi, Y. (1991). Reclamation and reuse of wastewater by biological aerated filter process. *Water Science & Technology*. 24 (9) 195 - 204.
- Addicks, R. (1990). Optimal simultaneous backwash of rapid granular-media filters with water and air in terms of three-phase-fluidisation. *5th World Filtration Congress - Nice*.
- Allen, T. (1981). Mercury Porosimetry. In: *Particle Size Measurement*, 3rded. Chapman and Hall. 564 - 582.
- Amar, D., Partos, J., Granet, C., Faup, G. M & Audic, J. M. (1986). The use of an upflow fixed bed reactor for treatment of a primary settled domestic sewage. *Water Research*. 20 (1) 9 - 14.
- American Water Works Association (AWWA) Standards Committee on Filtering Material. (1989). Standard for filtering material.
- Amirtharajah, A., McNelly, N., Page, G & McLeod, J. (1991). Optimum backwash of dual media filters and GAC filter adsorbers with air scour. *AWWA Conference Proceedings (June 1990)*.
- Amirtharajah, A & Cleasby, J.L. (1972). Predicting expansion of filters during backwash. *J.AWWA - Water Technology/Quality*. (January) 52 - 59.
- Amirtharajah, A & Trusler, S. (1982). Studies on loss of media during air scour. *AWWA Annual Conference Proceedings*.
- Amirtharajah, A & Wetstein, D. P. (1980). Initial degradation of effluent quality during filtration. *J. AWWA - Research and Technology*. 72 (9) 518 - 524.
- Amirtharajah, A. (1984). Fundamentals and theory of air scour. *J. Environmental Engineering*. 110 (3) 573
- Amirtharajah, A. (1988). Some theoretical and conceptual views of filtration. *J. AWWA - Research and Technology*. 80 (12) 36 - 46.
- Amirtharajah, A. (1993). Optimum backwashing of filters with air scour: a review. *Water Science & Technology*. 27 (10) 195 - 211.

- Anderson, G.K., Kasapgil, B & Ince, O. (1994). Comparison of porous and non-porous media in upflow anaerobic filters when treating dairy wastewater. *Water Research*. **28** (7) 1619 - 1624.
- Arden, E & Lockett, W.T. (1914). Experiments on the oxidation of sewage without the aid of filters. *J. Society of Chemical Industry*. **33** 523.
- Bach, H. (1937). The tank filter for the purification of sewage and trade wastes. Part 1 and 2. *Water works and sewerage*. 389.
- Baskervill, R. C & Gale, R. S. (1968). A simple automatic instrument for determining the filterability of sewage sludges. *Water Pollution Control*. **67** (2) 233.
- Bayfield, P. (1993). Factors affecting filter backwashing. *MSc Thesis*. Cranfield University, England.
- Baylis, J.R. (1959). Nature and effects of filter backwashing. *J.AWWA*. (January), 126-156.
- Boller, M., Kobler, D & Koch, G. (1997). Particle separation, solids budgets and headloss development in different biofilters. *Water Science & Technology*. **36** (4) 239-247.
- Boon, A. G., Hemfrey, J., Boon, K., Brown, M. ⁽¹⁹⁹⁷⁾ Recent developments in the biological filtration of sewage to produce high-quality nitrified effluents. *J. CIWEM*. **11** (December) 393-412.
- Boyle, W. C., Hellstrom, B. G & Ewing, L. (1988). Oxygen transfer efficiency measurements using off-gas techniques. *Water Science & Technology*. **21** 1295-1300.
- Breitenbucher, K., Siegl, M., Knupfer, A & Radke, M. (1989). Open-pore sintered glass as a high-efficiency support media in bioreactors: new results and long-term experiences achieved in high-rate anaerobic digestion. *Technical Advances in Biofilm Reactors - Nice*.
- British Effluent and Water Association (BEWA), (1993). Standard for the specification, approval and testing of granular filtering materials.
- Bryan, E.H. (1982). Development of synthetic media for biological treatment of municipal and industrial wastewaters. 89-111.
- Camp, T.R., Graber, S.D & Conklin, G.F. (1971). Backwashing of granular water filters. *J. Sanitary. Eng. Div.* **97** (SA6) 903 - 926.

- Ellis, K. V & Aydin, M. E. (1995). Penetration of solids and biological activity into slow sand filters. *Water Research*. **29** (5) 1333 - 1341.
- Fair, G. M *et al*, (1948). The behaviour of chlorine as a water disinfectant. *J. AWWA*. **40** (10).
- Fdez-Polanco, F., Mendez, F., Garcia, J.M & Blanco, C. (1996). Heterotroph growth in a nitrifying submerged biofilter. *IAWQ Biofilm 1996 Conference*.
- Fergusson, A. (1992). Operating experience and potential of a Colox® plant: an upward flow biological aerated filter. *IWEM Scientific Section Seminar, Matlock*.
- Figueroa, L. A & Silverstein, J. (1992). The effect of particulate organic matter on biofilm nitrification. *Water & Environmental Research*. **64** (5)728-733.
- Fitzpatrick, C.B.S. (1990). Detachment of deposits by fluid shear during filter backwashing. *Water Supply*. **8** 177 - 183.
- Fitzpatrick, C.S.B. (1993). Observations of particle detachment during filter backwashing. *Water Science & Technology*. **27** (10) 213 - 221.
- Fujie, K., Hu, H., Ikeda, Y & Urano, K. (1992). Gas-liquid oxygen transfer characteristics in an aerated submerged biofilter for wastewater treatment. *Chem. Eng. Sci.* **47** (13/14) 3745-3752.
- Fulton, G.P. (1988). Contending with filter media problems. *Public Works*. **119** (7) 67 - 70 and 110.
- Goldgrabe, J. C., Summers, R. S & Miltner, R. J. (1993). Particle removal and head loss development in biological filters. *J. AWWA - Research and Technology*. **86** (12) 94 - 106.
- Haarhoff, J & Malan, W.M. (1983). The disturbance of sand filter supporting layers by air scouring. *Water SA* **9** (2) 41 - 48.
- Hamoda, M. F & Abd-El-Bary, M. F. (1986). Operating characteristics of the aerated submerged fixed-film (ASFF) bioreactor. *Water Research*. **21** (8) 939 - 947.
- Harris, S. L. (1994). Aeration optimisation in biological aerated filters using off-gas analysis. *MSc Thesis*. Cranfield University, England.
- Harris, S. L., Stephenson, T & Pearce, P. (1995). Aeration investigation of biological aerated filters using off-gas analysis. *Water Science & Technology*. **34** (3/4) 307-314.
- Hewitt, S. R & Amiratharajah, A. (1984). Air dynamics through filter media during air scour. *J. Environmental Engineering ASCE*. **110** (3) 591-606.

Hoyland, G. (1979). Mass transfer model for aeration. *Prog. Wat. Tech.* **11**. (3) 237-246.

Humby, M. S (1994). Attrition of granular filter media. *MSc Thesis*. School of Water Sciences, Cranfield University, England.

Humby, M. S., Fitzpatrick, C. S. B. (1996). Attrition of granular filter media during backwashing with combined air and water. *Water Research*. **30** (2) 291-294.

Humby, M. S., Fitzpatrick, C.S.B & Stevenson, D.G. (1996). Development of a friability test for granular filter media. *Water and Environmental Management*. **10** (2) 87-91.

Indian Standards Institute. (1977). Indian Standard *IS 8419* (Part 1) - Requirements for filtration equipment.

Ives, K. J & Clough, G. (1985). Optical fibre investigations of filtration processes. 4th IAWPRC Workshop - Instrumentation and control of water and wastewater treatment and transport systems.

Ives, K. J. (1960). Rational design of filters. *Proc. Inst. Civ. Eng.* **16** 189-193.

Ives, K. J. (1965). Research on variables affecting filtration. *J. Sanit. Eng. Div. ASCE*. (SE4).

Ives, K. J. (1970). Rapid filtration. *Water Research*. **4** 201-223.

Ives, K. J. (1982). Fundamentals of filtration. *Conference Proceedings - Water Filtration, Belgium*.

Ives, K. J. (1989). Filtration studied with endoscopes. *Water Research* **23** (7) 861 - 866.

Ives, K.J. (1990). Testing of filter media. *J. Wat SRT - Aqua*. **39** (3) 144 - 151.

Ives + Coed (1987)

Iwasaki, T. (1937). Some notes on slow sand filtration. *J. AWWA*. **29** 1591-1602.

Kau, S. M & Lawler, D. F. (1995). Dynamics of deep-bed filtration: velocity, depth and media. *J. Env. Eng.* (December) 850 - 859.

Keim, P., Brandt, H-J., Aivasidis, A & Wandrey, C. (1988). Process control in anaerobic fluidized bed reactors using porous glass granules for microbial colonization. *Fifth Int. Symp. On Anaerobic Digestion - Bologna, Italy*.

Lacamp, B & Bourbigot, M. M. (1989). Advanced nitrogen removal processes for drinking and wastewater treatment. *Proceedings IAWPRC. Conference*. **2** 437-443.

Lang, J. S., Giron, J. J., Hansen, A. T., Trussell, R. R., Hodges, W. E. (1993). Investigating filter performance as a function of the ratio of filter size to media size. *JAWWA*. **85** (10) 122-130.

Langmuir, I. (1942). Filtration of aerosols and the development of filter materials. *Office of Scient. Res. Develop.*

Lee, K. M & Stensel, H. D. (1986). Aeration and substrate utilization in a sparged packed bed biofilm reactor. *J. WPCF*. **58** (11) 1066-1072.

Leglise, J. P., Faup, F. M & Ben, A. I. M. (1980). A new development in the biological aerated filter bed technology. *Annual water pollution control federation conference - Las Vegas*.

Le Tallec, X., Zeghal, S., Vidal, A., Lesouef, A. (1996). Effect of influent quality variability on biofilter operation. *IAWQ Biofilm Conference 1996*.

Lessar, A. (1993). Aeration in BAFs and the effects of bed depth. *MSc Thesis*. Cranfield Institute of Technology, England.

Letterman, R. D. (1980). Economic analysis of granular-bed filtration. *J. Env. Eng. Div.* **106** (EE2) 279 - 291.

Levenspiel, O. (1972). *Chemical Reaction Engineering*. 2nd Ed. Wiley, New York.

Lewis, W. K & Whitman, W. G. (1924). Principles of gas absorption. *Ind. Eng. Chem.* **43** 1215.

Mann, A., Fitzpatrick, C.S.B & Stephenson, T. (1995). A comparison of floating and sunken media biological aerated filters using tracer study techniques. *Trans. IChemE*. **73** (B) 137-143.

Mendoza-Espinosa, L., Mann, A & Stephenson, T. (1997). Determination of flow pattern and active volume in biological aerated filters under upflow and downflow conditions. *IChemE Jubilee Research Event Proceedings*. 121 - 124.

Messing, R. A. (1988). Immobilized cells in anaerobic waste treatment. In: *Bioreactor immobilized enzymes and cells - Fundamentals and applications*, M. Moo-Young (Ed). Elsevier Press. 311-316.

Metcalf & Eddy, (1991). *Wastewater Engineering - Treatment, Disposal, Reuse* (3rd Edition) McGraw-Hill, Inc .

Mintz, D. M. (1966). Modern theory of filtration. *IWSA 7th Congress, Barcelona*. 1 (10).

- Moran, M. C., Moran, D. C., Cushing, R. S & Lawler, D. F. (1993). Particle behaviour in deep-bed filtration: part 2 - particle detachment. *J. AWWA - Research and Technology*. (December) 82 - 93.
- Morgeli, B & Ives, K.J. (1979). New media for effluent filtration. *Wat.Res.* **13** 1001 - 1007.
- Mose Pedersen, B & la Coeur Jansen, J. (1992). Treatment of leachate-polluted groundwater in an aerobic biological filter. *European Water Pollution Control*. **2** (4) 40 - 45.
- O'Melia, C. R & Stumm, W. (1967). Theory of water filtration. *J. AWWA*. **59** 1393.
- O'Melia, C. R. (1974). The role of polyelectrolytes in filtration processes. *US EPA, Cincinatti, Ohio*.
- Odumosu, O.B & Muyibi, S.A. (1983). Filtration properties of local sands. *15th WEDC Conference - Nigeria*.
- Ogedengbe, O & Olawale, O. (1983). Palm kernel shells as filter media. *Filtration and Separation*. **20** (2) 138 and 140.
- Ogedengbe, O. (1982). Water filtration using locally available sand. *Water (Australia)*. **9** (6) 20 - 23.
- Ohashi, A., Viraj de Silva, D.G., Mobarry, B., Manem, J. A., Stahl, D. A & Rittmann, B. E. (1995). Influence of substrate c/n ratio on the structure of multi-species biofilms consisting of nitrifiers and heterotrophs. *Wat. Sci. Tech.* **32** (8) 75 - 84.
- Paffoni, C., Gousailles, M., Rogall, F & Gilles, P. (1990). Aerated biofilters for nitrification and effluent polishing. *Wat. Sci. Tech.* **22** (7/8) 181 - 189.
- Paolini, A. E. (1986). Effects of biomass on oxygen transfer in RBC systems. *J. WPCF*. **58** (4) 306-311.
- Parker, D. S & Richards, T. (1986). Nitrification in trickling filters. *J. WPCF*. **58** (9) 896-902.
- Parker, D., Lutz, M., Dahl, R & Bernkopf, S. (1989). Enhancing reaction rates in nitrifying trickling filters through biofilm control. *J. WPCF*. **61** (5) 618-631.
- Payatakes, A. C *et al*, (1981). A visual study of particle deposition and reentrainment during filtration of hydrosols with a polyelectrolyte. *Chem. Eng. Sci.* **36** 1319-1335.

- Payatakes, A. C., Tien, C & Turian, R. M. (1974). Trajectory calculation of particle deposition in deep bed filtration. *AIChE J.* **20** (5) 889 - 905.
- Peladan, J-G., Lemmel, H & Pujol, R. (1996). High nitrification rate with upflow biofiltration. *IAWQ Biofilm Conference 1996 Proceedings.*
- Pendse, H., Tien, C., Turian, R. M & Rajagopalan, R. (1978). Dispersion measurements in clogged filter beds - a diagnostic study on the morphology of particle deposition.
- Pujol, R., Lemmel, H., Gousailles, M & Vedry, B. (1996). Nitrification capacities with an up-flow biofiltration reactor. *IAWQ Biofilm Conference 1996 Proceedings.*
- Rajagopalan, R & Tien, C. (1976). Trajectory analysis of deep-bed filtration with the sphere-in-cell porous media model. *AIChE J.* **22** (3) 523 - 533.
- Rajagopalan, R & Tien, C. (1977). Single collector analysis of collection mechanisms in water filtration. *The Canadian J. Chemical Eng.* **55** (June) 246 - 255.
- Rao Bhamidimarri, S. M & See, T, T. (1992). Shear loss characteristics of an aerobic biofilm. *Wat. Sci. Tech.* **26** (3/4) 595 - 600.
- Reiber, S & Stensel, D. (1985). Biologically enhanced oxygen transfer in a fixed film system. *J. WPCF.* **57** (2) 135-142.
- Rusten, B. (1984). Wastewater treatment with aerated submerged biological filters. *J. WPCF.* **56** (5) 424-431.
- Ryhiner, G., Birou, B & Gros, H. (1992). The use of submerged structured packings in biofilm reactors for wastewater treatment. *Wat. Sci. Tech.* **26** (3-4) 723-731.
- Sagberg, P., Dauthuille, P & Hamon, M. (1992). Biofilm reactors: a compact solution for the upgrading of waste water treatment plants. *Wat. Sci. Tech.* **26** (3/4) 733-742.
- Särner, E. (1986). Removal of particulate and dissolved organics in aerobic fixed-film biological processes. *J. WPCF.* **58** (2) 165-172.
- Shah, J.S., Bokil, S.D & Chaudhuri, M. (1984). Characterisation of a basaltic water filter media. *J.Indian.W.W.A.* **16** (1) 33-38.
- Smith, A. J., Quinn, J. J., Hardy, P. J. (1990). Development of an aerated filter package plant. Presented: *1st International Conference on Advanced Waste Water and Environmental Managment, Lyon, France.*

- Smith, A. J & Hardy, P. J. (1992). High-rate sewage treatment using biological aerated filters. *J. IWEM*. **6** (April) 179-193.
- Smith, A. J & Hardy, P. J. (1997). The effect of variations in flow and load on the performance of a combined treatment biological aerated filter. *In Press*.
- Stensel, H. D., Brenner, R.C & Lubi, G. R.(1984). Aeration energy requirements in a sparged fixed film system. *Proceedings Second International Conference on Fixed Film Biological Processes*.
- Stensel, H. D & Reiber, S. (1983). Industrial wastewater treatment with a new biological fixed-film system. *Env. Progress*. **2** (2) 110-115.
- Stensel, H. D., Brenner, R. C., Lee, K. M., Melcer, H & Rakness, K. (1988). Biological aerated filter evaluation. *J. Env. Eng.* **114** (3) 655-671.
- Stephenson , T., Mann, A & Upton, J. (1993). The small footprint wastewater treatment process. *Chemistry & Industry* (19th July) 533-536.
- Stevenson, D.G. (1994). The specification of filtering materials for rapid-gravity filtration. *J.I.W.E.M.*, **8** (April) 527-533.
- Stevenson, D.G. (1995). Process conditions for the backwashing of filters with simultaneous air and water. *Wat. Res.* **29** (11) 2594-2597.
- Sundararajan, A & Ju, L-K. (1995). Biological oxygen transfer enhancement in wastewater treatment systems. *Wat. Env. Res.* **67** (5) 848-854.
- Tchobanoglous, G & Eliassen, R. (1970). Filtration of treated sewage effluent. *J. Sanit. Eng. Div. ASCE*. **96** (SA2) 243.
- Tebutt, T. H. (1971). An investigation into tertiary treatment by rapid filtration. *Wat. Res.* **5** (81).
- Tebbutt, R. H. Y & Shackleton, R. C. (1984). Temperature effects in filter backwashing. *The Public Health Engineer*. **12** (3) 174-178.
- Tien, C & Payatakes, A. C. (1979). Advances in deep bed filtration. *AIChE J.* **25** (5) 737-759.
- Tobiason, J. E., Johnson, G. S & Westerhoff, P. K. (1990). Particle size and filter performance: model studies. *Nat. Conf. Env. Eng. Conference Proceedings*.
- Upton, J & Cartwright, D. (1984). Basic design criteria and operating experience of a large nitrifying filter. *Wat. Pollut. Control*. **83**

- Upton, J & Churchley, J. (1996). Relative merits of aerated biofilters for compact treatment. *After the Outfall - Experience of Coastal Sewage Treatment, CIWEM Conference, Cambridge.*
- Upton, J & Stephenson, T. (1993). BAF - upflow or down flow - the choice exists. *Wastewater Treatment by Biological Aerated Filters - Latest Developments Symposium, Cranfield University.*
- Vigneswaran, S & Ben Aim, R. (1985). The influence of suspended particle size distribution in deep-bed filtration. *AIChE.* 31 321-324.
- Vigneswaran, S., Chang, J. S & Janssens, J. G. (1990). Experimental investigation of size distribution of suspended particles in granular bed filtration. *Wat. Res.* 24 927-930.
- Wen, C. Y & Yu, Y. H (1966). Mechanics of fluidisation. *Chem. Eng. Prog. Symp. Series no. 62.* New York: AIChE.
- Winkler, M. (1981). Biological Treatment of Wastewater. Ellis Horwood Ltd, England.
- WPCF. (1985a). Standard Methods for the Examination of Water and Wastewater.
- WPCF. (1985b). Standard Methods for the Examination of Water and Wastewater.
- Young, J.C. (1985). Operating problems with wastewater filters. *J.WPCF.* 57 (1) 22 - 29.